

UNCLASSIFIED

AD NUMBER

ADB019314

LIMITATION CHANGES

TO:

Approved for public release; distribution is unlimited.

FROM:

Distribution authorized to U.S. Gov't. agencies only; Test and Evaluation; 20 JAN 1977. Other requests shall be referred to Space and Missile Systems Organization, ATTN: SAMSO/RSSE, Los Angeles, CA 90009.

AUTHORITY

SAMSO ltr dtd 2 May 1978

THIS PAGE IS UNCLASSIFIED

THIS REPORT HAS BEEN DELIMITED
AND CLEARED FOR PUBLIC RELEASE
UNDER DOD DIRECTIVE 5200.20 AND
NO RESTRICTIONS ARE IMPOSED UPON
ITS USE AND DISCLOSURE.

DISTRIBUTION STATEMENT A

APPROVED FOR PUBLIC RELEASE;
DISTRIBUTION UNLIMITED.

AD B019314

SAMSO-TR-77-41

2

FG

ACOUSTIC RECESSION GAGE DEVELOPMENT

J. O. Vindum, R. L. Eichorn, T. F. Foster, J. T. Kelly,
T. K. Muller, R. E. Lundberg
Acurex Corporation/Aerotherm Division
485 Clyde Avenue
Mountain View, California 94042

DDC
JUN 27 1977
RECEIVED
C

20 January 1977

COPY AVAILABLE TO DDC DOES NOT
PERMIT FULLY LEGIBLE PRODUCTION

Final Report for Period 30 June 1975 - 30 November 1976

Distribution limited to U.S. Government agencies
only; Test and Evaluation; 20 January 1977.
Other requests for this document must be referred
to Space and Missile Systems Organization (SAMSO/
RSSE), Los Angeles, California, 90009.

AD NO.
DDC FILE COPY

Prepared for

SPACE AND MISSILE SYSTEMS ORGANIZATION
Air Force Systems Command/RSSE
Los Angeles, California 90009

SAMSO-TR-77-41

ACOUSTIC RECESSION GAGE DEVELOPMENT

J. O. Vindum, R. L. Eichorn, T. F. Foster, J. T. Kelly,
T. K. Muller, R. E. Lundberg
Acurex Corporation/Aerotherm Division
485 Clyde Avenue
Mountain View, California 94042

20 January 1977

Final Report for Period 30 June 1975 - 30 November 1976

Distribution limited to U.S. Government agencies
only; Test and Evaluation; 20 January 1977.
Other requests for this document must be referred
to Space and Missile Systems Organization (SAMSO/
RSSE), Los Angeles, California, 90009.

Prepared for

SPACE AND MISSILE SYSTEMS ORGANIZATION
Air Force Systems Command/RSSE
Los Angeles, California 90009

ACCESSION for	
NTIS	White Section <input type="checkbox"/>
DIC	Buff Section <input checked="" type="checkbox"/>
UNCLASSIFIED	<input type="checkbox"/>
JUSTIFICATION	
BY	
DISTRIBUTION/AVAILABILITY CODES	
Dist.	AVAIL. and/or SPECIAL
B	23 441

NOTICE

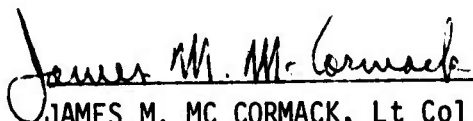
This final report was submitted by the Aerotherm Division of the Acurex Corporation located in Mountain View, California, 94042, under Contract F04701-75-C-0164, with the Space and Missile Systems Organization, Los Angeles, California, 90009. Capt. Don Jackson was the SAMSO/RSSE Project Officer-in-Charge.

This technical report has been reviewed and is approved for publication.



DON E. JACKSON, Capt, USAF
Project Officer

FOR THE COMMANDER:



JAMES M. MC CORMACK, Lt Col, USAF
Chief, Reentry Technology Division
Deputy for Reentry Systems

Unclassified

SECURITY CLASSIFICATION OF THIS PAGE (When Data Entered)

19 REPORT DOCUMENTATION PAGE		READ INSTRUCTIONS BEFORE COMPLETING FORM
1. REPORT NUMBER SAMS0-TR-77-41	2. GOVT ACCESSION NO.	3. RECIPIENT'S CATALOG NUMBER
4. TITLE (and Subtitle) ACOUSTIC RECESSION GAGE DEVELOPMENT.		5. TYPE OF REPORT & PERIOD COVERED Final Report for Period 6/30/75 - 11/30/76
7. AUTHOR(s) J. O. Vindum, R. L. Eichorn, T. F. Foster, J. T. Kelly, T. K. Muller, R. E. Lundberg		6. PERFORMING ORG. REPORT NUMBER FR 77-236, 77-237
9. PERFORMING ORGANIZATION NAME AND ADDRESS Acurex Corporation/Aerotherm Division 485 Clyde Avenue Mountain View, California 94042		8. CONTRACT OR GRANT NUMBER(s) F04701-75-C-0164
11. CONTROLLING OFFICE NAME AND ADDRESS SPACE AND MISSILE SYSTEMS ORGANIZATION Air Force Systems Command/RSSE Los Angeles, California 90009		10. PROGRAM ELEMENT, PROJECT, TASK AREA & WORK UNIT NUMBERS CDRL Item A001
12. MONITORING AGENCY NAME & ADDRESS (if different from Controlling Office) Aerotherm-TR-77-236		11. REPORT DATE 20 January 1977
		12. NUMBER OF PAGES 260
		13. SECURITY CLASS. (of this report) Unclassified
		14. DECLASSIFICATION/DOWNGRADING SCHEDULE
15. DISTRIBUTION STATEMENT (of this Report) Distribution limited to U.S. Government agencies only; Test and Evaluation; 20 January 1977. Other requests for this document must be referred to Space and Missile Systems Organization (SAMS0/RSSE), Los Angeles, California, 90009.		
17. DISTRIBUTION STATEMENT (of the abstract entered in Block 20, if different from Report) Final rept. 3p Jun 75-3p Nov 76,		
18. SUPPLEMENTARY NOTES		
19. KEY WORDS (Continue on reverse side if necessary and identify by block number) Acoustics Ablation Measurements Acoustic Gage Nosetips Resonating Acoustics Instrumentation Recession Gage Piezoelectric		
20. ABSTRACT (Continue on reverse side if necessary and identify by block number) Resonant Acoustic Measurement Gages have been developed under SAMS0 Contract F04701-75-C-0164. These gages were designed to determine the re- cession and shape of ablating reentry vehicle nosetips. A single-mode gage is used to determine recession only and a dual-mode gage was built to mea- sure both recession and shape. Details of the gage configurations, electronics, and associated tests are described. The tests include bench tests, 1 MW and 50 MW arc jet ablation		

DD FORM 1 JAN 73 1473

EDITION OF 1 NOV 68 IS OBSOLETE

Unclassified

SECURITY CLASSIFICATION OF THIS PAGE (When Data Entered)

407 435 iii

over
mt

Unclassified

SECURITY CLASSIFICATION OF THIS PAGE (When Data Entered)

20. Abstract (Continued)

tests. Also included are details of the acoustical analysis performed using several computer codes.

The main feature of the Resonant Acoustic Measurement Gage is that the object which is to be measured is acoustically excited at its resonant frequency or frequencies. It is from these frequencies that nosetip length and shape can be obtained.

Because of reduced funding levels in the instrumentation area, this program was temporarily halted. This report describes the status of the gages at the time the contract was halted.

Unclassified

SECURITY CLASSIFICATION OF THIS PAGE (When Data Entered)

TABLE OF CONTENTS

<u>Section</u>		<u>Page</u>
1	INTRODUCTION AND SUMMARY	5
2	RECOMMENDATIONS FOR DESIGN AND HARDWARE CHANGES	9
	2.1 Bench Tests	9
	2.2 Model Sizes	9
	2.3 1 MW and 50 MW Testing	9
	2.4 Applicable Carbon/Carbon Materials	10
	2.5 Design Changes	10
3	HARDWARE CONFIGURATION	11
	3.1 Electronics	11
	3.1.1 Design Status	11
	3.1.2 Flight Electronics	11
	3.1.3 Performance	27
	3.1.4 Application	30
	3.1.5 Reliability	30
	3.1.6 Test Electronics	33
	3.2 Mechanical Hardware Development	33
	3.2.1 Sensor Construction	38
	3.2.2 Crystal Study	40
	3.2.3 Transmitter and Receiver Construction	47
	3.2.4 Gage Attachment	55
	3.2.5 System Packaging	55
	3.3 50 MW Test Model Design	57
	3.3.1 Nosetip Configuration	57
	3.3.2 Support Hardware	58
	3.3.3 Model Instrumentation Support Hardware	58
4	DESIGN SUPPORT	61
	4.1 Bench Tests	61
	4.1.1 Bench Test Hardware	61
	4.1.2 Bench Test Objectives and Procedures	64
	4.1.3 Bench Test Results	66
	4.2 1 MW Tests	69
	4.2.1 Test Objectives	69
	4.2.2 Test Conditions - Test Matrix	69
	4.2.3 Model Description	74
	4.2.4 Test Procedure	74
	4.2.5 Test Results	75
	4.3 Analysis	75
	4.3.1 Methodology	83
	4.3.2 Applications	110
	REFERENCES	125
	APPENDIX A - DETAIL HARDWARE DRAWINGS	127
	APPENDIX B - ELECTRONIC SCHEMATICS AND WIRING DIAGRAMS	185
	APPENDIX C - ELECTRONIC COMPONENTS PARTS LIST	211
	APPENDIX D - NONSTANDARD PARTS APPROVAL REQUEST	239

LIST OF ILLUSTRATIONS

Figure		Page
1	Flight electronics block diagram	12
2	Power supply	14
3	Input buffer	15
4	Phase comparator	17
5	Filter	18
6	Voltage controlled oscillator	19
7	Power amplifier	21
8	Lock detector	22
9	Noise detector	24
10	Package	25
11	System interconnects	26
12	Loop response	29
13	50 MW single mode test using flight electronics	35
14	Concentric transmitter/receiver	37
15	In-line flexural transmitter and receiver	39
16	Prototype accelerometer	41
17	Useful temperature range of various piezoelectric materials	43
18	Desired piezoelectric crystal shapes	45
19	Crystal test fixtures	46
20	Crystal clamping	48
21	Transmitter construction	51
22	Waveguide performance	53
23	50 MW test models	54
24	Bimorph test configuration	62
25	50 MW models 0 to 100 kHz sweep	71
26	1 MW Test 1 lock detection signal history	76
27	1 MW Test 2 lock detection signal history	77
28	1 MW Test 1 tracked frequency vs. time	78
29	1 MW Test 2 tracked frequency vs. time	79
30	Nosetip surface temperature	80
31	Nosetip surface temperature	81
32	Base temperature	82

LIST OF ILLUSTRATIONS (Concluded)

<u>Figure</u>		<u>Page</u>
33	Schematic of SAP IV beam element applications to nosetip/waveguide system . .	84
34	SAP IV beam analysis predictions of tungsten bar resonant frequencies	87
35	Comparison of 1 MW arc SAP IV beam analysis predictions and measurements for tungsten nosetip	94
36	Tungsten elastic modulus as a function of temperature	95
37	Predicted 1 MW arc tungsten temperature distributions as a function of time	97
38	Comparison of 50 MW arc SAP IV beam analysis predictions and measurements for a tungsten nosetip	98
39	Elastic modulus versus temperature for representative commercial graphites . .	99
40	One MW arc test results for a carbon/carbon nosetip	100
41	Comparison of 50 MW arc SAP IV beam analysis predictions and measurements for a carbon/carbon nosetip	102
42	First and fourth flexural resonant frequencies versus midpoint length	103
43	Shape uncertainty as a result of predicted frequency uncertainty	104
44	SAP IV quadrilateral brick element analysis	108
45	Fourth flexural beam type responses (DIAL code)	112
46	Elastic modulus of carbon/carbon material versus temperature	116
47	First and fourth flexural resonant mode frequencies vs. midpoint length . . .	119
48	First and fourth flexural resonant mode vs. corner length	120
49	Carbon/carbon nosetip geometry and material properties	121

LIST OF TABLES

<u>Table</u>		<u>Page</u>
1	Accuracy	28
2	Standard Parts Used (Passive)	31
3	Standard Parts Used (Active)	32
4	Nonstandard Parts Used	34
5	Physical Properties of Piezoelectric Materials	42
6	Acoustic Impedance of Various Materials	49
7	Material Properties	52
8	Adhesive Properties	56
9	50 MW Model Frequencies	70
10	1 MW Test Matrix	73
11	1 MW Model Frequencies	74
12	Comparison of SAP IV Beam Analysis and Measured Nosetip/Waveguide Resonant Frequencies	89
13	MSV Nosetip with Single Crystal Waveguide	92
14	Aluminum Nosetip First Compressional Resonant Mode Frequencies	93
15	Comparison of SAP IV Beam Analysis Resonant Mode Frequency Predictions and Data for Various Nose Shapes	106
16	Comparison of SAP IV Beam and Quadrilateral Brick Element Predictions	107
17	Comparison of Resonant Mode Predictions Utilizing SAP IV, DIAL and Shell Shock	109
18	Comparison of SAP IV Beam and DIAL Predictions and Measurements	111
19	Relative Costs of Predictions Utilizing SAP IV, DIAL, and Shell Shock Codes	113
20	Effect of Temperature on Higher Order Modes	115
21	Sensitivity of Carbon/Carbon Flight Configuration Resonant Frequencies to Temperature	117
22	Nose Angle Uncertainty Due to Frequency Uncertainty	123

SECTION 1

INTRODUCTION AND SUMMARY

The purpose of this report is to describe all the engineering details of the Resonant Acoustic Measurement (RAM) gage. The design configurations, which were being developed at the time the program was temporarily halted and the design and test analysis which preceded the current gage configuration will be described. Because the gage program was halted during the developmental phase, the intent of this report is to serve as a detailed engineering report rather than an abbreviated final report. Appendices containing engineering details required for any subsequent startup of the program are included. These appendices contain reduced copies of blueprints, electronic schematics and layouts.

The Resonant Acoustic Measurement Gage was developed during the Passive Nosetip (PANT II) programs sponsored by the Space and Missile Systems Organization (SAMSO) under Contract F04701-75-C-0164. However, cutbacks in the funding level of the PANT III program resulted in the elimination of the gage developmental phase for 1977.

The two main objectives for the RAM gage program were to: (1) develop a flight-qualified recession gage for reentry vehicles, and (2) design and test a dual mode gage which would measure both recession and shape of an ablating nosetip.

Additionally, the RAM gage was developed to provide an instrument free from the disadvantages inherent in present (radioactive) gage designs and to also provide clear assessments of nosetip material performance in flight. This task was judged to be very important since advanced reentry system developments, including both flight tests and passive nosetip material evaluations, will continue during the next decade.

Specific material development activities considered were:

- 3-D carbon/carbon performance assessment
- Qualification of Rayon precursor substitute
- Qualification of low cost substitute of 3DCC
- Possible requirements for organometallic erosion resistant materials

- Possible requirements for shape controlled (soft core) materials

Furthermore, in light of the increased accuracy required from future RV's, it will be desirable to obtain shape as well as recession information during the flight.

Comparisons of data from past flights show that nosetip material characteristics significantly impact the shaping performance of the nosetip. Four shape regimes are known to exist:

- Laminar blunt
- Laminar cap with turbulent forecone
- Slender turbulent biconic
- Blunt turbulent biconic

The determination of when, during reentry, these various shape regimes occur is critical to the material performance evaluation. One material may, for example, undergo late boundary layer transition and hence, develop a slender, fracture prone shape; another may experience transition early and develop a blunter, more stable, biconic shape.

It is necessary, through ongoing programs, to quantify the major contributors to inaccuracy by thorough analysis of flight dynamics data. Measurements of nose bluntness, transition, and recession are needed to discriminate between the nosetip and frustum-related components of reentry dispersion.

The single mode, or recession RAM gage, has demonstrated the ability to accurately indicate the maximum heating ray recession in both graphitic and metal ablation tests. Bench tests of the dual mode or shape/recession gage verified that this type of gage can be used to determine the bluntness and length of a reentry vehicle nosetip.

The manner in which these gages function is as follows. The recession (or single mode) gage operates by setting up a single compressional standing wave in the ablating nosetip. Recession is determined from the frequency versus time information generated during reentry. The recession and bluntness (or dual mode) gage operates by setting up two compressional or flexural waves in the nosetip using the fundamental frequency and the fourth harmonic. The fundamental frequency is used for recession information, and the fourth can be used to derive the forecone angle of the nosetip versus time. From these data, bluntness during reentry can be extracted.

The recession point determined by the gage is the "midpoint" length which is measured from the backface of the nosetip to the intersection of the bisected cone angle and the forecone surface.

The single or dual standing waves are produced by exciting the back end of the nosetip with a piezoelectric crystal transmitter; single or dual piezoelectric receivers are used to detect the

motion of the backface of the nosetip. At resonance, the transmitted and received signal is 90° out of phase. This phase relationship is used to accomplish the frequency tracking during reentry for both the single and dual mode gages.

On a previous program, the single mode gage was tested in the 50 MW arc jet at Wright-Patterson Air Force Base. The objective of this program was to configure it for flight and to use flight approved hardware. The dual mode gage configuration was bench-tested and subjected to the 1 MW arc jet at Acurex.

Transmission of the flight data was relatively easy. Because the frequency of the transmitter is determined by a Voltage Controlled Oscillator (VCO), the input voltage to this oscillator is the only data that needs to be transmitted to the ground during reentry.

The electronics for the gage had also been configured so that changes in the boundary layer noise could be detected. It was expected that this would happen during boundary layer transition, hence the gage could also be used to detect transition.

The primary difficulty during the developmental tests has been testing flight hardware by using subscale tests. Subscale testing of the dual mode gage has proved particularly troublesome due to the interaction of the nosetip vibration with transducer resonance. These difficulties will be explained in more detail in Section 2 of this report.

Section 3 includes the details of the electrical and mechanical configurations. Hardware configurations at the time of the program termination and background data explaining the selection of the current configuration are included.

Design support tasks such as bench tests, 1 MW tests, and Acoustics Analysis are described in Section 4.

The appendices include details which were important to the program. Appendix A includes reduced blueprints of the mechanical components of the gage as well as test hardware and support equipment needed for bench, 1 MW, and 50 MW tests. Reduced electronic schematics and component layouts are included in Appendix B; Appendix C contains parts lists for the electronic components. Appendix D includes copies of the Nonstandard Parts Approval Requests which were submitted in order to qualify the required electronic components.

It should be noted that the Resonant Acoustic Measurement (RAM) gage is also referred to as the Acoustic Recession Gage (ARG). Both designations are used in this report.

SECTION 2

RECOMMENDATIONS FOR DESIGN AND HARDWARE CHANGES

This report describes the work done during the PANT II program to develop and build a Resonant Acoustic Measurement gage. Near the end of the program several factors important to the design of a flight gage were discovered which should change the procedure for developing further acoustic gage hardware. These factors relate to testing and test hardware.

2.1 BENCH TESTS

Many of the bench tests were performed with aluminum models rather than carbon/carbon nose-tip models since aluminum was easier to obtain and work with. The different acoustic velocities, damping coefficients and acoustic impedances at times led to erroneous test conclusions. It is therefore recommended that all tests be done with carbon/carbon materials or materials which would at least duplicate the composite nature of the carbon/carbon materials.

2.2 MODEL SIZES

Subscale nosetip models behave quite differently than full-scale models. The resonant frequency of a subscale model is much higher than that of a full-scale model. This can have serious effects on hardware which was designed for full-scale models. For example, the resonant frequency of a subscale model may be at the resonant point of the transmitter waveguide or gage housing.

Subscale models are usually acoustically stiffer than full-scale models since the length is scaled down, but the shank diameter is kept constant for proper attachment of the acoustic gage. This increased stiffness can also lead to erroneous results.

2.3 1 MW AND 50 MW TESTING

Because of model constraints in test facilities such as the 1 MW and 50 MW arcs, subscale nosetips are tested in these facilities to qualify flight hardware. This causes the type of problems described in Section 2.2. It is recommended that only full-scale tests be done in such facilities as the RPL nosetip test facility. Subscale testing is not an effective method of proving the flight worthiness of acoustic hardware designed for full-scale nosetips.

2.4 APPLICABLE CARBON/CARBON MATERIALS

Since the exact nosetip configuration is not too critical for bench tests, used nosetips from RPL tests for example, are an excellent source of test nosetips.

2.5 DESIGN CHANGES

One of the major limitations in the current design was the anticipated available electrical power on the Material Screening Vehicle* (MSV). It might be useful to consider an acoustic electronics package which has its own battery so that more power could be made available during the few seconds of reentry.

*Subscale reentry vehicle used for nosetip material testing.

SECTION 3

HARDWARE CONFIGURATION

This section describes the details of the electrical and mechanical hardware and the development and engineering which preceded the current configuration. The program was halted before the final flight configuration was completed, hence some of the design details may be missing or incomplete. The configurations to be used for planned 50 MW tests are also described.

3.1 ELECTRONICS

The description of the electronics has been divided into Design Status, Flight Electronics Description, Performance, Application, Reliability, and Test Electronics. Other details related to the electronics are included in Appendices B through D.

3.1.1 Design Status

The status of the electronics design at the time of termination was as follows:

1. All electronic subsystems were breadboarded and tested
2. Drafted schematics for the single mode gage were completed but not checked and finalized
3. Module layouts were completed and partially checked

The major efforts remaining were to finish the transformer and housing design and select the connectors and RFI filters as required. With completion of those tasks, a flight prototype could be fabricated.

3.1.2 Flight Electronics

The selected method of detecting nosetip recession is to continually excite the nosetip at its resonant frequency. To accomplish this, a phase-lock loop was used (see Figure 1, Flight Electronics Block Diagram).

A voltage controlled oscillator (VCO) excites the nosetip at some frequency close to resonance. A phase detector senses whether the phase angle between the transmitter and receiver is greater than or less than 90° , and commands the VCO to shift frequency in the appropriate direction to achieve the 90° phase angle characteristic of resonance.

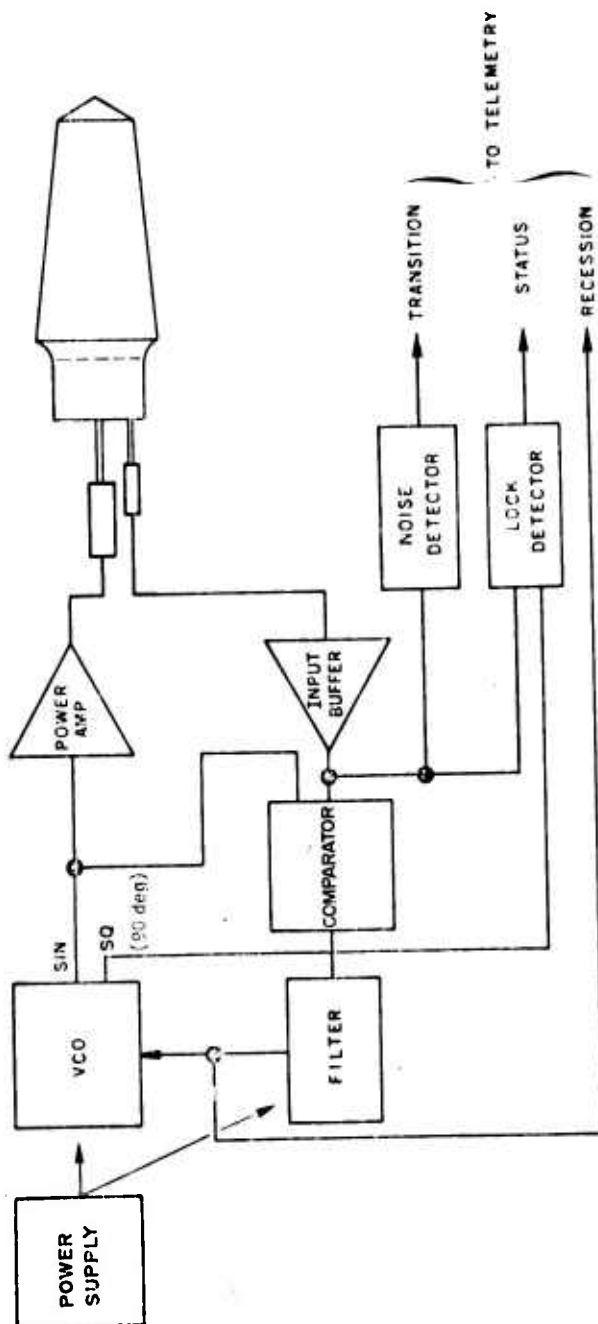


Figure 1. Flight electronics block diagram.

The VCO is designed so that the frequency is linearly proportional to input voltage, thus the VCO input may be fed directly to the telemetry system as an indication of resonant frequency.

Other functions provided in the flight electronics include a lock detector, which gives an indication as to whether the loop is locked to a good resonant peak, and a noise detector, which will hopefully provide information as to the occurrence of boundary layer transition. These two functions will be described in detail, along with the blocks in the recession gage loop, in the next section.

In addition, the flight circuitry incorporates a startup circuit which initializes the VCO to a predetermined frequency just below the anticipated nosetip resonance. The VCO then sweeps towards a higher frequency, causing the loop to sweep through the nosetip resonance, acquiring lock as it passes through resonance. Thus, it is guaranteed to lock to the appropriate nosetip resonance as it is turned on in flight.

The electronics is divided into several modules. Detailed descriptions of the modules are discussed here using simplified schematics. Detailed schematics are provided in Appendix B.

- a. Package — The package, which will be discussed in greater detail later, consists of six microwelded, potted cordwood modules enclosed in an aluminum housing. Certain electronic parts, such as power transistors, transformers, and parts which must be selected to customize the electronics to a specific nosetip is located external to the potted modules.
- b. Power Supply — The function of the power supply is to convert the incoming battery, with a voltage that can vary over a wide range, to a regulated DC voltage stable enough to obtain accurate system outputs. It provides two regulators of DC voltage. The first, V₂ (20.5 volts) (see Figure 2, Power Supply), is the main source of power and this requires a current driving pass transistor which is located external to the module, heatsunk to the aluminum chassis. The other voltage, V₁ (10.25 volts), is provided for bid levels only, and is obtained by dividing the main supply by 2 and by buffering with an operational amplifier. The regulator for the 20.5 volts is a standard integrated circuit, as shown in the simplified schematic.
- c. Input Buffer — The input buffer is a simple voltage follower (see Figure 3) which picks up the high impedance crystal signal and buffers it so that it can drive the next stages. In addition, the gain can be selected so as to accommodate a range of signal levels which may result depending on waveguide and nosetip configuration. Some configurations may actually require attention, thus the buffer is designed to have a gain range 0.1 to 10. The input is protected against high voltage transients by diodes to ground and V₂.

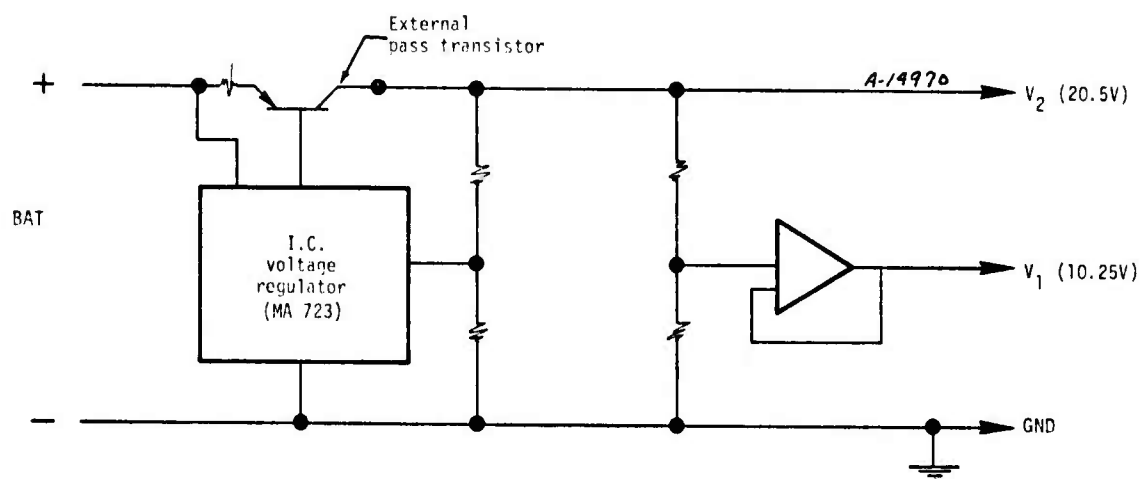


Figure 2. Power supply.

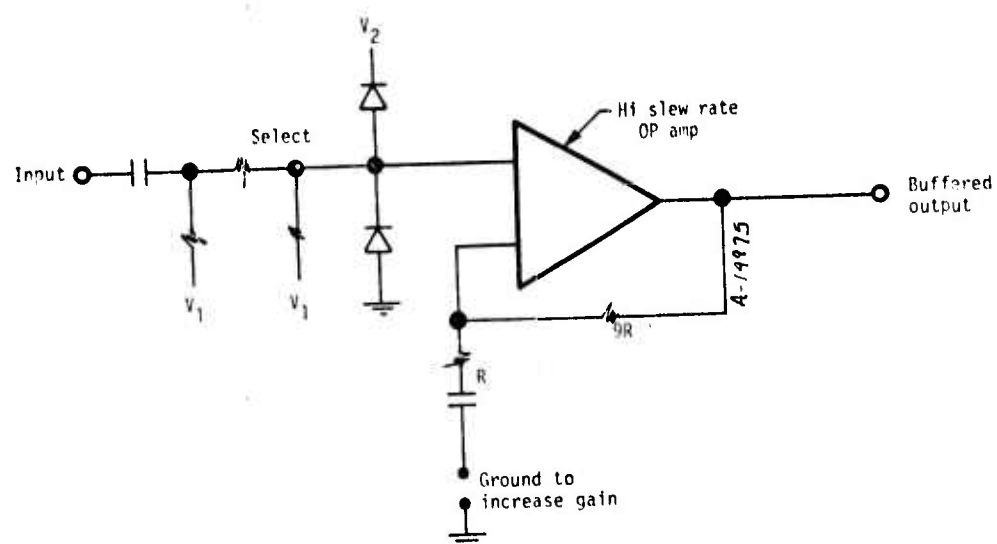


Figure 3. Input buffer.

- d. Phase Comparator — The phase comparator (Figure 4) is a linear integrated circuit multiplier. Thus the output is the product of the two input signals. It can be shown that when the two input signals are of the same frequency, the output consists of a double frequency component (not of interest) and a DC voltage which is positive when the signals are in phase, negative when they are 180° out of phase, and going to zero at a 90° phase angle. Thus the output is nulled when the phase is at the desired 90° phase which occurs at nosetip resonance. A phase compensation network is provided at the input which takes in the VCO signal. This corrects for the small phase error which occurs in the power amplifier and input buffer. Resistors must be selected to trim the multiplier output to zero at the desired 90° phase angle.
- e. Filter — The filter is a simple operational amplifier integrator which functions to remove the high frequency components from the multiplier, determines the frequency response of the loop, and eliminates the extraneous acoustic noise signals. The startup sequence is located in this section also; a startup circuit, in the module containing the input buffer controls a switch which places the filter in two different modes of operation. In the startup mode (see Figure 5), the input signal is locked out, and the output of the filter is biased at a fixed 5 volts DC. This condition exists until the power supplies have stabilized. When the startup circuit commands the search and lock mode, the filter becomes an integrator and a current is fed into the integrator input through the resistor to connect to V_2 . This causes the integrator voltage to ramp negative. Since the VCO input characteristics are such that decreasing voltage yields increasing frequency, the VCO frequency increases as the filter is ramping negative. When a large nosetip resonance is experienced, the signal at the input overwhelms the ramp current, and the integrator voltage stays locked at a fixed level. This level will be set to the specific nosetip frequency at 4.5 volts. This gives the output enough range to continue to decrease when the nosetip frequency increases due to recession.
- f. Voltage Controlled Oscillator — The voltage controlled oscillator (Figure 6) is an integrated circuit function generator with a frequency linearly proportional to the input current. A resistor network is placed on the front to convert the filter voltage to a current. A capacitor of the appropriate value is selected to make the VCO frequency equal to the nosetip resonant frequency with a 4.5-volt input. Since both the resistor network and the capacitor network directly control frequency, components with low temperature coefficients are chosen. In addition, two resistors are selected to minimize

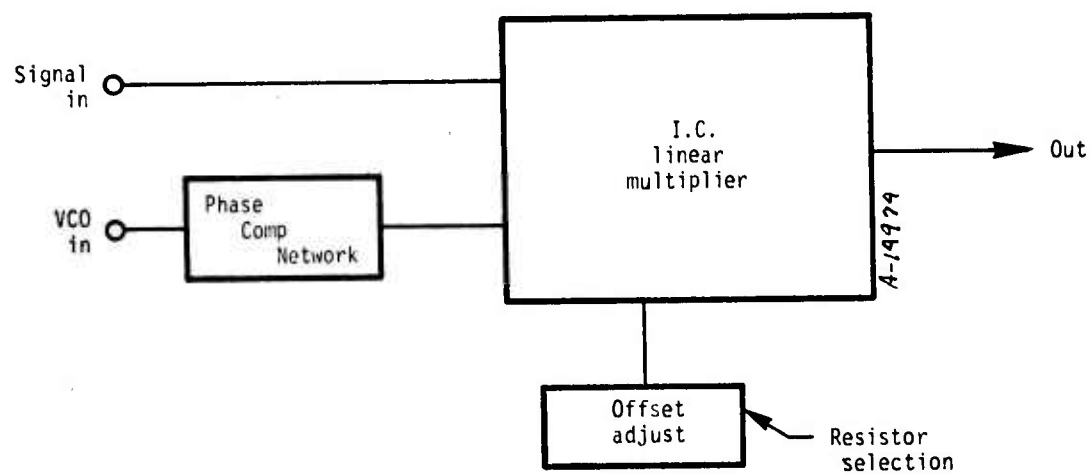


Figure 4. Phase comparator.

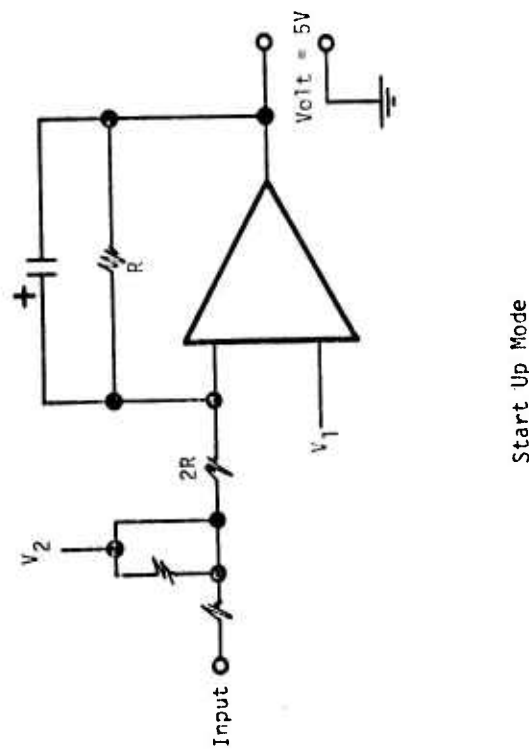
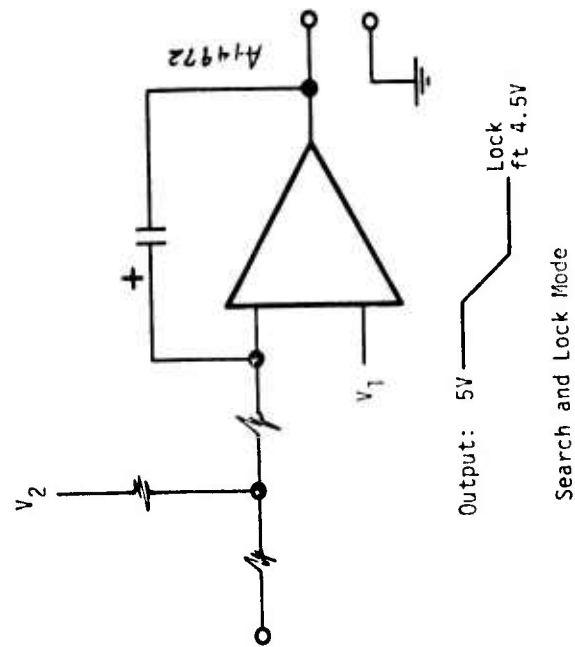


Figure 5. Filter.

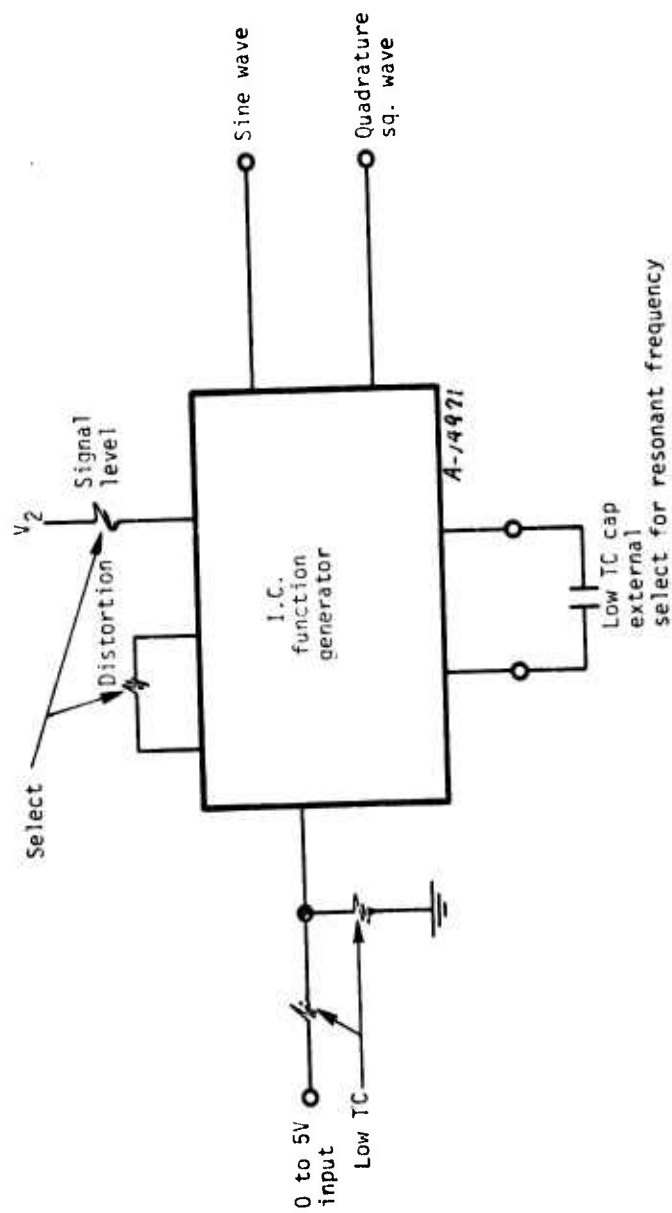


Figure 6. Voltage controlled oscillator.

sinewave distortion and to adjust the sinewave output to the appropriate amplitude. In addition to the sinewave output, the function generator has a squarewave output which is at 90° phase to the sinewave. This squarewave is used in the lock detector to be described later.

- g. Power Amplifier — The power amplifier consists of a high slew rate amplifier coupled to a power gain stage. The power transistors are external to the potted module and are heat sunk to the aluminum chassis. Power is supplied to the output directly from the battery, since high currents required to drive the crystal would result in a large power loss if supplied through the regulated supply. The power stage is designed to operate with peak voltages as close as possible to the power supply rails to minimize power consumption. A power transformer steps up the voltage from the power stage to the crystal in order to provide as large a driving force as possible. The turns ratio is dependent upon the size of the crystal used. Since the crystal is a capacitive load, the transformer reflects a load to the power stage which has a capacitive value equal to the turns ratio of the transformer squared, times the capacitance of the crystal. This reflected capacitance results in a power dissipation in the power stage which is expressed by:

$$P = \frac{VI}{\pi}$$

where V is the battery voltage and I is the peak output current into a capacitive load. Of course, I increases with capacitance and with frequency. The power stage is designed to handle about 1 amp into the transformer input, resulting in about 8.9 watts power dissipation. If the maximum frequency is 50 kHz and the peak output voltage is 12 volts (half the minimum supply voltage) then the reflected capacitance can be calculated to be 0.26 microfarad maximum. Thus, if a transmitter crystal selected has a total capacitance of 0.0026 microfarad, the maximum turns ratio is 10 and the output voltage to the transmitter is 120 volts peak, or 85 volts rms. Although the transformer design was never finalized, it was anticipated to be wound on a ferrite toroid of about 0.8-inch diameter. The power amplifier has an additional input provided so that when dual mode operation is desired the second VCO can be summed in. (Shown grounded in Figure 7.)

- h. Lock Detector — The lock detector circuit (Figure 8) is a synchronous demodulator and filter which used the squarewave output from the VCO to demodulate the input signal. The filter thus contains a DC level which corresponds to the magnitude of the phase component

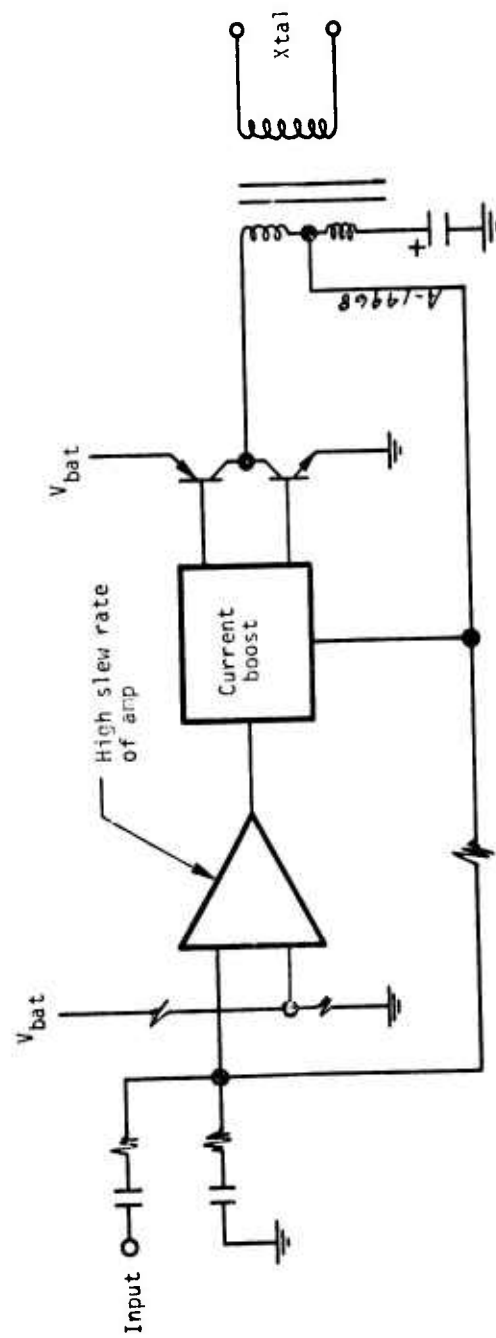


Figure 7. Power amplifier.

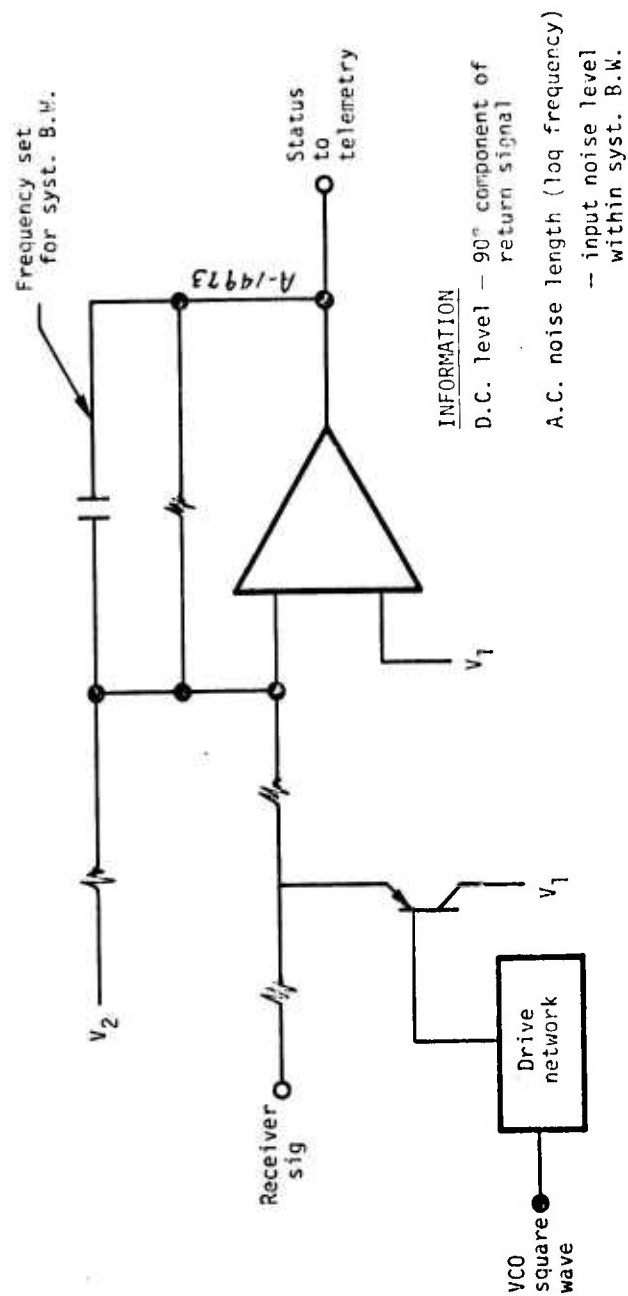


Figure 8. Lock detector.

of the received signal. Since the squarewave is in quadrature with the VCO sinewave signal, the lock detector responds to the 90° component of the input signal with respect to the crystal drive signal. Thus, a good resonance producing a strong quadrature component produces a large DC output. It is admittedly difficult to determine, considering that the strength of a resonance may vary during the conditions incurred during flight, at just what level indicated that lock is maintained. However, the lock detector can provide additional information to help interpret flight data from the recession gage. In addition, the lock detector will contain an AC noise signal which is proportional to the noise encountered within the bandwidth of the phase lock loop. Thus if the loop is overcome by acoustic noise, the lock detector will provide that information.

- i. Noise Detector — The noise detector is designed to measure the high frequency noise encountered during flight. Since the input signal contains the recession gage signal as well as the noise, the recession gage signal must be removed. This is the purpose of the bandpass filter at the noise detector input (see Figure 9). The design center for this filter was selected as 300 kHz, although any appropriate frequency within the response of the receiver transducer may be selected. The output from this filter is rectified and the DC component recovered with a low pass filter. Since the noise level could have a large dynamic range which is essentially unknown before flight, it was decided that a logarithmic output response was desired. Thus the rectified output is fed through a logarithmic amplifier and a level shifter to condition the signal to telemetry levels.
- j. Packaging — In order to meet the high shock and vibration environment, the electronics are packaged in six potted modules (welded cordwood construction) which are inserted into holes in an aluminum housing (see Figure 10). Transistors dissipating large power are attached directly to the aluminum housing. The module interconnects are soldered wires. External components which are selected to adapt to a specific nosetip are soldered to the module terminals. These interconnects and external components are potted in place before attaching the lid.

Figure 11 shows how the system is partitioned into modules and what external parts are required.

The electronics for a dual mode gage may be assembled by adding an additional phase and lock detector module and an integrator and VCO module. The interconnects between the two modules are identical, and the phase detectors share the same input. The output of the second VCO is attached to the unused input on the power amplifier.

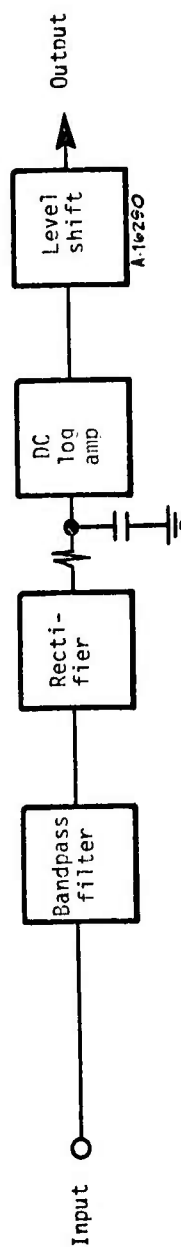


Figure 9. Noise detector.

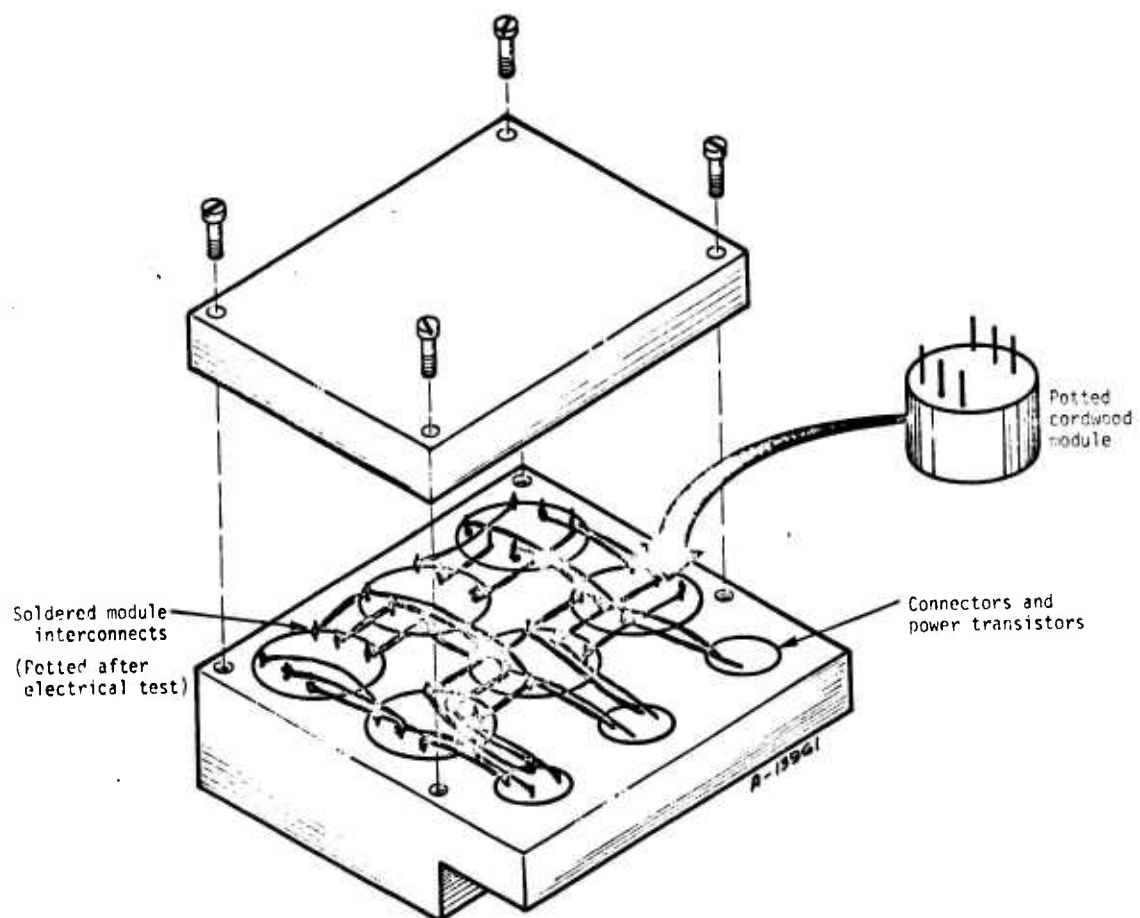


Figure 10. Package.

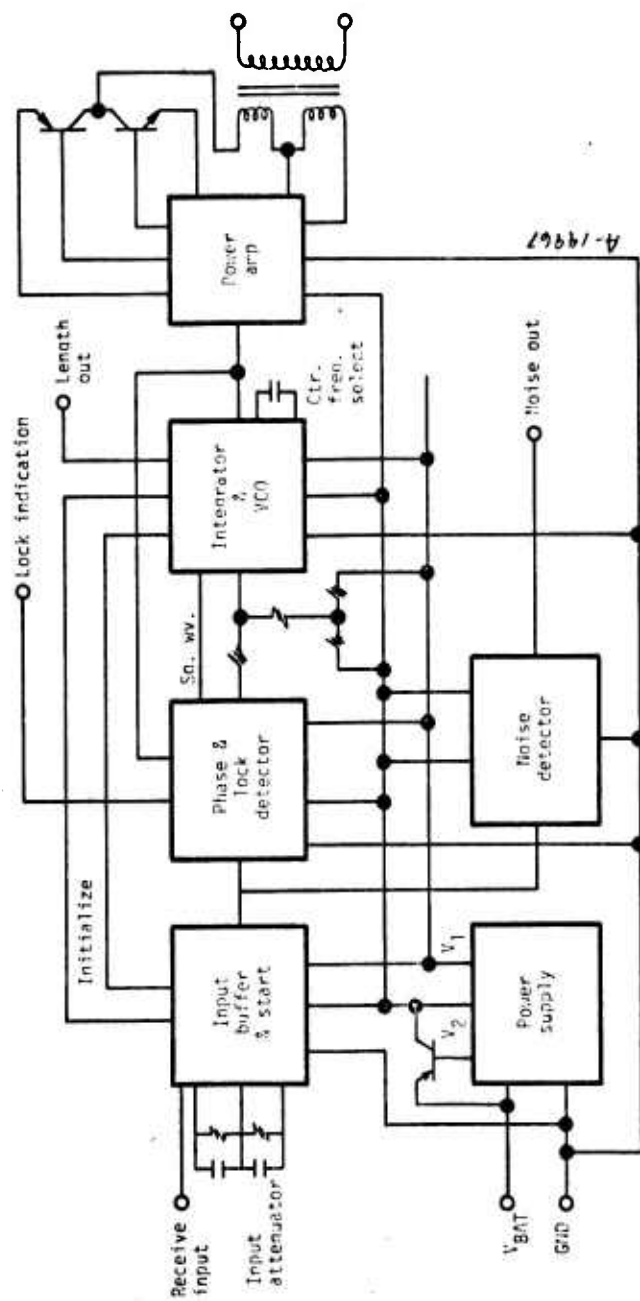


Figure 11. System interconnects.

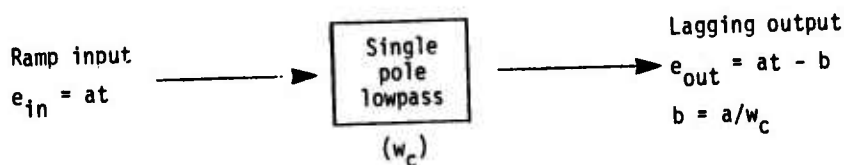
3.1.3 Performance

Accuracy – The error in the recession measurement due to the electronics is small compared to errors from various mechanical effects (such as heating). Table 1 lists the major error sources and the contribution to system error. The largest error source is the system lag, which is the amount the system falls behind a quickly recessing nosetip.

Frequency Response and Noise Rejection – The loop response for a typical loop response is shown in Figure 12. The response is a single pole rolloff beyond unity gain, thus assuring loop stability. The unity gain frequency is determined by the filter cutoff frequency in conjunction with the return signal level and phase comparator gain. Changing signal level in flight can change the loop response. The model lag, which does not affect loop response for this case, is determined by the model resonant bandwidth.

The unity gain cutoff frequency is chosen as a trade-off between noise rejection and speed of tracking. The minimum 28-Hz cutoff frequency was chosen as follows:

Required System Bandwidth



Assumptions: Starting resonant frequency 20 kHz
Ending resonant frequency 40 kHz
Time of event 4 sec

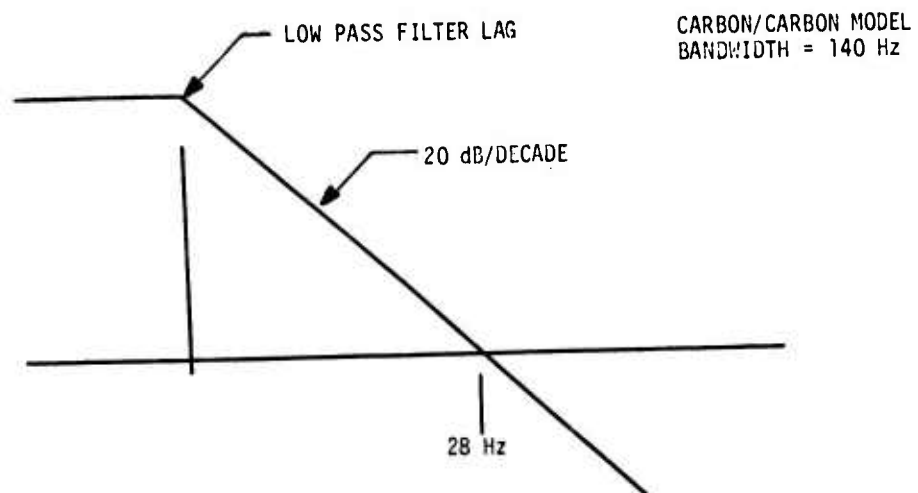
Requirement: Slew rate $\geq 5,000$ Hz/sec
Max lag ≥ 28 Hz*
 $w_c = 5,000/28 = 178$ rad/sec
 $F_c = 28$ Hz

Experiments have shown that the system can operate with a signal-to-noise ratio of 2.5 to 1 (noise being within the bandwidth of the system). Further experiments have indicated that the acoustic recession signal at nosetip resonance is as high as 30 g's rms. Thus the system could operate with about 12 g's rms of noise within the 28-Hz bandwidth. This represents a noise density of $2.27 \text{ g}/\sqrt{\text{Hz}}$, or a total noise of 1,200 g's in the 300-kHz bandwidth. Unfortunately, that much noise would saturate the input stage. The input amplifier is scaled to

* Model bandwidth 140 kHz, follow within 0.2 bandwidth.

TABLE 1. ACCURACY

Error Source	Contribution
Phase Detector — Static Error	0.03%
System Lag	0.13%
VCO Drift	0.10%
Capacitor Drift	0.05%
Resistor Drift	0.05%
	<u>RSS Total = 0.18%</u>
Assumptions: Model Q = 140	
Temperature Drift = 20°C	



TYPICAL LOOP RESPONSE (USED AT 50 MW)

Figure 12. Loop response.

accept a total noise signal five times the basic recession gage signal, or about 150 g's rms.

3.1.4 Application

Various nosetip lengths, shapes, and materials will result in differing nosetip initial resonant frequencies, bandwidths, and receiver signal strengths. In addition, various flight profiles may result in various recession rates and noise levels. It is therefore desirable to customize each unit to optimize the above parameters for the particular flight.

Each of the potted modules may be built far in advance, along with the housing and hardware. The unit can then be customized at final assembly by selection of a few components mounted external to the modules. A summary of the steps in customizing follows below.

Final Assembly Procedure

1. Insert fully tested, potted modules into housing
2. Wire interconnects, power transistors, EMI filtering, etc.
3. Temporarily install "custom" components
4. Perform functional test
5. Store this assembly until nosetip is known

Adapting Electronics to Specific Nosetip

1. The following nosetip/mission parameters must be known (Column 1). The electronic circuit parameter in Column 2 may then be calculated. The circuit parameter is then fixed by the selection of a passive component (resistor or capacitor).

<u>Nosetip Parameter</u>	<u>Circuit Parameter</u>
Resonant frequency	VCO center frequency
Receiver signal level	Input buffer gain
Maximum recession rate	Loop frequency response search speed
Nosetip bandwidth	Integrator time constant

2. Attach selected components
3. Perform functional test
4. Apply potting, lip
5. Acceptance testing

The calculation of values, final assembly, testing, and potting would take about 3 days. The time required for acceptance testing would depend on the requirements of the procuring agency.

3.1.5 Reliability

In order to assure a high reliability, a program was in progress in accordance with a program plan previously published (Reference 1). This plan defined the standard parts to be used, how the parts are to be applied, and the procedures for approval of nonstandard parts. In addition, various parts screening was called out. Tables 2 and 3 give a summary of the standard parts used, and

TABLE 2. STANDARD PARTS USED (PASSIVE)

Mil Designator	Mil Spec	Type	Qty
RCR07	MIL-R-39008	Resistor, Carbon	10
RNR55K	MIL-R-55182	Resistor, Metal Film	54
RNR55J	MIL-R-55182	Resistor, Metal Film (25 ppm)	4
RWR81	MIL-R-39007	Resistor, Power Wirewound	2
CKR05	MIL-C-39014	Capacitor, Ceramic	21
CSR13	MIL-C-39003	Capacitor, Solid Tantalum	8
CLR65	MIL-C-39006	Capacitor, Sintered Anode, Tant	3

TABLE 3. STANDARD PARTS USED (ACTIVE)

Part No.	Description	Quantity
2N2907A	Transistor, PNP, Low Power	3
2N2920	Transistor, NPN, Dual	1
2N2945A	Transistor, PNP, Chopper	4
2N3501	Transistor, NPN, Low Power	2
2N3637	Transistor, PNP, Low Power	2
2N3792	Transistor, PNP, High Power	2
1N4148	Diode, Signal	15
MA723	Voltage Regulator	1

Table 4 lists the nonstandard parts. In addition, complete parts lists and nonstandard parts approval requests are included in the documentation portion of this report.

3.1.6 Test Electronics

A set of test electronics was built for use in bench experiments and ground tests. This test box was built long before the flight electronics, and since the object was to prove the theory, the electronics was optimized for convenience and not for flight. However, functionally it performs the same as the flight electronics, but has additional features. It also contains the electronics for dual mode, which was successfully demonstrated on the bench. A schematic of the test electronics is included in the documentation section. Figure 13, shows a typical test setup for a 50 MW test using flight electronics. (This was for a single mode test, although a dual mode test would be similar.) Note, that since the nosetip is located 300 feet from the electronics, additional line drivers and receivers have been added. Also, the power amplifier must be located at the sting, since a large amount of power would be required to drive a transmission line at crystal voltage levels.

3.2 MECHANICAL HARDWARE DEVELOPMENT

For the design phase of the hardware development, design limitations were based upon the available packaging envelope for nosetip instrumentation on plug type nosetips intended for a vehicle such as an MSV. For this case, the maximum practical diameter for such instrumentation packages was 1.10 inches and approximately 3 to 4 inches long. It has been assumed that peripheral equipment such as the electronics could be located elsewhere in the vehicle body. The nosetip instrumentation consists of signal transducers, attachment components, signal cable connections and packaging; all located at the nosetip base.

The in-flight environmental conditions were subsequently defined by analyzing recent MSV flight histories. Of major concern during a flight, especially a weather flight, are nosetip base vibrations due to particle impingement. Past flights have revealed base temperatures of up to 500°F, vibration levels of 1,200 g's, shocks to 220 g's, and static accelerations to 25 g's. The nosetip instrumentation from this program is designed to withstand even greater extremes of temperature, vibration, shock and static acceleration (as outlined in the Minuteman II environmental specifications). Noting contract requirements and the above flight characterization, a system design lifetime can be defined as that associated with the following environmental exposure combinations:

1. Qualification tests
2. Acceptance tests and arc jet simulation tests
3. Acceptance tests and one flight (powered and reentry)

TABLE 4. NONSTANDARD PARTS USED

Part No.	Description	NSPAR	Qualification Required?		Qty
			Yes	No	
AD532SH	Multiplier (IC)	002		X	1
HA9-2510-8	Op Amp, High Slew	003		X	3
LM108	Op Amp, High Impedance	004		X	2
CYR41	Capacitor, Porcelain	005		X	1
2N5038	Transistor, NPN, High Power	006		X	1
XR2206M	Function Generator	007	X		1
None	Transformer	008	X		1
Not Identified	Logarithmic Amp	--		X	1
Not Identified	Connector, Co-Axial	--		X	2
Not Identified	Connector, System Interface	--		X	1

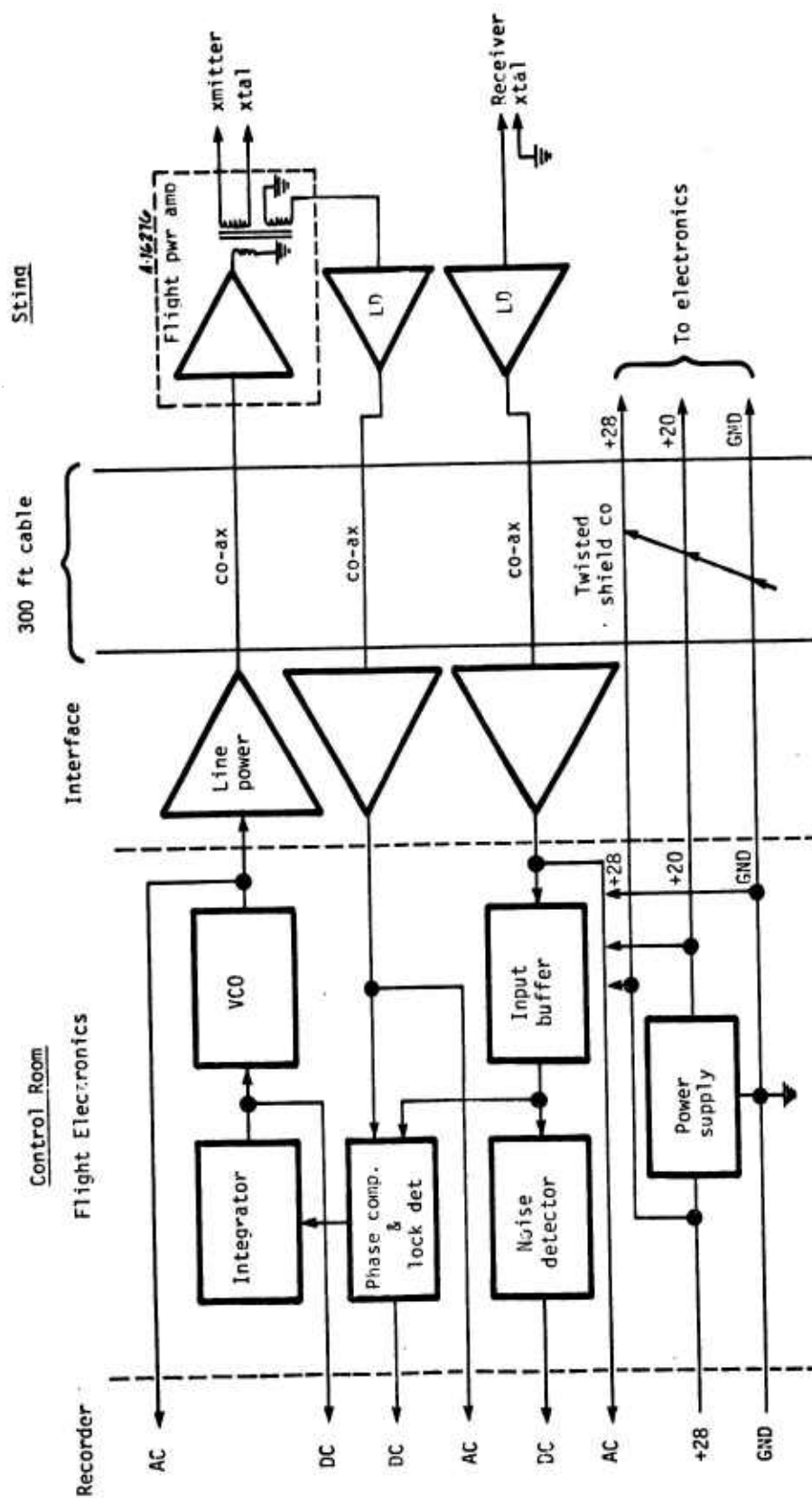


Figure 13. 50 MW single mode test using flight electronics.

The worst case loading situation is realized during acceptance tests and the arc jet simulation tests. Consequently, a design lifetime will consist of approximately 2.5 million stress reversal cycles at essentially a maximum 1,200-g rms stress level. This load characterization is a combination of axial and lateral loads experienced by the nosetip during exposure in the environment outlined above.

In the development of the acoustic gage as a measurement system, several areas of design must be addressed:

- Acoustic performance
- Structural considerations
- Thermal effects
- System packaging

Baseline acoustic performance had been demonstrated in previous work through bench and arc jet testing. The general conclusions were that more vibrations input to the nosetip are desirable to adequately track typical recession rates; the currently used receiver crystals were adequate and the general gage configuration excited the compressional mode of nosetip vibration as expected. The next step was to modify the ARG to withstand the environmental loads imposed without adversely affecting acoustic performance. This design modification also accounted for stresses induced by the thermal conditions to which the ARG system must be exposed. Ultimately, a flight qualified system package was sought to house the ARG.

Since feasibility was demonstrated using discrete vibration sensors, this general approach was again followed. Individual transmitter and receiver transducers constructed with piezoelectric crystals were employed; however, different configurations were considered. Two modes of nosetip vibration, single compressional mode and dual flexural mode were investigated. These two different modes of vibration are excited simply by locating the transmitter and receiver crystals at different orientations to the nosetip axis of symmetry. Three compressional configurations were conceptually evaluated: axial concentric transmitter and receiver, Figure 14, central transmitter with single or multiple eccentric receivers, Dwgs. #7141-080 and #7141-083, and a central receiver with single or multiple eccentric transmitters. Multiple transmitters were considered because of the need to increase vibration energy input to the nosetip; multiple receivers were considered due to the need for mass distribution radially to minimize excitation of flexural modes because of imbalance.

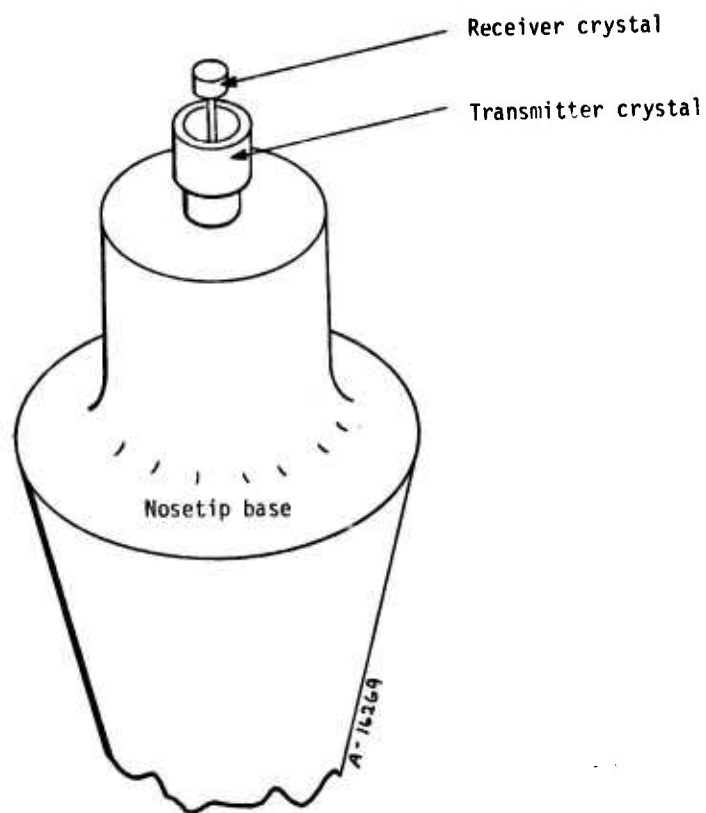


Figure 14. Concentric transmitter/receiver.

Three basic flexural configurations were also investigated: laterally opposing concentric transmitter and receiver, Dwg. #7141-064, lateral in-line transmitter and receiver, Figure 15, and axial eccentric transmitter and receivers, Dwgs. #7141-081, -082, and -099. Again these arrangements were built up of the individual sensor components, transmitters and receivers. These components are described in detail along with gage attachment and system packaging.

3.2.1 Sensor Construction

Since discrete components were to be employed, the individual sensors were analyzed in detail. The design goal was to boost transmitter output power to the nosetip and address the structural aspects of transmitter placement and support. The receiver acoustic performance, demonstrated to be sufficient in previous work, was analyzed for placement relative to the transmitter and structural support. Also, ways to miniaturize the receiver were investigated to allow more freedom in overall ARG configuration. The following basic design elements were considered:

1. Transducer construction optimization (transmitter, receivers)
2. Attachment to nosetip
3. System packaging

Individual components were studied to determine trade-offs between improvements in acoustic performance and structural weaknesses. A major problem faced was avoidance of resonant frequency operation at sensor assembly frequencies which lead to subsequent loss in ability to track the nosetip frequencies. Assembly resonant frequencies were to be in excess of 50 kHz range with 25 kHz being the anticipated nosetip resonance operating range. In light of the thermal environment and space constraints at the base of the typical MSV nosetip, attachment of ARG components is difficult. Directly attaching the piezoelectric crystals to the base where temperatures may briefly exceed 500°F seemed doubtful. System packaging was addressed to provide a means of protecting the ARG during fabrication, testing and installation on the reentry vehicle (a typical system lifetime).

Initially, commercially available accelerometers were thought to be an excellent choice for this application. They are available as packaged units; are flight tested and qualified; yield a broad banded flat response; have very compact geometry; are relatively inexpensive and readily available from several manufacturers. The only disadvantage at the outset was that recommended ranges of operation did not approach the frequency range of 25 kHz, since resonant frequencies of these transducers are quite low. Several models were tested as transmitters with the general conclusion that not enough vibration energy could be delivered to the nosetip; overdriving the accelerometers with higher than rated input power resulted in permanent damage. However, these accelerometers could

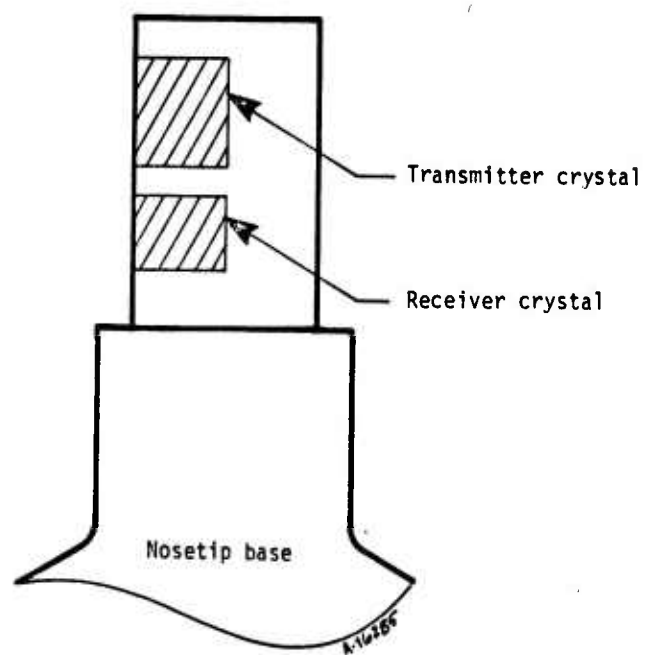


Figure 15. In-line flexural transmitter and receiver.

potentially be used as receivers if the nonlinear response near resonance could be cancelled out. A receiver crystal was fabricated (Dwg. #7141-079) and used for baseline comparison with the commercial accelerometers. Development of this particular design yielded significantly higher sensitivity and greater output signal; however, with a much lower resonant frequency. The natural frequency of this assembly was lower than 8 kHz, but no harmonics could be detected at higher frequencies which might degrade receiver performance. This receiver design was chosen because of the high output signal, acceptable frequency response and extremely compact size. Commercially available accelerometers tested were compared with the model and yielded reduced signal response with a given nosetip vibration input. Since improved receiver performance was obtainable, commercial accelerometers were eliminated entirely from the ARG system.

A prototype acoustic gage system in which a transmitter and receiver crystal were mounted within a single housing was fabricated for use in this program, Figure 16. Acoustic performance was poor with no significant difference in receiver crystal output signal whether attached or not to a bench test model nosetip. It was concluded that the receiver crystal was directly coupled acoustically to the transmitter crystal with no response to the nosetip.

Subsequently, the ARG components were examined and an optimization process begun with material selection and basic geometry definitions.

3.2.2 Crystal Study

Since previous work at Acurex dictated the use of piezoelectric transducers, only this type of crystal material was considered.

Table 5 lists some common piezoelectric materials with electrical and mechanical properties important for vibration transducer design. Initially, PZT-5 crystal material was chosen, primarily because of superior performance due to high values of electromechanical coupling coefficient, h_{33} , the dielectric constant and piezoelectric modulus, d_{33} ; and also a low value of the piezoelectric pressure constant, g_{33} , is desirable. This combination of parameters allows for large electrical energy storage in the crystal with subsequently high conversion to mechanical vibration, thus affecting maximum vibration energy input to the nosetip. Practical transducer design principles favored use of PZT-4 material because of greater material strength. Testing revealed no significant acoustic performance gain with PZT-5, as material properties would indicate, but revealed the loss in material strength. It was decided that the strength advantage of PZT-4 outweighed any acoustic performance differences. Both types of crystals have continuous operating temperature limits of at least the temperatures experienced at the nosetip backface during flight (Figure 17). Since exposure to this temperature range is extremely brief, crystal performance reduction would not be expected.

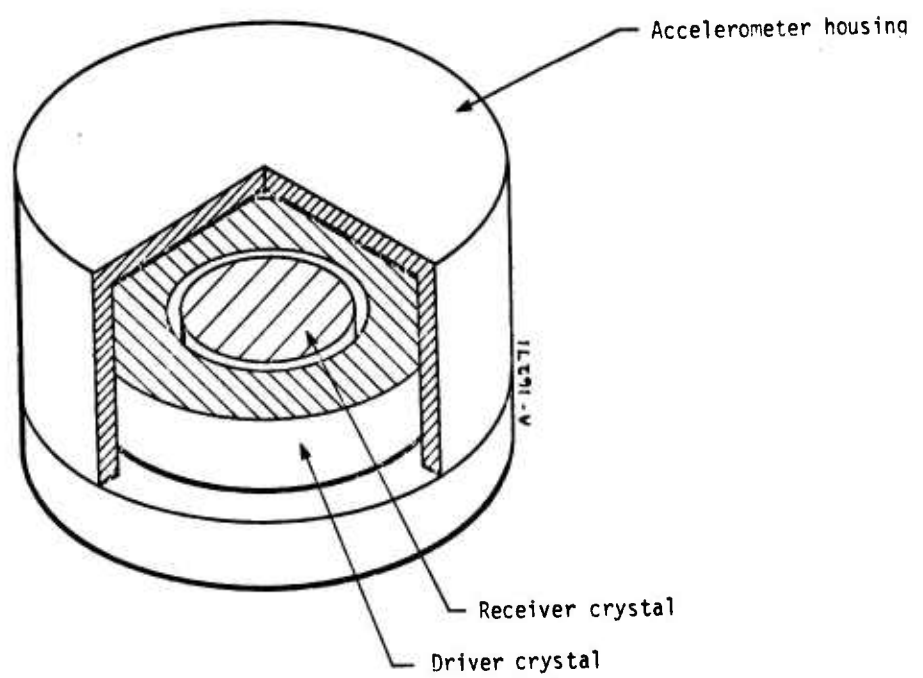


Figure 16. Prototype accelerometer.

TABLE 5. PHYSICAL PROPERTIES OF PIEZOELECTRIC MATERIALS

	Quartz	Lithium Sulfate	Barium Titanate	PZT-4	PZT-5	Lead Methacrylate
Density (lbm/in ³)	0.096	0.074	0.199	0.270	0.274	0.209
Maximum Operating Temperature (°C)	550	75	110	250	290	250
Dielectric Constant	4.5	10.3	1,250	1,300	1,750	225
Electromechanical Coupling Coefficient, k_{33}	0.1	0.4	0.46	0.68	0.71	0.42
Piezoelectric Modulus, d_{33} (10 ⁻¹² m/v)	2	16	145	280	380	85
Piezoelectric Pressure Constant, g_{33} [10 ⁻³ (V/m)/(N/m ²)]	58	175	13.1	25	25	42.5
Tensile Modulus (10 ⁶ psi)	11.6	--	17.1	11.8	7.8	4.2
Dynamic Tensile Strength (psi)	--	--	3,000	6,000	4,000	--
Bulk Acoustic Impedance (10 ⁵ lbm/ft ² sec)	29.9	--	52.2	50.5	41.4	26.5

T-140

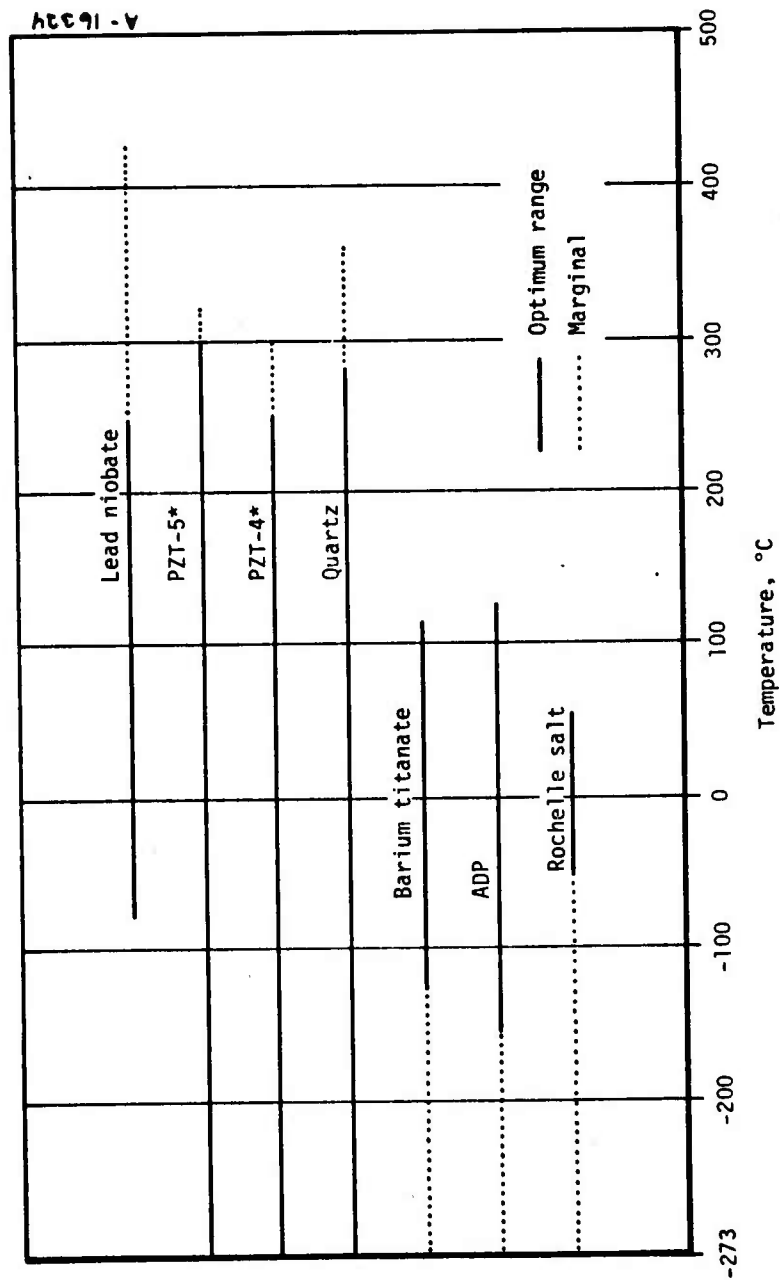


Figure 17. Useful temperature range of various piezoelectric materials.

One design goal throughout was to avoid component and system resonance of the ARG to provide flat response through the frequency range of operation. Both PZT-4 and PZT-5 work quite well in this respect because crystal dimensions were likely to be much less than 1 inch in thickness in the direction of vibration and resonant frequencies of such crystals would exceed several hundred kHz. Crystal orientation was well demonstrated in previous work at Acurex on the ARG and evolved with a "33" arrangement, namely, that crystal polarization and deflection are in the same direction. Such configurations are shown in Figure 18 for cylindrical, tubular, and wafer crystals. Initially it was felt that less complicated designs could result with use of such parallel, longitudinal crystals rather than shear types. The dish and tubular types were selected first to determine which shape and what general size crystal was required to generate enough vibrational excitation of the nostips. Bench tests were initiated to cover the spectrum of sizes selected for starting.

The following table covers the range of dimensions:

Diameter	Thickness			
	0.100"	1/8"	1/4"	5/8"
1/8" disk		X	X	
1/4" disk	X		X	X
3/8" disk	X			
1/2" disk, tube	X		X	
5/8" tube			X (1/8" wall)	
3/4" tube			X (1/8" wall)	

A small test rig was fabricated to house these crystals by mechanically clamping each between electrodes and mounting them to an aluminum nosetip simulating a MSV type nosetip, Figure 19. Previous work established good correlation between nosetip shape/length and resonant frequency; to facilitate bench testing turnaround time, test models were fabricated of 2024 T3 aluminum rather than carbon/carbon composite materials. Also, the bulk acoustic impedance of aluminum alloys is quite close to that of 2,2,3 carbon/carbon, thus aluminum is a reasonable simulation of an acoustic load to test acoustic drivers. Results of this work are discussed in Section 4.1. In short, acoustic performance seemed to track well with thin crystals of larger diameter; the amount of vibration energy output was proportional to crystal diameter. Consequently, disk and tubular crystals of 1/2-inch diameter and 0.100-inch thickness were tentatively chosen; these crystals also allowed a compact transducer design. Tubular crystals look attractive because the central hole allows freedom in housing and mechanical

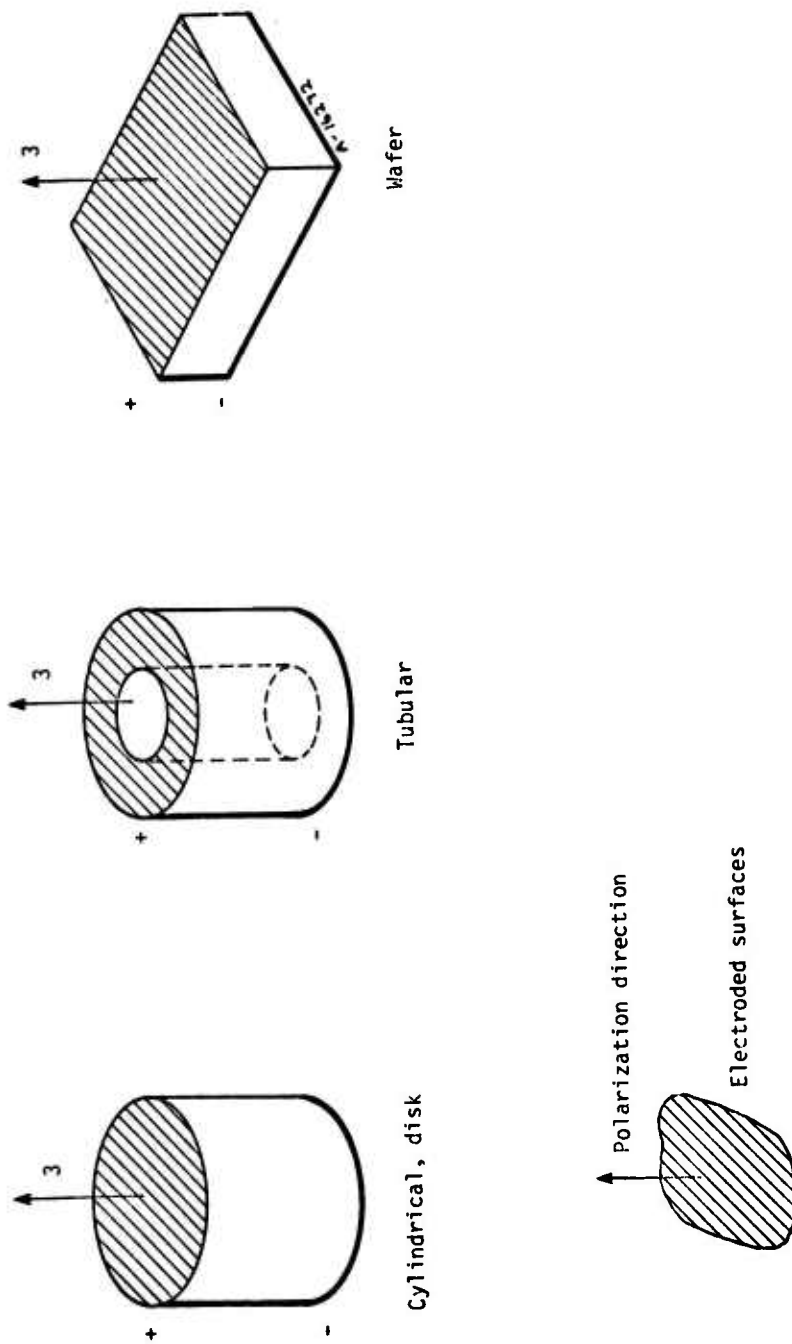


Figure 18. Desired piezoelectric crystal shapes.

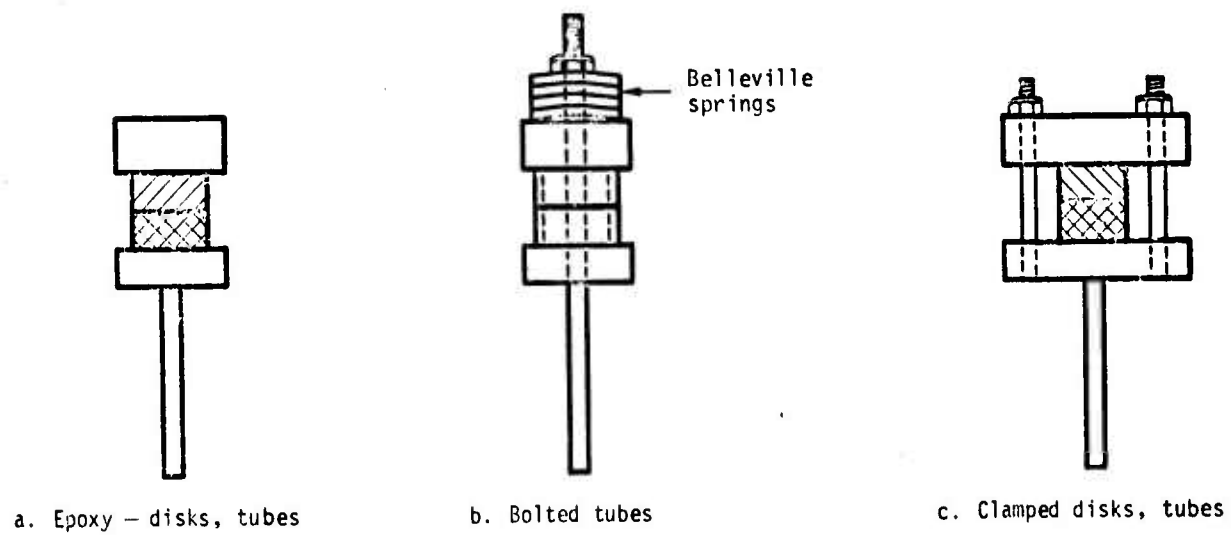


Figure 19. Crystal test fixtures.

attachment to a load, with a concentric bolt. The disk crystals were retained for design simplicity. Figure 20 indicates results on how the crystals should be housed with peripheral components; acoustic performance appears to be better for attachment with conductive epoxy (Ablebond 36-2 in this case) rather than mechanical clamping. Additionally, the mechanical clamping arrangements tended to degrade performance in that multiple components caused spurious vibration modes due to the complexity of the hardware; the number of interfaces increased reflections and back scattering causing a reduction in vibration energy being transmitted into the nosetip. Clearly, the design goal of reducing the number of components involved in the transducer construction is evident. Also, to get good acoustic energy transmission, the crystal must be tightly clamped to the load. During bench testing (in a setup as in Figure 20) the crystal output increased as the clamping pressure approached 3,000 psi; however, almost every crystal fractured at this clamping pressure. Crystals which were epoxy bonded gave better output performance with no clamping and exhibited no fracture failures.

3.2.3 Transmitter and Receiver Construction

The degree of nosetip excitation depends upon how the crystal output is coupled to the load, the nosetip. Both single and multiple crystals in a bimorph configuration, and epoxy bonded and mechanically clamped crystals were evaluated. Adequate nosetip vibration was achieved using a bonded, dual crystal bimorph similar to the design in Figure 19(a) and Dwg. #7141-065. Epoxy bonding allowed an acoustically clean design without bolts, springs, or awkward clamping dishes as in Figures 19(b) and 19(c). The thin (0.100-inch thickness) crystals yielded a very compact arrangement with strong acoustic output.

Conventional transducer design practice was used as a guide for the general approach of the transducer design. For this application some degree of directional acoustic transmission is desirable. To drive the nosetip, ideally the end of the transmitter must be firmly clamped to a rigid, nonabsorbing support, or one of high inertia with poor acoustic transmission. Practical design dictates that there be some physical interface between the crystals and the nosetip, with nonabsorbing and very high acoustic transmission capability.

A material search was undertaken to determine suitable candidate materials for such acoustic reflectors and transmitters; Table 6 is a listing of common materials of construction. By noting that the acoustic load in this application is the nosetip mode of carbon/carbon 2,2,3 and the crystal transmitter material selected was PZT-4, impedance matching considerations indicate clear material preferences. Spatially fixing the back side of the crystal is affected by a gross impedance



Figure 20. Crystal clamping.

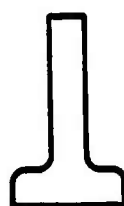
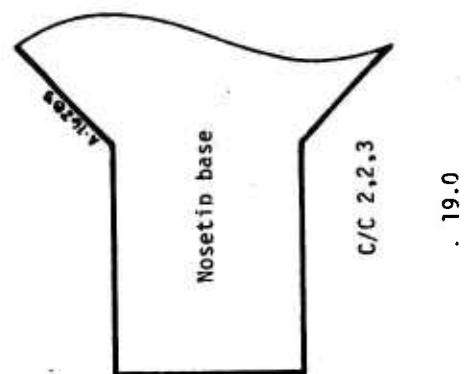
TABLE 6. ACOUSTIC IMPEDANCE OF VARIOUS MATERIALS

Material	Density (lbm/in ³)	Tensile Modulus (x 10 ⁶ psi)	Acoustic Impedance (x 10 ³ lbm/in ² sec)
C/C 2,2,2	0.067	13.9	19.0
PZT-4 Crystal	0.270	11.8	35.1
PZT-5 Crystal	0.274	7.8	28.8
Alumina	0.139	50	51.8
Aluminum 7075	0.101	10.4	20.1
Brass	0.304	15.0	42.0
Cast Iron (malleable)	0.266	26.5	52.2
Copper	0.323	17.0	46.1
Lead	0.410	2.0	17.8
Magnesium	0.064	6.5	12.7
Molybdenum	0.370	47.0	82.0
Nickel	0.321	30.0	61.0
Steel, Mild Carbon	0.283	30.0	57.3
Steel, Stainless	0.290	28.0	56.0
Titanium Alloy	0.160	16.5	31.9
Tungsten, Alloy	0.650	45.0	106.2

mismatch with a material such as tungsten. Good acoustic transmission into the nosetip is favored by connecting with a material with an impedance midway between that of the crystal material and the nosetip, namely aluminum or titanium. In light of material availability and fabricability, aluminum was chosen (Figure 21). A range of aluminum alloys was considered with the primary emphasis on fatigue strength and acoustic impedance, Table 7. Aluminum alloy 7075-T6 was chosen for highly stressed members and 2024-T3 for other components.

In general, the component geometry is a major factor in transmission; optimum transmission occurs in an intermediate medium of a thickness equal to one-quarter wavelength. In this application the frequency range of operation was anticipated to be on the order of 25 kHz; one-quarter wavelength in aluminum is approximately 2.0 inches, 1.8 inches in tungsten. However, bending stresses in a cantilevered beam due to lateral body vibration are proportional to the square of beam length. Therefore, waveguide length was varied during bench testing to determine a performance-structural trade-off. Also, the waveguide (crystal-nosetip interface medium) cross sectional profile was thought to affect acoustic performance. Figure 22 illustrates some of the waveguide shapes investigated. Since all were of the same length only the shape was varied with the performance differences resulting shown in Figure 23. The waveguide with highest acoustic performance also compared favorably from a structural standpoint. A large cross sectional area at the waveguide base, the location of the greatest bending moments of a cantilevered beam, would reduce bending stresses. The same criteria were used to size the tungsten backmass. This is important because of the high density and large moment area of this component. Bench testing revealed that a backmass of thickness comparable to that of the piezoelectric crystals was suitable. Dwg. #7141-065 illustrates the transmitter design resulting from the above considerations. The waveguide was sized primarily for a permissible stress level to provide a fatigue life of approximately 2.5 million bending stress reversal cycles. The results of the crystal study comparison suggested use of the PZT-4 crystal of 0.500-inch diameter and 0.100-inch thickness. The tungsten backmass is also 0.500-inch diameter and 0.100-inch thickness. The entire assembly is bonded together with a silver-filled, electrically conductive epoxy. The crystals are arranged in a bimorph (and thus expand outward in unison) configuration requiring a copper foil electrode on which to solder one of the input signal leads; the other signal lead is attached to the tungsten backmass and the aluminum waveguide. The entire assembly is then enclosed with heat skirt tubing to contain the delicate wiring.

As mentioned above, the design objective of receiver crystal modifications was to maintain vibration signal sensitivity while striving for miniaturization. Clearly for the compressional mode ARG with single transmitter and dual receivers, Dwg. #7141-065, savings in receiver diameter



Waveguide pedestal

7075 aluminum

20.1



Piezoelectric crystal

PZT-5

28.8



Backmass

Tungsten

106.2

Material:

Acoustic impedance:

Figure 21. Transmitter construction.

TABLE 7. MATERIAL PROPERTIES

Aluminum Alloy #	Machinability	Tensile Str (psi)	Shear Str (psi)	Endurance Limit (psi)	Tensile Modulus (psi)	Density (lbm/in ³)	Acoustic Impedance (lbm/in ² sec)
2014 (T4)	A	62,000	38,000	20,000	10.6 x 10 ⁶	0.101	20.3
2024 (T3)	A	70,000	41,000	20,000	10.6 x 10 ⁶	0.100	20.2
5052 (H38)	C	42,000	24,000	20,000	10.2 x 10 ⁶	0.097	19.6
5056 (H38)	C	60,000	32,000	22,000	10.3 x 10 ⁶	0.095	19.4
5090 (H38)	D	69,000	40,000	22,000	10.3 x 10 ⁶	0.095	19.4
5154 (H38)	D	48,000	28,000	21,000	10.2 x 10 ⁶	0.096	19.5
6061 (T6)	B	45,000	30,000	14,000	10.0 x 10 ⁶	0.098	19.5
7075 (T6)	A	83,000	48,000	23,000	10.4 x 10 ⁶	0.101	20.1
7079 (T6)	A	78,000	45,000	23,000	10.3 x 10 ⁶	0.099	19.8
7049 (T73)	A	72,000	48,000	23,000	10.2 x 10 ⁶	0.102	20.1

T-141

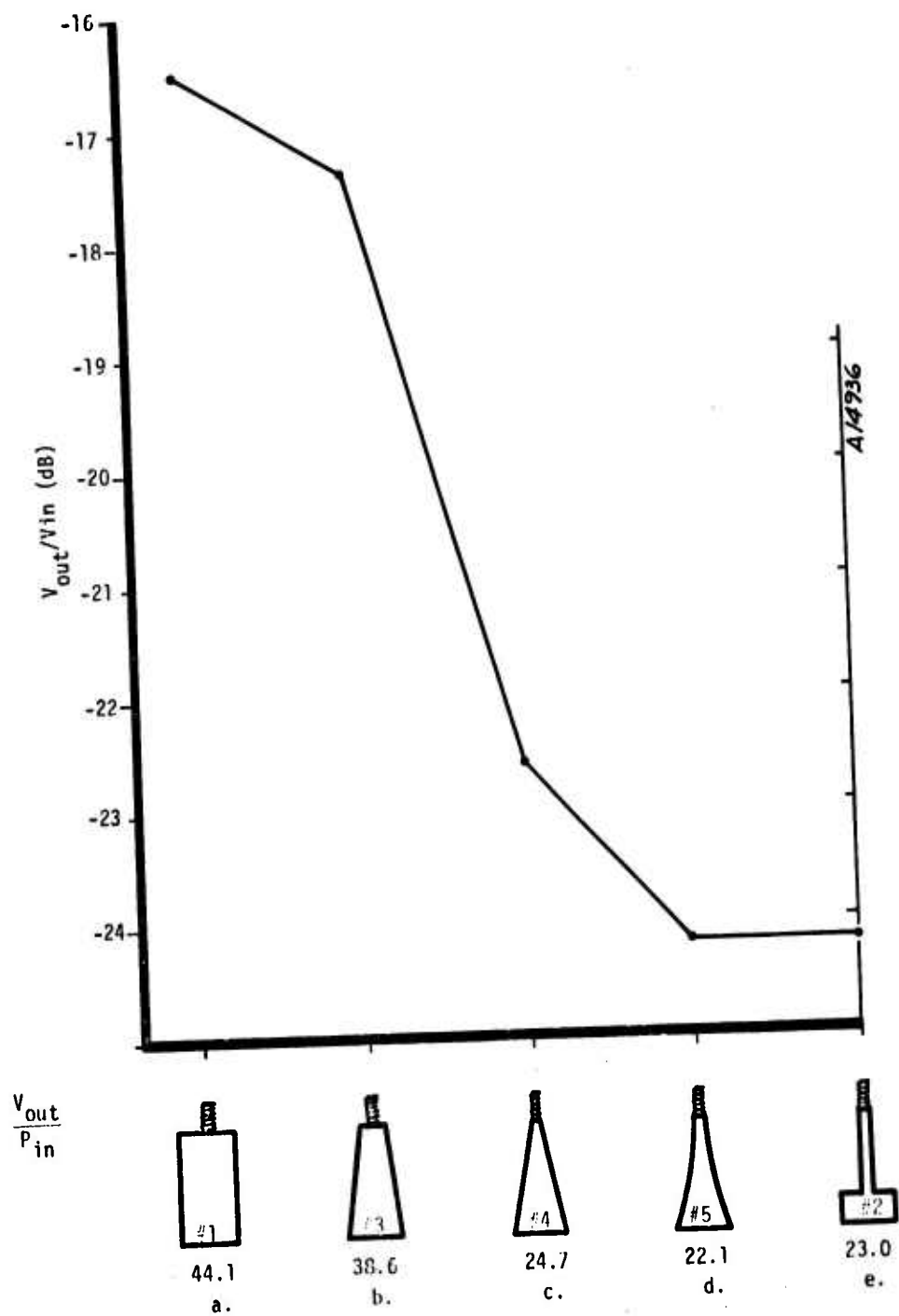


Figure 22. Waveguide performance.

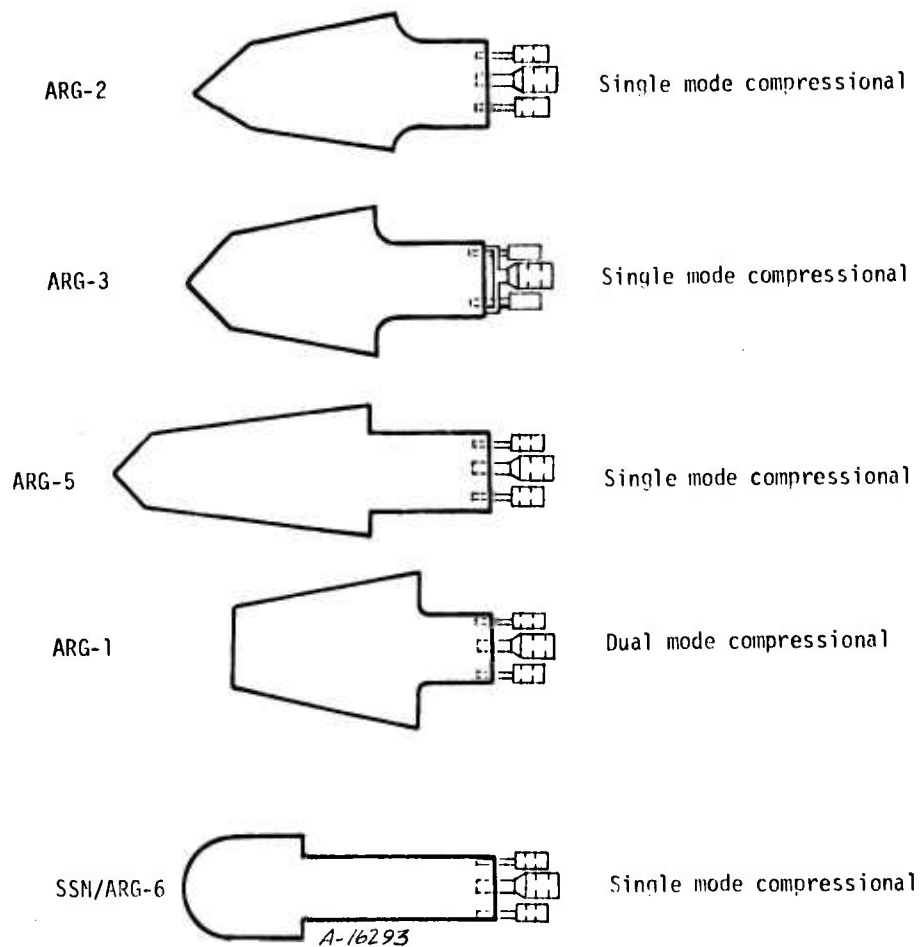


Figure 23. 50 MW test models.

or height reflect on length and diameter of the waveguide and hence, the load carrying capacity. Especially critical in this particular design, is the dimension tolerancing which is close in order to provide a minimum radius fillet at the waveguide base to reduce the local stress concentration. Details of the receiver assembly are shown in Dwg. #7141-079.

3.2.4 Gage Attachment

Several methods of attaching the ARG components to the nosetip base were investigated: screw threads, epoxy bonding and press fits. Press fits of an aluminum shaft (waveguide or receiver base) into carbon/carbon materials resulted in worsening the already high stress field due to relative thermal expansion during heatup. Epoxy bonding these components (with flat bottom surfaces) to a base plate (Dwgs. #7141-065 and #7141-063) which in turn was bonded to the nosetip base resulted in a packaged unit. However, several shortcomings were identified: acoustic performance with the added base plate deteriorated significantly and in spite of the high strength bonding provided by the epoxy (FM 400 as supported epoxy made by American Cyanamid), the 2,2,3 carbon/carbon material experienced a delamination of the first X-Y weave layer at relatively low amplitude lateral vibration levels. Subsequently, threaded fasteners were explored because transmitter and receiver loads could be distributed to many X-Y weave layers axially into the nosetip base. A coarse thread series is desirable to achieve full thread engagement with the unit cell of the carbon/carbon matrix. A relatively uniform stress distribution is favored with a very loose thread fit between aluminum and carbon composite materials if an unsupported epoxy is added to supply adhesion and fill the voids at the thread roots. A range of applicable epoxies appears in Table 8. Currently Hysol EA 934, an unsupported epoxy, is used to secure transmitter and receiver assemblies, Dwgs. #7141-080, -083, -081. This particular epoxy also has a relatively low cure temperature with good high temperature strength; cure temperatures are important during fabrication because of potential softening of the solder used to connect the cable assembly to the crystal electrode and backmass, also some weakening of the conductive epoxy used to assemble the crystals may occur.

3.2.5 System Packaging

The issue of encapsulating the ARG within a structural package is important for the following:

- Structural integrity
- Corrosion resistance of fragile components
- Hermetic sealing to prevent moisture condensation
- Handling protection during storage and installation

TABLE 8. ADHESIVE PROPERTIES

Epoxy	Max Temp (°F)	Core Temp (°F)	Tensile Str (psi)	Shear Str @ 77°F (psi)	Fatigue Str (psi)
Ablebond S17a	300	250 (1 hr)	5,000	2,500	800
Ablebond S50	260	300 (2 hrs)	--	6,000	1,000
Ablebond 293-14(EC)	--	260 (1 hr)	--	2,200	--
Scotch Weld 2214	350	225 (2 hrs)	--	2,000	900
FM 96	300	350 (2 hrs)	--	3,647	2,508
FM 460	420	350 (2 hrs)	--	4,010	1,850
FM 1000	180	340 (2 hrs)	--	7,200	3,500
Hysol 956	300	200 (1 hr)	--	2,500	1,000
Hysol EA 934	300	200 (1 hr)	--	3,100	1,000
Loctite 306	300	200 (1 hr)	--	1,800	1,400

600 psi @ 10⁷ cycles
No failures

- RFI shielding of components

The significance of good shielding was demonstrated in previous work; in arc simulation testing the plasma gas stream generates significant RFI noise which is easily received by unshielded signal cables. Dwg. #7141-065 illustrates shielding techniques employed; both receivers are completely sealed within an aluminum case bonded with an electrically conductive epoxy (Ablebond 36-2). This should prevent electrical cross-talk between the transmitter and receivers. To prevent outside noise interference with the transmitter signal, the entire ARG can be housed within an aluminum case again sealed with an electrically conductive epoxy. With this type of packaging the ARG system can be stored safely and applied to a nosetip with a single bonding operation.

3.3 50 MW TEST MODEL DESIGN

Although the 50 MW tests were never performed due to facility difficulties this section describes the hardware which was fabricated for those tests.

3.3.1 Nosetip Configuration

The nosetip material for the four ARG models was 1,1,3 carbon/carbon (c/c) (Billet No. 113-2, Preform No. 1005). The SSN/ARG-6 model was a 2,2,3 c/c with a 3/8-inch diameter TaC integral weave core. All models were subscale, but were designed to provide the maximum size and shape permissible for the stream conditions and testing mode. The four ARG models were flat face or biconic 15° half-angle cone frustums.

All ARG models were exposed to the steady-state, peaked enthalpy profile, high stagnation pressure condition for maximum recession rate. The biconic models were single mode compressional models designed to provide the maximum length change at these conditions for measurement of recession rate only. The flat face nosetip was designed to produce the maximum amount of shape change. This model was operated in the dual compressional mode for both recession rate and shape change information.

A 1.1-inch cylindrical shank was provided at the base of the conic nosetip to simulate expected flight vehicle nosetip shapes. The shank/cone interface provided a contoured attachment shoulder similar to that expected on flight nosetips. By operating the acoustic sensor at the nosetip first compressional mode of vibration, this attachment technique was optimized by placing the nosetip/holder attachment location near a vibration node resulting in minimum signal attenuation.

Two of the three ARG biconic nosetips were identical with the exception of the sensor configuration. The third model was 0.5 inch longer. The intent of the longer nosetip design was to investigate the gage performance through a flexural compressional mode crossover not expected during the length change of the two shorter models.

The SSN/ARG nosetip tested in this series was included to demonstrate the feasibility of the ARG in composite c/c material. The radically different shape, compared with the ARG models, was a result of the large core diameter (3/8 inch) and the preference for both an optimum overall diameter to core diameter ratio and an acoustically "clean" geometry (cylindrical). As in the case of the ARG models, the attachment shoulder was located near the first compressional node.

Due to the size of the model, the ramp mode of testing was employed. The hemispherical tip was utilized to detect transition and to monitor the core/parent material interface during recession.

A summary of the nosetip shapes is given in Figure 23. Detailed drawings of the nosetip are included in Appendix A.

3.3.2 Support Hardware

Each of the five nosetips was preassembled in carbon-phenolic (c-p) model holders which included a heat-treated stainless steel threaded adaptor to mate to the facility strut. Although the impedance mismatch of a copper holder would have been desirable acoustically, the long dwell time required for the desired 3/4 inch of recession warranted the use of a higher temperature c-p material.

To compensate for potential attenuation and frequency shifts resulting from a holder material similar in mechanical properties to that of the nosetip, the nosetip/holder interface was not bonded. The model was held in place by loose fitting c-p tangential pins.

This acoustically optimized design had the potential for high pressure, high enthalpy gas leakage to the strut interior in the event of model failure or improper injection. To protect against possible damage to facility equipment a silicone O-ring was installed at the nosetip shank/model holder interface and the aft portion of the stainless steel threaded adaptor was filled with an epoxy or RTV potting. This potting also served as a strain relief for the instrumentation leads.

3.3.3 Model Instrumentation Support Hardware

Each test model was a completely preassembled unit ready to thread to the facility strut. All instrumentation leads terminated in plugs. The leads were supported throughout the interior

of the strut by a 1/4-inch diameter split stainless steel tube and concentric split aluminum washers (Appendix A, Dwg. #7141-069). The leads were mated to extension cables and/or a line driver box located in an aft section of the sting. The 8-foot extension cable from the sting connected to facility terminal strips mounted on the carriage in the case of thermocouples (T/C) or to a power amplifier box in the case of acoustic gage signals. From the carriage location all leads were routed to the control room and data acquisition equipment via the normal facility conduit system.

SECTION 4

DESIGN SUPPORT

The design support tasks consisted of bench tests, 1 MW arc jet tests and computer analysis of the acoustical behavior of the gage and nosetip. The analysis was especially important in order to interpret the data correctly.

4.1 BENCH TESTS

During the development of both the flexural and the compressional sensor systems, several bench test series were conducted. These tests were designed to investigate the relative merits of different sizes and shapes of crystals, their orientation and attachment configurations, and the optimum packaging configuration for the chosen sensor system. In addition, tests were required on the ground test materials of interest. The nosetip vibrational response was characterized, the vibration modes to be "tracked" were identified and quantified, and the nosetip geometry effects were investigated. This section describes the hardware, test objectives, and test results of the developmental bench test program.

4.1.1 Bench Test Hardware

4.1.1.1 Crystal Test Fixture

A small crystal test fixture was constructed to investigate the various crystal sizes, shapes, stack configurations, attachment techniques, and polarity orientation. The fixture was large enough to accept the largest crystal configuration tested so that no mass change, other than that of the crystals, was experienced during the investigation. The entire fixture could be mounted to the test model. The transmission efficiency of the test configuration could be measured by mounting a standard receiver crystal on the opposite end of the test model. Effort was made to make the experiment as repeatable as possible by measuring the clamping torque at each assembly. A sketch of the crystal test fixture is shown in Figure 24.

4.1.1.2 Aluminum Nosetips

Aluminum nosetips were fabricated for the developmental portion of the bench test program. The basic nosetip shape chosen was that of a full scale MSV nosetip. The MSV was the expected gage

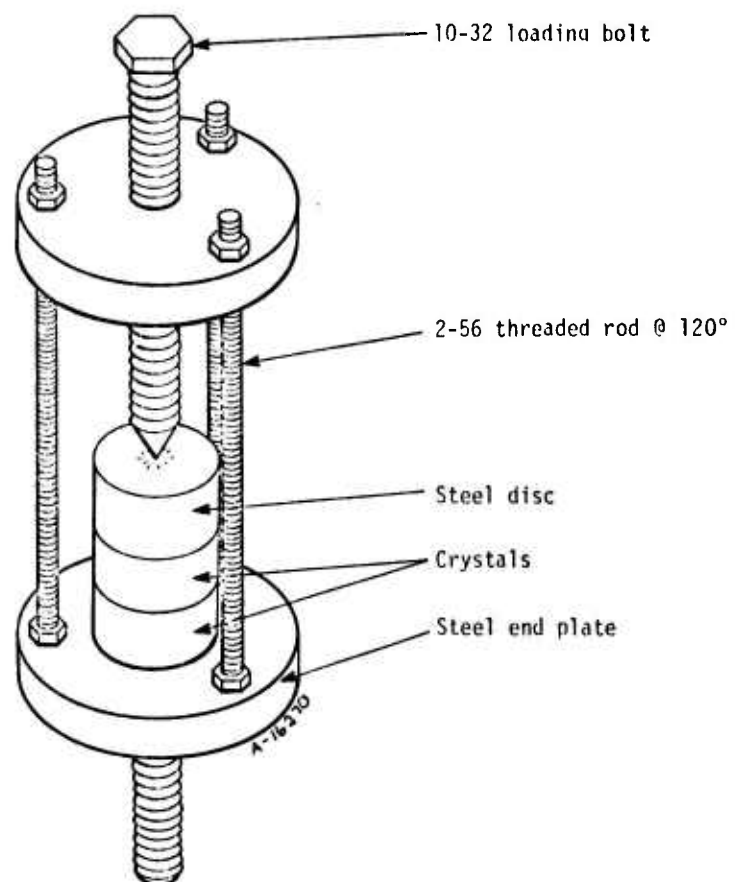


Figure 24. Bimorph test configuration.

test flight vehicle. Several shank geometries were investigated to determine the effect of increased diameter and shank extension. The intent was to achieve an optimum nosetip shape as large in diameter as the vehicle constraints would permit and as long as possible to reduce backface temperatures during reentry and to lower the resonant frequencies. Trade-offs were required between long shank extensions and "clean" vibration response.

The nosetip shape for most of the developmental tests was a flat face configuration. This shape provided a "clean" control case for the crystal studies and sensor configuration experiments. The flat face also provided a common location for a standard receiver throughout the testing of various transmitter configurations.

One of the aluminum nosetips was reserved for flexural excitation systems. Various schemes for attaching transmitter and receiver crystals to the base of the shank were investigated; such as brackets and cavities in the base of the model. These configurations were designed to hold the transmitter crystals in an orientation that would excite flexural vibrations while minimizing compressional vibrations.

Several models were designed to accept bonded sensor assemblies and sensor housings (canistors). Others were designed with threaded holes for direct attachment and bonding of transmitter systems.

4.1.1.3 Sensor Configurations

A prototype assembly of each sensor configuration was fabricated for testing and comparison on the aluminum nosetips. For those assemblies requiring bonding, several epoxies and adhesives were tried. A fast curing adhesive such as Eastman-910 or Micro-Measurements M-Bond 200 methyl-2-cyanoacrylate was used for the majority of bench testing because of its ease of application and short cure time. High temperature specs were not required for the bench testing development program.

After a sensor configuration was determined, several high temperature, high stress epoxies, both conductive and nonconductive, and both supported and nonsupported, were investigated for a nosetip bonding agent. Conductive and nonconductive epoxies were also compared in the crystal study portion of the program to determine the optimum methods of bonding crystals to each other as well as to waveguides and backmasses.

A detailed description of the sensor configurations investigated is given in Section 3.2.

4.1.1.4 Data Acquisition

The bench test data acquisition hardware included a dual trace oscilloscope, frequency counter, spectrum analyzer, and scope camera. In addition, the main instrument for determining the actual nosetip vibration and confirming the desired resonant mode was a "node probe."

The probe consisted of a small piezoelectric crystal and steel backmass with a directional probe (nail, small diameter drill bit, etc.) bonded to the end with conductive epoxy. The receiver crystal was encased in a hand held aluminum housing with connecting co-ax cable and BNC connector.

With the sensor and electronics operating at any selected resonant frequency, the entire model surface could be probed. In this manner resonances could be identified as being either flexural or compressional. Furthermore, by probing the side of the model for nodes (vibration nulls) the desired compressional or flexural frequency could be determined.

The majority of the bench test data were polaroid records of the nosetip response spectrum over a 0 to 100 kHz or 0 to 50 kHz bandwidth. All system resonances within these bandwidths were displayed in this manner. From these traces individual "peaks" could be isolated and probed for analysis and characterization.

4.1.2 Bench Test Objectives and Procedures

The developmental bench test program was conducted essentially in two parts. The first portion was structured to gather basic comparison data on the sensor configurations and individual components leading ultimately to an optimum sensor prototype. The second portion of the bench test program was devoted to fully characterizing the ground test model materials and determining the sensor response on these materials. One MW and fifty MW test nosetips were fabricated and characterized prior to testing.

In summary, the major bench test objectives were to determine the following:

1. Crystal material
2. Crystal size and shape
3. Number of crystals and polarization orientation
4. Crystal attachment configuration
5. Waveguide material and shape
6. Crystal backmass material and size
7. Optimum sensor packaging configuration (flexural and compressional)

8. Nosetip material characterization

9. Ground test model characterization and checkout

This section discusses briefly each of the above objectives.

Crystal Material - Two lead-zirconate-titanate (PZT) piezoelectric crystal materials were compared under identical conditions (PZT-4 and PZT-5).

Crystal Size and Shape - Disk crystals of various diameters and thicknesses were compared with each other and with tube crystals. Shear crystals were also included in the matrix, but were not tested in this program (see Reference 11 for detailed test matrix).

Number of Crystals and Polarization Orientation - All of the above sizes and shapes were tested in several combinations of multiple crystal and crystal polarization orientations. The standard bimorph configuration is defined as two identical crystals mated with a common pole at the interface [i.e., (-+)(+-)]. The center of gravity shift (e.g., shift) configuration is the reverse of the above, opposite poles at the common face [i.e., (-+)(-+)]. Various combinations of the two configurations were investigated with the intent of determining the optimum configuration; one that will result in a maximum receiver output voltage to power input ratio.

Crystal Attachment Configuration - Mechanical means of attaching the crystals to the model were investigated. For structural design considerations a mechanical clamping or threaded arrangement appear superior. Tube crystals with an internal central bolt and Belleville springs were compared with an external compressive harness. Both systems were then compared with the more acoustically "clean" but structurally inferior epoxy techniques.

Waveguide Material and Shape - Steel and aluminum waveguides were compared to confirm the prediction of the superior transmission properties of the lower impedance aluminum. Various lengths and shapes of waveguides were tested from large diameter cylinders to tapered (similar to exponential horn theory) small diameter systems. Although the "point source" 2-56 threaded rod used in previous ARG ground tests (Reference 9) was desirable acoustically, larger systems were required to satisfy the structural integrity problems at high reentry vibration levels.

Crystal Backmass Material and Size - Aluminum, steel and tungsten backmasses were added to several of the crystal combinations to determine the effect of impedance mismatch and increased signal transmission efficiency. Various sizes of each material were tested to

determine the optimum mass for each material while trying to minimize the potential structural problems of a heavy backmass attached to the rear of the crystals.

Optimum Sensor Packaging - The preliminary bench testing and screening mentioned above resulted in defining optimum sensor components. Several flexural and compressional excitation systems were tested with these components. Offset transmitters with receivers both parallel and perpendicular to the transmitter, single and dual receivers, systems with and without hermetically sealed enclosures, and transmitter/receiver assemblies with and without an integral aluminum base were all investigated. Based upon design trade-offs between maximum returned signal for a given input power and structural considerations, the sensor configurations were narrowed down to two. Several epoxies were tried as the sensor bonding agent. Both ground tests, 1 MW and 50 MW employed these designs.

Nosetip Material Characterization - The materials chosen for ground tests were analyzed with the chosen sensor configuration from above. Sweeps from 0 to 200 kHz were analyzed for nosetip and sensor vibrational response.

Ground Test Model Characterization and Checkout - Each 1 MW and 50 MW nosetip was instrumented and characterized. The flexural and compressional modes of interest were identified. Quantitative informations of return signal amplitude, frequency, and phase relationship were recorded for all phases of model build-up from nosetip alone to completely assembled and potted models.

4.1.3 Bench Test Results

The problems encountered in the developmental testing program are discussed in this section along with the results of the major phases of the bench test program.

4.1.3.1 Data Interpretation Problems

Several recurring problems with the bench test screening tests involving data repeatability and data acquisition are described below:

Crystal Study Test Fixture - The test fixture used for screening the various crystal and waveguide configurations, described in Section 4.1.1.1, was subject to data nonrepeatability problems. The test fixture itself was a significant part of the nosetips/sensor mass system. It had multiple resonances in the nosetip bandwidth of interest. Although the concentric single loading bolt and load distribution slug were constant throughout the testing, it is doubtful that the torque on the loading bolt could be repeated within 10 percent. Even

assuming repeatable torque settings uneven nonparallel crystal faces resulted in nonuniform, nonrepeatable stress distribution during loading. Thus uneven stress loading resulted in crystal fracture in some cases at moderate torque/compressive stress loadings.

Epoxy - To insure repeatable test conditions to the maximum extent possible, the fabrication of those test configurations involving crystal component or sensor assembly bonding should employ proper bonding techniques. Surface preparation, mixing, application and curing should all be performed to the specification of the adhesive manufacturer. This was not possible in the multiconfiguration, multitest point matrix of the crystal component screening tests. Consequently, a fast curing cyanoacrylate was used for most of the testing without the full complement of surface preparation procedures. While this was better than no adhesive, it was subsequently discovered that the bond strength was not always repeatable.

Model Size - The entire ARG program to date has involved carbon/carbon materials on a sub-scale basis only. The material has been analyzed and nosetip resonances characterized for specimens on the order of 3 to 3.5 inches in length. These short lengths result in relatively high first compressional modes of vibration. The spectrum is extremely "noisy" through 150 kHz and the fourth compressional mode. It would be desirable to develop the sensor on a full scale vehicle where the frequencies of interest would be lowered and distributed in a "cleaner" fashion throughout the spectrum.

Node Probe - The node probe was the only instrument available to determine the vibrational pattern of the nosetip. Although it was adequate for some cases, the data for most of the carbon/carbon nosetips were ambiguous. At times it was simply impossible to define the vibration as flexural or compressional, let alone which harmonic. The probe was not directional enough. The orientation with respect to the specimen was critical; slight shifts in the angle could produce opposite results.

In general, probing perpendicular to the model axis was easier than parallel, since lateral vibrations were transmitted when attempting to probe parallel to the axis. This made it difficult to determine the number of compressional nodes; and without an indication of where to search, it was at times, impossible. The computer estimation of response was an invaluable aid in this respect.

It would be desirable to perfect the probe technique in future work. Perhaps the orthogonal dual probe technique proposal initially merits further investigation. Plotting one output vs. the other and studying the resulting Lissajous figures would yield node locations by

displaying phase shifts. In the event the node probe cannot be improved, perhaps an optical technique of some kind can be developed to display nodal patterns. A stress-coat painting technique has also been suggested. In any event a better method of establishing the identity of the resonant peak is of paramount importance since it is critical to the overall theory and tracking success.

4.1.3.2 Crystal Configuration Selection

The transmitter crystal configuration chosen as a result of the bench test program and structural design trade-offs was the bimorph configuration with a high acoustic impedance tungsten backmass. A 0.5-inch long, 1/4-inch diameter, aluminum waveguide was used. The crystals were PZT-4, 0.5-inch diameter x 0.1-inch thick. Ablebond 36-2 conductive epoxy was used to mate the crystals and electrode interfaces. See Dwg. #7141-065.

The receiver crystal was a single PZT-4, 0.25-inch diameter x 0.1-inch thick crystal with a tungsten backmass. The entire receiver assembly was enclosed in a hermetically sealed thin walled aluminum can with attached coax cable (Dwg. #7141-079).

The choice of PZT-4 over PZT-5 was a design trade-off between the structural superiority of PZT-4 and the relatively minor increased efficiency of PZT-5. Bench test results showed the merits of PZT-5 to be within the data repeatability error band. Indeed the prediction of increased response of PZT-5 published by the manufacturer show only slight advantages for this material.

The choice of 0.1-inch thickness for the crystals was based upon bench test data which demonstrated that the thinner crystals had a higher output voltage/power input (V_{out}/P_{in}) ratio. The choice of the 0.5-inch diameter over other sizes, however, was not as direct. In some cases the smaller diameter crystal yielded a better (V_{out}/P_{in}) ratio than the 0.5-inch diameter case. The data were close to the error band. The larger size was chosen because it permitted a larger bonding surface for the multicrystal/mass assembly. The larger size also simplified handling during assembly and would adapt better to a 1/4-inch diameter waveguide.

4.1.3.3 Sensor Package Configuration Selection

Initially the objective of the sensor packaging was to have a single self-contained transmitter/receiver unit. The assembly would be hermetically sealed and ready for bonding to the nosetip surface (Dwg. #7141-065). Subsequent bench testing showed, however, that the single encapsulated unit generated numerous inherent sensor resonances and was subject to severe crosstalk problems. This phenomenon was apparent in both the proposed flexural and compressional systems.

Subsequent experimentation led to individually mounted transmitters and receivers and to the transmitter/aluminum base unit with separate receivers (Dwgs. #7141-080 to -083). These designs had only a few sensor resonances in the bandwidth of interest and these were sufficiently displaced from tracked frequencies that they did not interface.

Due to the relatively large contact area of the transmitter waveguide and receiver there still appeared to be minor crosstalk problems. Early ARG designs utilizing more directional waveguides on both transmitter and receiver (Reference 8) were not as severely affected by crosstalk.

4.1.3.4 50 MW Model Characterization

After the sensor had been bonded to the nosetip several spectrum analyzer sweeps were taken to display the nosetip vibrational response spectrum over the bandwidth of interest. Computer analysis results and the node probe, defined in Section 4.1.1.4, were used to identify the first compressional mode of vibration for the single mode models. The first and second compressional modes of vibration were identified for the one dual mode model. The frequencies tracked for each of the five models described in Section 3.3.1 are listed in Table 9. Figure 25 is a 0 to 100 kHz sweep for each of the five nosetips.

4.2 1 MW TESTS

4.2.1 Test Objectives

The main objective of the 1 MW ARG tests was to demonstrate the operation of the dual mode flexural sensor configurations for carbon/carbon material in a hyperthermal environment. The test was not considered a proof test of the dual mode flexural system, but a developmental test prior to 50 MW proof testing. The dual mode electronics and oscillograph data acquisition technique were also checked out in this test program.

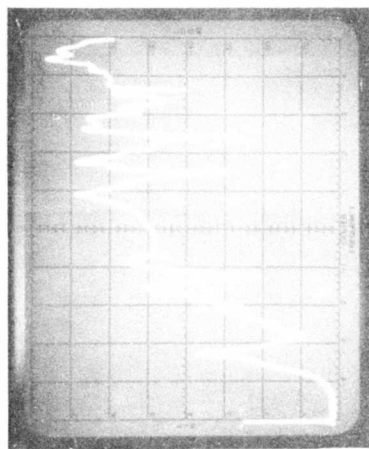
4.2.2 Test Conditions - Test Matrix

The Acurex/Aerotherm 1 MW Arc Plasma Generator (APG) provides a high enthalpy, low pressure, continuous flow test environment. Because of the low stagnation pressure, the heat transfer rate is less severe than that experienced at the 50 MW facility.

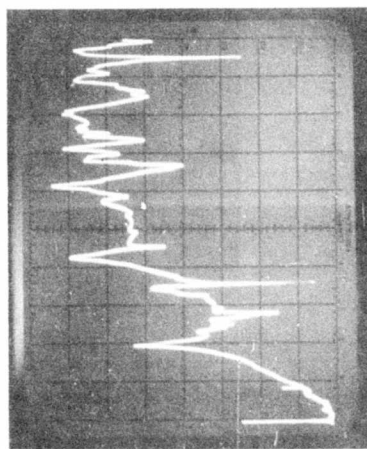
The effect upon the acoustic signal, however, should be more severe because of the increased test time and resulting temperature profile within the material. The temperature induced acoustic velocity changes, and hence the resulting frequency shifts, affect a greater portion of the nosetip for a longer period of time than that experienced in the 50 MW environment. The 1 MW environment, therefore, is a good checkout of the changes in material properties and their effect upon the transmitted acoustic signal. The test matrix for the two ARG tests is presented in Table 10.

TABLE 9. 50 MW MODEL FREQUENCIES

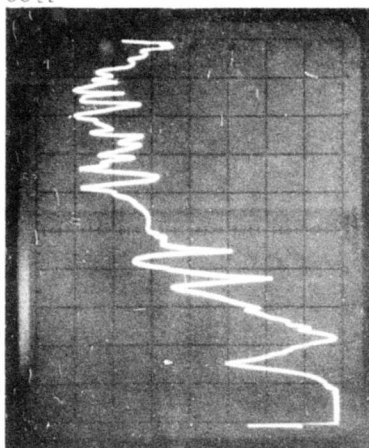
Model No.	f_{1c} (kHz)	f_{2c} (kHz)	Figure 23 Identification
ARG-1	59.3	93.6	a
ARG-2	61.4		b
ARG-3	61.6		c
ARG-5			d
SSN/ARG-6	48.0		e



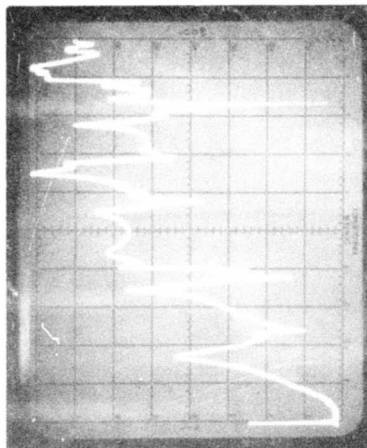
a. ARG-1



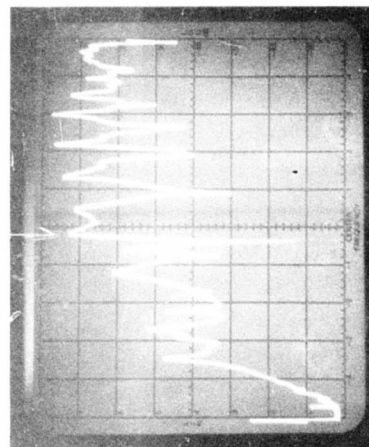
c. ARG-3



b. ARG-2



d. ARG-5



e. SSN/ARG-6

Note: • Log ref = 20 dBV
• Input voltage = 50 V p-p
• † = tracked frequency

Figure 25. 50 MW models 0 to 100 kHz sweep.

TABLE 10. 1 MW TEST MATRIX

APG Test No.	Model No.	C/C Material	$\dot{q}_{\text{flat face}}$ [Btu/(ft ² sec)]	P _{t2} (atm)	Approximate Time on G _L (sec)
2883	1 MW-1	Mod III _B	1,345	0.02	45
2884	1 MW-2	Mod III _B	1,388	--	34

4.2.3 Model Description

Both models were identical Mod III_B c/c nozetips. Approximately 1 inch in diameter, cylindrical, 3.25-inch long slugs tapered to a 0.5-inch diameter flat face were used (Dwg. #7141-073). The models were held in a loose fitting stainless steel adaptor with a loose fitting set screw. The adaptor was mated to a stainless steel tube to protect the sensor and instrumentation cables. This entire holder was encased in a circumferentially wrapped silica phenolic heatshield with a tapered graphite cap (Dwg. #7141-076).

The sensor configurations used were the offset transmitter and receiver configurations (Dwgs. #7141-081 and -082). For Model #1 MW-2 the sensor was threaded and bonded directly in the c/c nozetip base. The sensor for Model #1 MW-1 was a split aluminum base plate. The two semicircular sections contained the single transmitter and single receiver. The split base was bonded to the nozetip with supported epoxy.

The first and fourth flexural modes of vibration were tracked for this test. Table 11 lists the resonant frequencies for each model prior to the test.

TABLE 11. 1 MW MODEL FREQUENCIES

Model No.	Sensor Base Configuration	f_{1f} kHz	f_{4f} kHz
1 MW-1	Split Aluminum	15.1	68.9
1 MW-2	Direct	16.1	69.9

Model #1 MW-2 was instrumented with two type K base thermocouples (T/C). T/C #1 was located on ϕ in the c/c 1/4 inch in depth. T/C #2 was bonded directly to the nozetip base.

4.2.4 Test Procedure

An optical pyrometer was aligned 0.1 inch back from the stagnation point to monitor surface temperature and to determine when 0.1 inch of recession occurred during the test. A flat face calorimeter and a pitot probe were injected for stream calibration prior to model exposure. All stream conditions and model T/C data were recorded by a high-speed magnetic tape data acquisition system. All sensor instrumentation signals were recorded on the oscillograph. For each model and for each of the two oscillator loops of the dual mode electronics, the following signals were recorded:

- Loop #1 (f_4) and Loop #2 (f_1):
- Output of VCO - dc signal proportional to frequency
 - Phase lock detector output - dc signal monitoring status of loop lock

The tests were run to destruction. Shortly after the receiver signal was lost due to epoxy failure the test was terminated.

4.2.5 Test Results

Lock was lost within the first 1 to 3 seconds on one of the two resonances in both tests. It was not the same peak in each case. Overall recession was less than 0.1 inch indicating thermal effects resulted in loss of lock.

Figures 26 and 27 are the phase lock detector output signal histories for Tests #1 and #2, respectively. For Test #1 Figure 26 shows that a significant deviation from preset zero voltage occurred on Lock #1 loop (fourth flexural) around 20 seconds. This deviation indicates loss of lock and tracking capability. Lock #2 loop (first flexural) lost lock immediately, but recovered after the insertion vibration damped out. The reverse was true of Test #2.

Figures 28 and 29 are the frequency shift histories for both resonances of Models #1 and #2, respectively. The oscillograph sensitivity was adjusted for approximately 2 percent frequency shift based on previous 1 MW c/c data (Reference 8). The "end of data" or "no data" points indicate the frequency shift exceeded this value and the VCO/oscillograph amplifier saturated.

Figures 30 and 31 present the optical pyrometer output for Models 1 MW-1 and 1 MW-2, respectively. Note that the pyrometer was aligned 0.1 inch aft of the stagnation point. Figure 32 is the base temperature history for Model 1 MW-2. The plot indicates that the epoxy failure temperature was reached at approximately 20 seconds. The figure further indicates that the base was heated by conduction and not high temperature gas leakage through the loose fitting adaptor and heatshield. This was suspected initially because of rapid base temperature response during the test.

4.3 ANALYSIS

Theoretical analyses of the resonant acoustic response of nosetip/waveguide systems are needed to:

- Generate resonant frequency versus length and shape mass for data reduction purposes
- Correlate and extrapolate bench and arc test experimental results
- Establish the sensitivity of nosetip/waveguide system resonant frequencies to forecone shape and nosetip temperature distributions

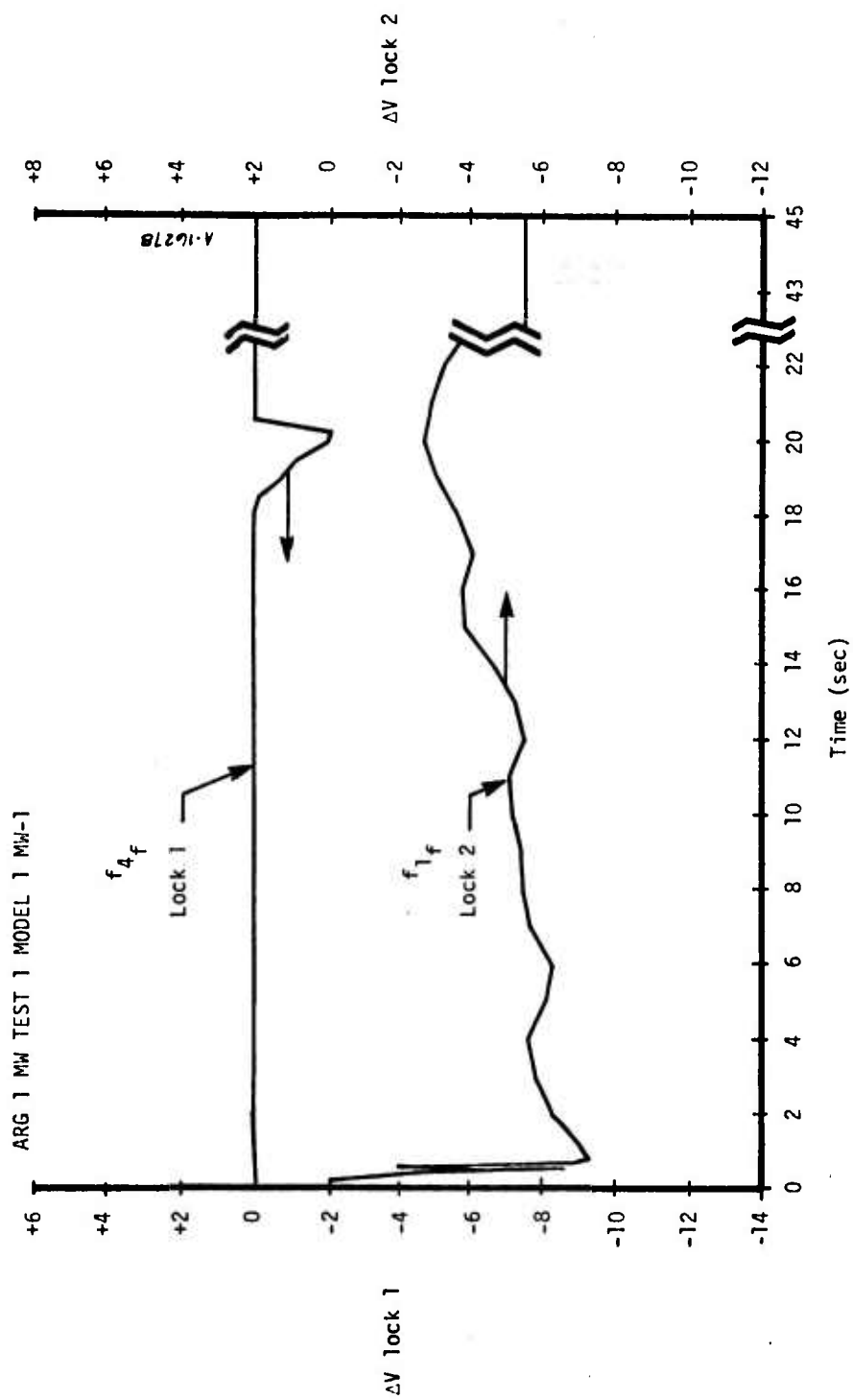


Figure 26. 1 MW Test 1 lock detection signal history.

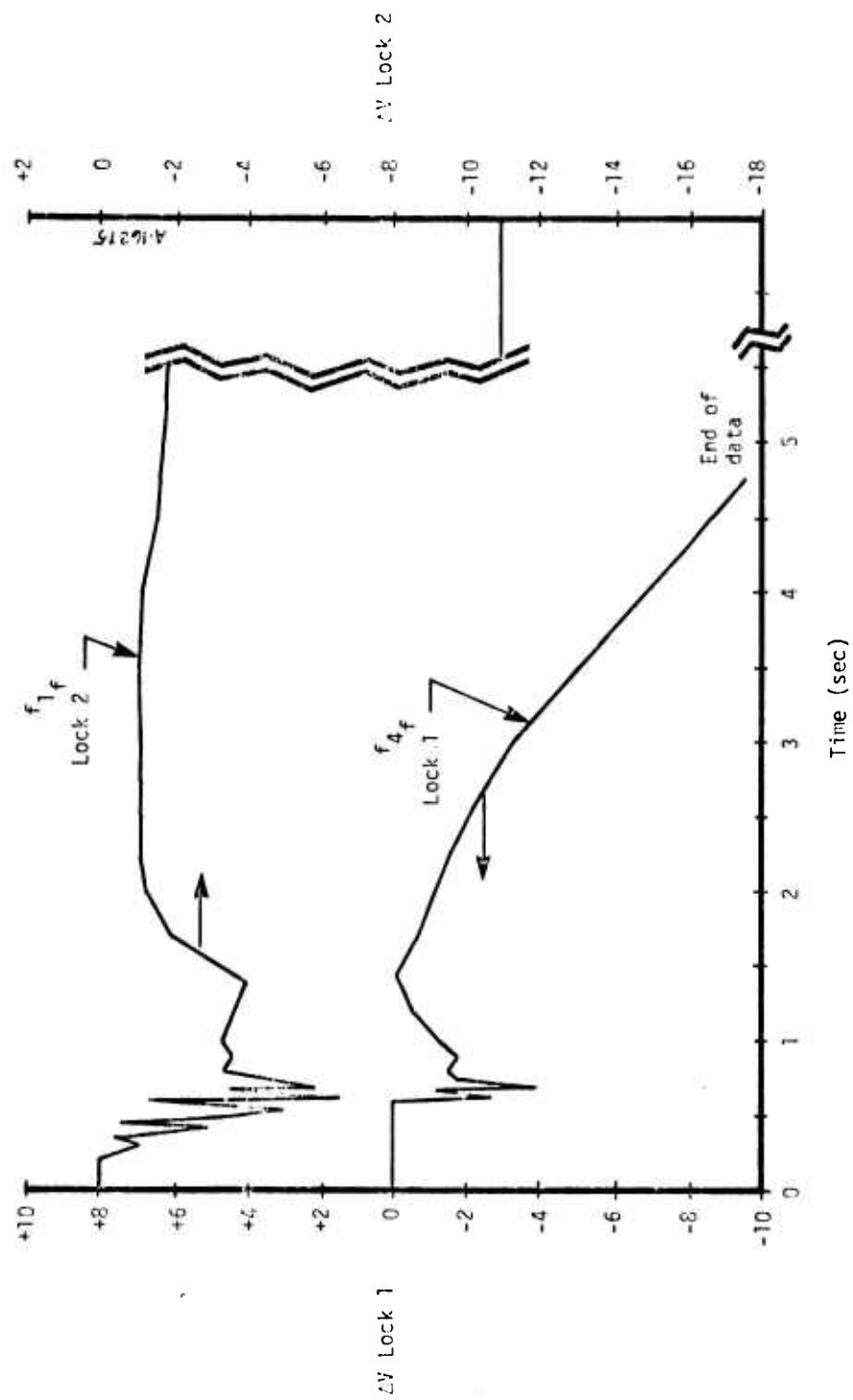


Figure 27. 1 MW Test 2 lock detection signal history.

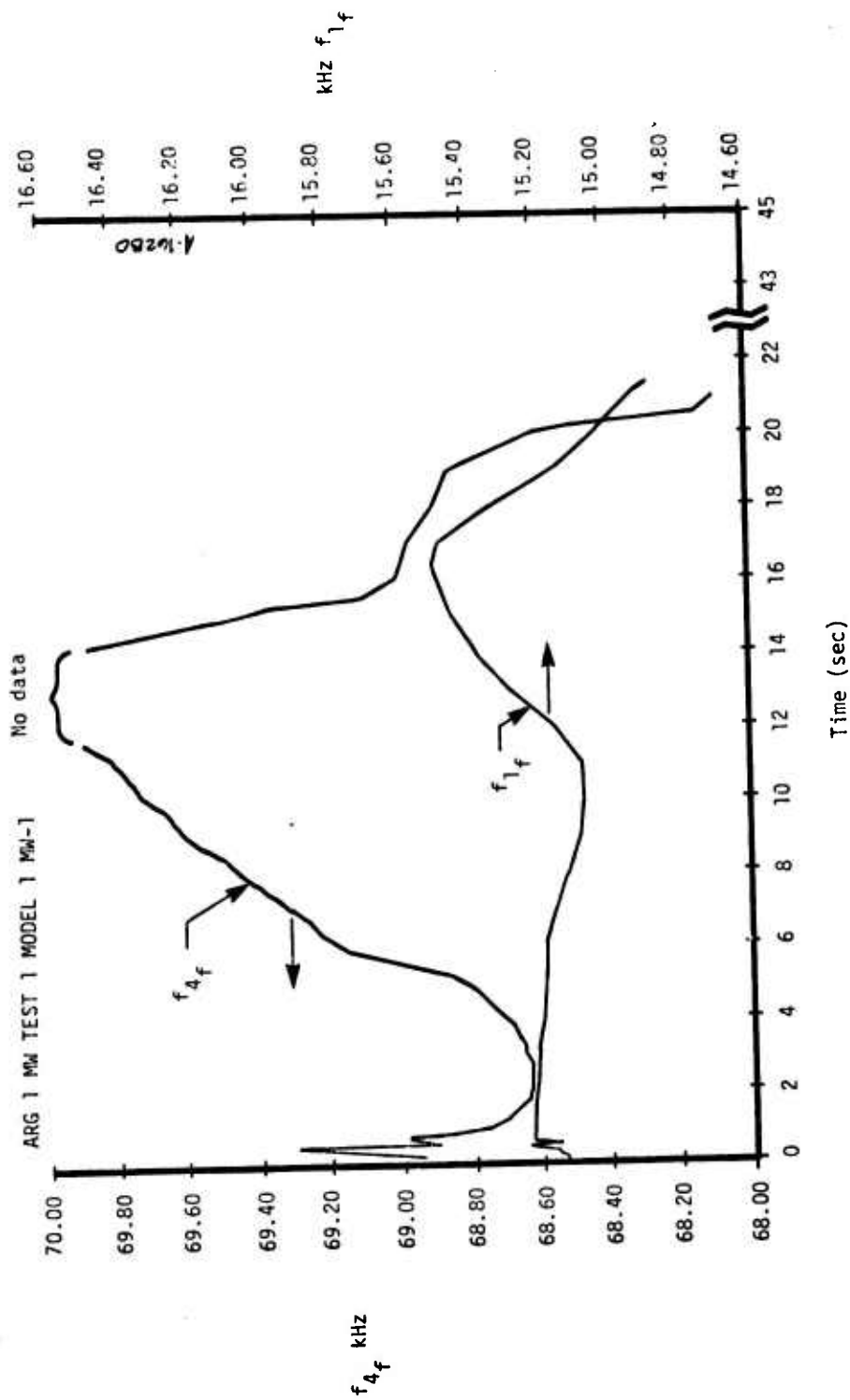


Figure 28. 1 MW Test 1 tracked frequency vs. time.

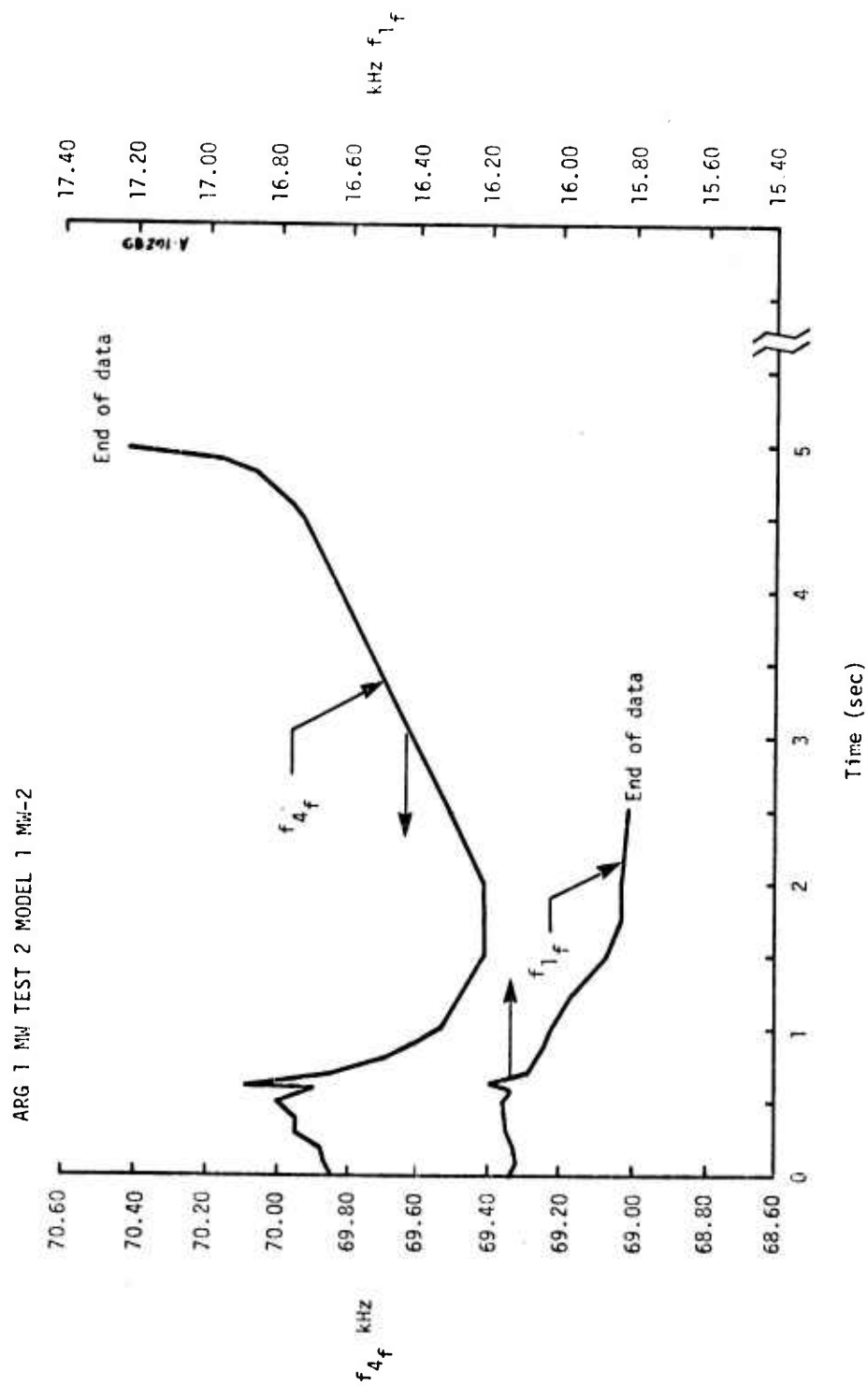


Figure 29. 1 MW Test 2 tracked frequency vs. time.

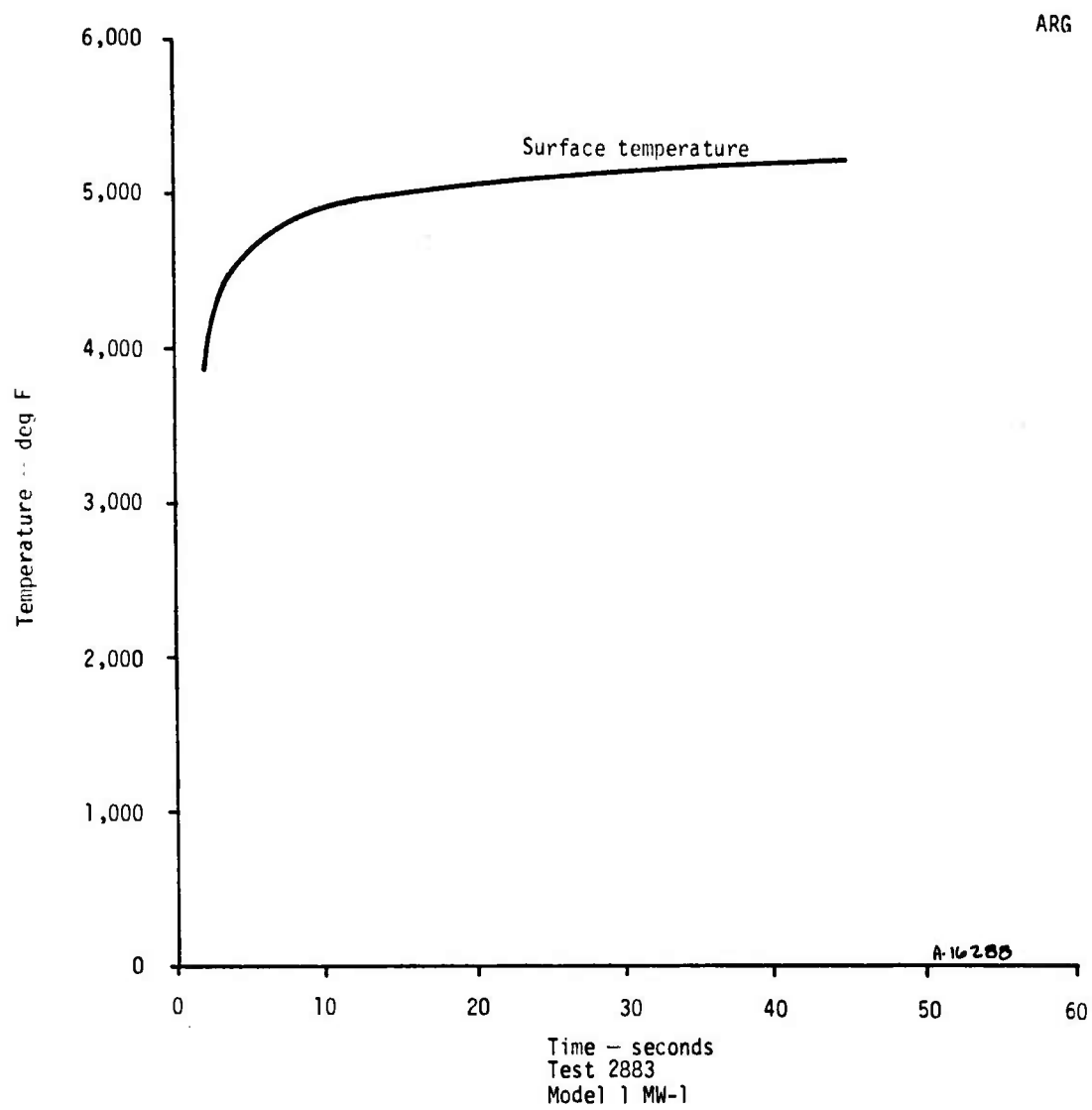


Figure 30. Nosetip surface temperature.

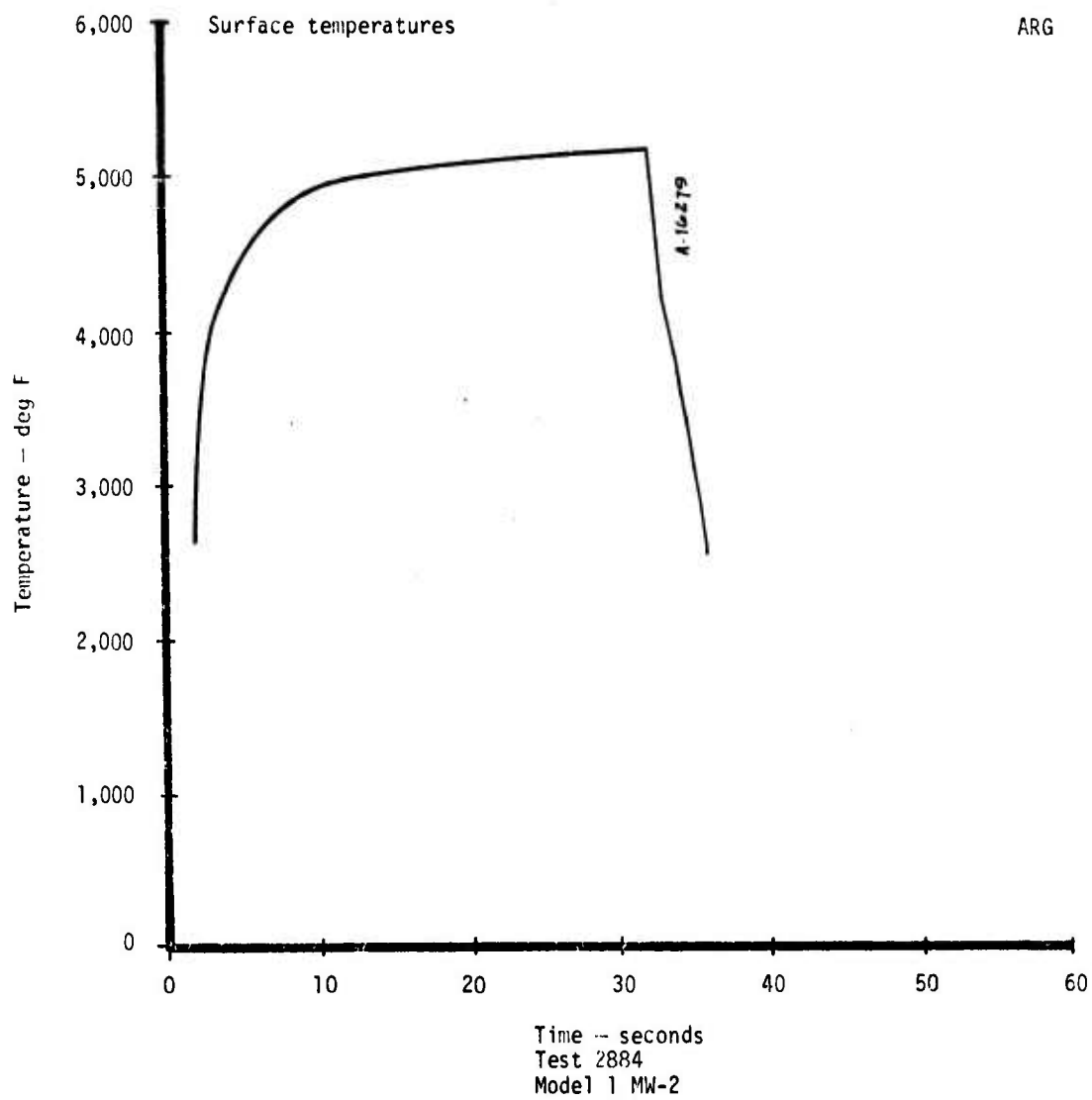


Figure 31. Nosetip surface temperature.

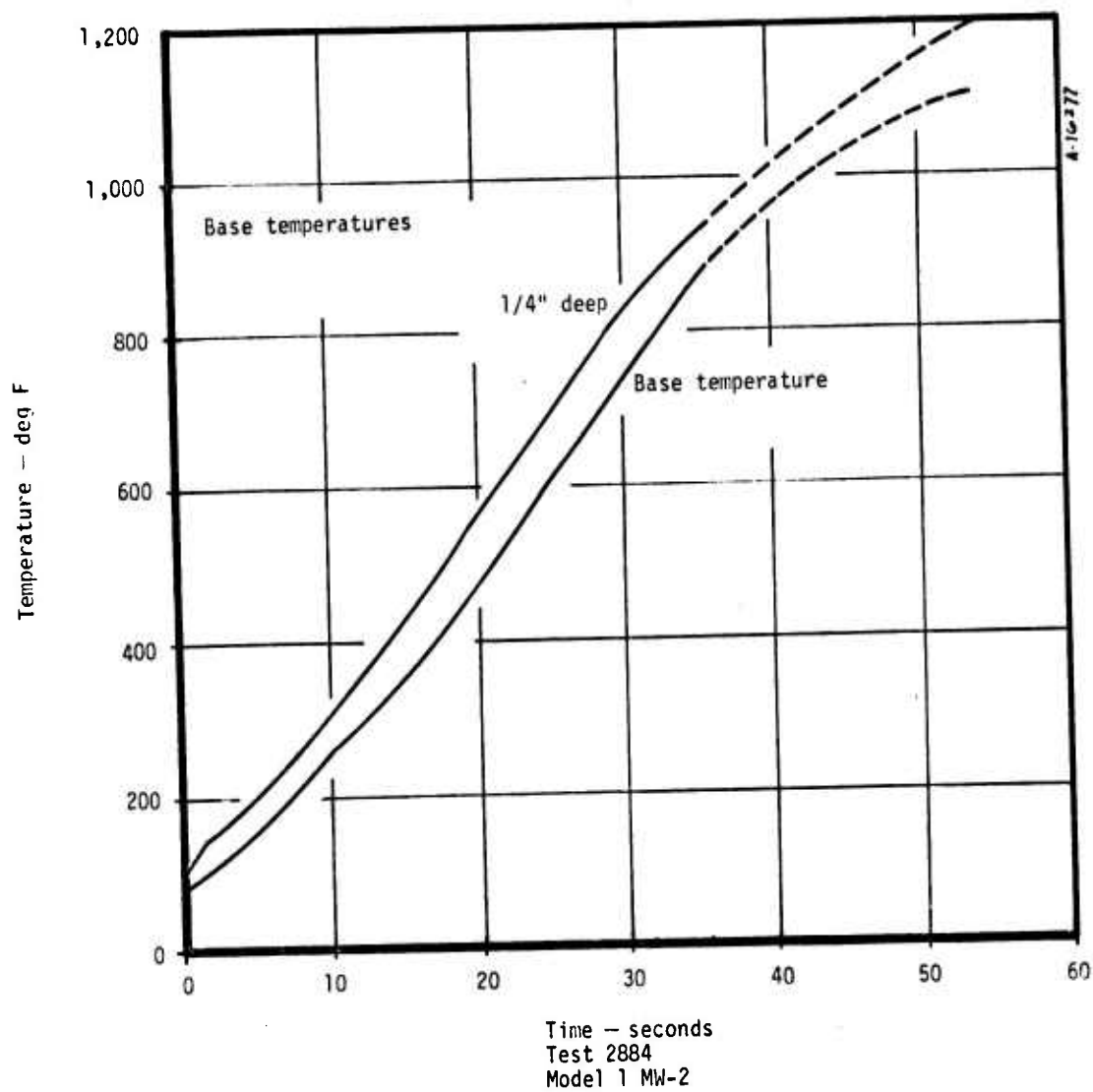


Figure 32. Base temperature.

- Assist designers in the optimization of the acoustic response of nosetip/waveguide systems

The following paragraphs discuss the theoretical methodology utilized in this study and some applications of the methodology to nosetip/waveguide systems.

4.3.1 Methodology

Since a large number of calculations were expected to be made during this program, a method was sought which would give adequate accuracy at minimal cost. Previous studies had indicated that simple analytical techniques could not provide the needed accuracy for the complex nosetip shapes and temperature distributions of interest. Consultations with an expert* indicated that a numerical finite element technique which is capable of predicting resonant frequencies (modal analysis) would be most suitable for application in this program. The finite element code selected for use in this study is the Structures Analysis Program (SAP IV) developed at the University of California at Berkeley (Reference 2). This code is widely available through various computer services and is typically well supported by their personnel. It is completely general allowing treatment of one-, two-, or three-dimensional configurations with the choice of eight different finite element types. Static, steady-state dynamic (i.e., modal analysis) as well as transient response predictions of arbitrary shaped bodies can be made with either isotropic or nonisotropic material properties. In summary, predictions of the full spectrum of nosetip/waveguide shapes and temperatures can be treated with this single code. However, the addition of successively more complex elements or material properties (e.g., nonisotropic, elastic modulus) increases the computational time and thereby the computational costs. Also, for the more complex elements (i.e., three-dimensional brick elements), problem setup time is greatly increased. Recognizing the cost impact of the more complex elements, the simple beam element analysis is applied to predict the first compressional resonant response of nosetip/waveguide systems. Accurate predictions of higher order resonant mode frequencies require a more sophisticated and costly approach.

4.3.1.1 Single Mode Gage

In the application of the beam element modal analysis to nosetip/waveguide systems, the nosetip and waveguide are broken into discs as illustrated in Figure 33. These discs are assumed to have stiffness properties characteristic of beams made of the same material with the same cross sectional shape. Since each beam element requires input of material properties, temperature effects

*Professor Hugh D. McNiven, U.C. at Berkeley.

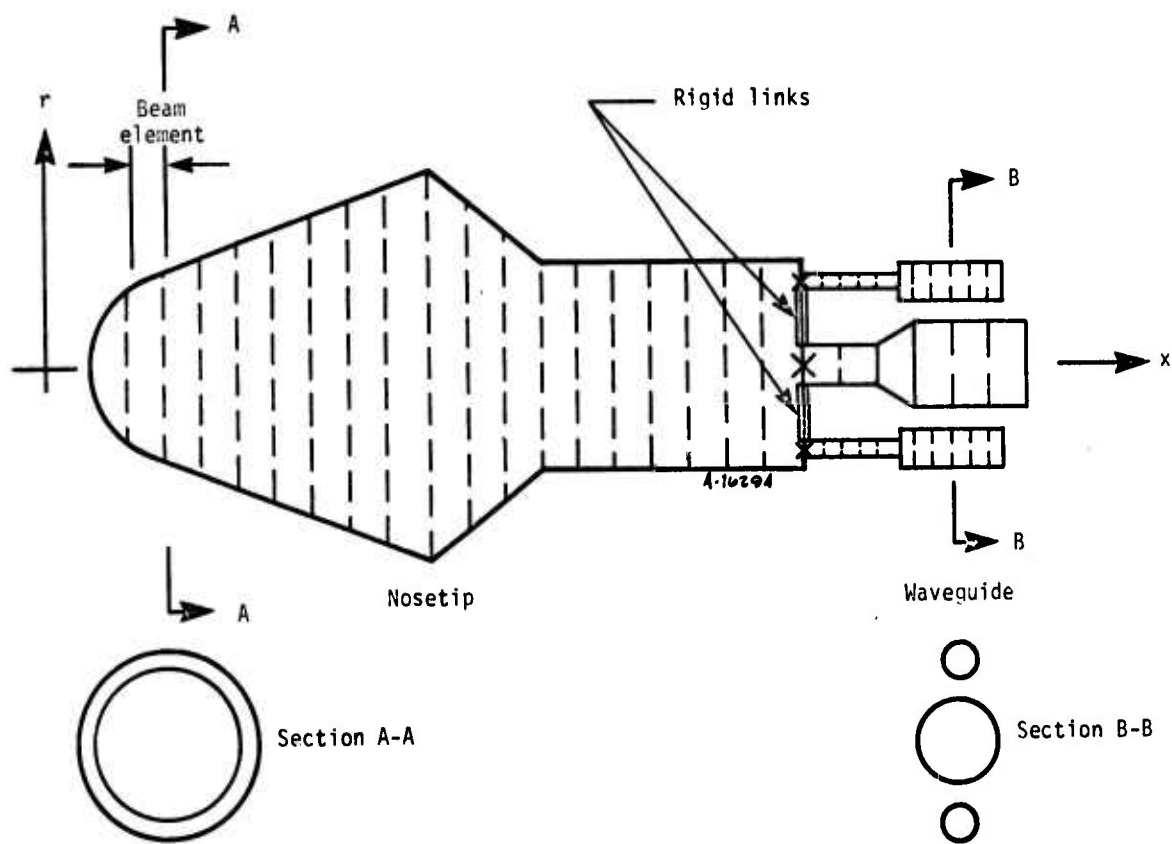


Figure 33. Schematic of SAP IV beam element applications to nosetip/waveguide system.

as a function of distance along the axis can be easily included in the analysis. With the use of a combination of rigid links* and beam elements, fully three-dimensional waveguide systems can be modeled with the beam analysis approach. Figure 33 illustrates a typical application of rigid links.

To reduce SAP IV beam element problem setup time, two auxiliary programs have been constructed by Aerotherm to generate beam element geometric input data from overall nosetip geometry. The first program, SAPINB, requires as input the nosetip overall length, plug dimensions, forecone and aftcone half angles and element lengths. The program generates nosetip element geometric data on punched cards which can be directly input into the SAP IV code. Waveguide geometric element data must be generated by hand and appended to the above data set to predict nosetip/waveguide system response. The second program, SAPINA, is constructed to interface with the Sandia Nosetip Analysis Procedure (SNAP) code (Reference 3). The SNAP code is a computational tool used to determine the shape and internal temperature distribution histories of nosetips during reentry into the atmosphere. At selected trajectory times during the calculations, shape and temperature distributions are automatically stored on magnetic tape to be retrieved at a later time. The SAPINA program accesses this data type and generates beam element geometric data from the predicted nosetip shape for direct input into the SAP IV code. This approach reduces the time consuming and error prone process of generating geometric data by hand. This approach is particularly useful for assessing the variation of resonant frequency under actual flight conditions over a complete reentry trajectory.

Given element geometric and material properties, the SAP IV code determines the nosetip/waveguide system resonant response by:

- Constructing mass and stiffness properties of all elements
- Linking elements together and forming a set of simultaneous equations
- Solving the simultaneous equation set for its eigenvalues (resonant mode frequencies) and eigenvectors (relative displacements along and perpendicular to the axis)

If desired, the results of the above modal analysis can be utilized as code input for a dynamic response analysis of the nosetip/waveguide system. Given a forcing function, the SAP IV dynamic response option determines, as a function of time, the absolute displacements and forces at the endpoints of all of the elements. The dynamic response option is useful in establishing forces within the nosetip/waveguide system as a result of nonacoustic gage generated vibrations and

* An element which connects other elements but which doesn't permit relative displacements between its endpoints.

phase relationships between the gage driver frequencies and receiver frequencies. It should be noted that the forcing function input for the dynamic response option must be defined in a discreet manner as a function of time. This input can become quite bulky for several periods of the driver oscillation. Also, the computer run time is increased over the modal analysis, and the output generated is bulky and not well suited for steady-state forced vibration problems. These negative aspects limit the extensive use of the dynamic analysis approach in this study.

The SAP IV beam element modal analysis has been validated via comparison with bench and arc test first compressional mode frequency data. In Figure 34, SAP IV beam element predictions of resonant frequencies are compared to values measured for several lengths of tungsten bar. Since the bars, especially of longer lengths, are beam-like, then good agreement is expected between predictions and measurements. In Figure 34 this is found to be the case for the first compressional mode, even for the shorter bar lengths. For the longer lengths, agreement is also found between the beam analysis and simple bar theory* for both compressional and flexural resonant modes.

It should be noted that the simple analytical bar theory for flexural vibrations differs from the beam analysis results and data at the shorter lengths. Since the shorter bar lengths have length-to-diameter ratios typical of nosetips, the above deviation illustrates the limitations inherent in applying simple bar theory analytical approaches to nosetip type shapes.

The good agreement between the first compressional mode, beam analysis predictions and measurement, for various bar lengths, prompted the use of the code in checking the "effective" elastic moduli of some materials used during the program. For these cases the material elastic moduli are established by adjusting the code input for these quantities until the predicted bar frequencies are equal to the measured values. The values found are typically close to published results but differ slightly by some nominal amount. The approach for checking elastic moduli is a valuable aid in

*For long bars of uniform length cross sectional shape it is found that

$$f_{\text{compressional}} = \frac{C_n}{L} \sqrt{\frac{E}{\rho}}$$

n	1	2	3
C _n	1	2	3

$$f_{\text{flexural}} = \frac{F_n}{L^2} \sqrt{\frac{EI}{w}}$$

n	1	2	3	4
F _n	3.56	9.82	19.24	31.31

where L = length, E = elastic modulus, ρ = density, w = mass per length, I = sectional moment of inertia, all in units of lbf-in-sec.

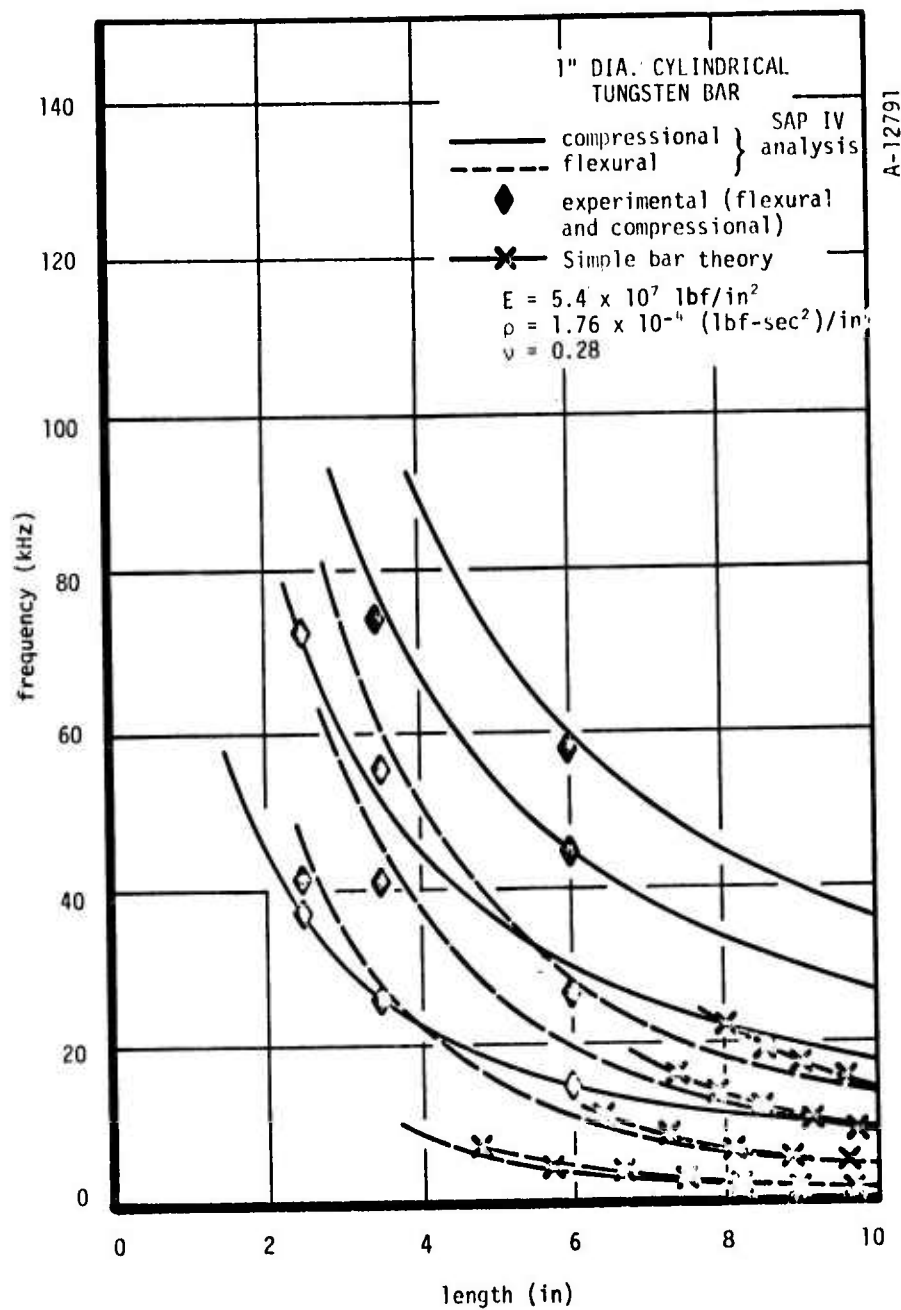


Figure 34. SAP IV beam analysis predictions of tungsten bar resonant frequencies.

developing code input data for nonisotropic carbon/carbon type materials. As previously indicated the beam analysis approach is essentially one-dimensional in nature and detailed nonisotropic material properties cannot be included in this option. However, if an "effective" elastic moduli is defined for the material based on a certain geometry then adequate predictions of frequencies can be made over a range of shapes and lengths which include this geometry. In essence, the beam analysis elastic moduli data is calibrated for beam analysis applications to nosetips which have nonisotropic material properties. The validity of this approach is demonstrated by arc test results which are discussed below.

In Table 12 SAP IV beam analysis predictions of 1 MW tungsten and carbon/carbon nosetip/waveguide system resonant frequencies are compared with measurements. The carbon/carbon "effective" elastic modulus input into the code was established from experiments on bar shaped samples of the material. The shapes of the nosetips deviate somewhat from the bar examples discussed previously. A major change from the bar examples is the inclusion of the asymmetric waveguide and crystal configurations in the analysis. The waveguides and crystals are constructed of materials different from the nosetip. For these cases, the presence of the waveguide system alters nosetip resonant frequencies. Also, several additional resonant frequencies appear which are associated primarily with the waveguides. In summary, the resonant response of the nosetip is altered and complicated by the presence of the waveguides. Since it is experimentally difficult to sort out the waveguide and body frequencies, several beam analysis predictions were made to try to evaluate the resonant response of some nosetip/waveguide systems used during this program.

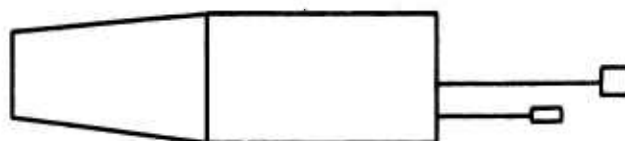
The comparison made in Table 12 indicates that resonant mode frequencies primarily associated with the body are predicted well for both tungsten and carbon/carbon nosetips. Though somewhat incomplete and not totally conclusive, the results presented in Table 12 indicate that the code can predict with reasonable accuracy responses associated primarily with the waveguides.

It should be noted that experimentally a resonant mode frequency was observed for both tungsten and carbon/carbon models which could not be associated with any beam analysis prediction of frequency. These responses might have arisen from either crystal resonances or nonbeam type (i.e., non-one-dimensional) responses of the nosetip. In a later discussion it will be demonstrated that nonbeam type responses can develop for nosetip type shapes. It is conjectured that the responses not predicted by the beam analysis approach shown in Table 12 are of this nature.

Besides the thin waveguides illustrated in Figure 33, the beam analysis approach, utilizing the same material properties has been applied to several aluminum nosetip shapes with massive waveguides. These waveguides are more typical of flight hardware than the thin waveguide cases

TABLE 12. COMPARISON OF SAP IV BEAM ANALYSIS AND MEASURED
NOSETIP/WAVEGUIDE RESONANT FREQUENCIES

a. 1 MW ARC TUNGSTEN MODEL



$$E = 5.4 \times 10^7 \text{ lbf/in}^2$$

$$\rho = 1.758 \times 10^{-3} \text{ (lbf-sec}^2\text{)/in}^4$$

$$\nu = 0.28$$

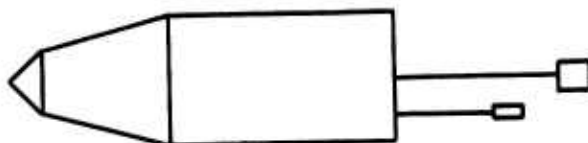
TUNGSTEN

Resonant Mode Type	Frequency (kHz)	
	Predicted	Measured
W, TX, f ^a	12.49	12.0
1 body flexural	14.53	
W, RC, L	17.18	
W, TX, f	25.69	
W, RC, f	26.09	
2 body flexural	29.53	28.8
1 body compressional	30.21	31.4
W, TX, f	43.02	40.0
3 body flexural	46.59	42.0
2 body compressional	53.94	56.3
W, TX, L	58.69	60.0
W, TX, f	63.64	
4 body flexural	64.33	

^aW = waveguide
TX = transmitter
RC = receiver
f = flexural
L = compressional

TABLE 12. Concluded

b. 1 MW ARC CARBON/CARBON MODEL



$$E = 3.65 \times 10^6 \text{ lbf/in}^2$$

$$\rho = 1.49 \times 10^{-4} \text{ (lbf-sec}^2\text{)/in}^4$$

$$\nu = 0.097$$

CARBON/CARBON

Resonant Mode Type	Frequency (kHz)	
	Predicted	Measured
1 body flexural	18.54	19.0
W, RCTX, f	25.73	25.0
W, RC, f	26.28	28.0
1 body compressional	31.41	31.4
2 body flexural	36.69	34.8
W, TX, f	43.19	43.0
2 body compressional	55.81	52.0
3 body flexural	56.70	55.0
W, TX, l	61.32	59.0
X, TX, f	63.99	65.0

48.0

illustrated in Table 12. The results presented in Table 13 demonstrate the agreement that can be achieved between predictions and measurement. As can be seen in Table 13, the beam analysis is adequate to predict second* compressional resonant response of a nosetip/waveguide system. Predictions of higher compressional resonant frequencies have larger deviations from measured values than the second compressional resonant response.

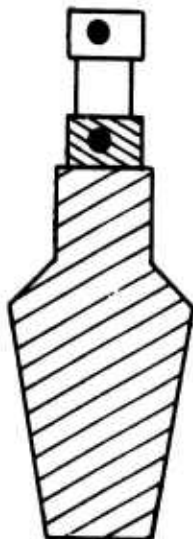
Having established the validity of the beam analysis approach for nosetip/waveguide systems, a series of calculations were made to demonstrate the accuracy of the method for a variety of nosetip forecone angles that represent nosetip shapes which are typical of flight shapes. Table 14 demonstrates the accuracy of the code in predicting first compressional resonant frequencies of a fixed length nosetip for forecone angles of 30°, 45°, 60°, and 90°. It should be noted that the deviation from experiment is always positive with the largest difference between deviations being 1.6 percent. These results indicate that the deviations could be reduced further by calibration of the elastic moduli to bring, for example, the 45° forecone angle case into direct agreement with the data.

To this point in the discussion, all examples presented have been for nosetip/waveguide systems at room temperature. When the nosetip is heated in an arc test or in flight the stiffness or elastic modulus of the material is altered. For very high temperatures typical of arc tests or flight, the elastic modulus of some materials can become a small fraction of the code value. Since resonant frequency is a function of the material stiffness (i.e., typically scales with the square root of the material stiffness) then resonant frequency can be strongly affected by temperature. Further, for some materials (e.g., tungsten) as the temperature rises, the material damping coefficient increases substantially. This alters both resonant frequency and the amplitude of the resonant response signal. Several beam analysis predictions of nosetip/waveguide systems under heating conditions were made during this study to demonstrate the validity of the beam modal analysis under actual flight type conditions.

Existing 1 MW tungsten arc test resonant frequency results are compared with first compressional beam analysis predictions in Figure 35. Agreement is seen to be good over the 20 second operating time period of the arc. The tungsten nosetip and waveguide configuration is similar to that given in Table 12. Elastic moduli properties were obtained from several sources and are summarized in Figure 36. The temperatures utilized to determine local elastic moduli along the length

*The second compressional nosetip/waveguide response for this system is equivalent in terms of body displacements to the first compressional response of the nosetip shown in Table 1. This is a result of the massive waveguide acting like an extension of the body. This is the frequency that would be tracked in flight.

TABLE 13. MSV NOSETIP WITH SINGLE CRYSTAL WAVEGUIDE



$$E = 9.704 \times 10^6 \text{ lbf/in}^2$$

$$\rho = 2.596 \times 10^{-4} \text{ (lbf-sec}^2\text{)/in}^4$$

$$\nu = 0.332$$

	Resonant Frequency (kHz)					
	Compressional			Flexural		
	I	II	III	I	II	III IV
SAP IV Beam	18.52	30.03	49.50	4.39	19.96	22.83 32.77
Experimental	17.42	29.93	44.60	4.08		
Percent Difference	5.9	1.7	9.9	7.1		

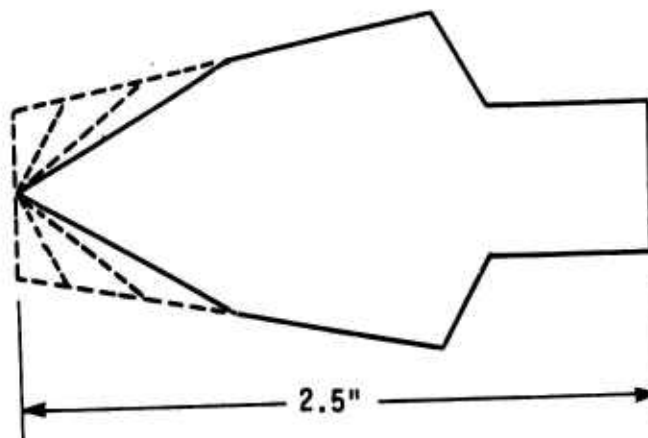
TABLE 14. ALUMINUM NOSETIP FIRST COMPRESSIONAL
RESONANT MODE FREQUENCIES

$$\rho = 2.596 \times 10^{-4} \text{ (lbf-sec}^2\text{)/in}^4$$

$$E = 9.704 \times 10^6 \text{ lbf/in}^2$$

$$\nu = 0.332$$

Forecone Angle	Frequency (kHz)		
	SAP IV	Measured	Percent Change
30	53.85	51.19	5.2
45	50.08	48.34	3.6
60	48.75	46.95	3.8
90	47.36	45.55	4.0



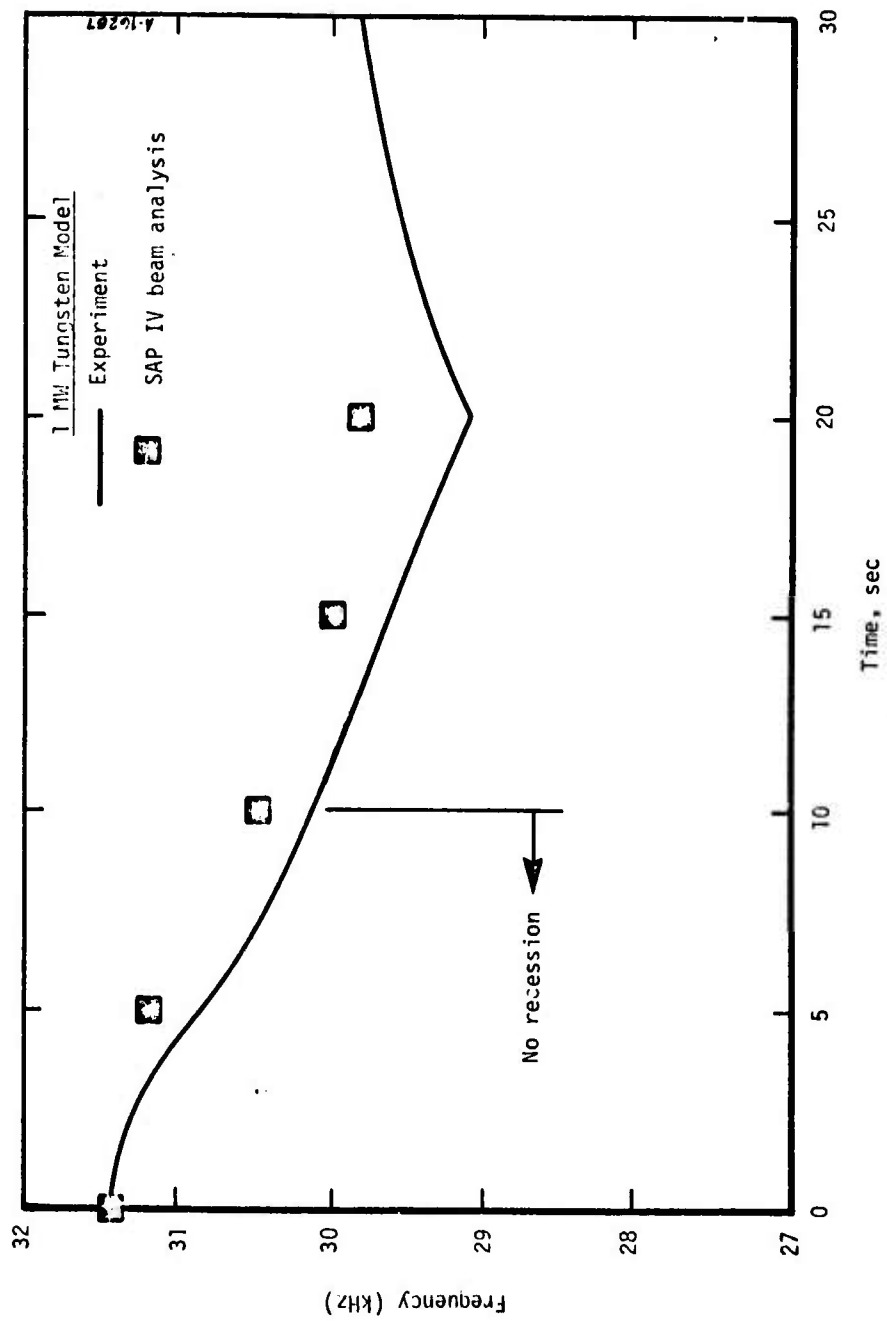


Figure 35. Comparison of 1 MW arc SAP IV beam analysis predictions and measurements for tungsten nosetip.

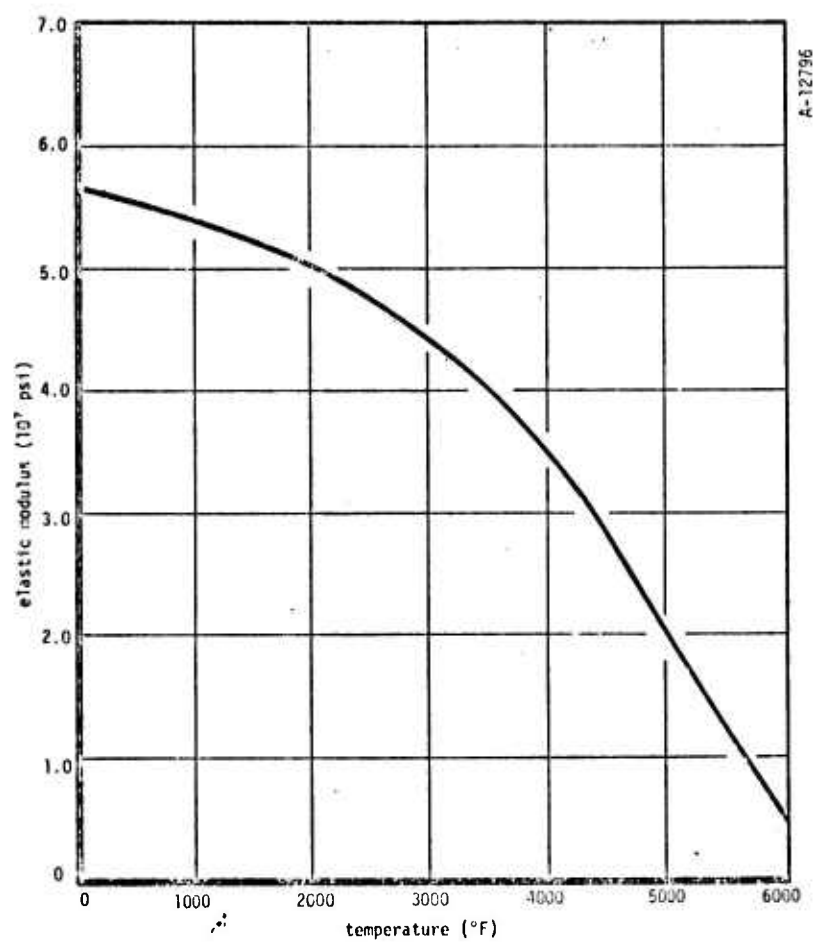


Figure 36. Tungsten elastic modulus as a function of temperature.

of the nosetip were generated using a one-dimensional heat conduction code and the measured nose and backface temperature during the arc test. Due to the one-dimensionality of the predictions, the accuracy of the temperature distributions shown in Figure 37 are not very good, and yet, predicted frequencies are close to measured values as is shown in Figure 35. This indicates that resonant frequencies are not very sensitive to temperature effects.

Under actual flight conditions the heating rate is much greater and the heating time at this rate much less than that in the 1 MW arc jet test facility. The amount of material at high temperature under these conditions is limited to a narrow region close to the surface. Therefore, the effect of temperature on resonant frequency for the flight case should be less than that experienced in the 1 MW arc jet. This is confirmed by the high heating rate 50 MW tungsten arc test results shown in Figure 38. The predicted frequencies are in good agreement with measured values even though "cold" elastic moduli values were utilized as input into the SAP IV beam analysis. It can then be concluded that for the high heating rates and short heating times encountered during flight, temperature effects for tungsten can be adequately handled by the beam analysis approach.

Unlike tungsten, there is evidence that carbonaceous materials increase in stiffness as temperature increases. This is illustrated in Figure 39 for a number of graphitic materials. However, at extremely high temperatures the stiffness of the material will eventually decrease as is indicated in Figure 39. Carbon/carbon fiber type materials, though significantly stronger than graphite itself, exhibit similar elastic moduli trends with temperature (Reference 5). Since temperatures within nosetips under flight conditions vary from relatively cold in-depth to extremely hot near the surface then it is expected that portions of the nosetip will have increased stiffness, whereas other sections will have reduced stiffness. On the whole, it is expected that local temperature effects will tend to cancel each other leaving the first compressional resonant frequency relatively unchanged from its cold value. This assumption is substantiated in Figure 40 by the plot of measured first compressional frequency versus time for the carbon/carbon nosetip in the 1 MW arc. The nosetip and waveguide system for this case is similar to that presented in Table 12. During the test the carbon/carbon material at the surface was heated to very high temperatures. Negligible recession occurred during the test period and, therefore, most of the frequency change is a result of temperature effects. Neglecting the initial abrupt drop in frequency shown in Figure 40, it can be seen that as the model is heated the frequency first rises as stiffness increases then falls as the surface temperature rises to very high values. Finally, as the steady state is approached the entire nosetip becomes hot, driving up the frequency. The variation in frequency reaches a maximum of

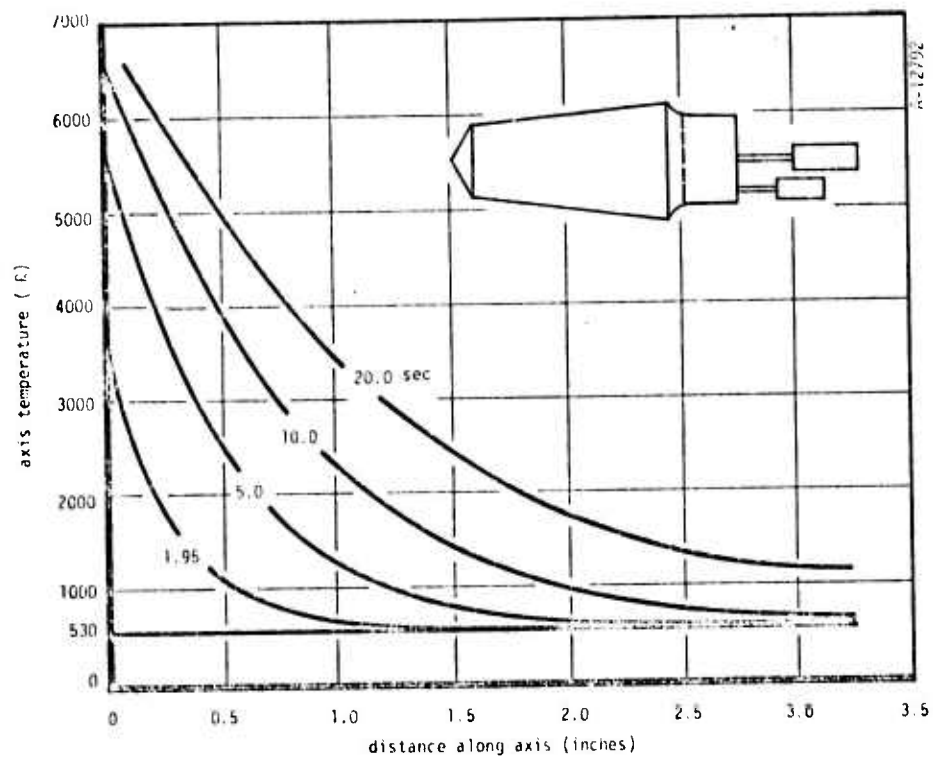


Figure 37. Predicted 1 MW arc tungsten temperature distributions as a function of time.

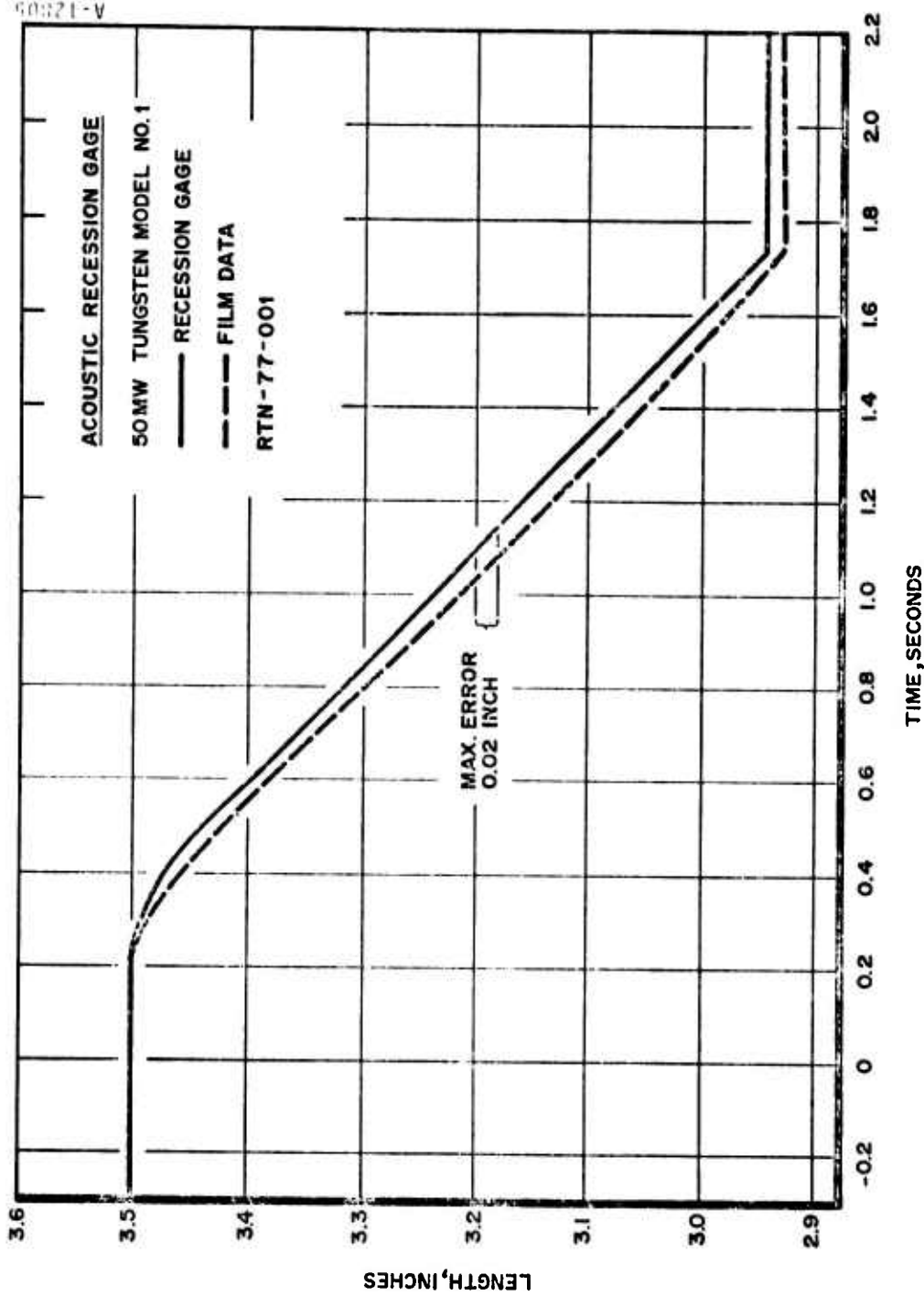


Figure 38. Comparison of 50 MW arc SAP IV beam analysis predictions and measurements for a tungsten nosetip.

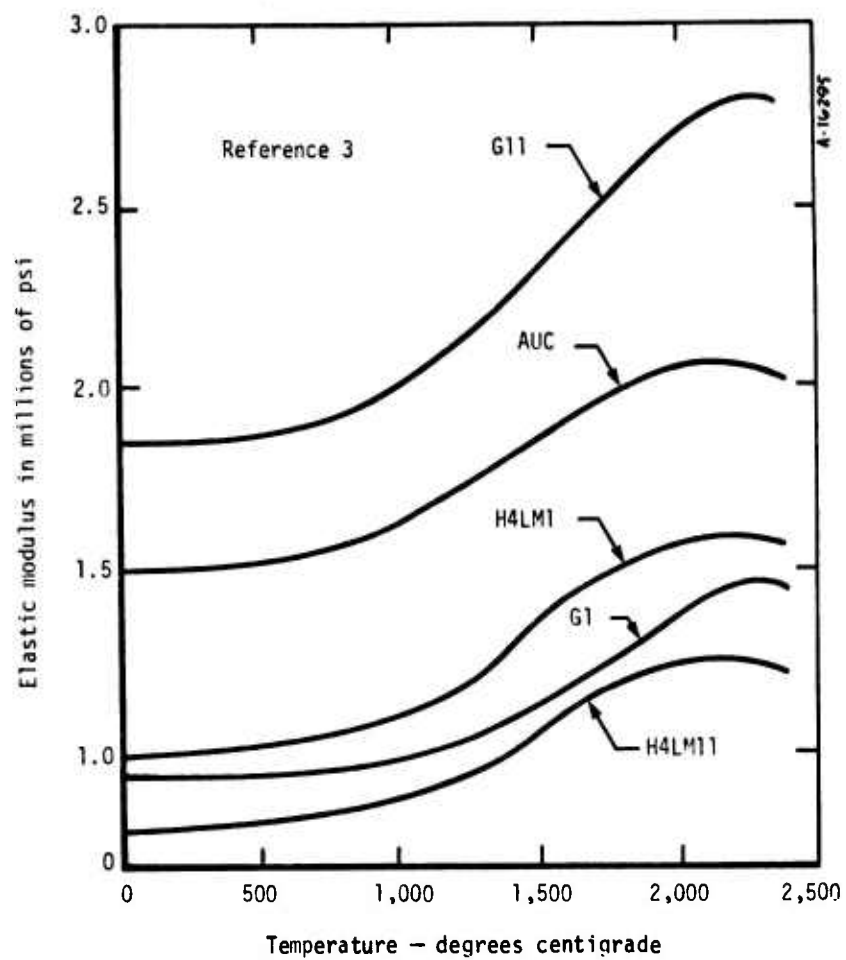


Figure 39. Elastic modulus versus temperature for representative commercial graphites.

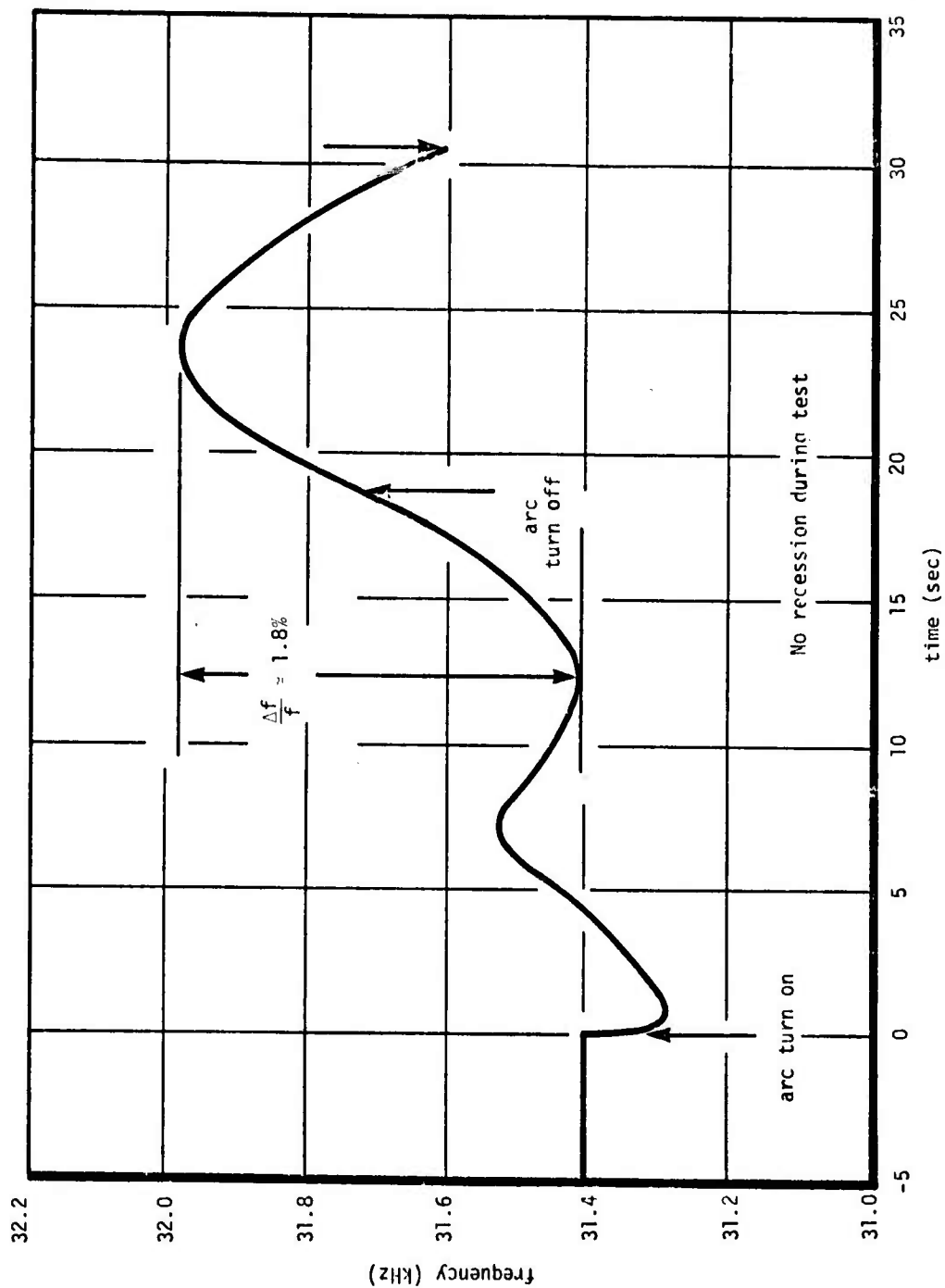


Figure 40. One MW arc test results for a carbon/carbon nosetip.

1.8 percent during the heating event. In terms of uncertainty in length measurement,* this frequency change is negligible.

These results indicate that carbon/carbon nosetip resonant frequency is not a sensitive function of temperature. For high heating rate cases typical of flight, this conclusion should be even more applicable. This is illustrated by the high heating rate 50 MW arc test results, which show good correlation with data in Figure 41, even without any correction for temperature.

4.3.1.2 Dual Mode Gauge

In the previous section, the relationship between a single resonant mode frequency and overall nosetip length was discussed. Predictions and measurements of first compressional resonant mode frequencies as a function of length indicate that there is sufficient sensitivity to accurately infer length from measured frequency. Given two resonant mode frequencies, simultaneous shape and nosetip overall length can be established. As in the overall nosetip length measurement approach, the first flexural or compressional resonant mode is selected as one of the frequencies to be measured. Previous studies have shown that the fourth flexural resonant mode frequency in combination with the first flexural will provide the most sensitivity for determining both shape and length. However, the sensitivity for measuring shape is not as great as that for measuring length. Therefore, the analysis approach must be reexamined to determine if accuracy is sufficient to accurately infer shape from frequency measurements. Figure 42 gives the beam analysis predictions of the first and fourth flexural resonant frequencies of an aluminum nosetip as a function of midpoint length. Midpoint length is defined as the measured length from the plug end of the nosetip to the intersection of the major cone angle bisector with the nosetip forecone face (see schematic in Figure 42). From Figure 42 it can be seen that the first flexural resonant frequencies fall on a single line for all nosetip forecone angles, whereas the fourth flexural frequencies are spread out over a frequency band which is a function of a nosetip forecone angle and midpoint length. The frequency band is not very wide, particularly for the blunter forecone angles. Utilizing the results of Figure 42, Figure 43 illustrates the shape uncertainty produced as a result of a small 1-percent frequency uncertainty. These results indicate that accurate shape inference for blunt nosetips require accurate predictions of both first and fourth flexural frequencies.

Predictions made for the single mode acoustic gauge have demonstrated the validity of using the SAP IV beam analysis approach to determine first flexural resonant mode frequencies. However,

* Length uncertainty is directly proportional to frequency uncertainty for simple bars (i.e., $\Delta L/L \propto -\Delta f/f$).

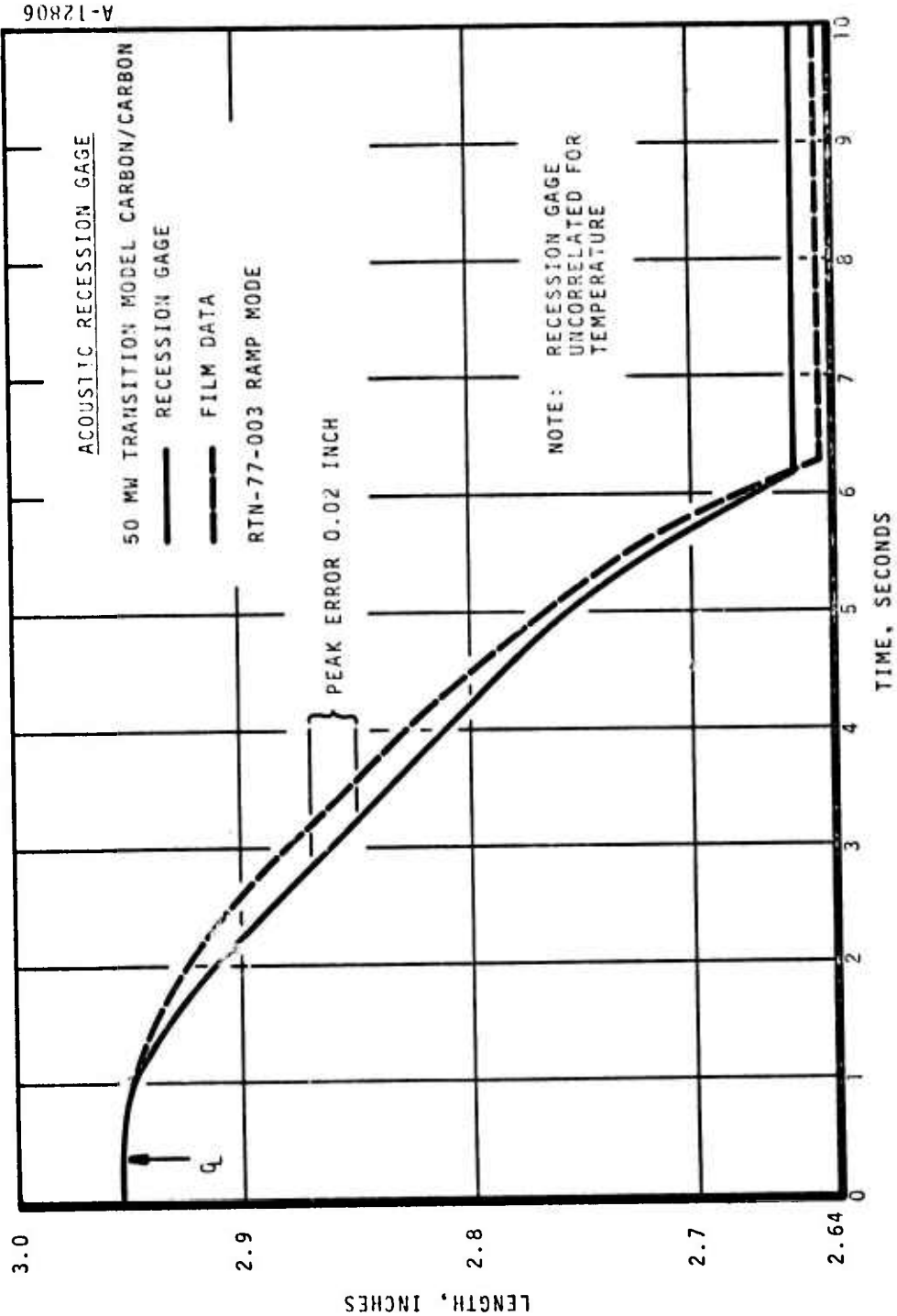


Figure 41. Comparison of 50 MW arc SAP IV beam analysis predictions and measurements for a carbon/carbon nosetip.

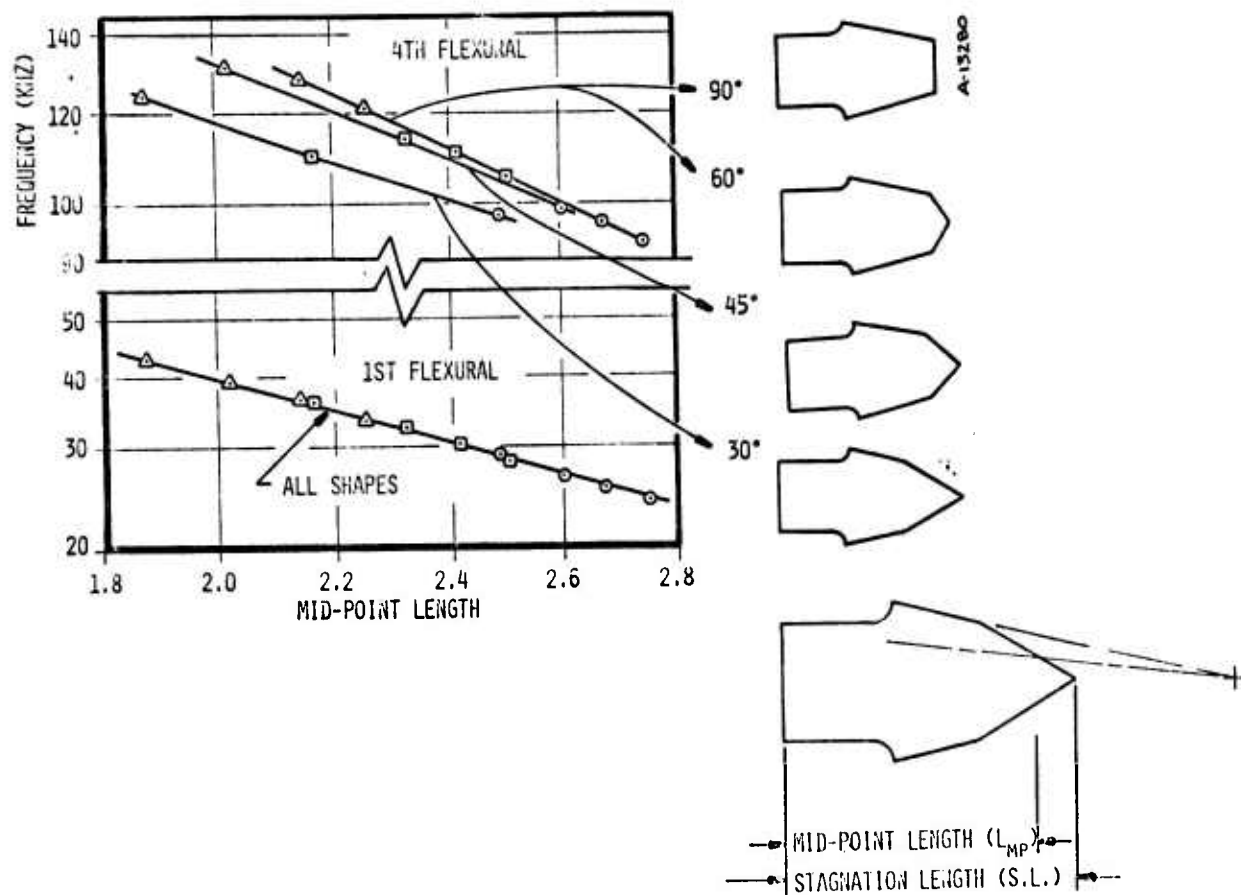


Figure 42. First and fourth flexural resonant frequencies versus midpoint length.

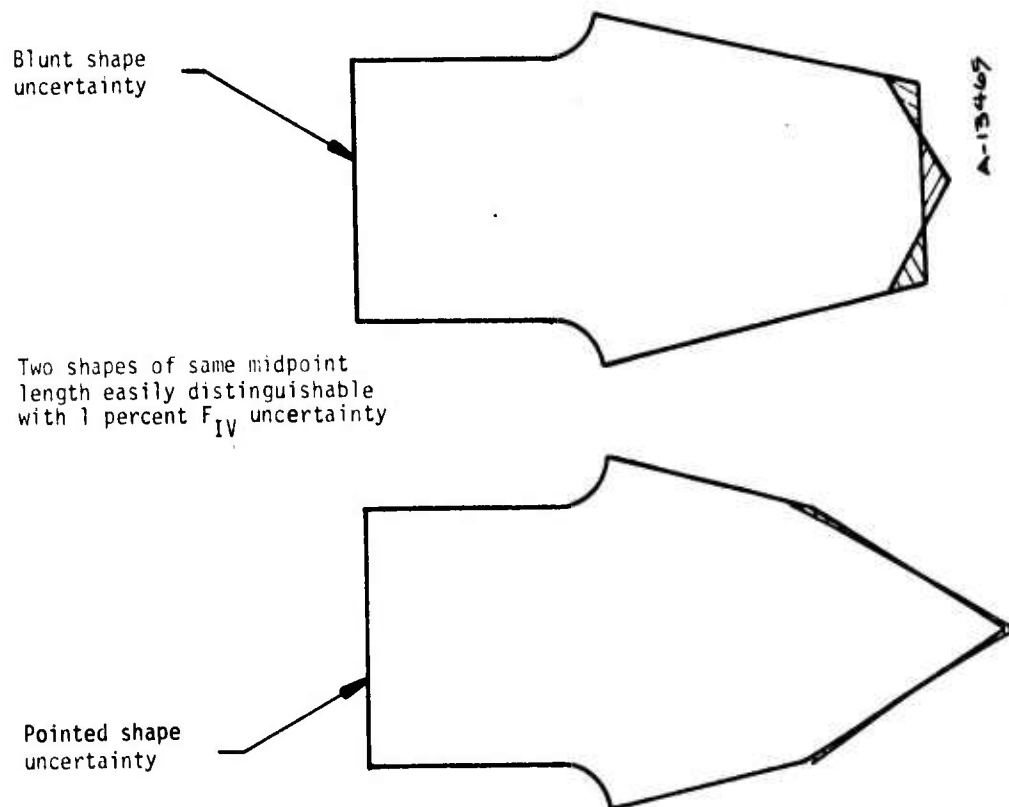


Figure 43. Shape uncertainty as a result of predicted frequency uncertainty.

SAP IV beam element predictions of higher order flexural or compressional mode frequencies are consistently higher than measured data. This is illustrated in Table 15, where beam analysis predictions and measurements of several flexural and compressional resonant mode frequencies for an aluminum nosetip of 30°, 45°, 60°, and 90° forecone angles are compared. These results demonstrate the increased deviation between predicted and measured frequencies for the higher order modes. A probable cause for this deviation is that the beam elements do not allow sufficient distortions to adequately model the three-dimensional solid body displacements produced at the higher frequency modes. Because of this restriction of the degrees of freedom, this causes the body to be artificially "stiff", increasing the predicted resonant frequency above the measured values.

To test the artificial stiffness hypothesis, a two-dimensional analysis of a nosetip-type shape was carried out, utilizing both SAP IV beam elements and the more sophisticated SAP IV quadrilateral brick elements. The brick elements model the detailed displacement in two-dimensions, whereas the beam elements only give displacements along the axis of the body. As shown in Table 16, the frequencies predicted using quadrilateral brick elements were lower than those using the beam elements. Also, the detailed brick element analysis gave additional resonant modes which were not predicted by the beam analysis. These are nonclassical beam type vibrations which, like the results shown in Figure 44, exhibit considerable distortion of initially flat planes. These vibrations may account for several resonant mode peaks found experimentally that cannot be identified with classical beam type vibrations as discussed previously.

Even though the SAP IV quadrilateral brick element planar calculation demonstrated the value of applying a more sophisticated element approach to calculate higher order modes for shape determination, the large increases in problem setup and computer time for the two-dimensional case precluded the use of SAP IV on a large matrix of three-dimensional cases. A search was then made to find a finite element code which, for a reasonable cost, could perform a detailed and accurate analysis of higher order axisymmetric nosetip resonant modes. A limited search uncovered the DIAL (Reference 6) and Shell Shock (Reference 7) codes, which nominally fit the analysis and cost objectives. Both utilize a Fourier decomposition of the flexural modes of axisymmetric bodies. This approach reduces the three-dimensional acoustic response problem (which SAP IV solves directly) to a much simpler two-dimensional problem. The corresponding problem setup and computer costs are thereby reduced significantly.

To check the relative accuracy of the SAP IV beam, DIAL and Shell Shock analyses, resonant mode calculations for a truncated aluminum cone were carried out and the predicted resonant frequencies compared. As indicated in Table 17, DIAL and Shell Shock resonant frequency predictions are

TABLE 15. COMPARISON OF SAP IV BEAM ANALYSIS RESONANT MODE FREQUENCY PREDICTIONS
AND DATA FOR VARIOUS NOSE SHAPES

$$E = 9.704 \times 10^6 \text{ lbf/in}^2$$

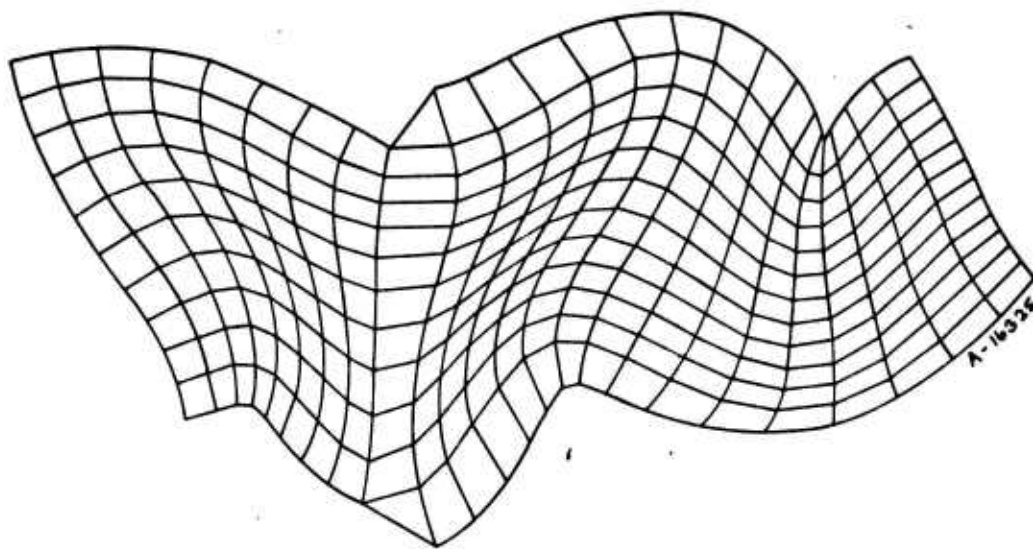
$$\rho = 2.596 \times 10^{-4} \text{ (lbf-sec}^2\text{)/in}^4$$

$$\nu = 0.332$$

	Forecone Angle	Resonant Mode Frequencies of 2.5-Inch Long Aluminum Model (kHz)						
		Compressional		Flexural				
		I	II	I	II	III	IV	
Test Results	90	45.55	75.88	25.66	47.23	67.46	92.8X	
	60	46.95	78.69	27.60	50.30	69.43	95.1X	
	45	48.34	81.30	29.32	53.00	70.76	95.8X	
	30	51.19	84.70	31.96	54.95	70.40	93.9X	
Analysis	90	47.36	79.43	28.51	54.86	81.36	105.7X	
	60	48.75	82.53	30.43	58.39	85.27	111.0X	
	45	50.08	85.49	32.13	61.23	87.95	114.0X	
	30	53.85	86.39	35.99	63.56	93.22	110.2X	
Percent Difference	90	4.0	4.7	11.1	16.2	20.6	13.9	
	60	3.8	4.6	10.3	16.1	22.8	16.7	
	45	3.6	5.2	9.5	15.5	24.3	19.0	
	30	5.2	2.0	12.6	15.7	32.4	17.3	

TABLE 16. COMPARISON OF SAP IV BEAM AND QUADRILATERAL BRICK ELEMENT PREDICTIONS

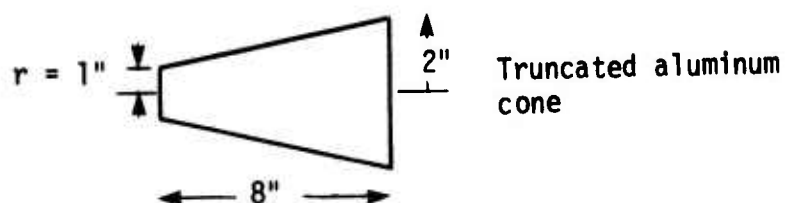
Approach	Resonant Mode Frequencies of a 2.5-Inch Aluminum Noretip (kHz)					
	Compressional		Flexural			
	I	II	I	II	III	IV
Beam	41.974	76.575	28.655	54.471	79.917	104.12
2-D Plane	40.591	72.129	25.560	44.563	61.743 65.602	86.276
Percent Difference	0.034	0.062	0.121	0.222	0.294 0.218	0.207



Modal frequency, 86.276 kHz

Figure 44. SAP IV quadrilateral brick element analysis.

TABLE 17. COMPARISON OF RESONANT MODE PREDICTIONS
UTILIZING SAP IV, DIAL AND SHELL SHOCK



Type ^a	Frequency (kHz)		
	SAP IV Beam ^b	DIAL	Shell Shock
t ₁		9.24	9.41
l ₁	13.77	13.57	13.56
t ₂		16.88	17.16
t ₃		24.71	25.04
l ₂	26.62	25.39	25.31
l ₃	39.58	27.88	28.39
t ₄		32.51	32.77
l ₄	52.47	34.29	33.74
t ₅		40.19	
l ₅		40.21	
f ₁	7.89		6.85
f ₂	16.97		14.10
f ₃	26.40		21.30
f ₄	35.48		25.60
f ₅	44.27		29.70
f ₆	52.74		31.50
f ₇			33.40
f ₈			36.80

^at = torsion; l = compressional; f = flexural

^bMay not correspond to l₁, l₂, ..., etc.

quite close to each other whereas SAP IV predictions are consistently higher, particularly for the higher order modes. Further, SAP IV beam and DIAL predictions of resonant frequencies for an aluminum nosetip are compared with measured values in Table 18. Deviations between SAP IV beam analysis results and data vary from -1.3 to 21 percent over the range of resonant modes predicted. The deviations of DIAL predictions from data varied from -3 to -6 percent. It should be noted that the material properties utilized in both calculations were identical. If material properties for the calculations were adjusted to give "exact" agreement for first flexural mode then, as shown in Table 18, the DIAL code would have much better agreement with data than the SAP IV analysis. Also, the DIAL code predicts two fourth flexural mode type responses consistent with measurement, whereas the SAP IV beam element only predicts one mode in that frequency range. Examining the displacement plots produced by the DIAL code shown in Figure 45, it can be seen that the two fourth flexural responses are quite similar except for some detailed displacements located near the outer edges of the nosetip and at the cone/plug juncture. The SAP IV beam analysis is not capable of defining these regions and, therefore, only a single resonant mode is found.

These comparisons clearly demonstrate the superiority of the DIAL and Shell Shock codes over the SAP IV beam analysis method for predicting shape.

Besides demonstrating the accuracy of the various methods, the truncated cone calculations also provide some information on the relative costs of the different methods. Table 19 summarizes the estimated relative costs of the different methods for problem setup, run and generation of displacement plots for the truncated cone case. Also included in Table 19 are some general comments relating to the methods. Based on a SAP IV two-dimensional brick element calculation, a rough order of magnitude cost estimate for a fully three-dimensional SAP IV calculation is included in Table 19. Except for a few baseline predictions, the cost penalty of the SAP IV three-dimensional method is prohibitive for a large number of cases.

Because of the easy problem setup and moderate cost, the DIAL code is applied to all dual mode gauge calculations requiring accurate higher frequency mode and detailed displacement predictions. The SAP IV beam analysis procedure is emphasized for all other calculations where shape predictions are not required.

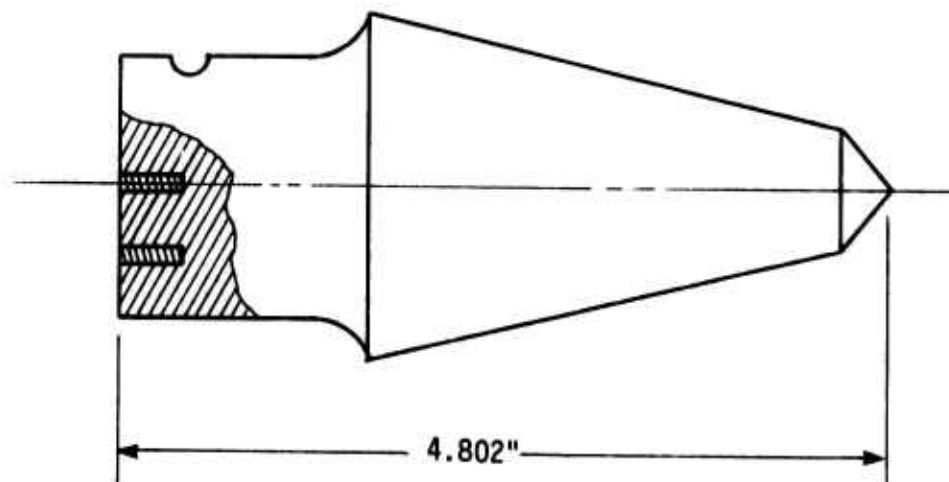
4.3.2 Applications

During this study a large number of resonant acoustic response calculations were made. This section focuses on the results of calculations which demonstrate the sensitivity of dual mode gauge frequencies to temperature and nosetip length and shape.

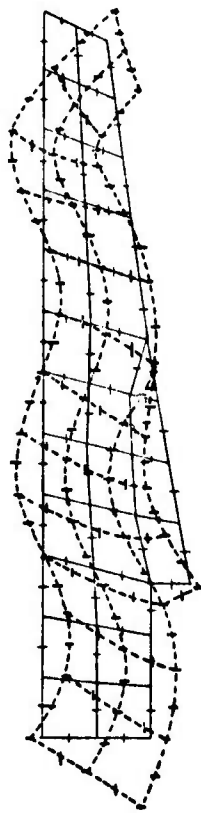
TABLE 18. COMPARISON OF SAP IV BEAM AND DIAL PREDICTIONS AND MEASUREMENTS

Compressional Frequencies (kHz)							
Mode	Measured	Beam	%	Adjusted %	DIAL	%	Adjusted %
1	25.51	25.19	- 1.3	- 5.9	23.90	-6.0	XXXX
2	42.97	44.22	+ 2.9	- 1.7	41.30	-4.0	XXXX
3	59.55	61.73	+ 3.7	- 0.9	57.20	-4.0	XXXX
4		82.07			68.50		

Flexural Frequencies (kHz)							
Mode	Measured	Beam	%	Adjusted %	DIAL	%	Adjusted %
1	11.66	12.20	+ 4.6	0.0	10.94	-6.0	XXXX
2	23.00	24.77	+ 7.7	3.1	22.19	-4.0	XXXX
3	34.63	37.97	+ 9.6	5.0	33.39	-4.0	XXXX
4	45.62	55.22	+21.6	16.4	44.32	-3.0	XXXX
4	47.78	55.22	+15.6	11.0	46.36	-3.0	XXXX



Frequency: 44.3 kHz



Frequency: 46.4 kHz

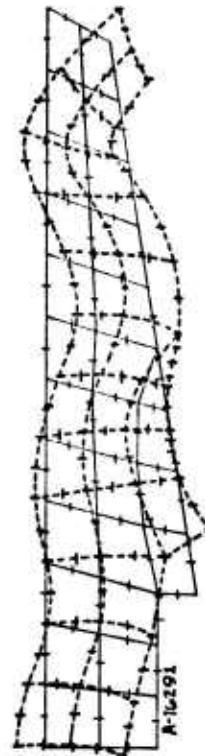


Figure 45. Fourth flexural beam type responses (DIAL code).

TABLE 19. RELATIVE COSTS OF PREDICTIONS UTILIZING
SAP IV, DIAL, AND SHELL SHOCK CODES

	Relative Cost	Comments
SAP IV Beam	1.0 ^a	Easy problem setup, cheap, adequate for low frequency modes, can model 3-D waveguides, isotropic material properties
SAP IV Three-Dimensional	~30	Difficult problem setup, expensive, accurate for all modes, can model 3-D waveguides, orthotropic material properties
DIAL	2.5	Easy problem setup, moderate cost, accurate for all modes, axisymmetric waveguide only, orthotropic material properties
Shell Shock	4.0	Moderate problem setup, moderate cost, accurate for all modes, axisymmetric waveguides only, orthotropic material properties

^aBaseline

4.3.2.1 Sensitivity of Higher Order Resonant Modes to Temperature

In Section 4.3.1 the impact of temperature on the first compressional resonant mode frequency was determined for tungsten and carbon/carbon nosetips. It was found that temperature effects could be accounted for in the predictions for tungsten and that no correction was required for carbon/carbon materials. For dual mode gauge purposes the effect of temperature on the relative position of the frequency maps is needed. This is of importance because the relative position between the frequencies establishes shape, and accurate predictions of frequency position are needed to reduce shape uncertainty to reasonable levels.

To assess the impact of temperature effects on relative frequency position the SAP IV beam analysis results for the 1 MW tungsten arc test model were reexamined. Geometry of the nosetip and waveguide are given in Table 1 and elastic modulus and temperature distributions as a function of time are given in Figures 36 and 37. Table 20 gives the results of the predictions for 0- (cold) second case are -0.59 to -4.74 at 5 seconds, and -3.0 to -9.9 at 10 seconds. The variation in relative position between the first and fourth flexural resonant mode frequency is 1.2 percent at 5 seconds and -1.2 percent at 10 seconds. If no temperature correction were applied, then the uncertainty of nosetip shape would be approximately that shown in Figure 33 for 1 percent uncertainty. With some correction for temperature the shape uncertainty could be reduced even further.

For carbon/carbon nosetips, temperature corrections are not needed for establishing nosetip length from first compressional mode frequency. However, as in the case of tungsten, dual mode gauge applications require accurate predictions to reduce nose shape uncertainty. To assess the impact of temperature on the relative spacing of first and fourth flexural resonant mode frequencies, SAP IV beam analysis predictions were carried out on nosetip type shapes utilizing cold and hot carbon/carbon material properties. Both sharp and blunt ablated nosetip shapes were calculated to ensure bounding the temperature effect. Shapes and internal temperature distributions were generated using the SNAP code. Material property variation with temperature, given in Figure 46, was a compilation of several sources of data (Reference 5). The resonant mode frequencies calculated for the blunt and sharp shapes under cold and hot conditions are given in Table 21. Results for the sharp shape indicate that the relative position of the first and fourth flexural frequencies only varies by 0.4 percent in going from hot to cold conditions. The blunt shape variations of relative position is 1.2 percent for the first and fourth flexural frequency. As in the tungsten nosetip case, the shape uncertainty created by roughly 1 percent frequency uncertainty would be similar to that given in Figure 33. With some correction for temperature the shape uncertainty could be reduced below that illustrated in Figure 33.

TABLE 20. EFFECT OF TEMPERATURE ON HIGHER ORDER MODES

Resonant Mode Frequencies of a Tungsten Nosetip on a 1 MW Tungsten Arc Test Model					
Mode ^a (cold)	t = 0	t = 5 sec	% 10 sec Change	t = 10 sec	% 0-10 sec Change
f ₁	14.53	14.36	-0.59	13.94	-4.1
f ₂	30.48	29.79	-2.27	28.21	-7.5
L ₁	31.19	30.93	-0.94	30.25	-3.0
f ₃	48.11	46.69	-4.74	43.37	-9.9
L ₂	55.64	54.46	-3.97	51.67	-7.1
f ₄	66.01	64.30	-1.90	64.11	-2.9

^af = flexural

L = compressional

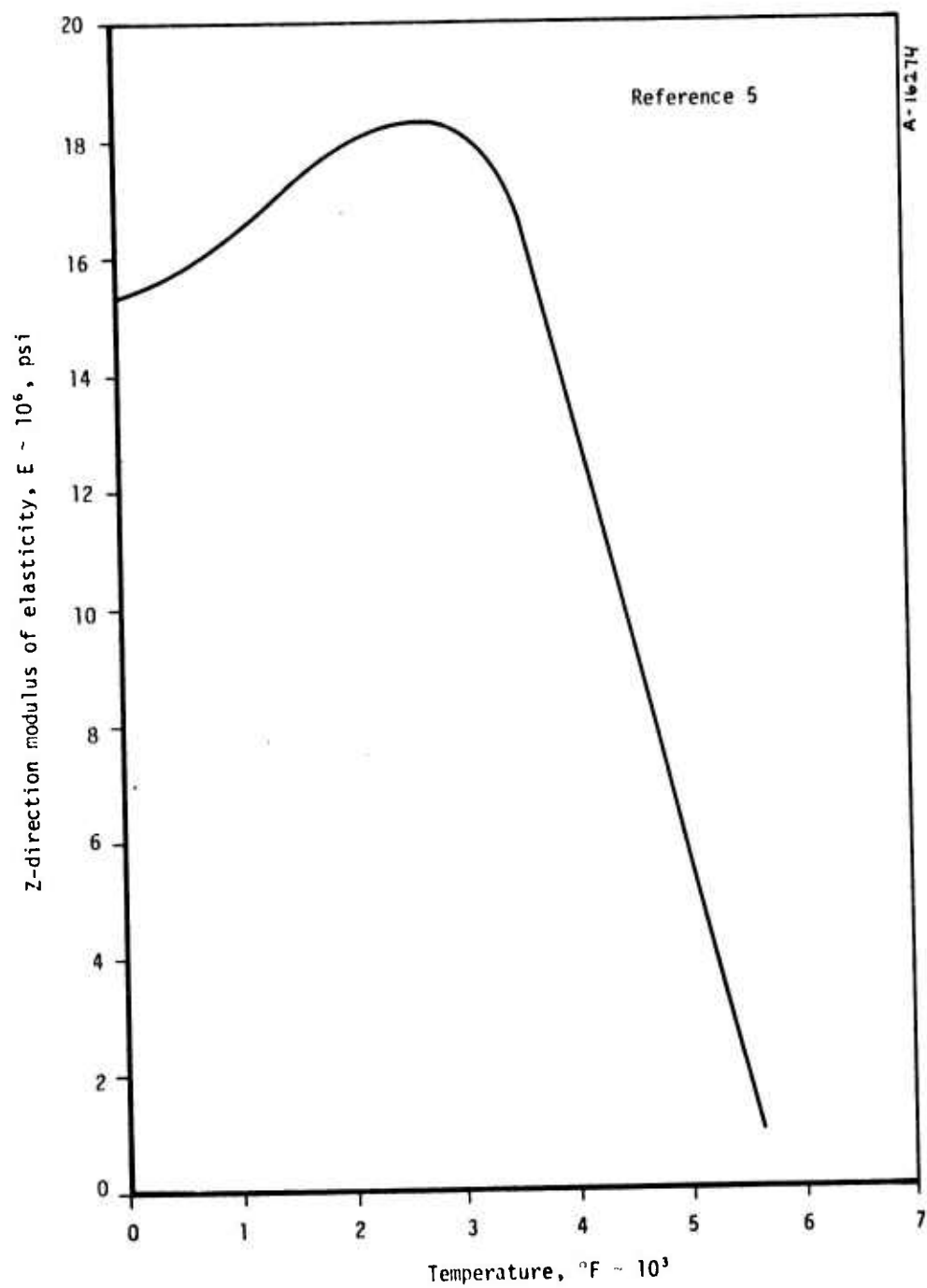


Figure 46. Elastic modulus of carbon/carbon material versus temperature.

TABLE 21. SENSITIVITY OF CARBON/CARBON FLIGHT CONFIGURATION RESONANT FREQUENCIES TO TEMPERATURE

Resonant Mode Frequencies (kHz) of Blunt Shapes											
Analysis Type	Compressional				Flexural						
	I	II	III	IV	I	II	III	IV	V	VI	VII
Cold	27.079	42.262	70.200	86.950	14.803	31.799	44.717	59.534	75.529	81.036	95.701
Hot	27.287	42.887	71.410	87.832	14.892	32.278	45.229	60.154	74.248	82.134	97.438
Hot/Cold	1.00768	1.01479	1.01724	1.01014	1.00601	1.01506	1.01145	1.01881	1.00978	1.01355	1.01815

Resonant Mode Frequencies (kHz) of Sharp Shapes											
Analysis Type	Compressional				Flexural						
	I	II	III	IV	I	II	III	IV	V	VI	VII
Cold	25.131	37.953	60.952	79.600	13.097	25.827	38.482	47.457	58.867	70.331	77.269
Hot	25.253	38.223	61.693	80.300	13.145	26.094	38.847	47.880	58.696	68.990	76.156
Hot/Cold	1.00485	1.00711	1.01216	1.00000	1.00366	1.01034	1.00948	1.00891	1.99710	1.98093	1.98560

4.3.2.2 Sensitivity of Carbon/Carbon

In the operation of the acoustic gage either one or two resonant mode frequencies are tracked as a function of time. The magnitude of these frequencies alters as the nosetip shape, length and material properties change. A primary purpose of analysis is to assess the sensitivity of the resonant mode frequencies to nosetip shape and length changes. From the predictions it can be established if sufficient sensitivity is available for inferring nosetip shape and length even before the nosetip/waveguide system is manufactured. Also, the predictions indicate if any resonant frequencies will interfere or cross during nosetip shape and length change. The interference of resonant frequencies can make frequency tracking difficult during flight.

As an example of the assessment of the effects of nosetip shape and length changes on resonant mode frequencies, DIAL code predictions of carbon/carbon nosetips resonant frequencies are presented in Figures 47 and 48. Figure 49 gives the nosetip geometry and material properties input into the code for this case. The geometry is characteristic of those typically employed during subscale, subvelocity flight tests for material screening purposes. For simplicity, waveguides are not included in the predictions. Two overall lengths, 4.5 and 5.5 inches, at four forecone nose angles, 80°, 60°, 45°, and 30°, were calculated to characterize the resonant frequencies under the assumed nosetip shape and length change. Figure 47 presents the results in terms of midpoint length whereas Figure 48 gives the results in terms of the "corner" length (length from the nosetip plug end to the intersection of the nosetip major cone and forecone faces). It is apparent that results presented in terms of "corner" length give a better straight line fit of all first flexural resonant frequencies. This makes it easier to interpret the fourth flexural frequency results in terms of sensitivity to nose shape. However, it should be noted that for dual mode gage applications, there is nothing fundamental or unique about the presentation of the data in this manner. For flight data reduction purposes a much more precise map of resonant frequencies in terms of overall nosetip length is probably more appropriate than the maps presented in Figures 47 and 48.

From Figure 47 it can be seen that, at a 4.25-inch corner length, an 8.5-, 1.1-, and 1.7-kHz fourth flexural frequency change is produced by going from 30° to 45°, 45° to 60°, and 60° to 80° nosetip forecone angles, respectively. These frequency bands represent 13.7, 1.6, and 2.5 percent of the absolute frequency found at the initial forecone angle. If it is assumed that a frequency error of 1 percent can exist between modal analysis predictions and measurements in flight due to:

- Temperature effects on material properties
- Nonconical nose shapes

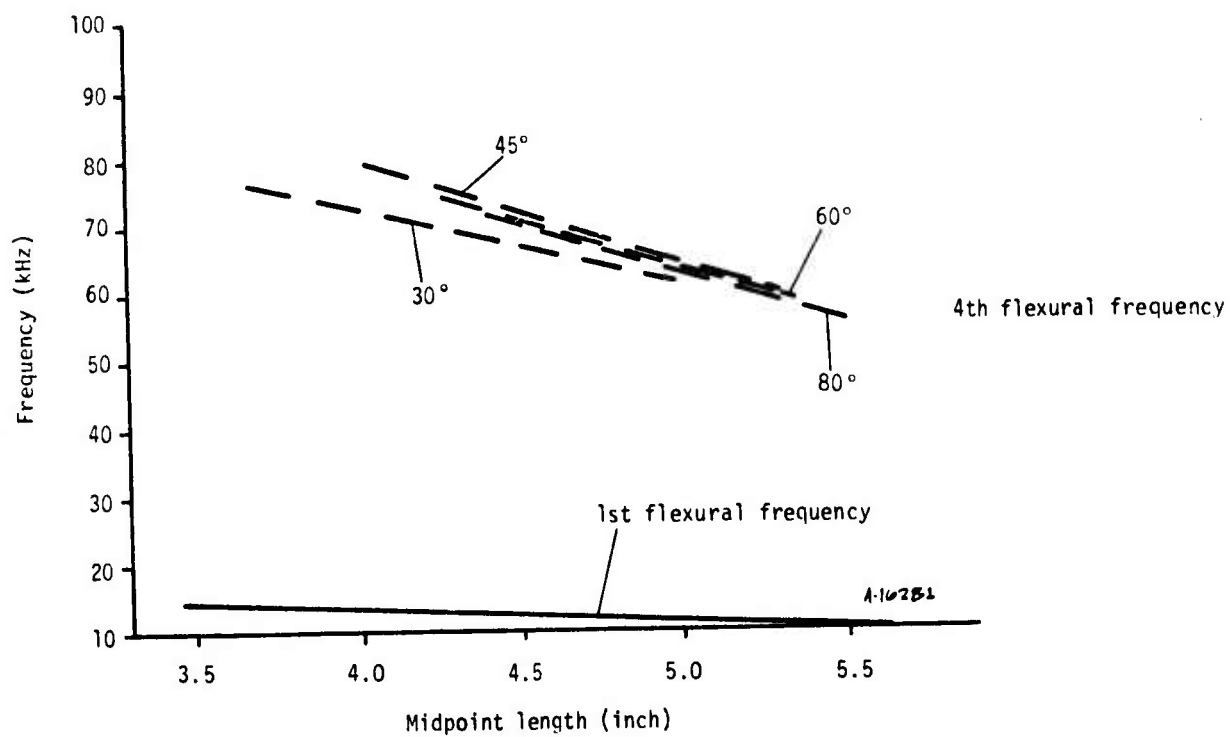


Figure 47. First and fourth flexural resonant mode frequencies vs. midpoint length.

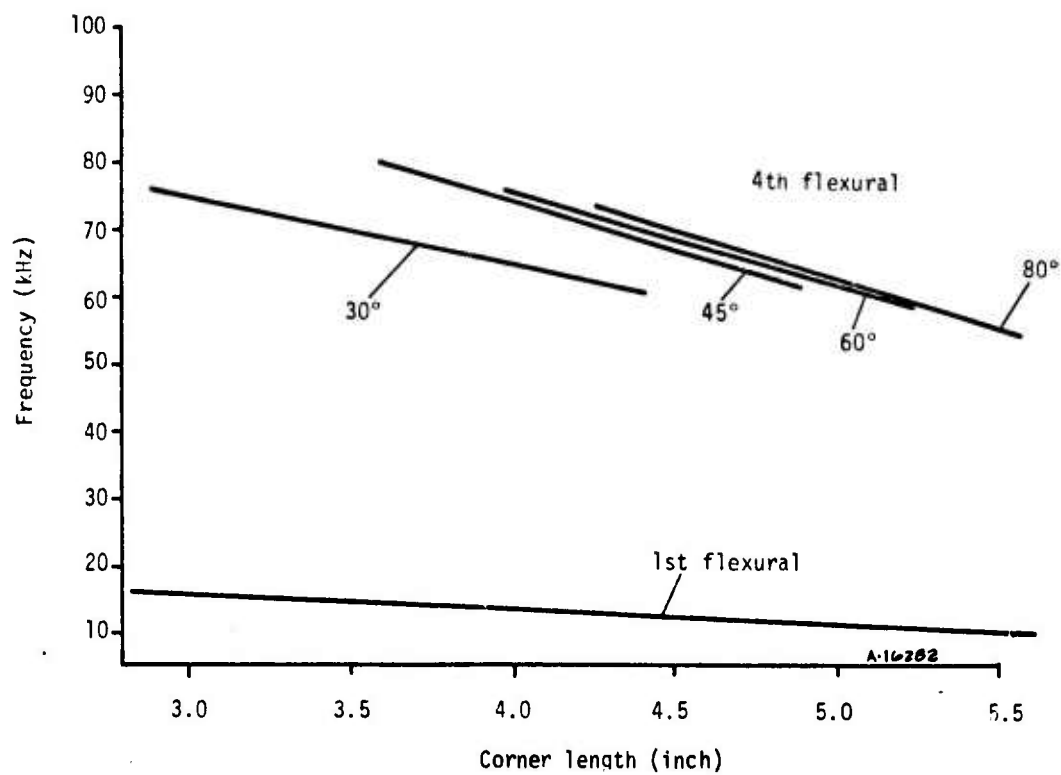
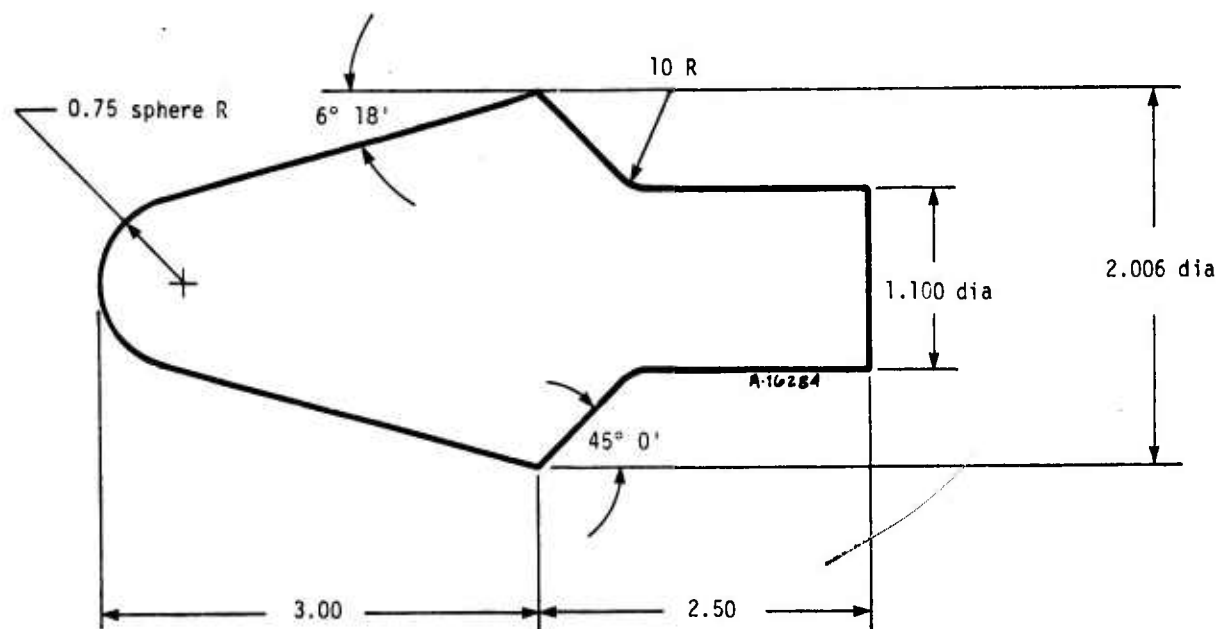


Figure 48. First and fourth flexural resonant mode vs. corner length.



Material Properties

$$E = 15.25 \times 10^6 \text{ lbf/in}^2$$

$$\rho = 1.713 \times 10^{-4} \text{ (lbf-sec}^2\text{)/in}^4$$

$$\nu = 0.097$$

Figure 49. Carbon/carbon nosetip geometry and material properties.

- Complex waveguides
- Nonideal boundary conditions
- Forced response and damping
- Crystals and electronics

then a forecone angle uncertainty can be defined. Table 22 summarizes the angle uncertainties produced by a 1-percent fourth flexural frequency uncertainty. The angle uncertainties are only average values for the specified nose angle intervals. Predictions for several more forecone angles would yield a smoother distribution of angle uncertainty. From these results, it may be concluded that, when applied to the first and fourth flexural resonant modes of the above nosetip, the acoustic gage can determine sharp shapes with good accuracy and blunter shapes with less accuracy. The gage would certainly indicate whether the nosetip was sharp or blunt. For different selections of resonant mode frequencies or other nosetip/waveguide geometries and materials the above conclusion might be altered.

TABLE 22. NOSE ANGLE UNCERTAINTY DUE TO
FREQUENCY UNCERTAINTY

Nose Angle Band	Angle Uncertainty
30° - 45°	$\pm 1^\circ$
45° - 60°	$\pm 9^\circ$
60° - 80°	$\pm 8^\circ$

REFERENCES

1. "Acoustic Recession Gage Program Plan for the Parts, Materials, Processes Control Board," C/N 7141.206, May 10, 1976.
2. Bathe, K., Wilson, E. L., and Peterson, F. E., "SAP IV, A Structural Analyses Program for Static and Dynamic Response of Linear Systems," University of California Earthquake Engineering Research Center, Report EERC 73-11, June 1973.
3. Rafinejad, D. and Derbidge, T. C., "User's Manual: Sandia Nosetip Analysis Procedure (SNAP)," Aerotherm Acurex Corporation Report UM-74-58, December 1974.
4. Armstrong, P. E. and Brown, H. L., "Dynamic Youngs Modulus Measurements Above 1000°C on Some Pure Polycrystalline Metals and Commercial Graphites," Transactions of Metallurgical Society of A.I.M.E., Vol. 230, August 1964, pp. 962-968.
5. Köster, W., Z. Metallk., 1948, Volume 39, p. 1.
6. Iannuzzi, F. A., "SSN Thermal and Structural Test Report (Preliminary)," Southern Research Institute, letter report to J. Dodson, Aerotherm, March 1976.
7. Ferguson, G., "DIAL User's Manual," Lockheed Missiles and Space Corporation Report, in preparation.
8. Grant, J. E. and Gabrielson, V. K., "Shell Shock Structural Code," Sandia Laboratories Report SAND75-8013, April 1975.
9. Hartman, C. D., Foster, T. F., Eichorn, R. L., and Lundberg, R. E., "Acoustic Recession Gage Development during February - June 1975," Aerotherm Report TM-75-78, August 1975.
10. "Resonant Acoustic Recession Gage," SAMSO/Aerospace Briefing, Aerotherm C/N 7141-145, February 1976.
11. "Acoustic Recession Gage Bench Test Plan," CDRL Item A005, Aerotherm C/N 7141.263, June 1976.

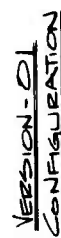
APPENDIX A
DETAIL HARDWARE DRAWINGS

TABLE OF CONTENTS FOR APPENDIX A

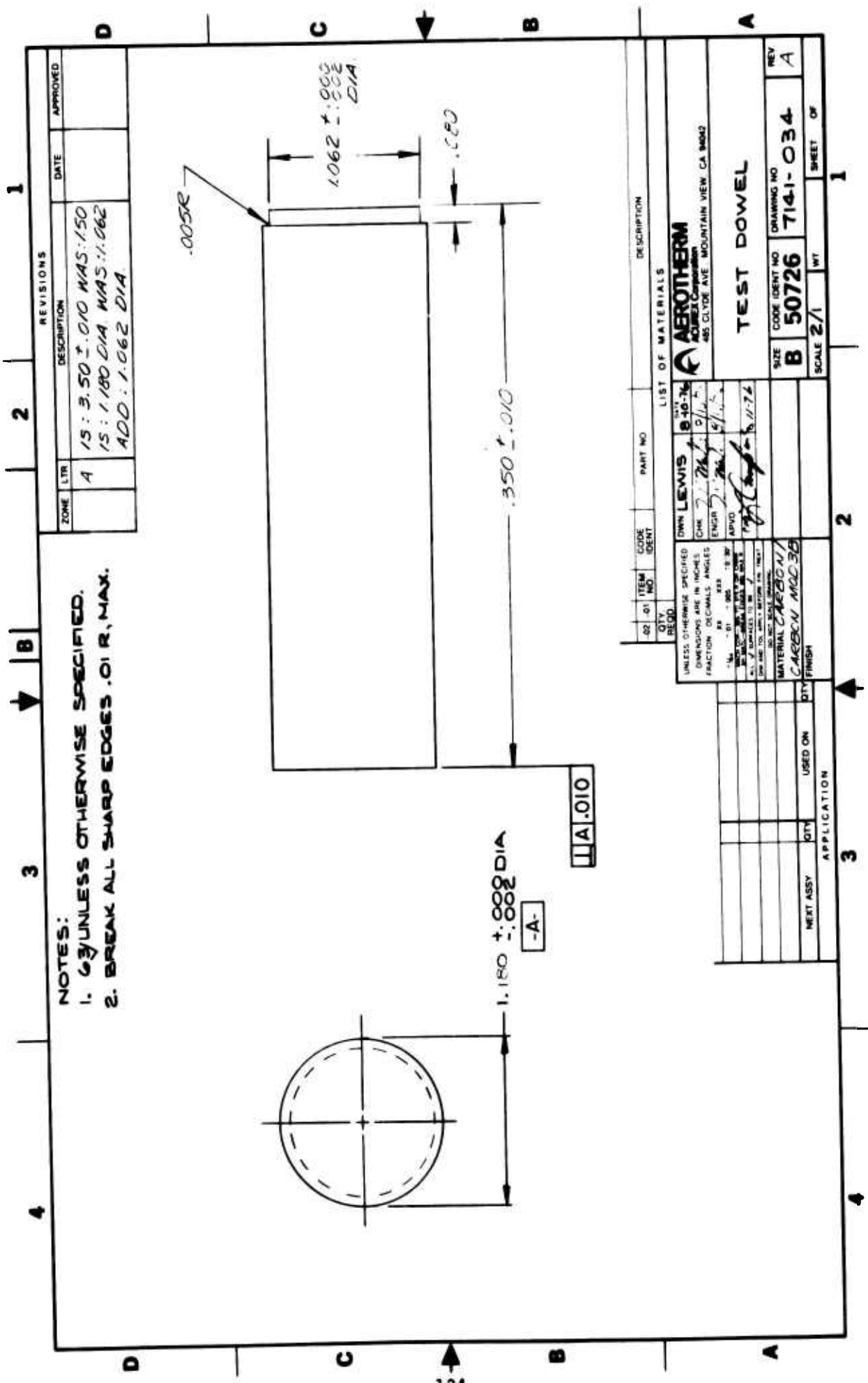
Description	Drawing No.	Page
MSV Nosetip Acoustic Gage Bench Test Model (Pre-Modifications)	7141-030	131
Flexural Receiver Back Mass (Mod I Assembly)	7141-032	132
Flexural Transmitter Back Mass (Mod I Assy)	7141-033	133
Test Dowel	7141-034	134
Concentric Flexural Waveguide (Mod I Assembly)	7141-035	135
Cover, Concentric Flexural Housing (Mod I Assembly)	7141-036	136
Concentric Flexural Housing (Mod I Assy)	7141-037	137
Ablative Washer - ARG 50 MW Arc-Jet Test Unit	7141-041	138
Acoustic Recession Gage, 50 MW Carbon/Carbon Tip - Nosetip	7141-042	139
Adapter - ARG 50 MW Test III	7141-043	140
Model Holder	7141-044	141
Acoustic Recession Gage, 50 MW Model Assembly	7141-045	142
Heat Shield - 1 MW	7141-046	143
Model Holding Fixture, Shake Test	7141-056	144
Receiver Back Mass - Mod I	7141-058	145
Transmitter Back Mass - Mod I	7141-059	146
Receiver Base - Mod I	7141-060	147
Gage Outer Case - Mod I	7141-061	148
Receiver Case - Mod I	7141-062	149
Transmitter Base and Pedestal - (Mod I Compressional)	7141-063	150
Flexural Acoustic Gage Assembly (Dual Mode Sensor) Mod I	7141-064	151
Compressional Acoustic Gage Assembly (Single Mode Sensor) Mod I	7141-065	152
Transmitter Electrode	7141-066	153
50 MW Nose Tip Test Assembly (Dual Mode Sensor)	7141-067	154
50 MW Nose Tip Test Assembly (Single Mode Sensor)	7141-068	155
Cable Support Tube	7141-069	156
Acoustic Recession Gage - 50 MW	7141-070	157
Holder - 1 MW	7141-072	158
Test Model - 1 MW	7141-073	159
Model Holder - 1 MW	7141-074	160
Mounting Flange - 1 MW	7141-075	161

TABLE OF CONTENTS FOR APPENDIX A (Concluded)

Description	Drawing No.	Page
1 MW Test Assembly - with Flexural Acoustic Gage (Dual Mode Sensor) Mod I	7141-076	162
Housing, Flexural Acoustic Gage - Mod II	7141-077	163
Housing, Flexural Acoustic Gage - Mod III	7141-078	164
Receiver Assembly - Compressional Acoustic Gage (Single Mode Sensor) Mod I	7141-079	165
50 MW-III Acoustic Gage Assembly (Single Mode Compressional Sensor) Mod II	7141-080	166
Flexural Acoustic Gage Assembly (Dual Mode Sensor) Mod IV	7141-081	167
Flexural Acoustic Gage Assembly (Dual Mode Sensor) Mod V	7141-082	168
50 MW-III Acoustic Gage Assembly (Dual-Single Mode Compressional Sensor) Mod III	7141-083	169
Flexural Acoustic Gage Assembly (Dual Mode Sensor) Mod III	7141-083	170
50 MW SSN/ARG Model 6 Assy	7141-085	171
50 MW SSN/ARG-6 Model Holder	7141-086	172
50 MW SSN/ARG-6 Noisetip	7141-087	173
Threaded Receiver Base Mod II Assembly	7141-088	174
Threaded Transmitter Waveguide	7141-089	175
50 MW-III Nose Tip Assembly (Single Mode Compressional Sensor)	7141-090	176
50 MW-III Nose Tip Assembly (Dual Mode Compressional Sensor)	7141-092	177
Acoustic Recession Gage Carbon/Carbon Noisetip	7141-093	178
Acoustic Recession Gage 50 MW-III Model Assembly	7141-094	179
50 MW-III ARG Model Holder	7141-095	180
Acoustic Recession Gage - 50 MW Test Assy	7141-096	181
Modified Transmitter Base and Pedestal - (Mod II Assembly)	7141-097	182
Flexural Acoustic Gage Base (Mod II Assembly)	7141-098	183
Flexural Acoustic Gage Assembly (Dual Mode Sensor) Mod II	7141-099	184



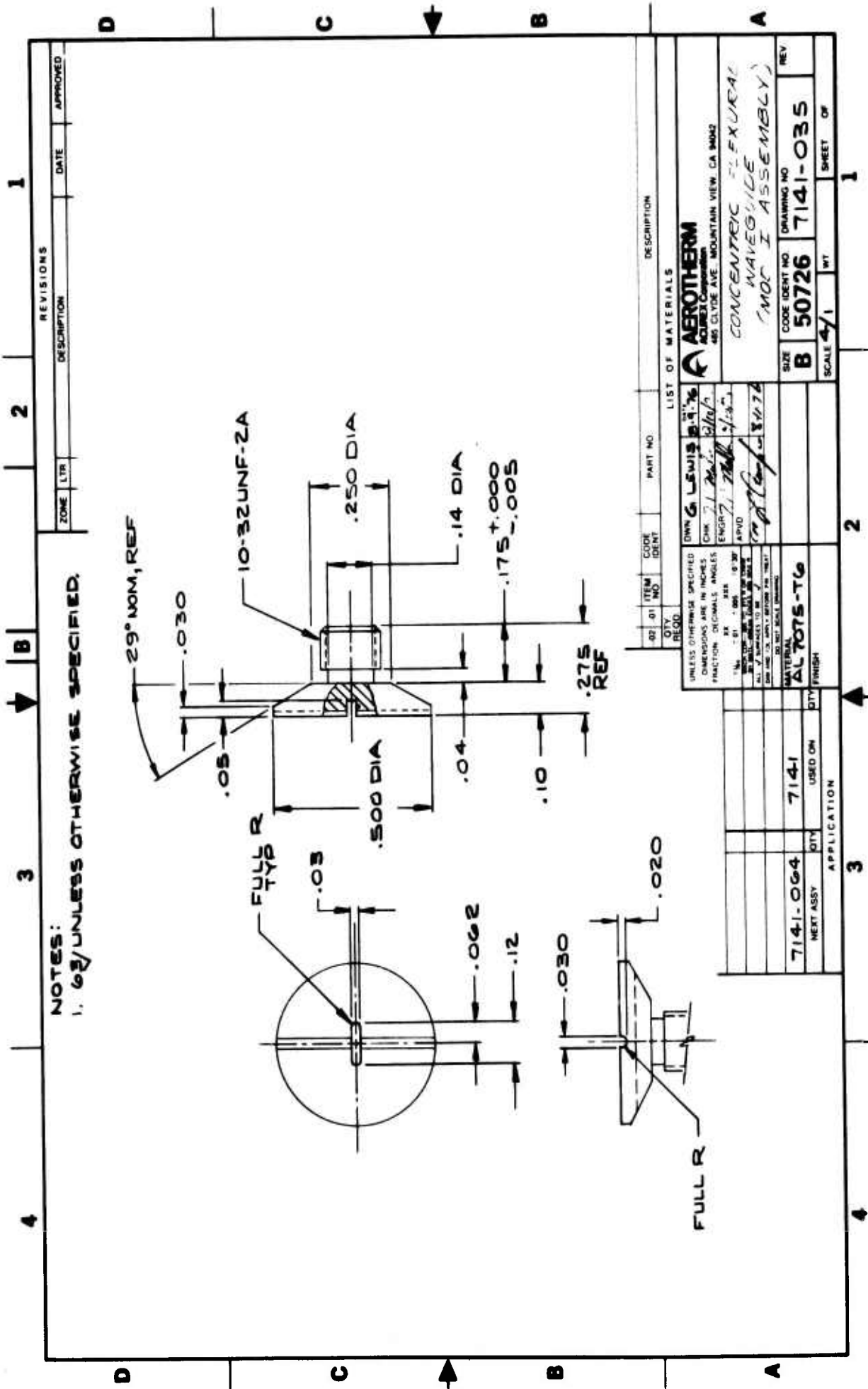
I



NOTES:
 1. 63/UNLESS OTHERWISE SPECIFIED.
 2. BREAK ALL SHARP EDGES .01 R, MAX.

REVISIONS		DATE	APPROVED
ZONE	DESCRIPTION		
A	13: 3.50 ± .010 WAS: 1.50		
	15: 1.180 DIA. WAS: 1.062		
	ADD: 1.062 DIA		

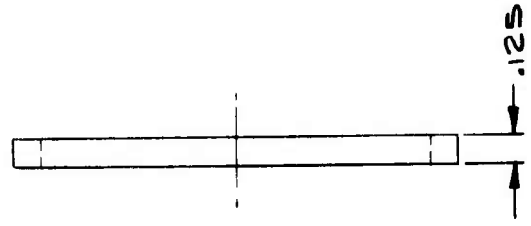
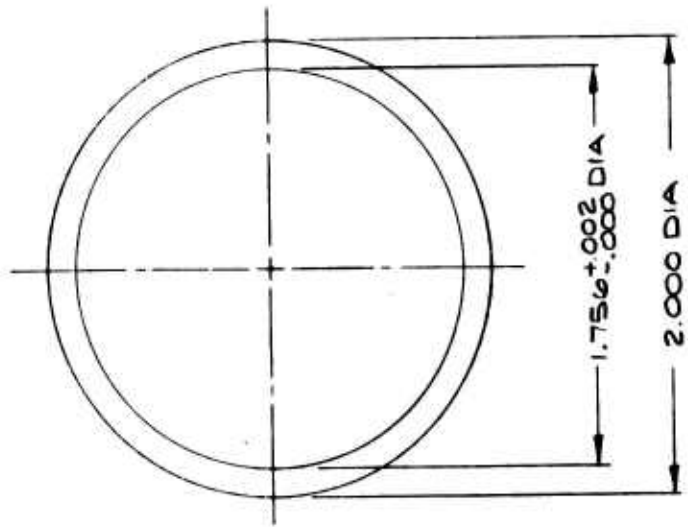
ITEM NO.		CODE IDENT	PART NO.	DESCRIPTION
QTY. REQD.		LIST OF MATERIALS		
UNLESS OTHERWISE SPECIFIED		AEROTHERM		
DIMENSIONS ARE IN INCHES		ACUREX Corporation		
FRACTION DECIMALS ANGLES		485 CLYDE AVE. MOUNTAIN VIEW CA 94042		
1/16 1/8 1/4 3/8 1/2 3/4 1 1 1/2 2 3 4 5 6 8 10 12 16 20 24 30 36 48 60 72 96 120 144 180 216 240 288 360 432 480 576 720 864 1080 1296 1440 1728 2160 2592 2880 3456 4320 5184 6480 7776 9600 11520 14400 17280 21600 25920 31680 38880 47520 58320 71040 86400 103680 126720 155520 191040 232320 282240 343680 418560 509760 621120 757440 921600 1120320 1376640 1688880 2069760 2527680 3083520 3750000 4548000 5500800 6729600 8256000 10137600 12422400 15273600 18758400 23040000 28224000 34368000 41856000 50976000 62112000 75744000 92160000 112032000 137664000 168888000 206976000 252768000 308352000 375000000 454800000 550080000 672960000 825600000 1013760000 1242240000 1527360000 1875840000 2304000000 2822400000 3436800000 4185600000 5097600000 6211200000 7574400000 9216000000 11203200000 13766400000 16888800000 20697600000 25276800000 30835200000 37500000000 45480000000 55008000000 67296000000 82560000000 101376000000 124224000000 152736000000 187584000000 230400000000 282240000000 343680000000 418560000000 509760000000 621120000000 757440000000 921600000000 1120320000000 1376640000000 1688880000000 2069760000000 2527680000000 3083520000000 3750000000000 4548000000000 5500800000000 6729600000000 8256000000000 10137600000000 12422400000000 15273600000000 18758400000000 23040000000000 28224000000000 34368000000000 41856000000000 50976000000000 62112000000000 75744000000000 92160000000000 112032000000000 137664000000000 168888000000000 206976000000000 252768000000000 308352000000000 375000000000000 454800000000000 550080000000000 672960000000000 825600000000000 1013760000000000 1242240000000000 1527360000000000 1875840000000000 2304000000000000 2822400000000000 3436800000000000 4185600000000000 5097600000000000 6211200000000000 7574400000000000 9216000000000000 11203200000000000 13766400000000000 16888800000000000 20697600000000000 25276800000000000 30835200000000000 37500000000000000 45480000000000000 55008000000000000 67296000000000000 82560000000000000 101376000000000000 124224000000000000 152736000000000000 187584000000000000 230400000000000000 282240000000000000 343680000000000000 418560000000000000 509760000000000000 621120000000000000 757440000000000000 921600000000000000 1120320000000000000 1376640000000000000 1688880000000000000 2069760000000000000 2527680000000000000 3083520000000000000 3750000000000000000 4548000000000000000 5500800000000000000 6729600000000000000 8256000000000000000 10137600000000000000 12422400000000000000 15273600000000000000 18758400000000000000 23040000000000000000 28224000000000000000 34368000000000000000 41856000000000000000 50976000000000000000 62112000000000000000 75744000000000000000 92160000000000000000 112032000000000000000 137664000000000000000 168888000000000000000 206976000000000000000 252768000000000000000 308352000000000000000 375000000000000000000 454800000000000000000 550080000000000000000 672960000000000000000 825600000000000000000 1013760000000000000000 1242240000000000000000 1527360000000000000000 1875840000000000000000 2304000000000000000000 2822400000000000000000 3436800000000000000000 4185600000000000000000 5097600000000000000000 6211200000000000000000 7574400000000000000000 9216000000000000000000 11203200000000000000000 13766400000000000000000 16888800000000000000000 20697600000000000000000 25276800000000000000000 30835200000000000000000 37500000000000000000000 45480000000000000000000 55008000000000000000000 67296000000000000000000 82560000000000000000000 101376000000000000000000 124224000000000000000000 152736000000000000000000 187584000000000000000000 230400000000000000000000 282240000000000000000000 343680000000000000000000 418560000000000000000000 509760000000000000000000 621120000000000000000000 757440000000000000000000 921600000000000000000000 1120320000000000000000000 1376640000000000000000000 1688880000000000000000000 2069760000000000000000000 2527680000000000000000000 3083520000000000000000000 3750000000000000000000000 4548000000000000000000000 5500800000000000000000000 6729600000000000000000000 8256000000000000000000000 10137600000000000000000000 12422400000000000000000000 15273600000000000000000000 18758400000000000000000000 23040000000000000000000000 28224000000000000000000000 34368000000000000000000000 41856000000000000000000000 50976000000000000000000000 62112000000000000000000000 75744000000000000000000000 92160000000000000000000000 112032000000000000000000000 137664000000000000000000000 168888000000000000000000000 206976000000000000000000000 252768000000000000000000000 308352000000000000000000000 375000000000000000000000000 454800000000000000000000000 550080000000000000000000000 672960000000000000000000000 825600000000000000000000000 1013760000000000000000000000 1242240000000000000000000000 1527360000000000000000000000 1875840000000000000000000000 2304000000000000000000000000 2822400000000000000000000000 3436800000000000000000000000 4185600000000000000000000000 5097600000000000000000000000 6211200000000000000000000000 7574400000000000000000000000 9216000000000000000000000000 11203200000000000000000000000 13766400000000000000000000000 16888800000000000000000000000 20697600000000000000000000000 25276800000000000000000000000 30835200000000000000000000000 37500000000000000000000000000 45480000000000000000000000000 55008000000000000000000000000 67296000000000000000000000000 82560000000000000000000000000 101376000000000000000000000000 124224000000000000000000000000 152736000000000000000000000000 187584000000000000000000000000 230400000000000000000000000000 282240000000000000000000000000 343680000000000000000000000000 418560000000000000000000000000 509760000000000000000000000000 621120000000000000000000000000 757440000000000000000000000000 921600000000000000000000000000 1120320000000000000000000000000 1376640000000000000000000000000 1688880000000000000000000000000 2069760000000000000000000000000 2527680000000000000000000000000 3083520000000000000000000000000 3750000000000000000000000000000 4548000000000000000000000000000 5500800000000000000000000000000 6729600000000000000000000000000 8256000000000000000000000000000 10137600000000000000000000000000 12422400000000000000000000000000 15273600000000000000000000000000 18758400000000000000000000000000 23040000000000000000000000000000 28224000000000000000000000000000 34368000000000000000000000000000 41856000000000000000000000000000 50976000000000000000000000000000 62112000000000000000000000000000 75744000000000000000000000000000 92160000000000000000000000000000 112032000000000000000000000000000 137664000000000000000000000000000 168888000000000000000000000000000 206976000000000000000000000000000 252768000000000000000000000000000 308352000000000000000000000000000 375000000000000000000000000000000 454800000000000000000000000000000 550080000000000000000000000000000 672960000000000000000000000000000 825600000000000000000000000000000 1013760000000000000000000000000000 1242240000000000000000000000000000 1527360000000000000000000000000000 1875840000000000000000000000000000 2304000000000000000000000000000000 2822400000000000000000000000000000 3436800000000000000000000000000000 4185600000000000000000000000000000 5097600000000000000000000000000000 6211200000000000000000000000000000 7574400000000000000000000000000000 9216000000000000000000000000000000 11203200000000000000000000000000000 13766400000000000000000000000000000 16888800000000000000000000000000000 20697600000000000000000000000000000 25276800000000000000000000000000000 30835200000000000000000000000000000 37500000000000000000000000000000000 45480000000000000000000000000000000 55008000000000000000000000000000000 67296000000000000000000000000000000 82560000000000000000000000000000000 101376000000000000000000000000000000 124224000000000000000000000000000000 152736000000000000000000000000000000 187584000000000000000000000000000000 230400000000000000000000000000000000 282240000000000000000000000000000000 343680000000000000000000000000000000 418560000000000000000000000000000000 509760000000000000000000000000000000 621120000000000000000000000000000000 757440000000000000000000000000000000 921600000000000000000000000000000000 1120320000000000000000000000000000000 1376640000000000000000000000000000000 1688880000000000000000000000000000000 2069760000000000000000000000000000000 2527680000000000000000000000000000000 3083520000000000000000000000000000000 3750000000000000000000000000000000000 4548000000000000000000000000000000000 5500800000000000000000000000000000000 6729600000000000000000000000000000000 8256000000000000000000000000000000000 10137600000000000000000000000000000000 12422400000000000000000000000000000000 15273600000000000000000000000000000000 18758400000000000000000000000000000000 23040000000000000000000000000000000000 28224000000000000000000000000000000000 34368000000000000000000000000000000000 41856000000000000000000000000000000000 50976000000000000000000000000000000000 62112000000000000000000000000000000000 75744000000000000000000000000000000000 92160000000000000000000000000000000000 112032000000000000000000000000000000000 137664000000000000000000000000000000000 168888000000000000000000000000000000000 206976000000000000000000000000000000000 252768000000000000000000000000000000000 308352000000000000000000000000000000000 375000000000000000000000000000000000000 454800000000000000000000000000000000000 550080000000000000000000000000000000000 672960000000000000000000000000000000000 825600000000000000000000000000000000000 1013760000000000000000000000000000000000 1242240000000000000000000000000000000000 1527360000000000000000000000000000000000 1875840000000000000000000000000000000000 2304000000000000000000000000000000000000 2822400000000000000000000000000000000000 3436800000000000000000000000000000000000 4185600000000000000000000000000000000000 5097600000000000000000000000000000000000 6211200000000000000000000000000000000000 7574400000000000000000000000000000000000 9216000000000000000000000000000000000000 11203200000000000000000000000000000000000 13766400000000000000000000000000000000000 16888800000000000000000000000000000000000 20697600000000000000000000000000000000000 25276800000000000000000000000000000000000 30835200000000000000000000000000000000000 37500000000000000000000000000000000000000 45480000000000000000000000000000000000000 55008000000000000000000000000000000000000 67296000000000000000000000000000000000000 82560000000000000000000000000000000000000 101376000000000000000000000000000000000000 124224000000000000000000000000000000000000 152736000000000000000000000000000000000000 187584000000000000000000000000000000000000 230400000000000000000000000000000000000000 282240000000000000000000000000000000000000 343680000000000000000000000000000000000000 418560000000000000000000000000000000000000 509760000000000000000000000000000000000000 621120000000000000000000000000000000000000 757440000000000000000000000000000000000000 921600000000000000000000000000000000000000 1120320000000000000000000000000000000000000 1376640000000000000000000000000000000000000 1688880000000000000000000000000000000000000 2069760000000000000000000000000000000000000 2527680000000000000000000000000000000000000 3083520000000000000000000000000000000000000 37500 4548000000000000000000000000000000000000000 5500800000000000000000000000000000000000000 6729600000000000000000000000000000000000000 8256000000000000000000000000000000000000000 10137600000000000000000000000000000000000000 12422400000000000000000000000000000000000000 152736				



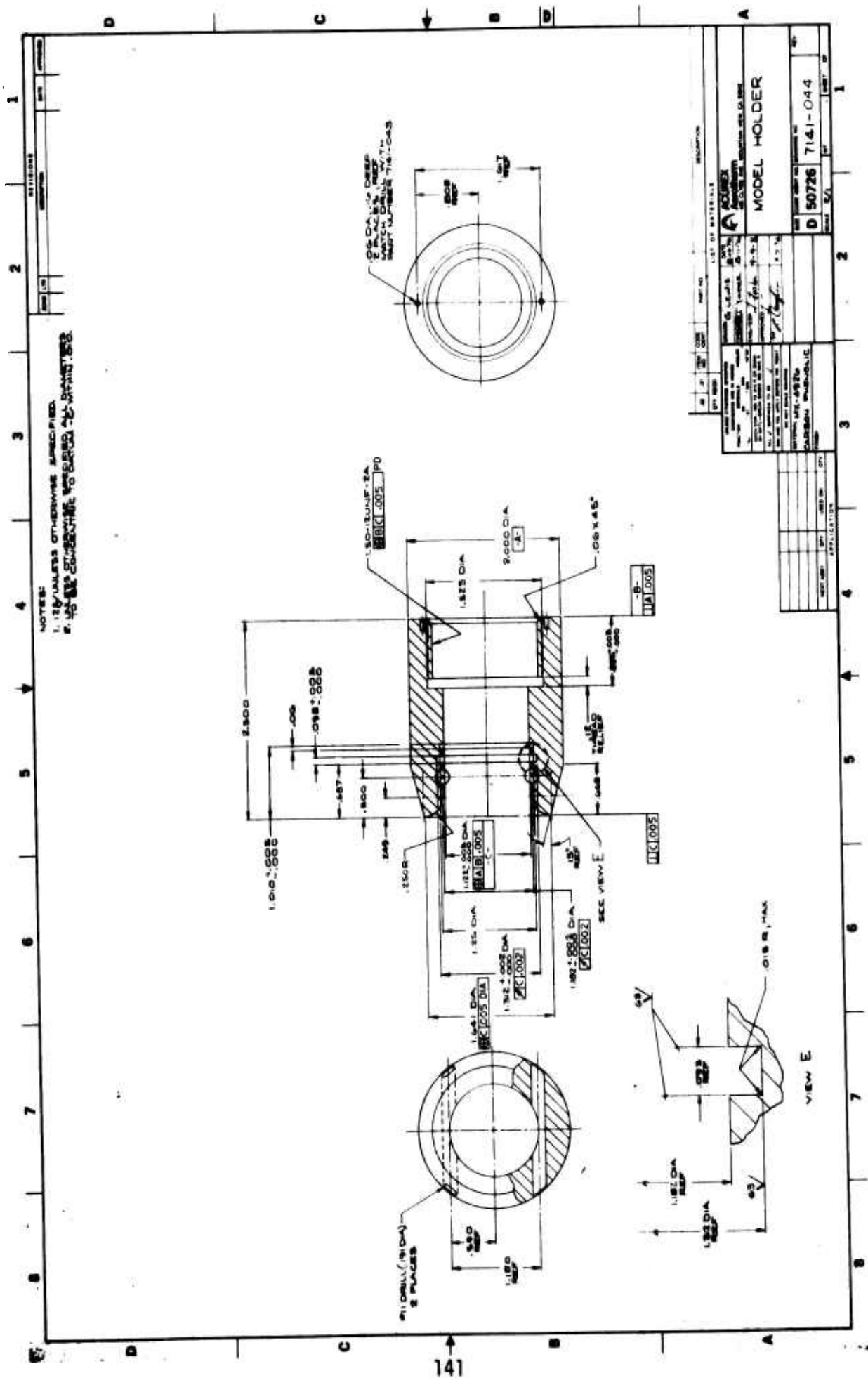
4 3 2 1

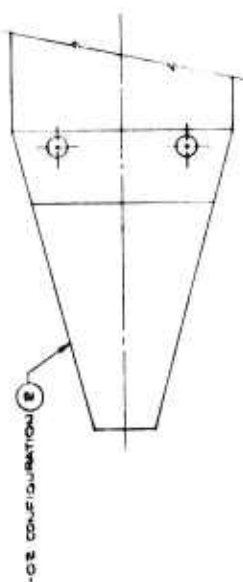
NOTES:
1. MATL: SILICA FILLED PHENOLIC (G-11).

REVISIONS		
ZONE	DESCRIPTION	DATE
1		



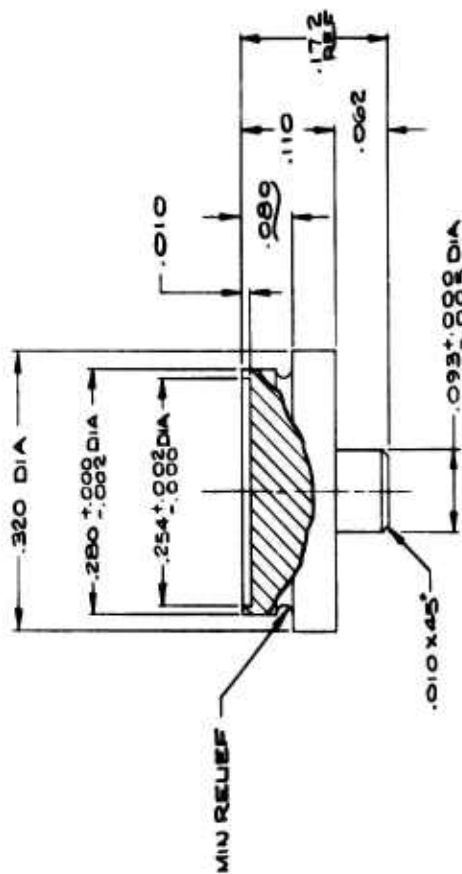
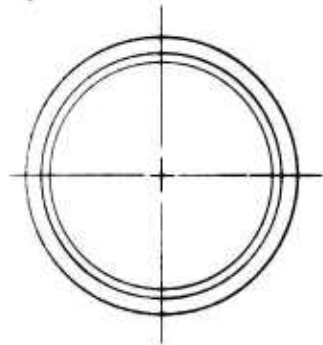
QTY		02	01	ITEM NO	CODE IDENT	PART NO	LIST OF MATERIALS	DESCRIPTION			
RECD		DWN G. LEWIS 8-10-76 5-11-76 9-9-76 1-1-77						AEROTHERM ABLATIVE WASHER-ARG SOMW ARC-JET TEST UNIT			
UNLESS OTHERWISE SPECIFIED DIMENSIONS ARE IN INCHES FRACTION DECIMALS ANGLES		XX .01 .005 .030 .001 .002 .005 .010 .015 .020 .030 .040 .050 .060 .070 .080 .090 .100 .125 .150 .175 .200 .250 .300 .375 .500 .625 .750 .875 1.000 1.250 1.500 1.750 2.000 2.500 3.000 3.750 4.000 5.000 6.000 7.000 8.000 9.000 10.000 ALL V SURFACES TO BE .7 DIM AND TO APPLY DECIMAL IN INCHES DO NOT SCALE DRAWING						SIZE B	CODE IDENT NO 50726	DRAWING NO 7:41-041	REV
MATERIAL SEE NOTE 1		NEXT ASSY		QTY		USED ON		SCALE 2/1	WT 	SHEET 1	OF
APPLICATION											



[illegible][illegible]

143

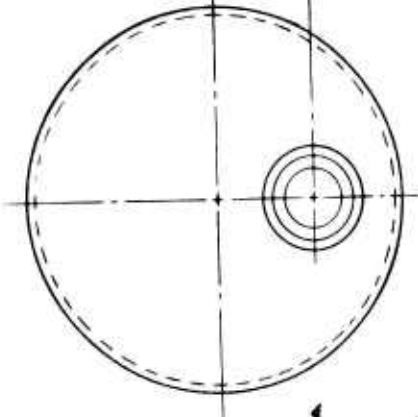
NOTES:
 1. UNLESS OTHERWISE SPECIFIED,
 2. BREAK ALL SHARP EDGES.
 3. UNLESS OTHERWISE SPECIFIED, ALL
 DIAMETERS TO BE CONCENTRIC
 WITHIN .005.



REVISIONS		DATE	APPROVED
ZONE	LTR		

DRAWING G. LEWIS		DATE 8-17-76	ACUREX Aerotherm 405 CLYDE AVE. MOUNTAIN VIEW, CA 94042	
CHECKED A. G. LEWIS	ENGINEER J. H. LEWIS	APPROVED J. H. LEWIS	RECEIVER BASE - MOD I	
UNLESS OTHERWISE SPECIFIED DIMENSIONS ARE IN INCHES		SIZE CODE IDENT NO DRAWING NO		
FRACTION DECIMALS ANGLES		C 50726 7141-060		
1/16 .001 1/2 1/4 1/8 3/16 3/8 1/2 3/4 1 1 1/2 2 3 4 5 6 8 10 12 14 16 18 20 22 24 26 28 30 32 34 36 38 40 42 44 46 48 50 52 54 56 58 60 62 64 66 68 70 72 74 76 78 80 82 84 86 88 90 92 94 96 98 100		SCALE 10/1		
DO NOT SCALE DRAWING		SHEET 1 OF 1		
MATERIAL AL 7075-T6		REV		
FINISH				

QTY	REVISION	DESCRIPTION	DATE	APPROVED
7141-0605	7141	USED ON		
7141-0605	7141	APPLICATION		

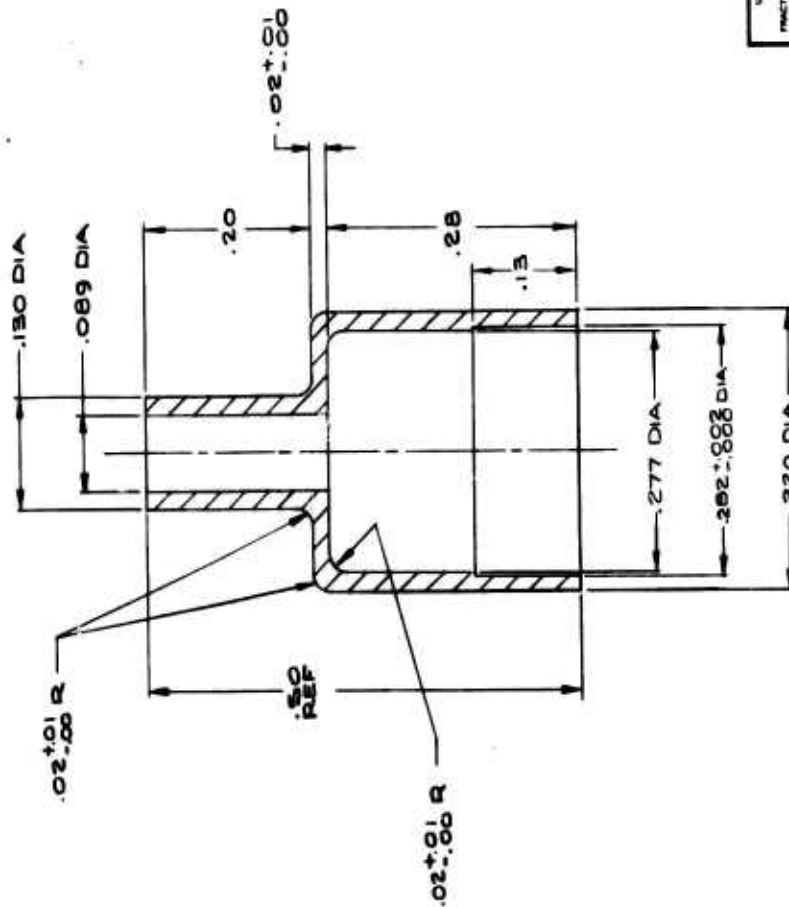


NOTES.

1. 63 UNLESS OTHERWISE SPECIFIED.
2. BREAK ALL SHARPEGES. OIR, MAX.
3. UNLESS OTHERWISE SPECIFIED. ALL DIAMETERS TO BE CONCENTRIC WITH .005 TOTAL.

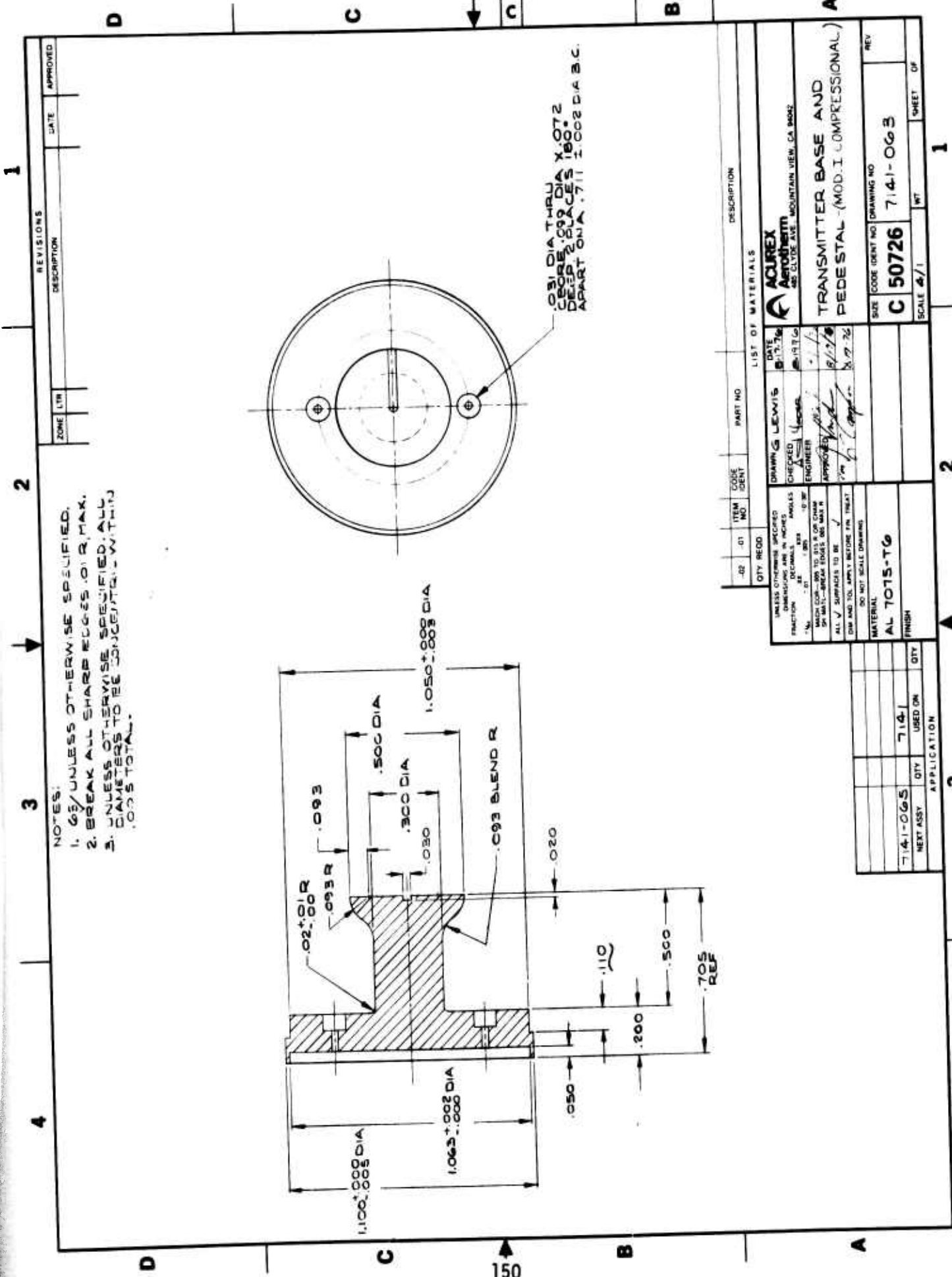
REVISIONS				
ZONE	LTR	DESCRIPTION	DATE	APPROVED

[illegible]



- NOTES:
1. G3 UNLESS OTHERWISE SPECIFIED.
 2. BREAK ALL SHARP EDGES 0.1R MAX.
 3. UNLESS OTHERWISE SPECIFIED, ALL DIAMETERS TO BE CONCENTRIC WITHIN .005.

[illegible]



NOTES:
 1. G3/ UNLESS OTHERWISE SPECIFIED.
 2. BREAK ALL SHARP EDGES .012 MAX.
 3. UNLESS OTHERWISE SPECIFIED, ALL DIAMETERS TO BE CONCENTRIC WITHIN .005 TOTAL.

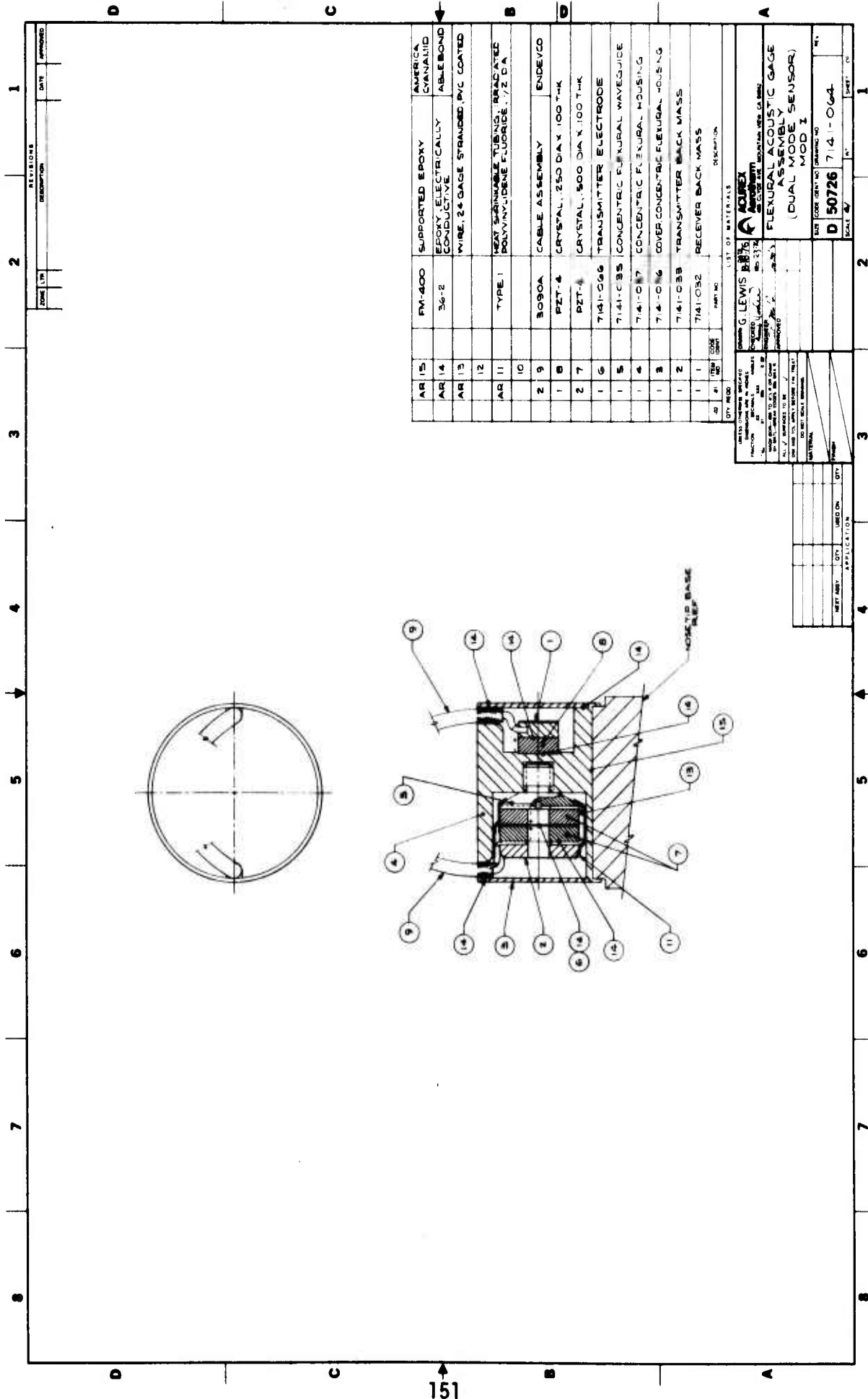
ZONE 1		ZONE 2		ZONE 3		ZONE 4	
REVISIONS		DESCRIPTION		DATE		APPROVED	
1							
2							
3							
4							

ITEM		CODE		PART NO		DESCRIPTION	
NO		IDENT					
.02		.01				QTY REQD	

DRAWING		DATE		LIST OF MATERIALS	
G LEWIS		8/13/76		ACUREX Aerotherm	
CHECKED		8/13/76		200 GLENN AVE. MOUNTAIN VIEW, CA 94039	
ENGINEER		8/13/76		TRANSMITTER BASE AND	
APPROVED		8/13/76		PEDESTAL (MOD. I COMPRESSIONAL)	
BY		8/13/76			

SIZE		CODE IDENT NO		DRAWING NO		REV	
C 50726		7141-063					
SCALE 4/1		WT		SHEET		OF	
1		2		3		4	

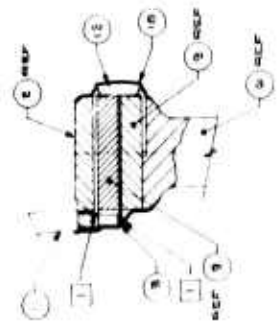
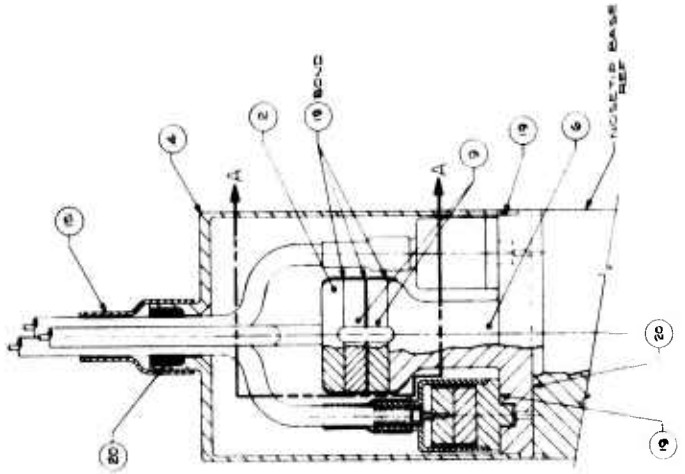
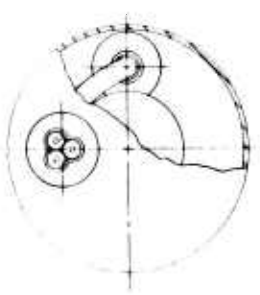
MATERIAL		FINISH		QTY		APPLICATION	
AL 7075-T6							
7141-063		7141		QTY USED ON		QTY	
NEXT ASSY							



QTY	REV	DATE	DESCRIPTION
1	1		RECEIVER BACK MASS
1	2		TRANSMITTER BACK MASS
1	3		COVER CONCENTRIC FLEXURAL HOUSING
1	4		CONCENTRIC FLEXURAL HOUSING
1	5		CONCENTRIC FLEXURAL WAVEGUIDE
1	6		TRANSMITTER ELECTRODE
2	7		CRYSTAL, 500 DIA X 100 THK
1	8		PZT-4
2	9		CABLE ASSEMBLY
10	10		ENDEVCO
12	11		TYPE 1
12	12		HEAT SHRINKABLE TUBING, RADIATED POLYVINYLIDENE FLUORIDE, 1/2 DIA
12	13		WIRE, 24 GAGE STRANDED, PVC COATED
12	14		ABLE BOND CONDUCTIVE
12	15		AMERICA CYANALOID

G. LEWIS
 FLEXURAL ACOUSTIC GAGE ASSEMBLY (DUAL MODE SENSOR) MOD 1
 DATE 50726 7/4/64
 DRAWING NO. 7/4-064
 SHEET 1

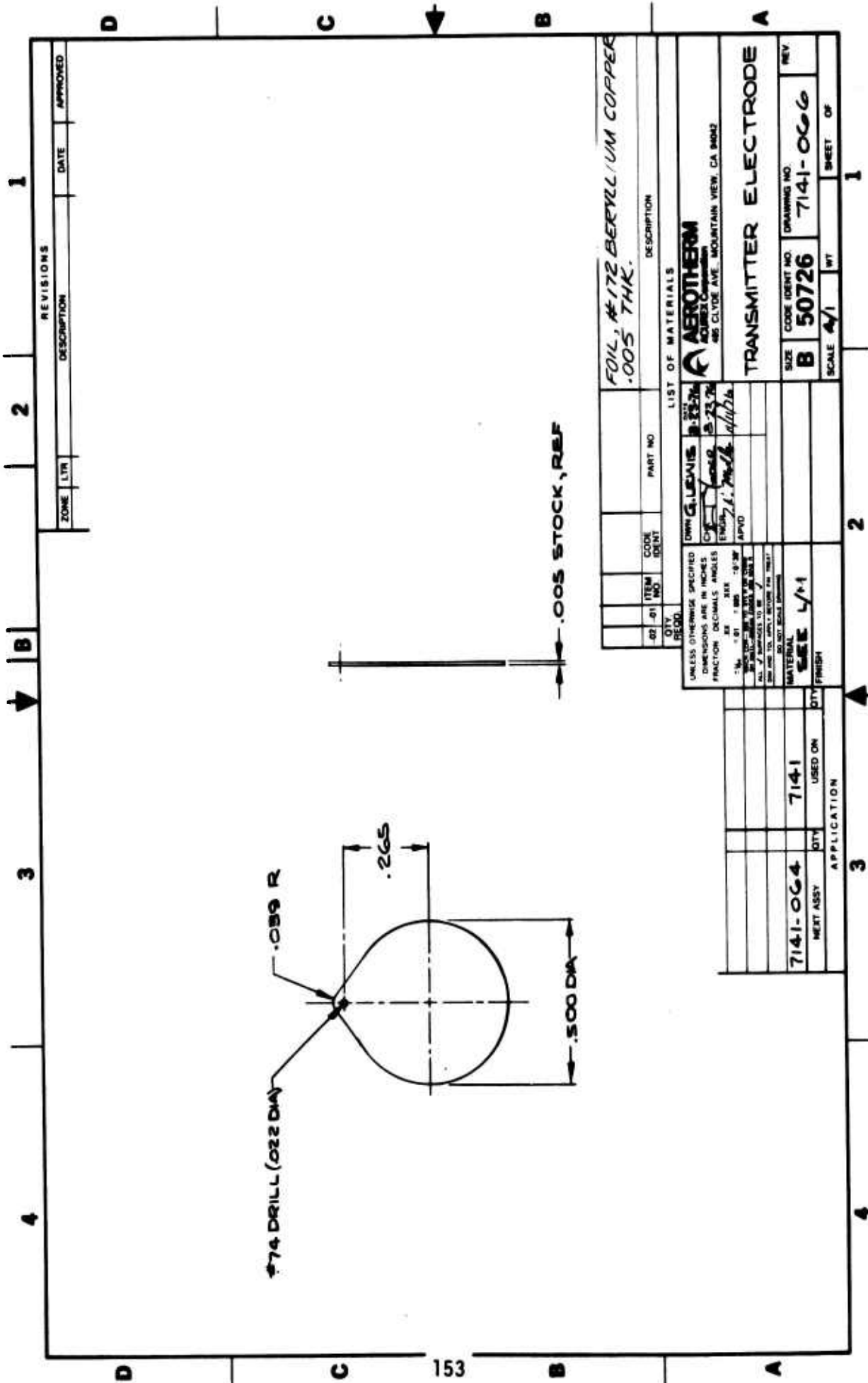
NOTES:
 1. ELECTRICAL GRADE SOLDER TO BE USED
 2. ON ALL SOLDER JOINTS



VIEW A-A

QTY	DESCRIPTION	UNIT	QTY	DESCRIPTION	UNIT
AR 20	EPOXY		AR 20	EPOXY	
AR 19	30-2		AR 19	30-2	
AR 18	TYPE 1		AR 18	TYPE 1	
AR 17			AR 17		
AR 16			AR 16		
AR 15			AR 15		
AR 14			AR 14		
AR 13			AR 13		
AR 12			AR 12		
AR 11			AR 11		
AR 10			AR 10		
AR 9			AR 9		
AR 8			AR 8		
AR 7			AR 7		
AR 6			AR 6		
AR 5			AR 5		
AR 4			AR 4		
AR 3			AR 3		
AR 2			AR 2		
AR 1			AR 1		

DRAWN: G. LEWIS
 CHECKED: [Signature]
 APPROVED: [Signature]
 DATE: 4-10-68
 SCALE: 4/1
 D 50726



FOIL, #172 BERYLLIUM COPPER
.005 THK.

QTY	ITEM	CODE	PART NO	DESCRIPTION
REQD	NO	IDENT		

LIST OF MATERIALS

A AEROTHERM
AEROTHERM CORPORATION
485 CLYDE AVE. MOUNTAIN VIEW, CA 94042

TRANSMITTER ELECTRODE

SIZE	CODE IDENT NO	DRAWING NO	REV
B	50726	7141-0606	
SCALE	WT	SHEET OF	
4/1		1	

UNLESS OTHERWISE SPECIFIED
DIMENSIONS ARE IN INCHES
FRACTION DECIMALS ANGLES

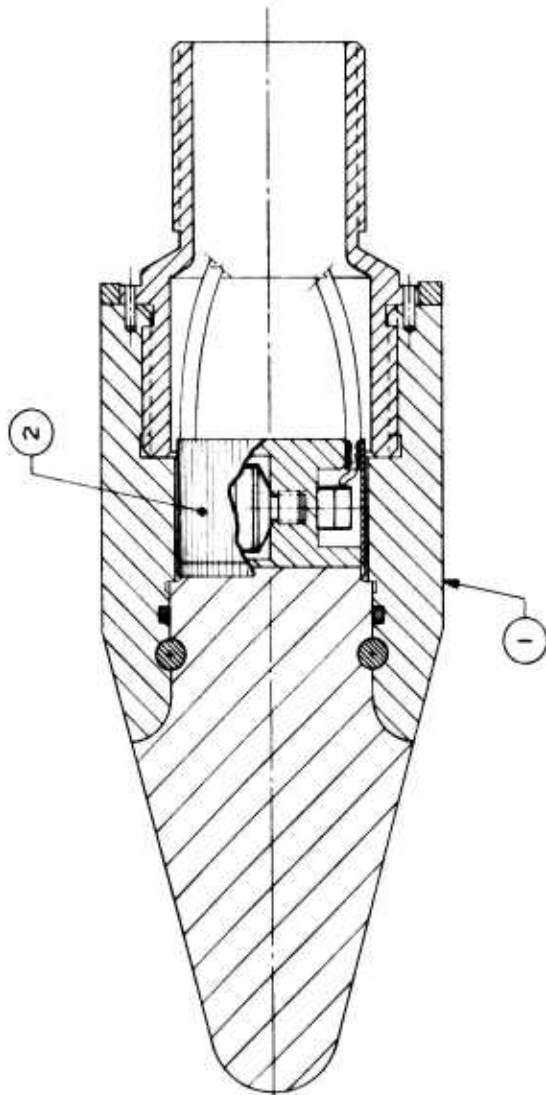
1/16" = .0625"
1/32" = .03125"
1/64" = .015625"
ALL DIMENSIONS TO BE
HOLD AND TO APPLY BEFORE FINISH

MATERIAL
SEE 4/1

FINISH

QTY	USED ON	QTY	APPLICATION
7141-0604	7141		
NEXT ASSY			

REVISIONS				
ZONE	LTR	DESCRIPTION	DATE	APPROVED

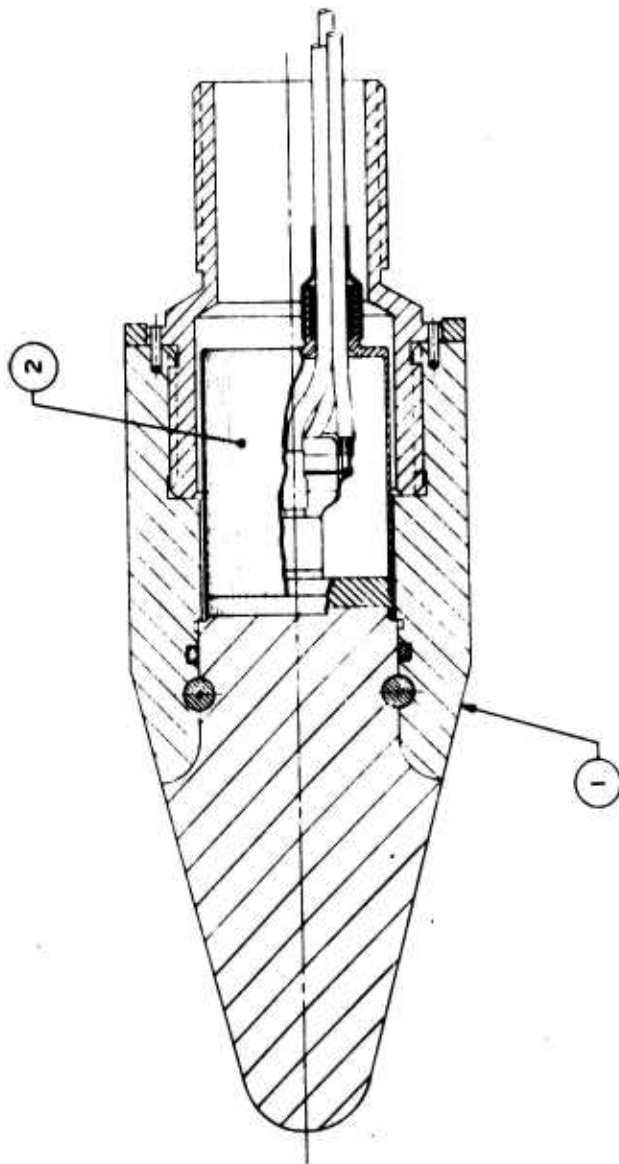


ITEM	CODE	PART NO.	DESCRIPTION
1	2	7141-004	FLEXURAL ACOUSTIC GAGE ASSEMBLY (DUAL MODE SENSOR)
1	1	7141-045	ACOUSTIC RECESSION GAGE, 50 MW-

QTY	RECD	NO.	IDENT	PRINT NO.	LIST OF MATERIALS
UNLESS OTHERWISE SPECIFIED DIMENSIONS ARE IN INCHES FRACTION DECIMALS XXX ANGLES - 1/4 - 01 * .005 MACH COR - .005 TO .015 R OR CHAM 3/4 WALL - SHEAR EDGES .005 MAX R		DRAWING LEW'S CHECKED <i>LEW'S</i> ENGINEER <i>LEW'S</i> APPROVED <i>LEW'S</i>		DATE 8-23-76 8-23-76 9-9-76 9-9-76	
ALL \sqrt SURFACES TO BE \sqrt DIM AND TOL APPLY BEFORE FIN TREAT DO NOT SCALE DRAWING		SIZE CODE IDENT NO DRAWING NO C 50726 7141-067		REV 1	
MATERIAL FINISH		SCALE 2 1/2" = 1"		SHEET NO	

[illegible]

REVISIONS		DATE	
ZONE	LTR	DESCRIPTION	
1			



ITEM NO	QTY REQD	CODE IDENT	PART NO	DESCRIPTION
1	2		7141-065	COMPRESSIONAL ACOUSTIC GAGE ASSEMBLY (SINGLE MODE SENSOR)
2	1		7141-045	ACOUSTIC RECESSION GAGE, 50 MW

LIST OF MATERIALS

DRAWN G. LEM/S		DATE 8-18-76
CHECKED A. L. J.	DATE 8-18-76	
ENGINEER J. L. J.		
APPROVED J. L. J.		
DO NOT SCALE DRAWING		
MATERIAL		
FINISH		
NEXT ASSY		
QTY USED ON		
QTY APPLICATION		

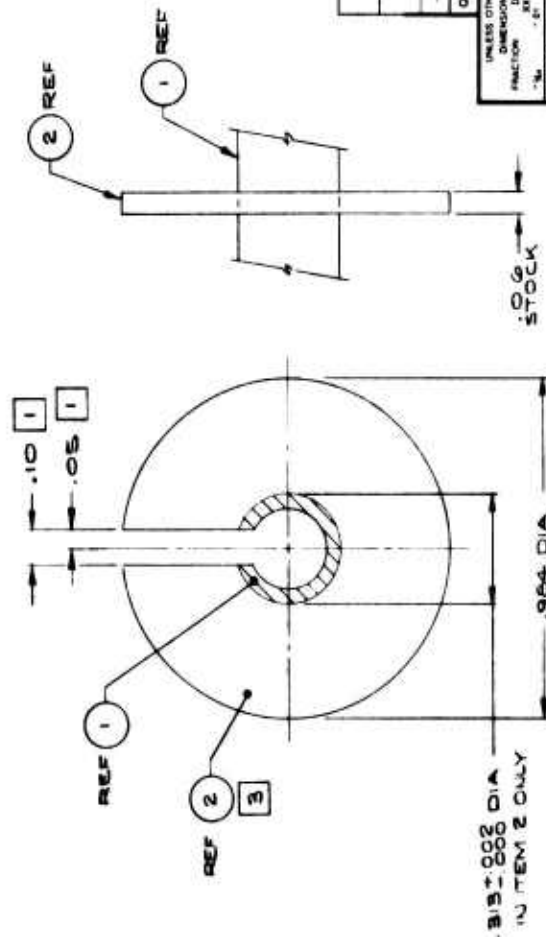
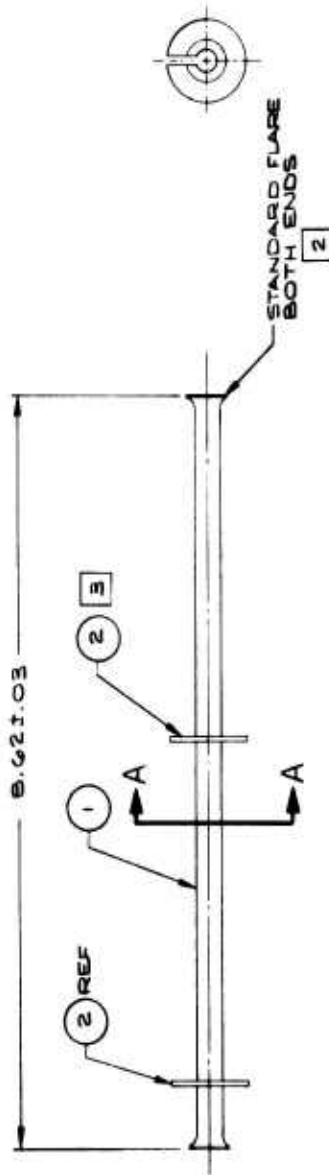
A		B		C		D	
1		2		3		4	

A		B		C		D	
1		2		3		4	

A		B		C		D	
1		2		3		4	

4 3 2 1

- NOTES:
1. SLOT TO BE MACHINED IN BOTH ITEM 1 AND 2 PRIOR TO THEIR ASSEMBLY.
 2. PRIOR TO FLARING ENDS OF ITEM 1, ASSEMBLE ITEM 2 ONTO ITEM 1, AS SHOWN.
 3. INDICATED PARTS TO BE ALLOCINE PRIOR TO ASSEMBLY.
 4. BREAK ALL SHARPEDES .01 R, MAX.

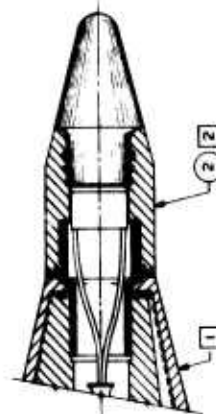


QTY	REQD	ITEM NO	CODE IDENT	PART NO	DESCRIPTION
2	2	-2			AL 6061-T6 OR 7075-T656 X1.00 DIA
1	1	-1			TUBING, SST 304, 5/16 OD X .02 WALL X
					8.62 LONG

LIST OF MATERIALS

DRAWING G. LEWIS		DATE	8/20/76
CHECKED	ENGINEER	APPROVED	
ACUREX Aerotherm 485 CLUTE AVE. MOUNTAIN VIEW, CA 94042			
CABLE SUPPORT TUBE		SIZE	C 50726
DRAWING NO		7141-069	REV
SCALE		1/1	WT
SHEET		1	OF

4 3 2 1



NOTES:

1 EXISTING PARTS PER DRAWING NUMBER
STITCHING U.S. AIR FORCE, WRIGHT PATERSON
AIR FORCE BASE, OHIO.

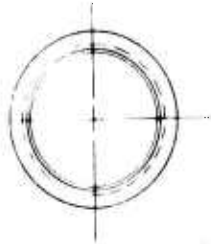
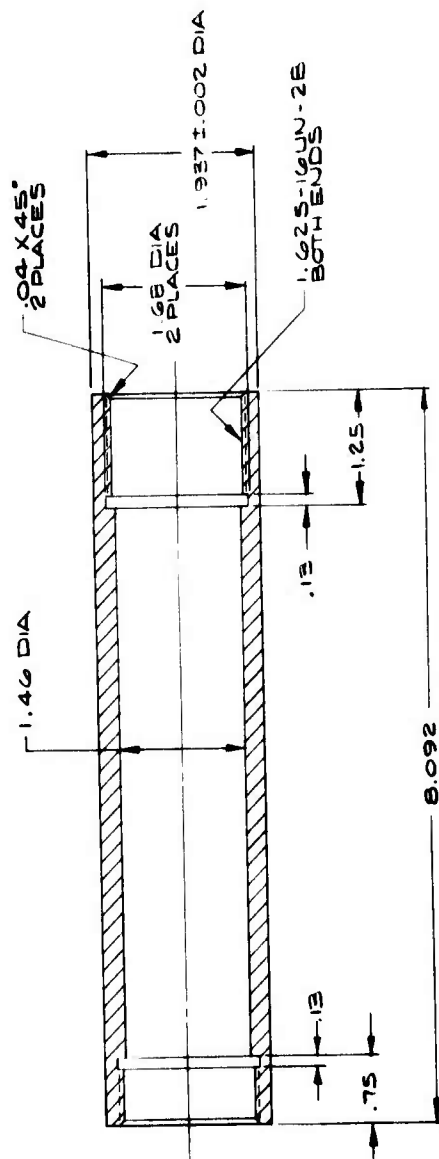
2 TO BE FURNISHED BY AEROTHERMAL-CLARK CORP.
AS A PRE-ASSEMBLED UNIT.

1	1	7				
		9				
		5				
		4				
		3				
1	1	1	714-059			CABLE SUPPORT TUBE ASSEMBLY
		2	714-067			30 MM NOSE TIE TEST ASSEMBLY (DUAL MOORE BANDSON)
1	1		714-048			30 MM NOSE TIE TEST ASSEMBLY (SINGLE MOORE BANDSON)
		1				
		1				

[illegible][illegible]

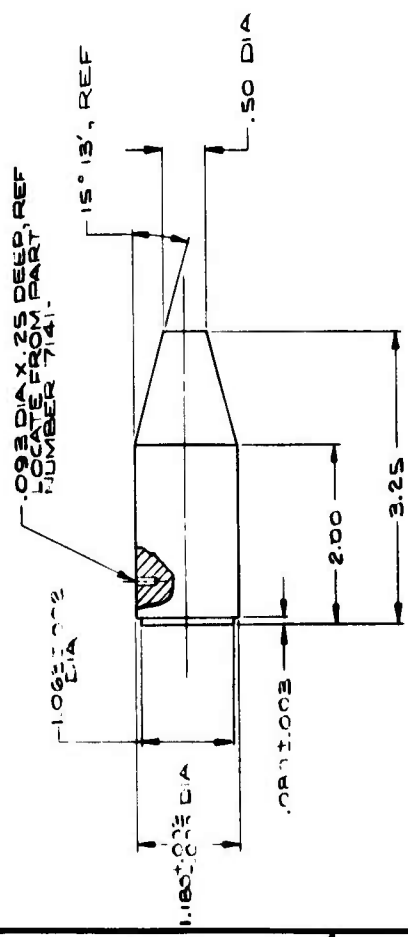
4 3 2 1

NOTES:
1. 125/UNLESS OTHERWISE SPECIFIED.
2. BREAK ALL SHARP EDGES .02 R, MAX.



QTY. REQD.		QTY. USED ON		QTY. USED ON		QTY. USED ON		QTY. USED ON		QTY. USED ON	
ITEM NO.	CODE IDENT	ITEM NO.	CODE IDENT	ITEM NO.	CODE IDENT	ITEM NO.	CODE IDENT	ITEM NO.	CODE IDENT	ITEM NO.	CODE IDENT
714-1-076		714-1									
NEXT ASSY		APPLICATION		APPLICATION		APPLICATION		APPLICATION		APPLICATION	
714-1-076		714-1		714-1		714-1		714-1		714-1	
FINISH		FINISH		FINISH		FINISH		FINISH		FINISH	
SST 316		SST 316		SST 316		SST 316		SST 316		SST 316	
DO NOT SCALE DRAWING		DO NOT SCALE DRAWING		DO NOT SCALE DRAWING		DO NOT SCALE DRAWING		DO NOT SCALE DRAWING		DO NOT SCALE DRAWING	
ALL SURFACES TO BE		ALL SURFACES TO BE		ALL SURFACES TO BE		ALL SURFACES TO BE		ALL SURFACES TO BE		ALL SURFACES TO BE	
MACH. CON. TO 0.005 IN. OR CHAM		MACH. CON. TO 0.005 IN. OR CHAM		MACH. CON. TO 0.005 IN. OR CHAM		MACH. CON. TO 0.005 IN. OR CHAM		MACH. CON. TO 0.005 IN. OR CHAM		MACH. CON. TO 0.005 IN. OR CHAM	
BY MAT. - BREAK EDGES AND MAX. R		BY MAT. - BREAK EDGES AND MAX. R		BY MAT. - BREAK EDGES AND MAX. R		BY MAT. - BREAK EDGES AND MAX. R		BY MAT. - BREAK EDGES AND MAX. R		BY MAT. - BREAK EDGES AND MAX. R	
CHECKED		CHECKED		CHECKED		CHECKED		CHECKED		CHECKED	
ENGINEER		ENGINEER		ENGINEER		ENGINEER		ENGINEER		ENGINEER	
APPROVED		APPROVED		APPROVED		APPROVED		APPROVED		APPROVED	
DATE 8-28-76		DATE 8-28-76		DATE 8-28-76		DATE 8-28-76		DATE 8-28-76		DATE 8-28-76	
DRAWN G. LEWIS		DRAWN G. LEWIS		DRAWN G. LEWIS		DRAWN G. LEWIS		DRAWN G. LEWIS		DRAWN G. LEWIS	
ACUREX Aerotherm		ACUREX Aerotherm		ACUREX Aerotherm		ACUREX Aerotherm		ACUREX Aerotherm		ACUREX Aerotherm	
480 CLYDE AVE. MOUNTAIN VIEW, CA 94042		480 CLYDE AVE. MOUNTAIN VIEW, CA 94042		480 CLYDE AVE. MOUNTAIN VIEW, CA 94042		480 CLYDE AVE. MOUNTAIN VIEW, CA 94042		480 CLYDE AVE. MOUNTAIN VIEW, CA 94042		480 CLYDE AVE. MOUNTAIN VIEW, CA 94042	
DESCRIPTION		DESCRIPTION		DESCRIPTION		DESCRIPTION		DESCRIPTION		DESCRIPTION	
HOLDER - 1 MW		HOLDER - 1 MW		HOLDER - 1 MW		HOLDER - 1 MW		HOLDER - 1 MW		HOLDER - 1 MW	
SIZE CODE IDENT NO		SIZE CODE IDENT NO		SIZE CODE IDENT NO		SIZE CODE IDENT NO		SIZE CODE IDENT NO		SIZE CODE IDENT NO	
C 50726		C 50726		C 50726		C 50726		C 50726		C 50726	
DRAWING NO		DRAWING NO		DRAWING NO		DRAWING NO		DRAWING NO		DRAWING NO	
7141-072		7141-072		7141-072		7141-072		7141-072		7141-072	
SCALE 1/1		SCALE 1/1		SCALE 1/1		SCALE 1/1		SCALE 1/1		SCALE 1/1	
SHEET OF		SHEET OF		SHEET OF		SHEET OF		SHEET OF		SHEET OF	
1		1		1		1		1		1	

REVISIONS		DATE	APPROVED
ZONE	LTR		

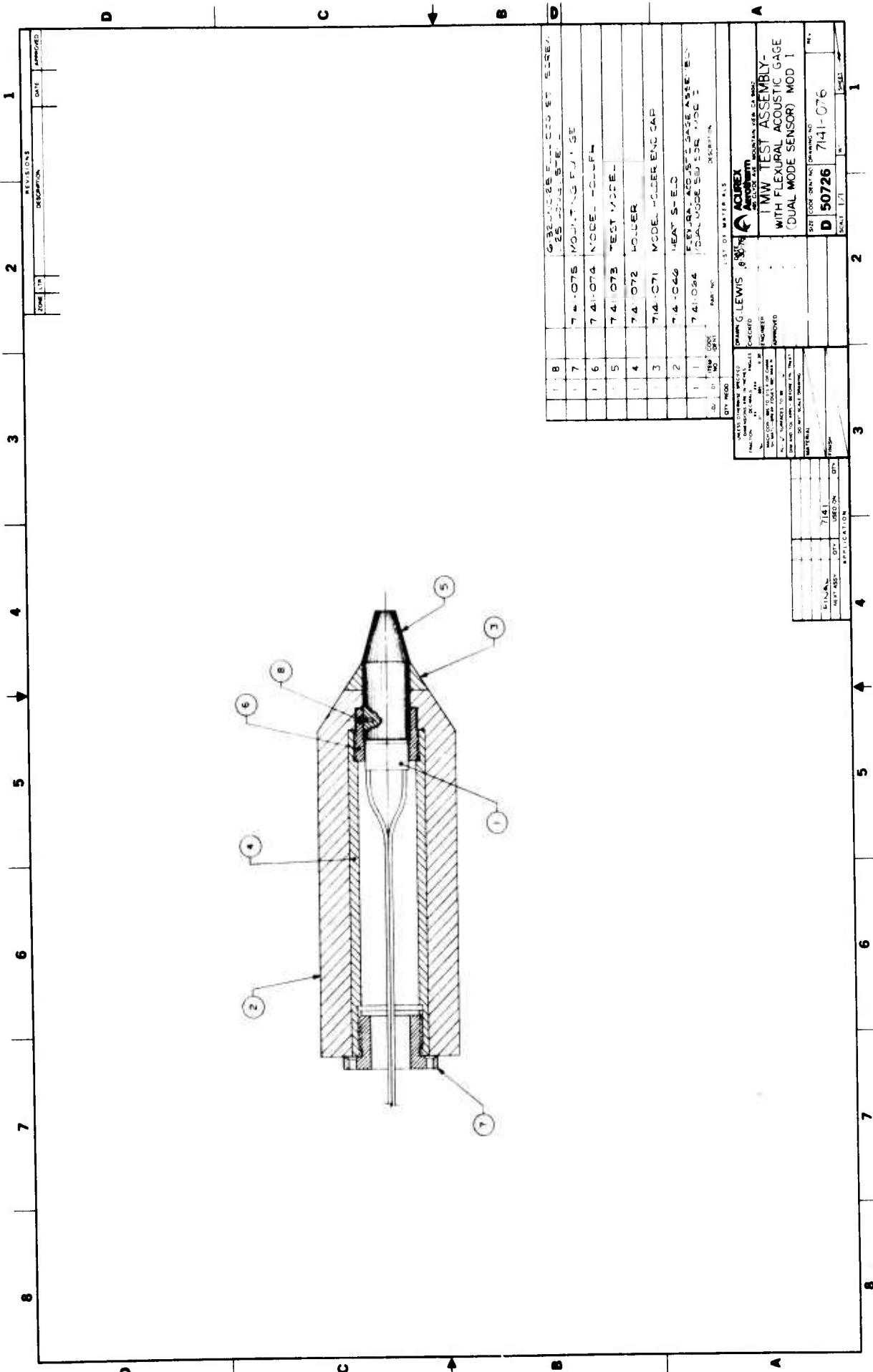


QTY. REQD.		ITEM NO.	CODE IDENT	PART NO.	DATE	DESCRIPTION
UNLESS OTHERWISE SPECIFIED DIMENSIONS ARE IN INCHES		DRAWN G. LEWIS		ACUREX Aerotherm 28 CLYDE AVE., MOUNTAIN VIEW, CA 94042		
FRACTION	DECIMALS	CHECKED	ENGINEER	TEST MODEL - 1 MW		
1/16	0.0625			SIZE CODE IDENT NO. DRAWING NO. REV.		
1/8	0.125			C 50726 7141-073		
1/4	0.25			SCALE 1/1		
3/8	0.375			SHEET OF		
1/2	0.5			1		
5/8	0.625					
3/4	0.75					
7/8	0.875					
1	1.0					
1 1/8	1.125					
1 1/4	1.25					
1 3/8	1.375					
1 1/2	1.5					
1 5/8	1.625					
1 3/4	1.75					
1 7/8	1.875					
2	2.0					
2 1/8	2.125					
2 1/4	2.25					
2 3/8	2.375					
2 1/2	2.5					
2 5/8	2.625					
2 3/4	2.75					
2 7/8	2.875					
3	3.0					
3 1/8	3.125					
3 1/4	3.25					
3 3/8	3.375					
3 1/2	3.5					
3 5/8	3.625					
3 3/4	3.75					
3 7/8	3.875					
4	4.0					
4 1/8	4.125					
4 1/4	4.25					
4 3/8	4.375					
4 1/2	4.5					
4 5/8	4.625					
4 3/4	4.75					
4 7/8	4.875					
5	5.0					
5 1/8	5.125					
5 1/4	5.25					
5 3/8	5.375					
5 1/2	5.5					
5 5/8	5.625					
5 3/4	5.75					
5 7/8	5.875					
6	6.0					
6 1/8	6.125					
6 1/4	6.25					
6 3/8	6.375					
6 1/2	6.5					
6 5/8	6.625					
6 3/4	6.75					
6 7/8	6.875					
7	7.0					
7 1/8	7.125					
7 1/4	7.25					
7 3/8	7.375					
7 1/2	7.5					
7 5/8	7.625					
7 3/4	7.75					
7 7/8	7.875					
8	8.0					
8 1/8	8.125					
8 1/4	8.25					
8 3/8	8.375					
8 1/2	8.5					
8 5/8	8.625					
8 3/4	8.75					
8 7/8	8.875					
9	9.0					
9 1/8	9.125					
9 1/4	9.25					
9 3/8	9.375					
9 1/2	9.5					
9 5/8	9.625					
9 3/4	9.75					
9 7/8	9.875					
10	10.0					
10 1/8	10.125					
10 1/4	10.25					
10 3/8	10.375					
10 1/2	10.5					
10 5/8	10.625					
10 3/4	10.75					
10 7/8	10.875					
11	11.0					
11 1/8	11.125					
11 1/4	11.25					
11 3/8	11.375					
11 1/2	11.5					
11 5/8	11.625					
11 3/4	11.75					
11 7/8	11.875					
12	12.0					
12 1/8	12.125					
12 1/4	12.25					
12 3/8	12.375					
12 1/2	12.5					
12 5/8	12.625					
12 3/4	12.75					
12 7/8	12.875					
13	13.0					
13 1/8	13.125					
13 1/4	13.25					
13 3/8	13.375					
13 1/2	13.5					
13 5/8	13.625					
13 3/4	13.75					
13 7/8	13.875					
14	14.0					
14 1/8	14.125					
14 1/4	14.25					
14 3/8	14.375					
14 1/2	14.5					
14 5/8	14.625					
14 3/4	14.75					
14 7/8	14.875					
15	15.0					
15 1/8	15.125					
15 1/4	15.25					
15 3/8	15.375					
15 1/2	15.5					
15 5/8	15.625					
15 3/4	15.75					
15 7/8	15.875					
16	16.0					
16 1/8	16.125					
16 1/4	16.25					
16 3/8	16.375					
16 1/2	16.5					
16 5/8	16.625					
16 3/4	16.75					
16 7/8	16.875					
17	17.0					
17 1/8	17.125					
17 1/4	17.25					
17 3/8	17.375					
17 1/2	17.5					
17 5/8	17.625					
17 3/4	17.75					
17 7/8	17.875					
18	18.0					
18 1/8	18.125					
18 1/4	18.25					
18 3/8	18.375					
18 1/2	18.5					
18 5/8	18.625					
18 3/4	18.75					
18 7/8	18.875					
19	19.0					
19 1/8	19.125					
19 1/4	19.25					
19 3/8	19.375					
19 1/2	19.5					
19 5/8	19.625					
19 3/4	19.75					
19 7/8	19.875					
20	20.0					
20 1/8	20.125					
20 1/4	20.25					
20 3/8	20.375					
20 1/2	20.5					
20 5/8	20.625					
20 3/4	20.75					
20 7/8	20.875					
21	21.0					
21 1/8	21.125					
21 1/4	21.25					
21 3/8	21.375					
21 1/2	21.5					
21 5/8	21.625					
21 3/4	21.75					
21 7/8	21.875					
22	22.0					
22 1/8	22.125					
22 1/4	22.25					
22 3/8	22.375					
22 1/2	22.5					
22 5/8	22.625					
22 3/4	22.75					
22 7/8	22.875					
23	23.0					
23 1/8	23.125					
23 1/4	23.25					
23 3/8	23.375					
23 1/2	23.5					
23 5/8	23.625					
23 3/4	23.75					
23 7/8	23.875					
24	24.0					
24 1/8	24.125					
24 1/4	24.25					
24 3/8	24.375					
24 1/2	24.5					
24 5/8	24.625					
24 3/4	24.75					
24 7/8	24.875					
25	25.0					
25 1/8	25.125					
25 1/4	25.25					
25 3/8	25.375					
25 1/2	25.5					
25 5/8	25.625					
25 3/4	25.75					
25 7/8	25.875					
26	26.0					
26 1/8	26.125					
26 1/4	26.25					
26 3/8	26.375					
26 1/2	26.5					
26 5/8	26.625					
26 3/4	26.75					
26 7/8	26.875					
27	27.0					
27 1/8	27.125					
27 1/4	27.25					
27 3/8	27.375					
27 1/2	27.5					
27 5/8	27.625					
27 3/4	27.75					
27 7/8	27.875					
28	28.0					
28 1/8	28.125					
28 1/4	28.25					
28 3/8	28.375					
28 1/2	28.5					
28 5/8	28.625					
28 3/4	28.75					
28 7/8	28.875					
29	29.0					
29 1/8	29.125					
29 1/4	29.25					
29 3/8	29.375					
29 1/2	29.5					
29 5/8	29.625					
29 3/4	29.75					
29 7/8	29.875					
30	30.0					
30 1/8	30.125					
30 1/4	30.25					
30 3/8	30.375					
30 1/2	30.5					
30 5/8	30.625					
30 3/4	30.75					
30 7/8	30.875					
31	31.0					
31 1/8	31.125					
31 1/4						

[illegible]

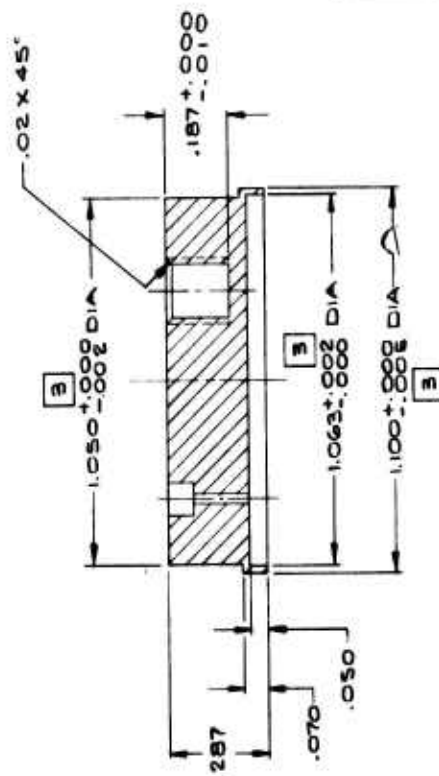
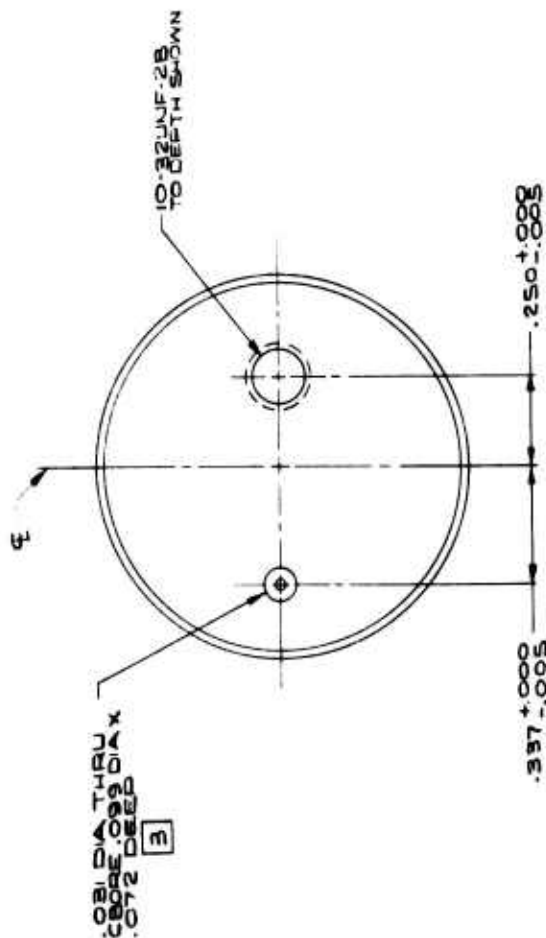
.187 DIA THRU
CSINK .312 DIA X .82.
8 PLACES EQUALLY SPACED
ON A 1.937 DIA B.C.

[illegible]

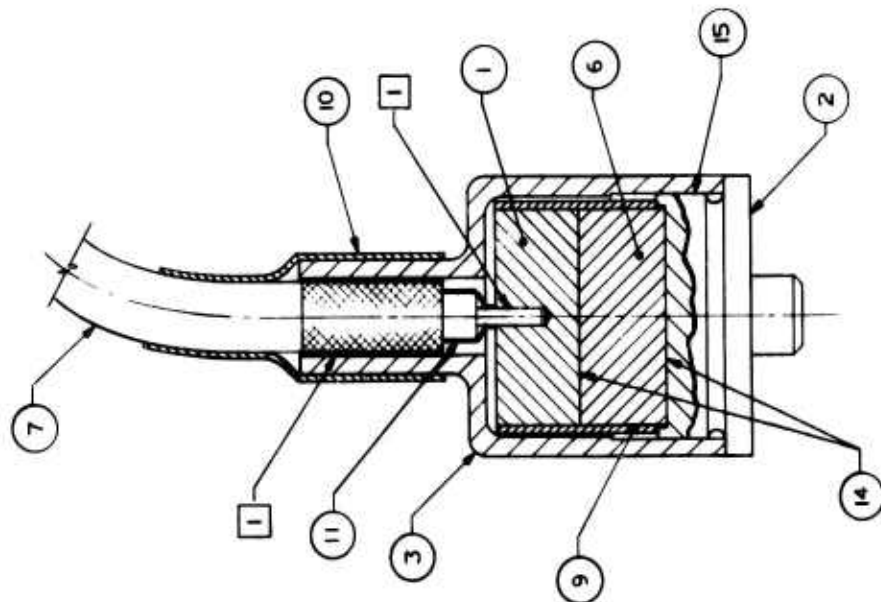
[illegible]

1

NOTES:
1. GRUNLESS OTHERWISE SPECIFIED.
2. BREAK ALL SHARP EDGES. O.R. MAX.
3. DIAMETERS INDICATED ARE TO BE
OBTAINED WITH THE RESULT OF
ELECTRICALLY STRIPPED CABLES.

[illegible][illegible]

NOTES:
 1 ELECTRICAL GRADE SOLDER TO BE USED ON ALL SOLDER JOINTS.



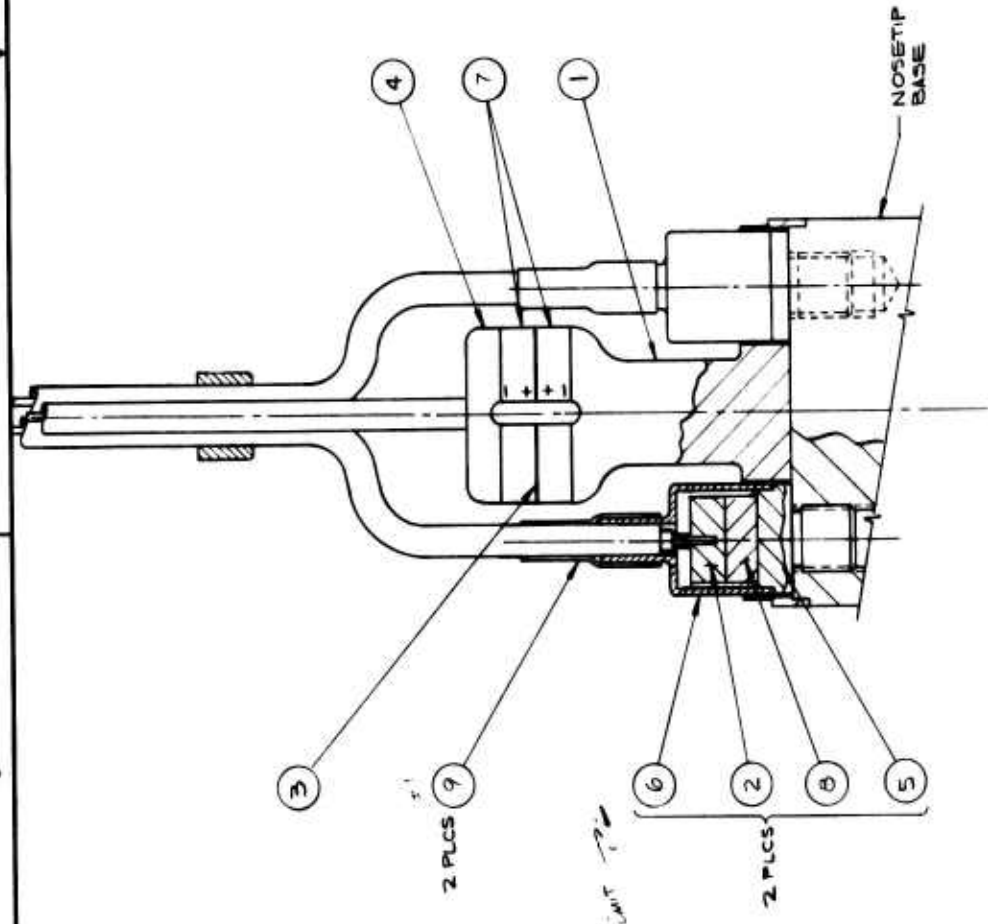
ITEM NO.	CODE IDENT	PART NO.	DESCRIPTION
AR 14	36-2		EPOXY, ELECTRICALLY CONDUCTIVE
AR 13			
AR 12			
AR 11			HEAT SHRINKABLE TUBING, IRRADIATED FLEXIBLE POLYVINYL CHLORIDE, 1/16 DIA
AR 10			HEAT SHRINKABLE TUBING, IRRADIATED FLEXIBLE POLYVINYL CHLORIDE, 3/16 DIA
AR 9	TYPE 1		HEAT SHRINKABLE TUBING, IRRADIATED, POLYVINYLIDENE FLUORIDE, 1/4 DIA
AR 8			
1 7	3090A		CABLE ASSEMBLY ENDEVCO
1 6	PZT-4		CRYSTAL, .250 DIA X .100 THK
1 5			
1 4			
1 3	7141-062		RECEIVER CASE
1 2	7141-060		RECEIVER BASE
1 1	7141-058		RECEIVER BACK MASS

ACUREX Acoustic Research 48 CLAYDE AVE. MOUNTAIN VIEW, CA 94039	
DRAWN G. LEWIS CHECKED ENGINEER APPROVED	DATE 9-1-76 RECEIVER ASSEMBLY- COMPRESSIONAL ACOUSTIC GAGE (SINGLE MODE SENSOR) MOD I
SIZE CODE IDENT NO DRAWING NO C 50726 7141-079	REV
SCALE 10/1	WT
SHEET 1	

APPLICATION	QTY	USED ON	QTY
7141-065		7141	
NEXT ASSY			

1 2 3 4

REVISIONS		
ZONE	DESCRIPTION	DATE
LTR		



QTY	RECD	ITEM NO	CODE IDENT	PART NO	DESCRIPTION
1	02	01		7141-062	BLACK PVC HEAT SHRINK TUBING
2		08		7141-088	PZT-4 CRYSTALS (.25 DIA X .100 THK) IDENTICAL POLARITY ORIENTATION
2		07		7141-059	PZT-4 CRYSTALS (.50 DIA X .100 THK) RECEIVER CASE
2		06		7141-066	THREADED RECEIVER BASS
2		05		7141-059	TRANSMITTER BACK MASS
1		04		7141-066	TRANSMITTER CENTER ELECTRODE (CRYSTAL (+) FACE COMMON)
1		03		7141-058	RECEIVER BACK MASS
1		02		7141-097	MODIFIED TRANSMITTER BASE AND PEDESTAL (WAVEGUIDE)

ACUREX Acoustic Research 58 CLYDE AVE., MOUNTAIN VIEW, CA 94032	
50 MW-III ACOUSTIC GAGE ASSEMBLY (SINGLE MODE COMPRESSIONAL SENSOR) MOD II	
SIZE C 50726	CODE IDENT NO 7141-080
SCALE 4/1	
SHEET 1 OF 1	

QTY	APPLICATION
7141	USED ON
	NEXT ASSY

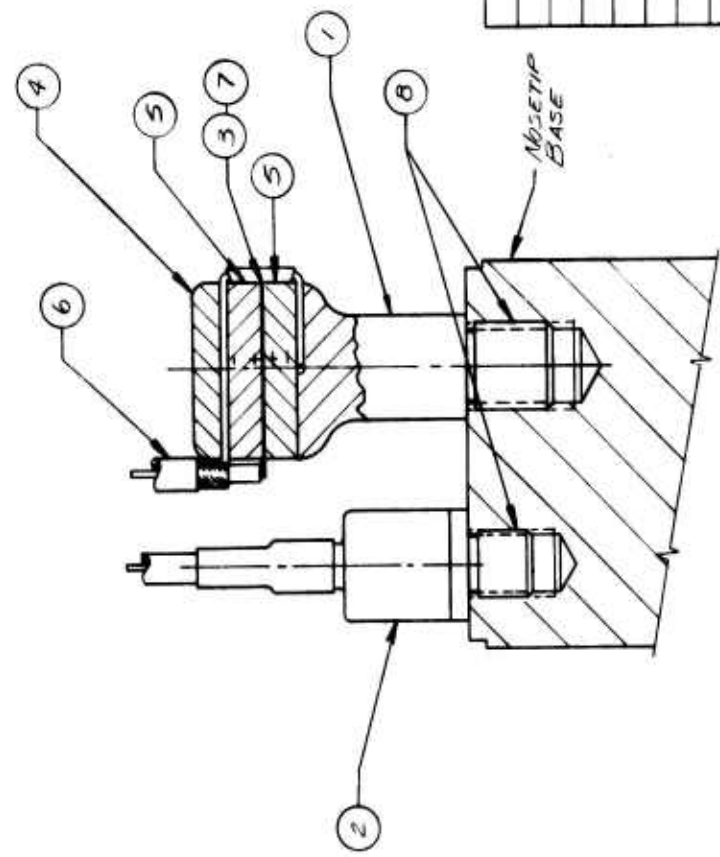
1 2 3 4

REVISIONS		DATE	APPROVED
ZONE	LTR		

2

3

4



ITEM NO.	CODE IDENT	PART NO.	DESCRIPTION
AR 8			HY50L E4956 STRUCTURAL EPOXY
AR 7			ABLEBAND 36-2 CONDUCTIVE EPOXY
1 6			COAX CABLE ASSEMBLIES ENDEVCO 3990-A
2 5			PBT-4 PEROELECTRIC CRYSTALS .500 IN DIA X .100 THICK
1 4		7141-059	TRANSMITTER BACK MASS
1 3		7141-066	TRANSMITTER ELECTRODE
1 2		7141-083	THREADED RECEIVER ASSEMBLY
1 1		7141-089	THREADED TRANSMITTER WAVEGUIDE

AGOREX 25 CLAY AVE. MOUNTAIN VIEW, CA 94032	
FLEXURAL ACOUSTIC GAGE ASSEMBLY (DUAL MODE SENSOR) MOD IV	
SIZE C 50726	DRAWING NO. 7141-081
SCALE 1/1	
SHEET OF 1	

QTY	USED ON	QTY	APPLICATION

1

2

3

4

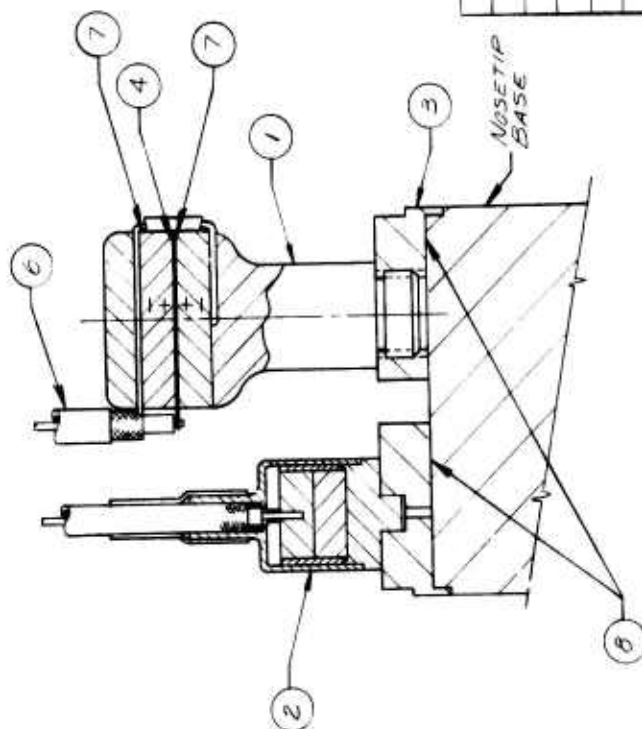
1

2

3

4

REVISIONS		DATE	APPROVED
ZONE	LTR		



QTY	REQD	ITEM NO	CODE IDENT	PART NO	DESCRIPTION
1	1	1		7141-089	TRANSMITTER WAVE SLIDE
1	1	2		7141-085	BONDED RECEIVER ASSEMBLY
1	1	3		7141-098	FLEXURAL ACOUSTIC GAGE BASE, MOD. W/ SLIT
1	1	4		7141-086	TRANSMITTER ELECTRODE
1	1	5		7141-054	TRANSMITTER BACK MASS
1	1	6			ENVELOPE CAN CABLE ASSEMBLY - 3000 A
1	1	7			PRT 4 PNEUMATIC CRYSTALS - 500 IN DIA
1	1	8			HYGOL EA956 STRUCTURAL EPOXY

ACUREX Aeroflex 45 GLEN AVE, MOUNTAIN VIEW, CA 94039	
FLEXURAL ACOUSTIC GAGE ASSEMBLY (DUAL MODE SENSOR) MOD. V	
SIZE C 50726	DRAWING NO 7141-082
SCALE 4/1	WT 1
SHEET 1 OF 1	

1

2

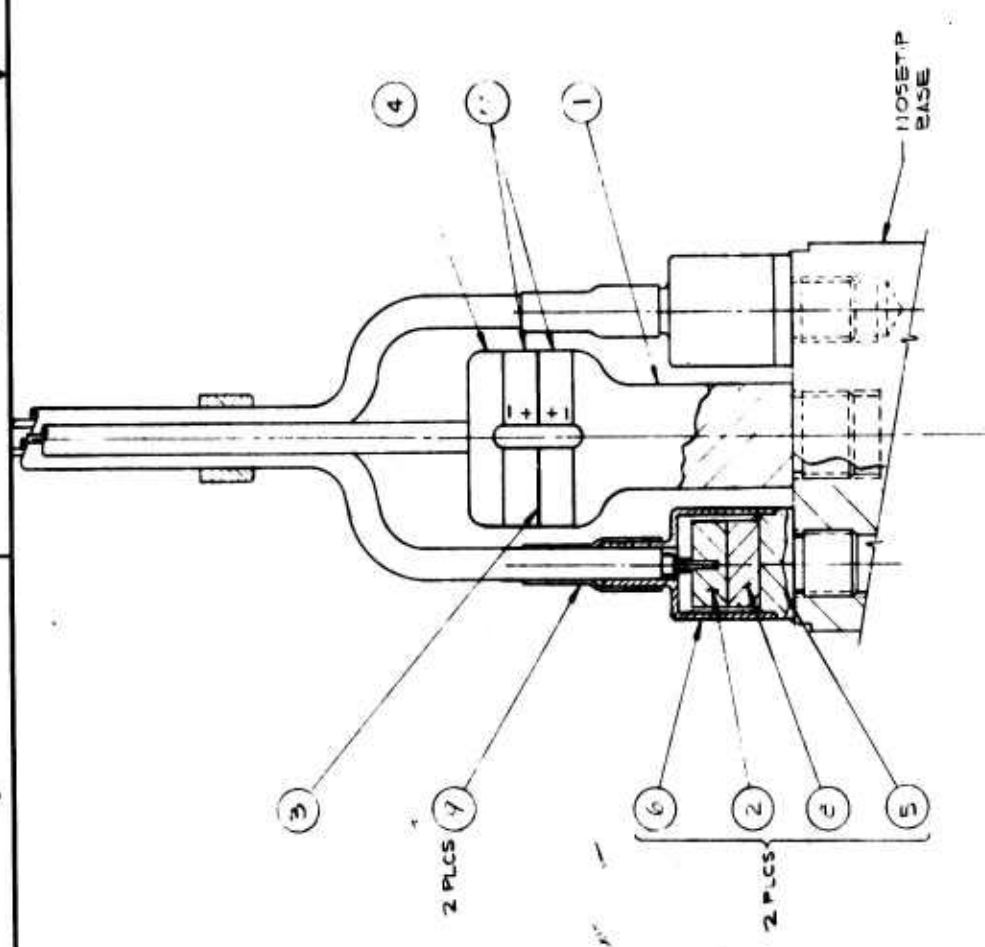
3

4

1 2 3 4

D C B A

REVISIONS		DATE	APPROVED
ZONE	LYN		

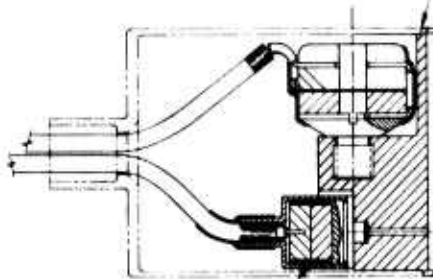


ITEM NO	QTY	DESCRIPTION
1	1	BLACK PVC HEAT SHRINK TUBING
2	2	P2T-4 CRYSTALS (7" DIA X .100 THK) IDENTICAL POLARITY ORIENTATION
3	2	P2T-4 CRYSTALS (7" DIA X .100 THK)
4	2	RECEIVER CASE
5	2	THREADED RECEIVER BARS
6	1	TRANSMITTER BACK MASS
7	1	TRANSMITTER CENTER ELECTRODE (CRYSTAL (+) FACE COMMON)
8	1	RECEIVER BACK MASS
9	1	THREADED TRANSMITTER WAVEGUIDE

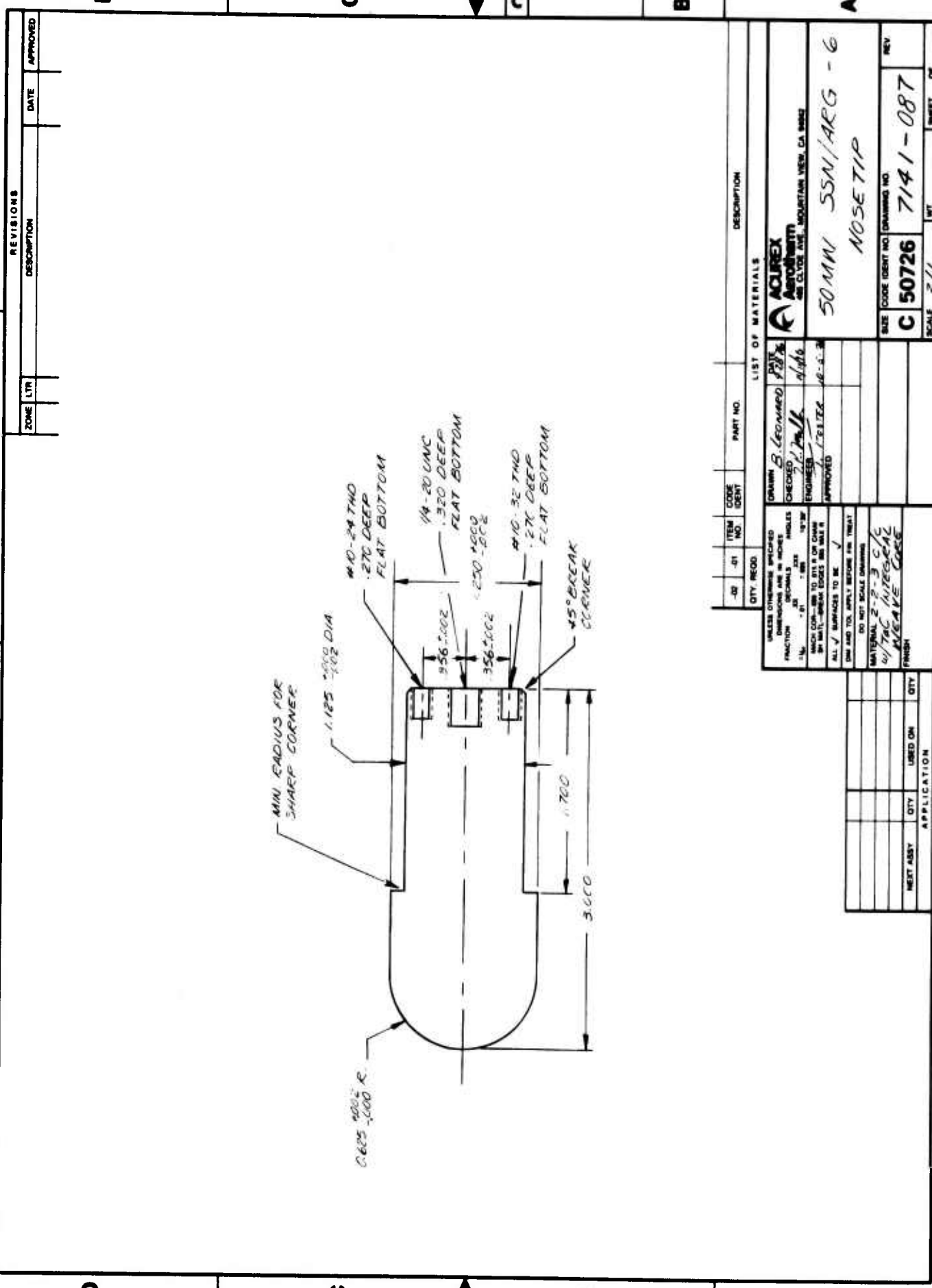
LIST OF MATERIALS	
ACUREX	DATE 8-15-74
50 MW-III ACOUSTIC GAGE ASSEMBLY (DUAL-SENSOR) MOD III	BY CLYDE AVE. MOUNTAIN VIEW, CA 94038
DATE CODE IDENT NO	7141-083
SCALE	4/1
WT	
SHEET 1 OF 3	

UNLESS OTHERWISE SPECIFIED DIMENSIONS ARE IN INCHES	
FINISH	ALL SURFACES TO BE
ALL DIMENSIONS TO CENTER UNLESS OTHERWISE SPECIFIED	DO NOT SCALE DRAWING
DO NOT SCALE DRAWING	
NOTED	
7141	7141
QTY USED ON	QTY
APPLICATION	

1 2 3 4

[illegible]

4 3 2 1

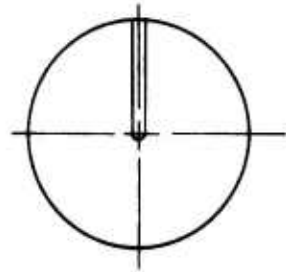



REVISIONS		DATE	APPROVED
ZONE	LTR		

ACUREX Aerospace 400 CLOVE AVE. MOUNTAIN VIEW, CA 94032		50MM SSN/ARG - 6 NOSETIP	
SIZE CODE IDENT NO DRAWING NO C 50726 7141-087		REV 1	
SCALE 2/1		WT 1	
SHEET OF 1		1	

ITEM NO	QTY	RECD	DESCRIPTION

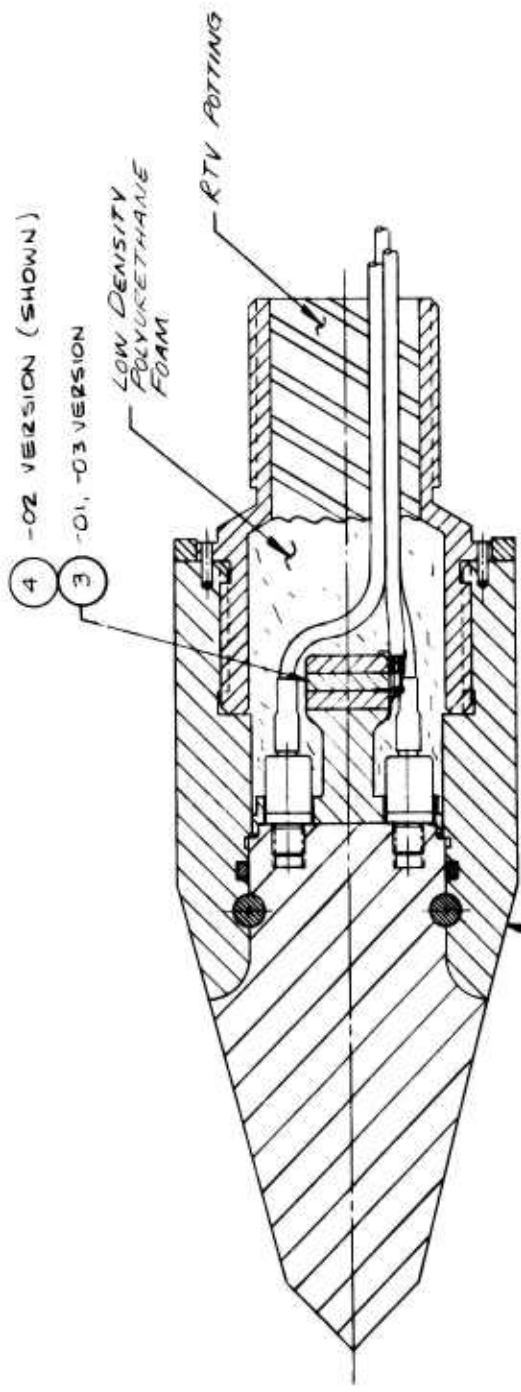
DIMENSIONS UNLESS OTHERWISE SPECIFIED FRACTIONS IN INCHES DECIMALS IN MILLIMETERS TOLERANCES FRACTIONS .125 .250 .375 .500 .750 1.000 1.500 2.000 3.000 4.000 5.000 6.000 7.000 8.000 9.000 10.000 12.000 15.000 20.000 25.000 30.000 35.000 40.000 45.000 50.000 60.000 70.000 80.000 90.000 100.000 DECIMALS .005 .010 .015 .020 .030 .040 .050 .060 .070 .080 .090 .100 .125 .150 .175 .200 .250 .300 .350 .400 .450 .500 .600 .700 .800 .900 1.000 1.250 1.500 1.750 2.000 2.500 3.000 3.500 4.000 4.500 5.000 6.000 7.000 8.000 9.000 10.000 12.000 15.000 20.000 25.000 30.000 35.000 40.000 45.000 50.000 60.000 70.000 80.000 90.000 100.000 ALL SURFACES TO BE <input checked="" type="checkbox"/> FINISHED DIM AND TOL APPLY BEFORE FIN TREAT DO NOT SCALE DRAWING MATERIAL 2-2-3 C/C w/ TAC INTEGRAL REAVE CASE FINISH	DRAWN B. LEONARD CHECKED J. J. J. ENGINEER J. J. J. APPROVED J. J. J.
---	--



DESCRIPTION	OF MATERIALS		
		AEROTHERM AQUATHER Corporation 485 CLYDE AVE. MOUNTAIN VIEW, CA 94039	
	THREADED TITANIUM WAVEGUIDE		
	SIZE	CODE IDENT NO.	DRAWING
	B	50726	712
	SCALE 4/1		WT

4 3 2 1

REVISIONS		
ZONE	DESCRIPTION	DATE
1		



-01, -02 VERSION 1
-03 VERSION 2

VERSION	MODEL NO	SENSOR CONFIGURATION	NOSE TIP CONFIGURATION
-01	ARG-2	COMPRESSORIAL MOD III THREADED TRANSMITTER WAVEGUIDE AND RECEIVER BASES	7141-083
-02	ARG-3	COMPRESSORIAL MOD II INTEGRAL ALUMINUM BASE W/ RECEIVER THRU HOLES	7141-080
-03	ARG-5A	COMPRESSORIAL MOD III, NO INTEGRAL ALUMINUM BASE	7141-083

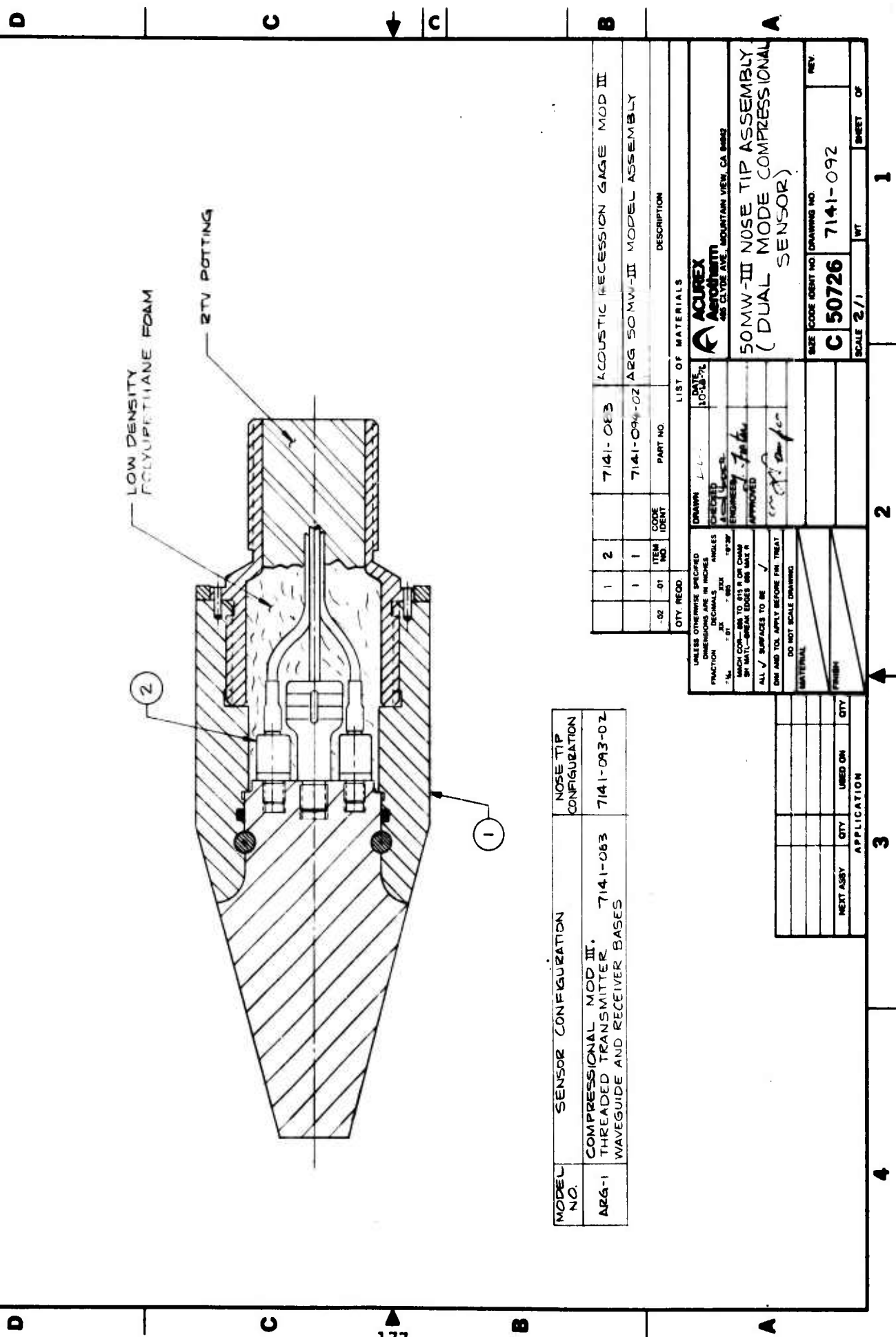
ACUREX Aerochem 400 E. 10th Ave. Mountain View, CA 94040	
DRAWN: E.C. 11/70 CHECKED: [] ENGINEER: [] APPROVED: []	DATE: 10/73 PART NO: [] CODE IDENT: []
LIST OF MATERIALS UNLESS OTHERWISE SPECIFIED DIMENSIONS ARE IN INCHES FRACTION DECIMALS ANGLES 1/16 .01 .005 10 30 MATCH COR- AND TO .015 X OR CHAM SH MATL-BREAK EDGES .005 MAX R ALL SURFACES TO BE [] DIM AND TOL. APPLY BEFORE FIN. TREAT DO NOT SCALE DRAWING	
MATERIAL: [] FINISH: []	

50MM-III NOSE TIP ASSEMBLY (SINGLE NOSE COMPRESSORIAL SENSOR)	
SIZE: CODE IDENT NO: 50726 DRAWING NO: 7141-080	REV: []
SCALE: 2/1	WT: [] SHEET OF: 1

APPLICATION	QTY	USED ON	QTY
NEXT ASSY			

4 3 2 1

4 3 2 1



REVISIONS		
ZONE	LTR	DESCRIPTION

DATE	APPROVED

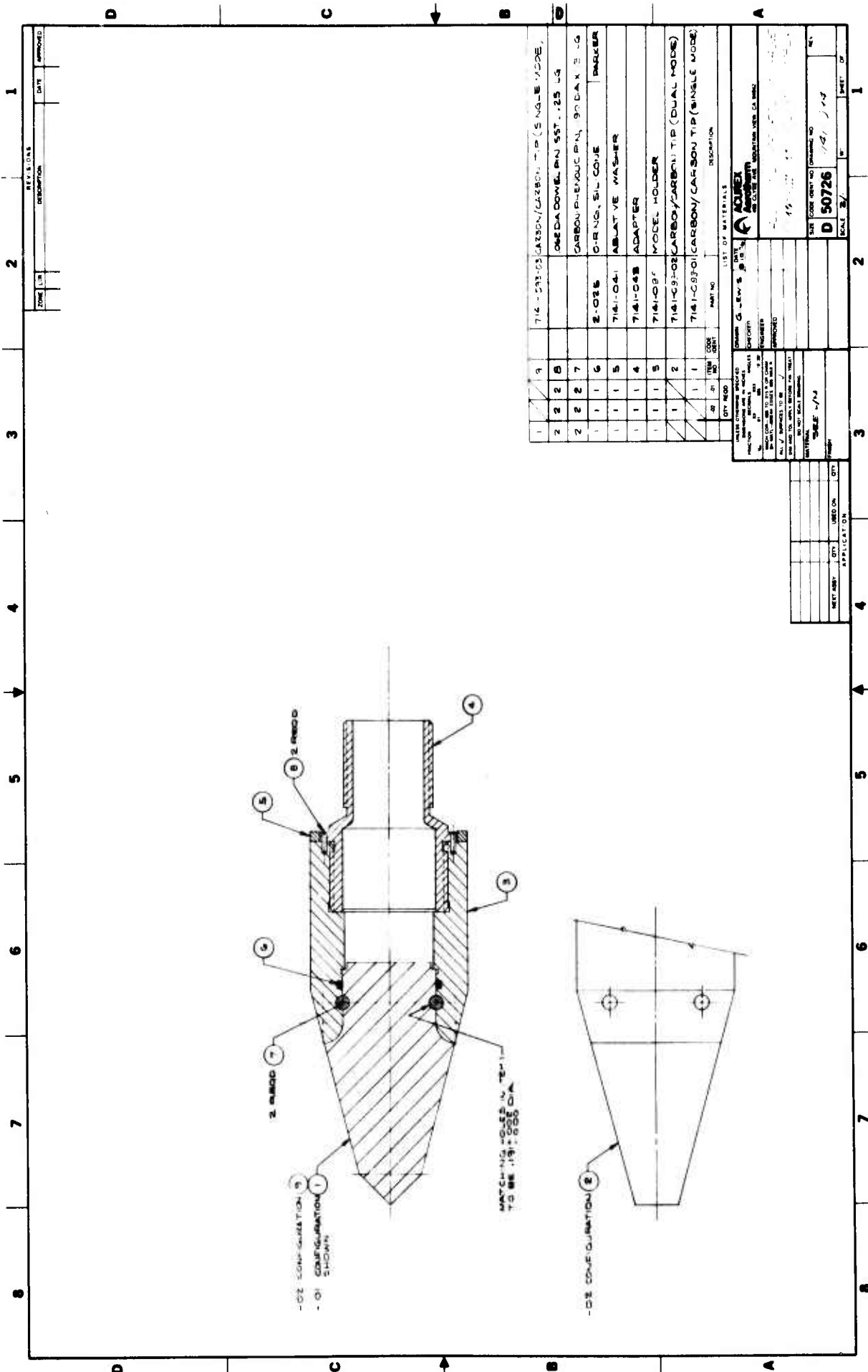
MODEL NO.	SENSOR CONFIGURATION	NOSE TIP CONFIGURATION
ARG-1	COMPRESSIONAL MOD III, THREADED TRANSMITTER, WAVEGUIDE AND RECEIVER BASES	7141-093-02

ITEM NO.	CODE IDENT	PART NO.	DESCRIPTION
1	01	7141-093	ACOUSTIC RECESSION GAGE MOD III
2	02	7141-094-02	ARG 50MW-III MODEL ASSEMBLY

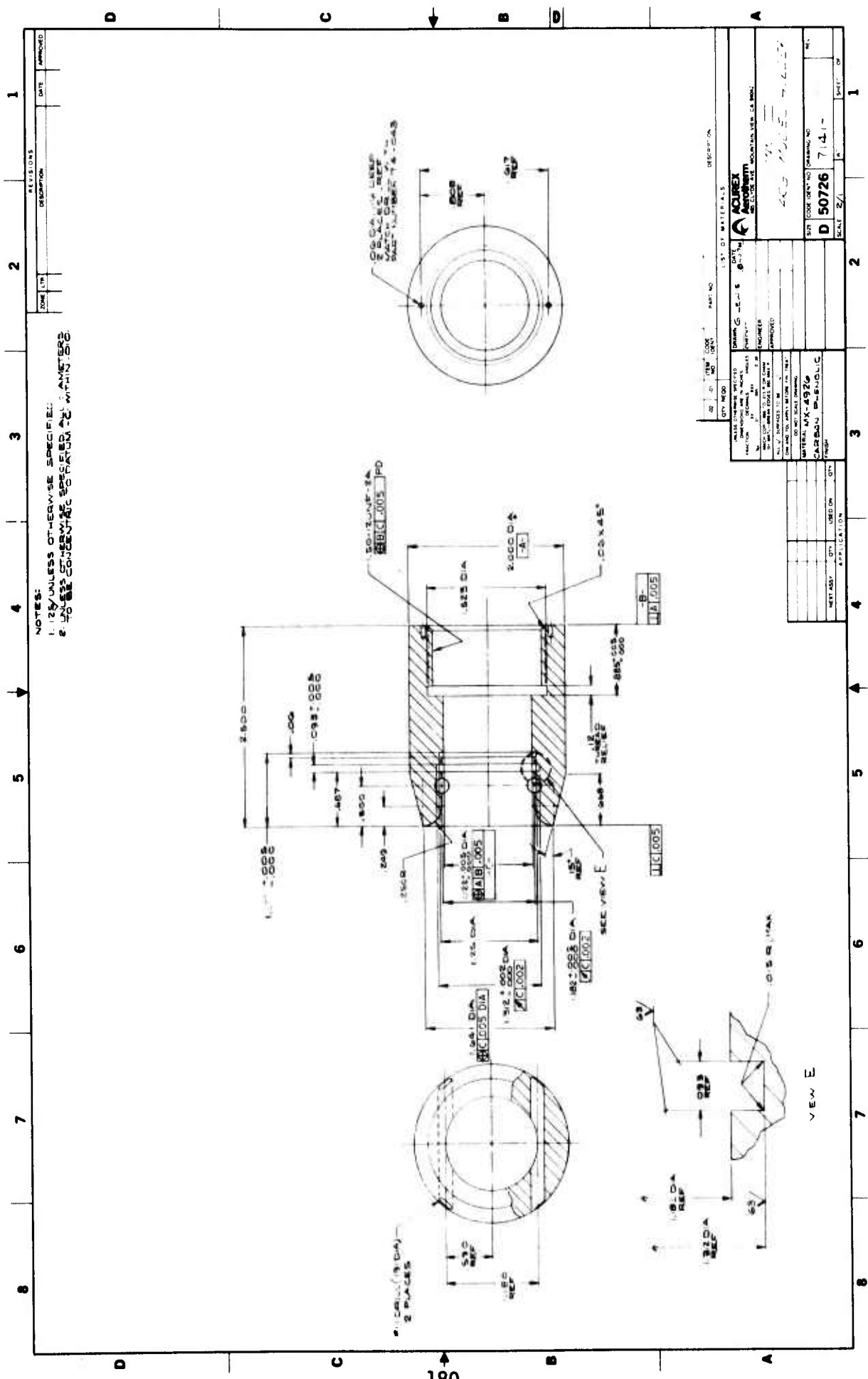
ACUREX Acurex Corporation 400 CLYDE AVE., MOUNTAIN VIEW, CA 94039	
50MW-III NOSE TIP ASSEMBLY (DUAL MODE COMPRESSIONAL SENSOR)	
SIZE C 50726	DRAWING NO 7141-092
SCALE 2/1	
REV	

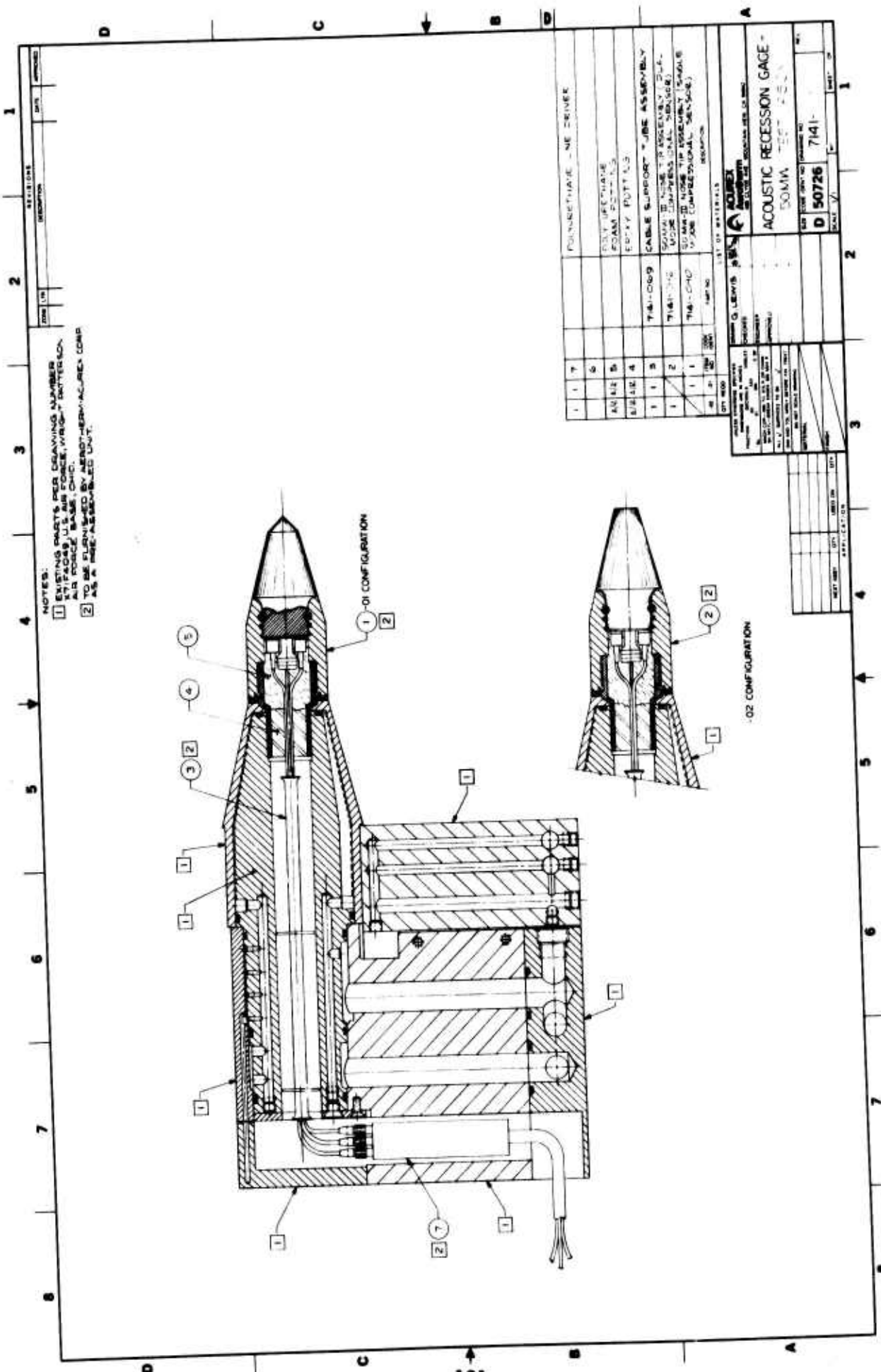
QTY	USED ON	QTY

4 3 2 1



1	1	3	714-1-037-02 CARBON/CARBON TIP (SINGLE MODE)																																																																																																																																																																																																																																																																																																																																																																																																																																																																																																																																																																																																																																																																																																																																																																																																																																																																																																																																																																																																																																																																																																																																																																																																																																																																																																																																																																																																													
---	---	---	--	--	--	--	--	--	--	--	--	--	--	--	--	--	--	--	--	--	--	--	--	--	--	--	--	--	--	--	--	--	--	--	--	--	--	--	--	--	--	--	--	--	--	--	--	--	--	--	--	--	--	--	--	--	--	--	--	--	--	--	--	--	--	--	--	--	--	--	--	--	--	--	--	--	--	--	--	--	--	--	--	--	--	--	--	--	--	--	--	--	--	--	--	--	--	--	--	--	--	--	--	--	--	--	--	--	--	--	--	--	--	--	--	--	--	--	--	--	--	--	--	--	--	--	--	--	--	--	--	--	--	--	--	--	--	--	--	--	--	--	--	--	--	--	--	--	--	--	--	--	--	--	--	--	--	--	--	--	--	--	--	--	--	--	--	--	--	--	--	--	--	--	--	--	--	--	--	--	--	--	--	--	--	--	--	--	--	--	--	--	--	--	--	--	--	--	--	--	--	--	--	--	--	--	--	--	--	--	--	--	--	--	--	--	--	--	--	--	--	--	--	--	--	--	--	--	--	--	--	--	--	--	--	--	--	--	--	--	--	--	--	--	--	--	--	--	--	--	--	--	--	--	--	--	--	--	--	--	--	--	--	--	--	--	--	--	--	--	--	--	--	--	--	--	--	--	--	--	--	--	--	--	--	--	--	--	--	--	--	--	--	--	--	--	--	--	--	--	--	--	--	--	--	--	--	--	--	--	--	--	--	--	--	--	--	--	--	--	--	--	--	--	--	--	--	--	--	--	--	--	--	--	--	--	--	--	--	--	--	--	--	--	--	--	--	--	--	--	--	--	--	--	--	--	--	--	--	--	--	--	--	--	--	--	--	--	--	--	--	--	--	--	--	--	--	--	--	--	--	--	--	--	--	--	--	--	--	--	--	--	--	--	--	--	--	--	--	--	--	--	--	--	--	--	--	--	--	--	--	--	--	--	--	--	--	--	--	--	--	--	--	--	--	--	--	--	--	--	--	--	--	--	--	--	--	--	--	--	--	--	--	--	--	--	--	--	--	--	--	--	--	--	--	--	--	--	--	--	--	--	--	--	--	--	--	--	--	--	--	--	--	--	--	--	--	--	--	--	--	--	--	--	--	--	--	--	--	--	--	--	--	--	--	--	--	--	--	--	--	--	--	--	--	--	--	--	--	--	--	--	--	--	--	--	--	--	--	--	--	--	--	--	--	--	--	--	--	--	--	--	--	--	--	--	--	--	--	--	--	--	--	--	--	--	--	--	--	--	--	--	--	--	--	--	--	--	--	--	--	--	--	--	--	--	--	--	--	--	--	--	--	--	--	--	--	--	--	--	--	--	--	--	--	--	--	--	--	--	--	--	--	--	--	--	--	--	--	--	--	--	--	--	--	--	--	--	--	--	--	--	--	--	--	--	--	--	--	--	--	--	--	--	--	--	--	--	--	--	--	--	--	--	--	--	--	--	--	--	--	--	--	--	--	--	--	--	--	--	--	--	--	--	--	--	--	--	--	--	--	--	--	--	--	--	--	--	--	--	--	--	--	--	--	--	--	--	--	--	--	--	--	--	--	--	--	--	--	--	--	--	--	--	--	--	--	--	--	--	--	--	--	--	--	--	--	--	--	--	--	--	--	--	--	--	--	--	--	--	--	--	--	--	--	--	--	--	--	--	--	--	--	--	--	--	--	--	--	--	--	--	--	--	--	--	--	--	--	--	--	--	--	--	--	--	--	--	--	--	--	--	--	--	--	--	--	--	--	--	--	--	--	--	--	--	--	--	--	--	--	--	--	--	--	--	--	--	--	--	--	--	--	--	--	--	--	--	--	--	--	--	--	--	--	--	--	--	--	--	--	--	--	--	--	--	--	--	--	--	--	--	--	--	--	--	--	--	--	--	--	--	--	--	--	--	--	--	--	--	--	--	--	--	--	--	--	--	--	--	--	--	--	--	--	--	--	--	--	--	--	--	--	--	--	--	--	--	--	--	--	--	--	--	--	--	--	--	--	--	--	--	--	--	--	--	--	--	--	--	--	--	--	--	--	--	--	--	--	--	--	--	--	--	--	--	--	--	--	--	--	--	--	--	--	--	--	--	--	--	--	--	--	--	--	--	--	--	--	--	--	--	--	--	--	--	--	--	--	--	--	--	--	--	--	--	--	--	--	--	--	--	--	--	--	--	--	--	--	--	--	--	--	--	--	--	--	--	--	--	--	--	--	--	--	--	--	--	--	--	--	--	--	--	--	--	--	--	--	--	--	--	--	--	--	--	--	--	--	--	--	--	--	--	--	--	--	--	--	--	--	--	--	--	--	--	--	--	--	--	--	--	--	--	--	--	--	--	--	--	--	--	--	--	--	--	--	--	--	--	--	--	--	--	--	--	--	--	--	--	--	--	--	--	--	--	--	--	--	--	--	--	--	--	--	--	--	--	--	--	--	--	--	--	--	--	--	--	--	--	--	--	--	--	--	--	--	--	--	--	--	--	--	--	--	--	--	--	--	--	--	--	--	--	--	--	--	--	--	--	--	--	--	--	--	--	--	--	--	--	--	--	--	--	--	--	--	--	--	--	--	--	--	--	--	--	--	--	--	--	--	--	--	--	--	--	--	--	--	--	--	--	--	--	--	--	--	--	--	--	--	--	--	--	--	--	--	--	--	--	--	--	--	--	--	--	--	--	--	--	--	--	--	--	--	--	--	--	--	--	--	--	--	--	--	--	--	--	--	--	--	--	--	--	--	--	--	--	--	--	--	--	--	--	--	--	--	--	--	--	--	--	--	--	--	--	--	--	--	--	--	--	--	--	--	--	--	--	--	--	--	--	--	--	--	--	--	--	--	--	--	--	--	--	--	--	--	--	--	--	--	--	--	--	--	--	--	--	--	--	--	--	--	--	--	--	--	--	--	--	--	--	--	--	--	--	--	--	--	--	--	--	--	--	--	--	--	--	--	--	--	--	--	--	--	--	--	--	--	--	--	--	--	--	--	--	--	--	--	--	--	--	--	--	--	--	--	--	--	--	--	--	--	--	--	--	--	--	--	--	--	--	--	--	--	--	--	--	--	--	--	--	--	--	--	--	--	--	--	--



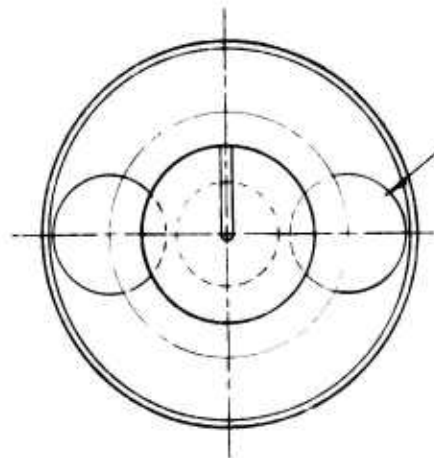


NOTES:
 1 EXISTING PARTS, PER DRAWING NUMBER
 1 EXISTING U.S. AIR FORCE, WRIGHT PATTERSON
 AIR FORCE BASE, OHIO.
 2 TO BE FURNISHED BY AEROTHERM-AEREX CORP.
 AS A RE-ASSEMBLED UNIT.

LIST OF MATERIALS	
1	7
2	5
3	4
4	3
5	2
6	1
7	1
8	1
9	1
10	1
11	1
12	1
13	1
14	1
15	1
16	1
17	1
18	1
19	1
20	1
21	1
22	1
23	1
24	1
25	1
26	1
27	1
28	1
29	1
30	1
31	1
32	1
33	1
34	1
35	1
36	1
37	1
38	1
39	1
40	1
41	1
42	1
43	1
44	1
45	1
46	1
47	1
48	1
49	1
50	1
51	1
52	1
53	1
54	1
55	1
56	1
57	1
58	1
59	1
60	1
61	1
62	1
63	1
64	1
65	1
66	1
67	1
68	1
69	1
70	1
71	1
72	1
73	1
74	1
75	1
76	1
77	1
78	1
79	1
80	1
81	1
82	1
83	1
84	1
85	1
86	1
87	1
88	1
89	1
90	1
91	1
92	1
93	1
94	1
95	1
96	1
97	1
98	1
99	1
100	1

ACQUICK
 ACQUICK REVISION GAGE
 50MM
 7141-
 D 50726
 7141-
 1

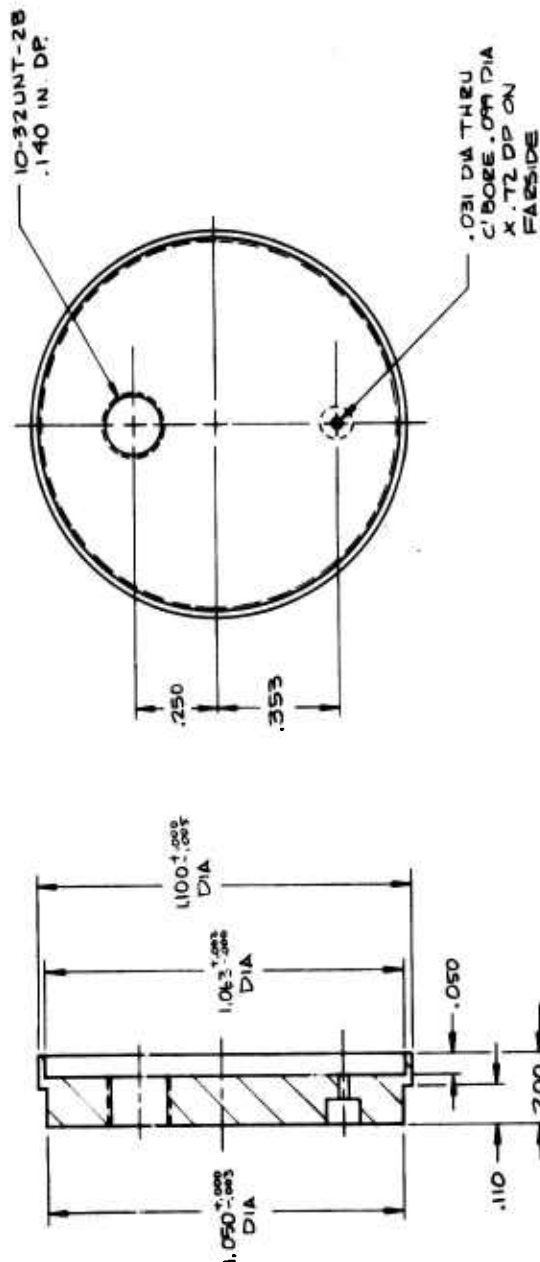
REVISIONS				
ZONE	LIN	DESCRIPTION	DATE	APPROVED



339 N. DIA (=R DRILL) THRU
2 HOLES 180° APART
ON .712 I: 885 DIA B.C.

[illegible]

REVISIONS				
ZONE	LTR	DESCRIPTION	DATE	APPROVED

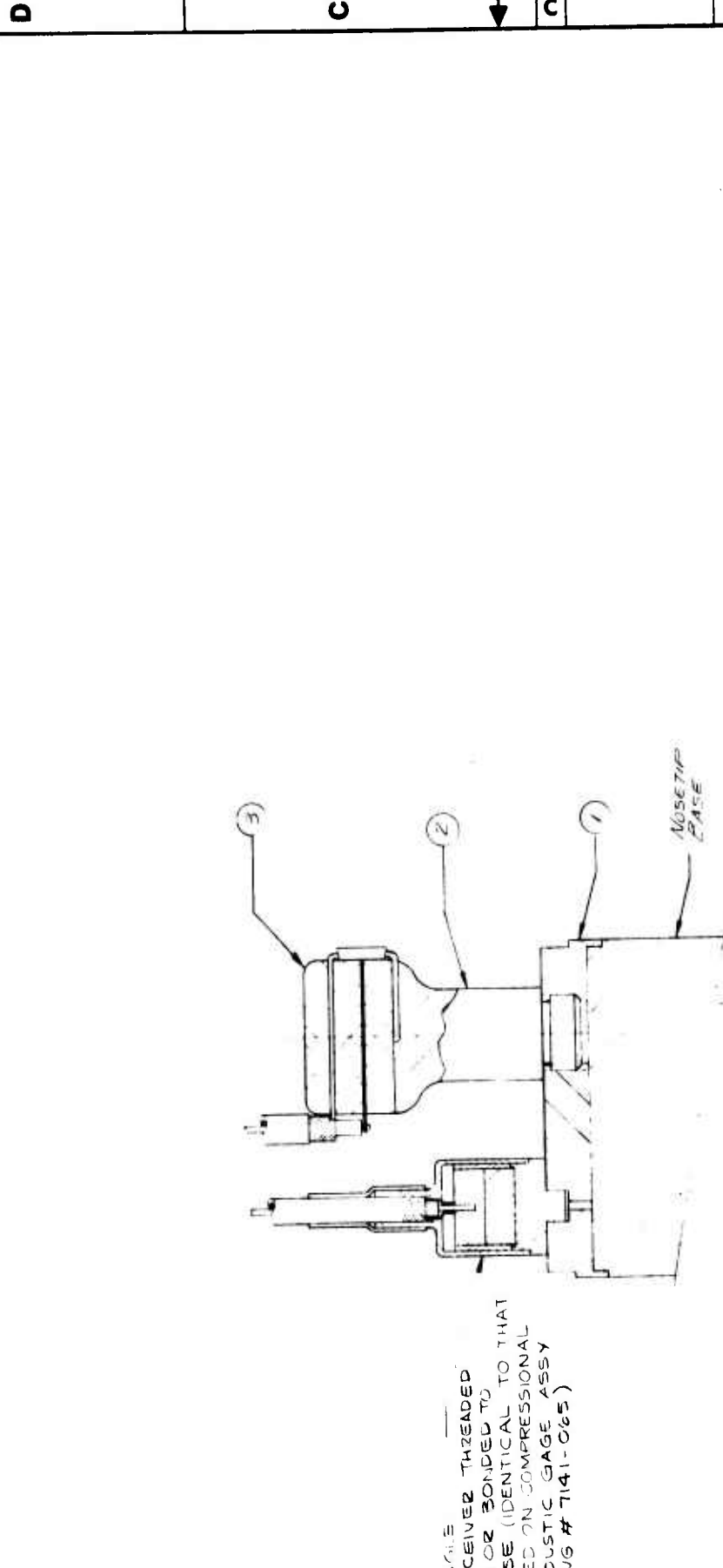


NOTES :
1. 63/ UNLESS OTHERWISE SPECIFIED
2. SAND BLAST ON EPOXY SURFACES
3. ALL DIAMETERS CONCENTRIC
WITHIN .005 TOTAL
4. BREAK ALL SHARP EDGES .01R
MAXIMUM.

[illegible]

1 2 3 4

REVISIONS		DATE	APPROVED
ZONE	LTR		



RECEIVER THREADED
ON OR BONDED TO
BASE (IDENTICAL TO THAT
USED ON COMPRESSIONAL
ACOUSTIC GAGE ASSY
DWG # 7141-065)

ITEM	NO	CODE	PART NO	DESCRIPTION
1	3		7141-059	FLEXURAL TRANSMITTER BACKMASS
1	2		7141-089	THREADED TRANSMITTER WAVEGUIDE
1	1		7141-098	FLEXURAL ACOUSTIC GAGE BASE (MOD II)

ACUREX Aerotherm 485 CLYDE AVE MOUNTAIN VIEW CA 94042	
DRAWN CHECKED ENGINEER APPROVED	DATE 10-15-72
FLEX-RA-120057-C GAGE ASSEMBLY (JULI MODE SENSOR) MOD II	
SIZE C	CODE IDENT NO 50726
DRAWING NO 7141-099	
REV	
SCALE 4/1	WT
SHEET OF 1	

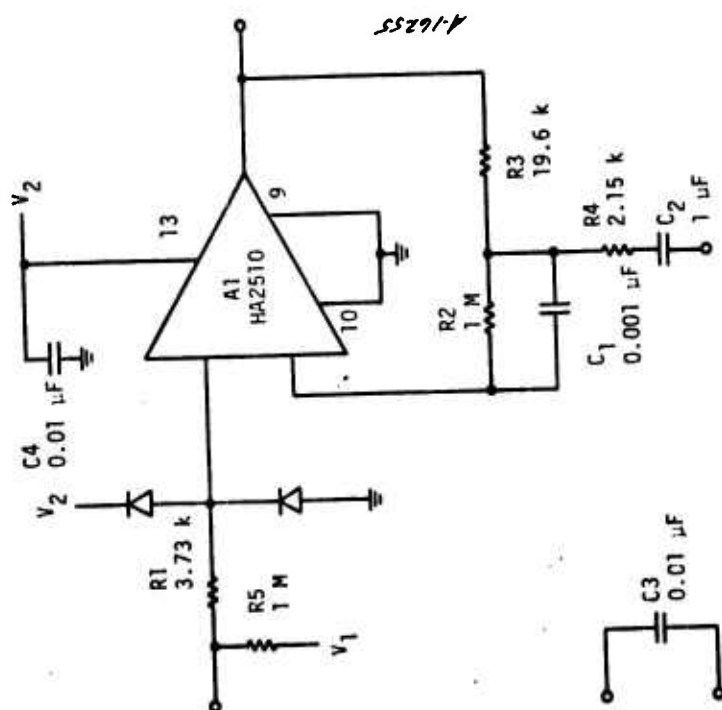
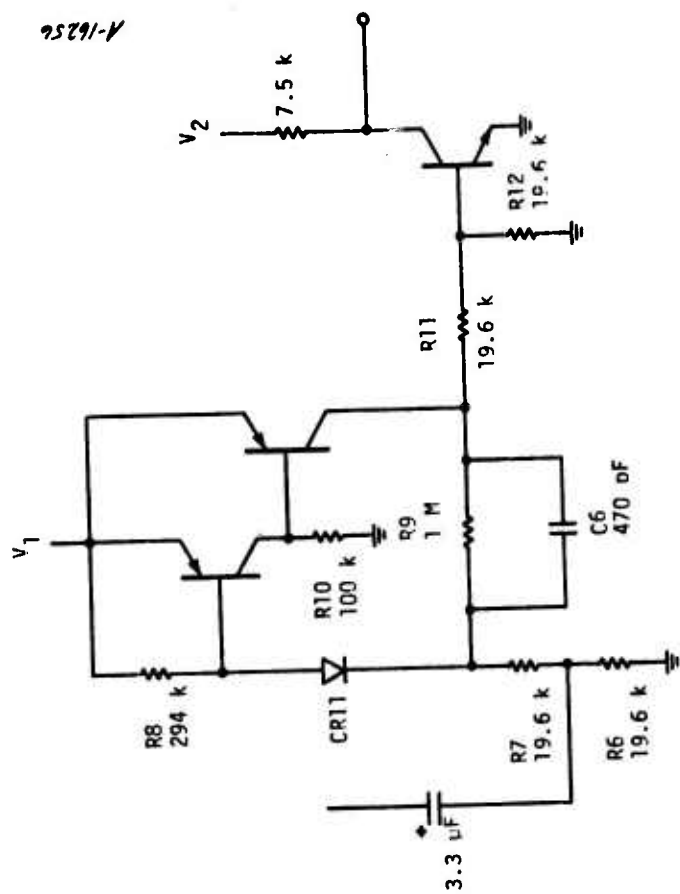
1 2 3 4

DTY REQD	UNLESS OTHERWISE SPECIFIED	DTY
01	INCHES	
02	DECIMALS	
03	ANGLES	
04	D 30	
05	D 30	
06	D 30	
07	D 30	
08	D 30	
09	D 30	
10	D 30	
11	D 30	
12	D 30	
13	D 30	
14	D 30	
15	D 30	
16	D 30	
17	D 30	
18	D 30	
19	D 30	
20	D 30	
21	D 30	
22	D 30	
23	D 30	
24	D 30	
25	D 30	
26	D 30	
27	D 30	
28	D 30	
29	D 30	
30	D 30	

APPENDIX B
ELECTRONIC SCHEMATICS AND WIRING DIAGRAMS

TABLE OF CONTENTS FOR APPENDIX B

Description	Page
Input Buffer and Start Circuit	189
Module #2 - Power Supply	190
Schematic, Power Supply	191
Module #3 Power Amplifier	192
Schematic - Power Amplifier	193
Module 4 - Phase Comparitor & Lock Detector	194
Schematic, Phase Comparitor & Lock Detector	195
Module 5 Integrator & VCO	196
Schematic - Integrator & VCO	197
Noise Detector	198
Input Buffer	199
Input Buffer	200
Module #2 - Power Supply	201
Module #2 - Power Supply	202
Module #3 Power Amplifier	203
Module #3 Power Amplifier	204
Module 4 - Phase Comparitor & Lock Detector	205
Module 4 - Phase Comparitor & Lock Detector	206
Noise Detector	207
Noise Detector	208
Module #5 - Integrator & VCO	209
Module #5 - Integrator & VCO	210



INPUT BUFFER AND START CIRCUIT

PARTS LIST

LINE NO.	QTY REQD				FWD NO.	DWG SIZE	PART NO.	REV LTR	DESCRIPTION	REF DESIG
	1	2	3	4						
1	2								MODULE 2 ESTAK	
2										
3	R								MODULE 2 SCHEMATIC	
4										
5										
6										
7	1								INTEGRATED CIRCUIT μ A723	A1
8	1								INTEGRATED CIRCUIT HA9-2510-B	A2
9										
10	1								CAPACITOR 22 μ fd, 100V, TANT CLR65	C1
11	2								CAPACITOR 100 μ fd, 200V, CERAMIC CKR08	C2,5
12	2								CAPACITOR 1.0 μ fd, 25V, TANT, -SR13	C3,4
13										
14	2								DIODE 1N4148 JAN1KV	CR1,2
15										
16	3								RESISTOR, 12.1 Ω RLR07C	R1,23
17	3								RESISTOR, 2.15K Ω RLR07C	R2,8,14
18	1								RESISTOR, 1.47K RLR07C	R5
19	1								RESISTOR SELECT RLR07C	R6
20	1								RESISTOR 511 Ω RLR07C	R9
21	2								RESISTOR 19.6K RLR07C	R10,11
22	1								RESISTOR 100K RLR07C	R12
23	1								RESISTOR 3.83K RLR07C	R13
24										
25	4								TRANSISTOR 2N46-1	Q1,2
26										3,5
27	1								TRANSISTOR 2N5501	Q4
28										
29										
30										
31										
32										
33										
34										
35										
36										
37										
38										
39										
40										

DATE	BY	DATE	BY
01/10/76	01/10/76	01/10/76	01/10/76
CHK	CHK	CHK	CHK
APVD	APVD	APVD	APVD
EN	EN	EN	EN


ACUREX Aerotherm 488 CLYDE AVE, MOUNTAIN VIEW, CA 94042	
MODULE #2 - POWER SUPPLY	
SIZE B	CODE IDENT NO. 50726
DRAWING NO. PL-	REV.

LTR	DATE	APVD	NEXT ASSY	USED ON
REVISIONS	APPLICATION			

PL-

PARTS LIST

LINE NO.	QTY REQD				PND NO.	DWS SIZE	PART NO.	REV LTR	DESCRIPTION	REF DESIG
	1	2	3	4						
1	2					4/11			MODULE 3 ESTAR	
2										
3	R								MODULE 3 SCHEMATIC	
4										
5										
6										
7	1								INTEGRATED CIRCUIT HA9-2510	A1
8										
9	2								CAPACITOR .01uf 100V 10% CKR05	C12
10	1								CAPACITOR .10uf 50V 10% CKR05	C3
11	1								CAPACITOR 30pf 200V 10% CKR05	C4
12	1								CAPACITOR 47uf 50V 20% CLR05	C5
13	2								CAPACITOR 1uf 50V 20% CSR13	C6,7
14										
15	6								DIODE 1N4143	CR1-6
16										
17	4								RESISTOR 10K 1/4W 2% RLR07	R1,2,6,7
18										
19	1								RESISTOR 75K 1/4W 2% RLR07	R3
20	2								RESISTOR 19.6K 1/4W 2% RLR07	R4,5
21	2								RESISTOR 3.01K 1/4W 2% RLR07	R8,9
22	1								RESISTOR 15K 1/4W 2% RLR07	R10
23	2								RESISTOR 249Ω 1/4W 2% RLR07	R11,12
24	2								RESISTOR 200Ω 1/4W 2% RLR07	R13,14
25	2								RESISTOR 33.2Ω 1/4W 2% RLR07	R15,16
26	2								RESISTOR 0.5Ω 1/4W 2% RLR07	R17,18
27										
28	1								TRANSISTOR 2N2907A	Q1
29	1								TRANSISTOR 2N3501	Q2
30	1								TRANSISTOR 2N3637	Q3
31										
32										
33										
34										
35										
36										
37										
38										
39										
40										

DESIGNED BY	DATE	 ACUREX Aerotherm 485 CLYDE AVE., MOUNTAIN VIEW, CA 94042			
CHECKED BY					
APPROVED BY					
DATE					
MODULE #3 POWER AMPLIFIER		SIZE B CODE IDENT NO. 50726 DRAWING NO. PL- REV.			
LTR	DATE	APVD	NEXT ASSY	USED ON	SHEET 1 OF 1
REVISIONS APPLICATION					

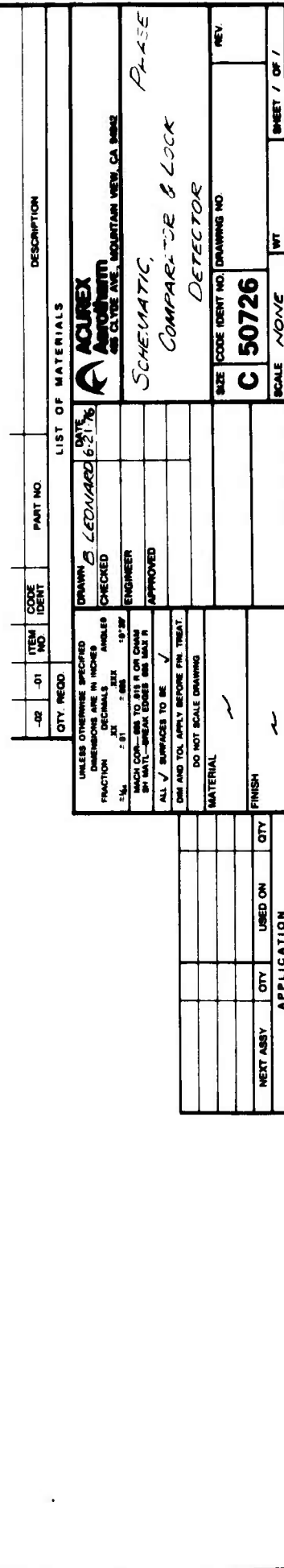
PL-

PARTS LIST

LINE NO.	QTY	REQD	FIND NO.	DWG SIZE	PART NO.	REV LTR	DESCRIPTION	REF DESIG
1	2						MODULE 4 E-7AK	
2								
3	R						MODULE 4 SCHEMATIC	
4								
5								
6								
7	1						INTEGRATED CIRCUIT AD532SH	A1
8	1						INTEGRATED CIRCUIT LM108A	A2
9								
10	4						CAPACITOR .1mfd CKR05	C1,2
11								5,6
12	2						CAPACITOR 100pfd CKR05	C3,8
13	1						CAPACITOR 4700pfd CKR05	C4
14							CAPACITOR 022mfd CKR05	C7
15								
16	8						RESISTOR 19.6K RLR07C	R1-4
17								10-13
18	1						RESISTOR 1.96K RLR07C	R5
19	1						RESISTOR SELECT RLR07C	R6
20	1						RESISTOR SELECT RLR07C	R7
21	1						RESISTOR SELECT RLR07C	R8
22	1						RESISTOR 10K RLR07C	R9
23	1						RESISTOR 316K RLR07C	R14
24	1						RESISTOR 196K RLR07C	R15
25	1						RESISTOR 3.33K RLR07C	R16
26								
27	1						TRANSISTOR 2N2945A	Q1
28								
29								
30								
31								
32								
33								
34								
35								
36								
37								
38								
39								
40								

PL-

DATE	6-29-76	ACUREX	
CHK		Aerotherm	
TRNG		485 CLYDE AVE, MOUNTAIN VIEW, CA 94042	
APVS		MODULE 4 - PHASE COM-	
CEL		PARITOR & LOCK DETECTOR	
SIZE	B	CODE IDENT NO.	50726
DRAWING NO.	PL-	REV.	
LTR	DATE	APVD	NEXT ASSY
REVISIONS			USED ON
			APPLICATION



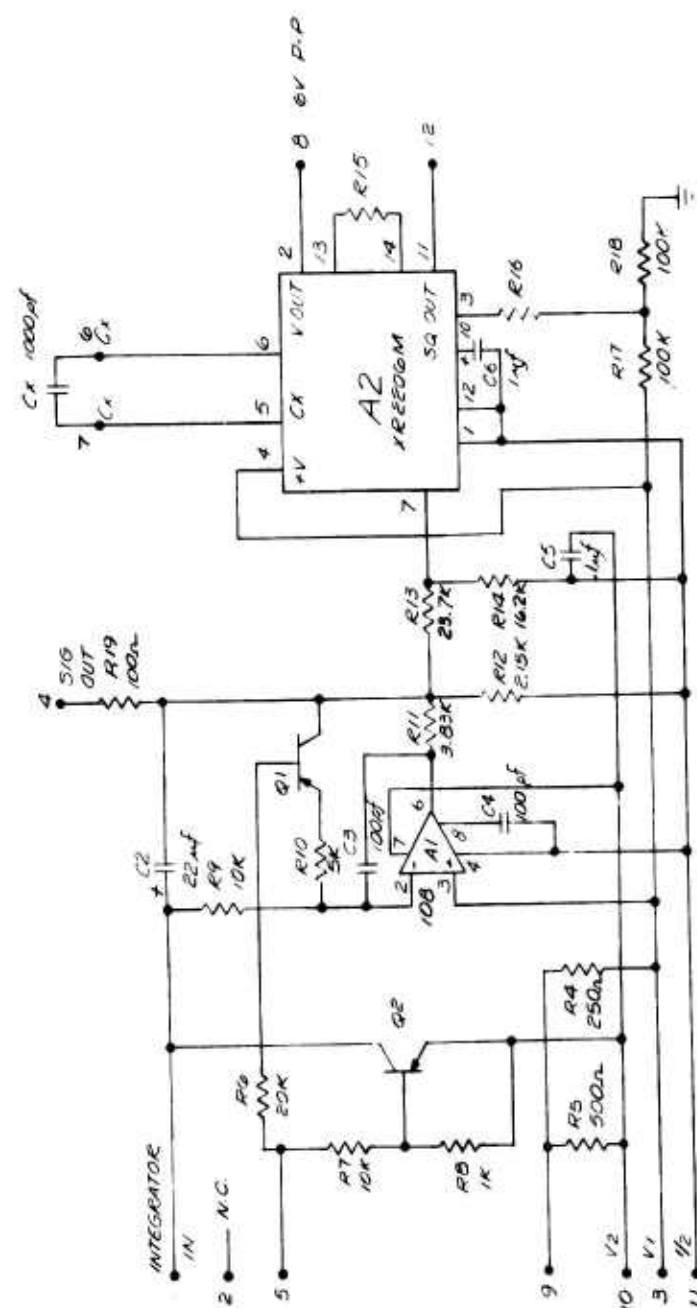
PARTS LIST

LINE NO.	QTY REQ'D				PND NO.	DWS SIZE	PART NO.	REV LTR	DESCRIPTION	REF DESIG
	1	2	3	4						
1	2					A/W			MODULE 5 ESTAR	
2										
3	R								MODULE 5 SCHEMATIC	
4										
5										
6										
7	/								INTEGRATED CIRCUIT LM108	A1
8	/								INTEGRATED CIRCUIT XR2206M	A2
9										
10	3								CAPACITOR 100pfd CKR05	C1,3,4
11	/								CAPACITOR 22mfd 25V CLR65	C2
12	/								CAPACITOR .1mfd CKR05	C5
13	/								CAPACITOR 1.0mfd CSR13	C6
14										
15	2								DIODE 1N4148	CR1,2
16										
17	2								RESISTOR 56.2K	R1,13
18	4								RESISTOR 100K	R2,4,7,8
19										
20	2								RESISTOR 38.3K	R3,14
21	/								RESISTOR 348K	R5
22	3								RESISTOR 1MEG	R6,9,10
23										
24	/								RESISTOR 3.83K	R11
25	/								RESISTOR 2.15K	R12
26	/								RESISTOR SELECT $\approx 200\Omega$	R15
27	/								RESISTOR SELECT } $\approx 50K$	R16
28	/								RESISTOR SELECT }	R17
29										
30	3								TRANSISTOR	Q1-3
31										
32										
33										
34										
35										
36										
37										
38										
39										
40										

DWN CHK ENGR APVD CTR				DATE 11/20/76		ACUREX Aerotherm 485 CLYDE AVE, MOUNTAIN VIEW, CA 94048	
						MODULE 5 INTEGRATOR & VCO	
SIZE B		CODE IDENT NO. 50726		DRAWING NO. PL-		REV. 1	
LTR REVISIONS		DATE APVD NEXT ASSY USED ON APPLICATION		SHEET / OF /			

PL-

REVISIONS		DATE	APPROVED
ZONE	LYR		



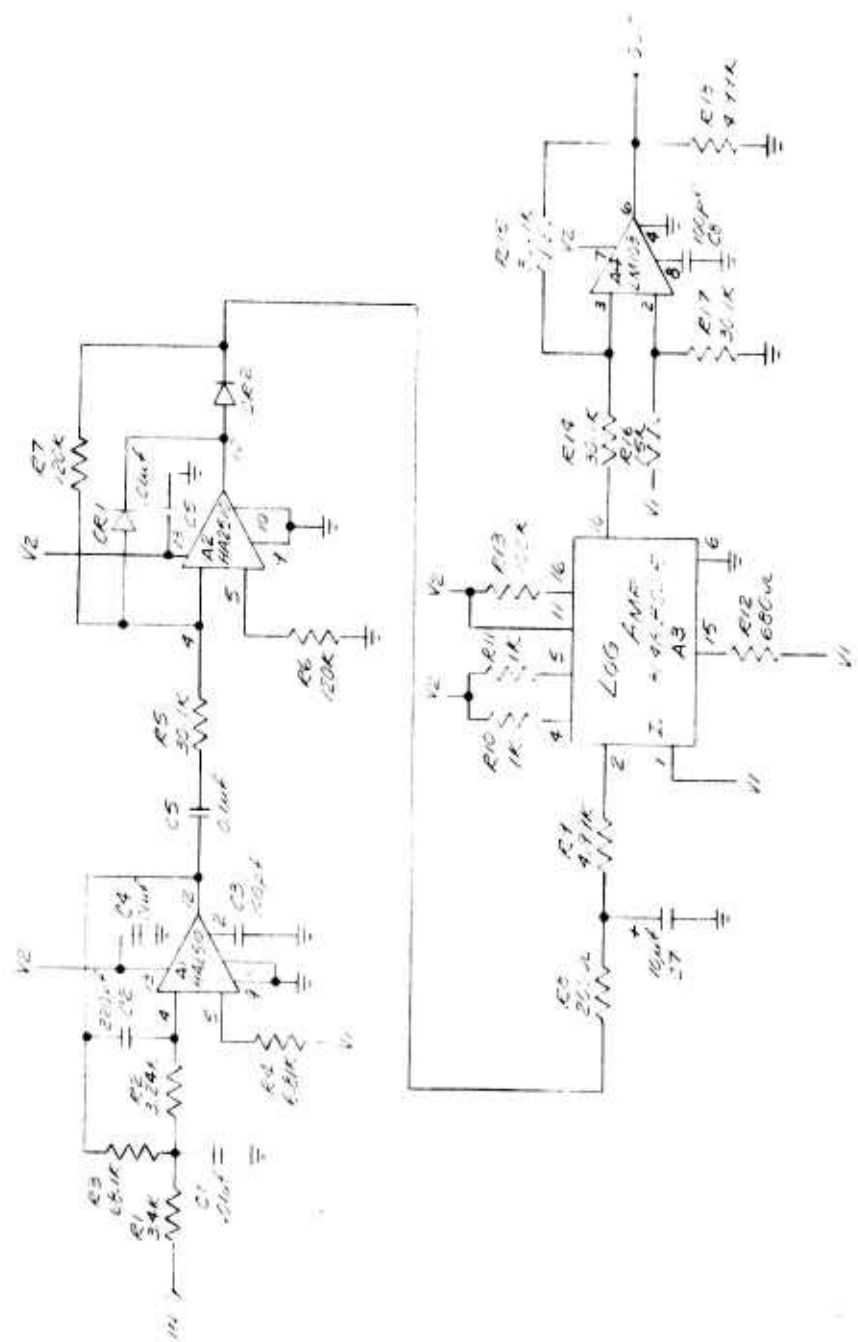
NOTES - UNLESS OTHERWISE SPECIFIED:
 1. ALL TRANSISTORS - 2N29A5A.
 2. ALL RESISTORS - 1/8W.
 3. $V_E = 20.5$
 $V_I = 10.25$

QTY. REQD.		ITEM NO.	CODE IDENT	PART NO.	DESCRIPTION
-02		-01			

UNLESS OTHERWISE SPECIFIED DIMENSIONS ARE IN INCHES FRACTION DECIMALS INCHES MILLIMETERS MACH CON - 98 TO .015 & OR CHAM BY MATL - BREAK EDGES ARE SHOWN ALL SURFACES TO BE DIM AND TOL APPLY BEFORE FIN. TREAT DO NOT SCALE DRAWING MATERIAL FINISH		DATE 6/22/78	DRAWN S. LEONARD	CHECKED S. LEONARD	ENGINEER S. LEONARD	APPROVED S. LEONARD
--	--	-----------------	---------------------	-----------------------	------------------------	------------------------

AUREX Aurora Electronics 25 CLAY AVE., MOUNTAIN VIEW, CA 94042		SCHEMATIC -	
INTEGRATOR & VCO			
SIZE	CODE IDENT NO.	DRAWING NO.	REV.
C	50726		
SCALE	NONE	WT	SHEET 1 OF 1

REVISIONS				
ZONE	LTR	DESCRIPTION	DATE	APPROVED



QTY REQD		ITEM NO	QTY	IDENT	PART NO	DESCRIPTION
-02	-01					

LIST OF MATERIALS		DATE
DRAWN	AS (CONVARD)	1/1/76
CHECKED		
ENGINEER		
APPROVED		

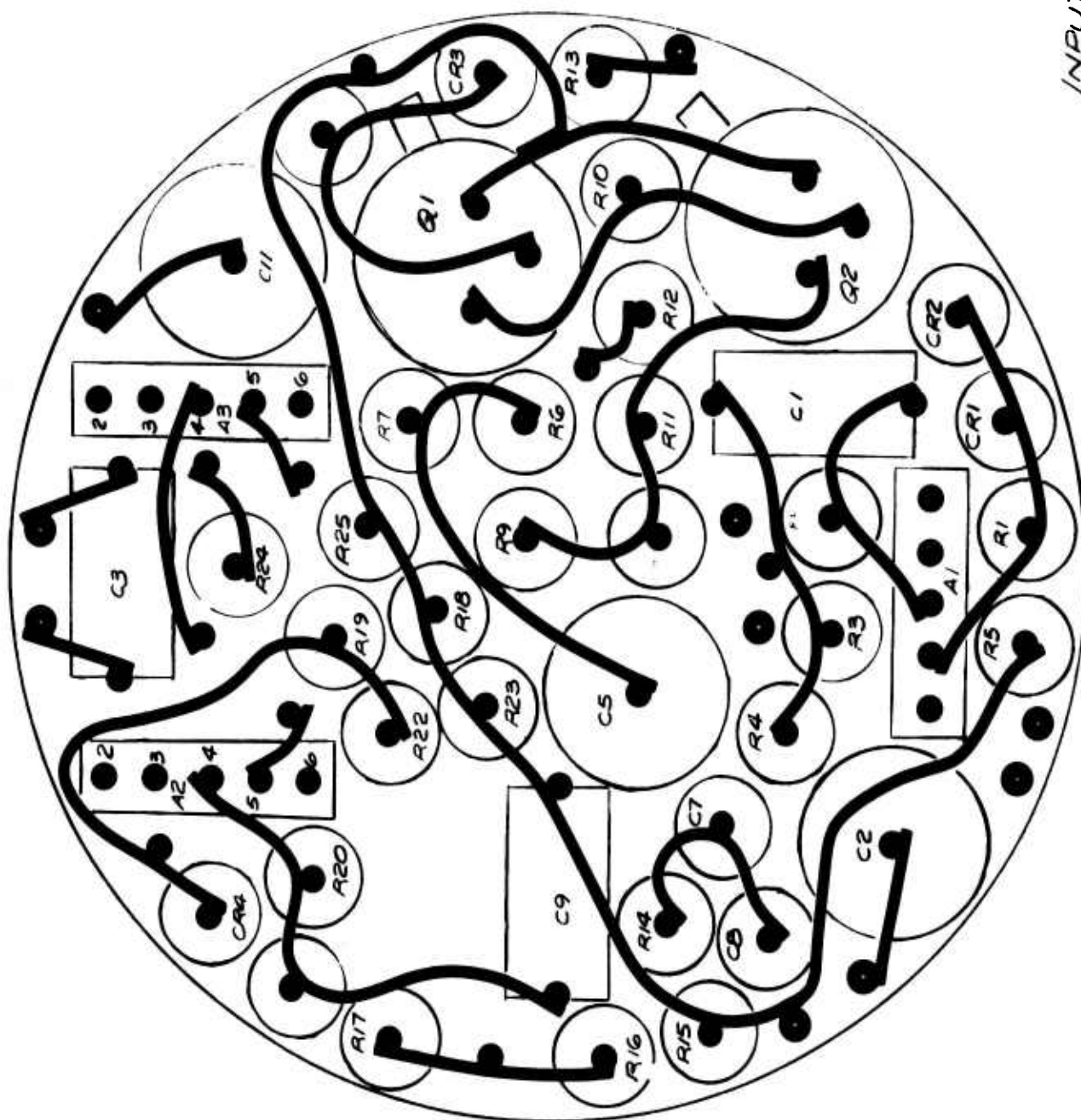
AEROTHERM	
AEROTHERM Corporation	
485 CLYDE AVE MOUNTAIN VIEW, CA 94042	
NOISE DETECTOR	

SIZE	CODE	IDENT NO	DRAWING NO	REV
C	50726			REV

SCALE	WT	SHEET	OF
1/16" = 1"			

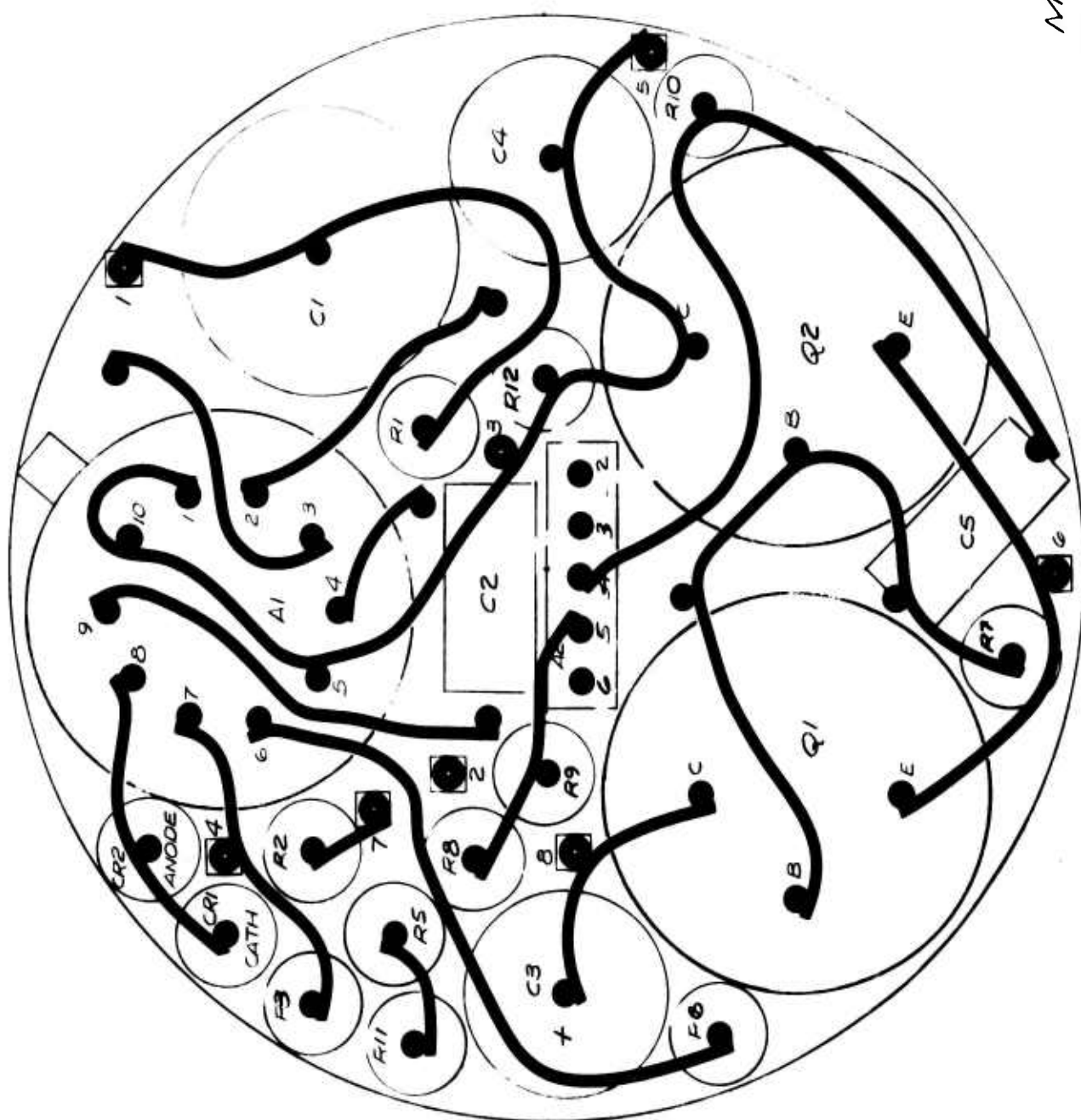
FINISH		APPLICATION	
NEXT ASSY	QTY	USED ON	QTY

INPUT BUFFER

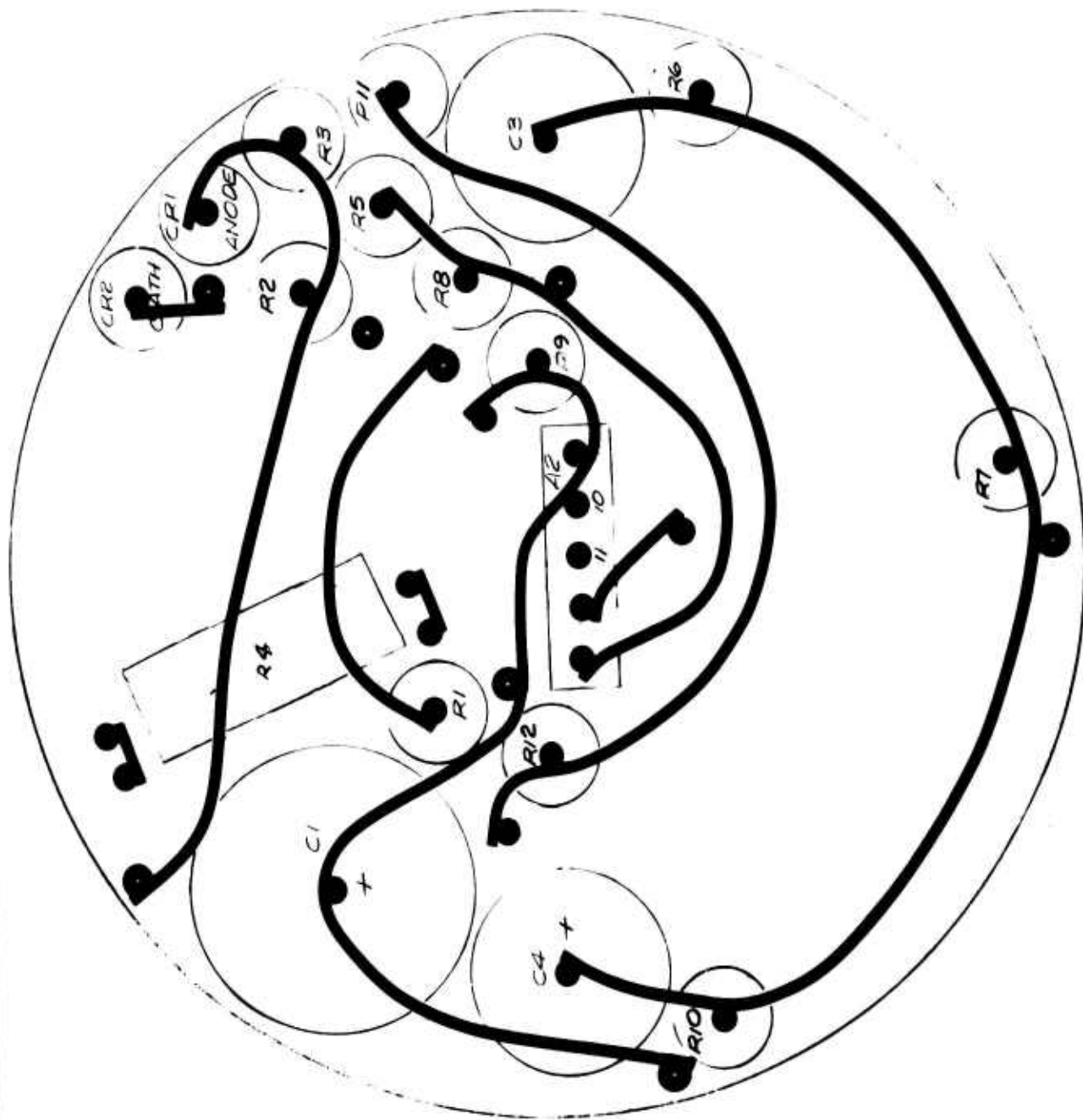




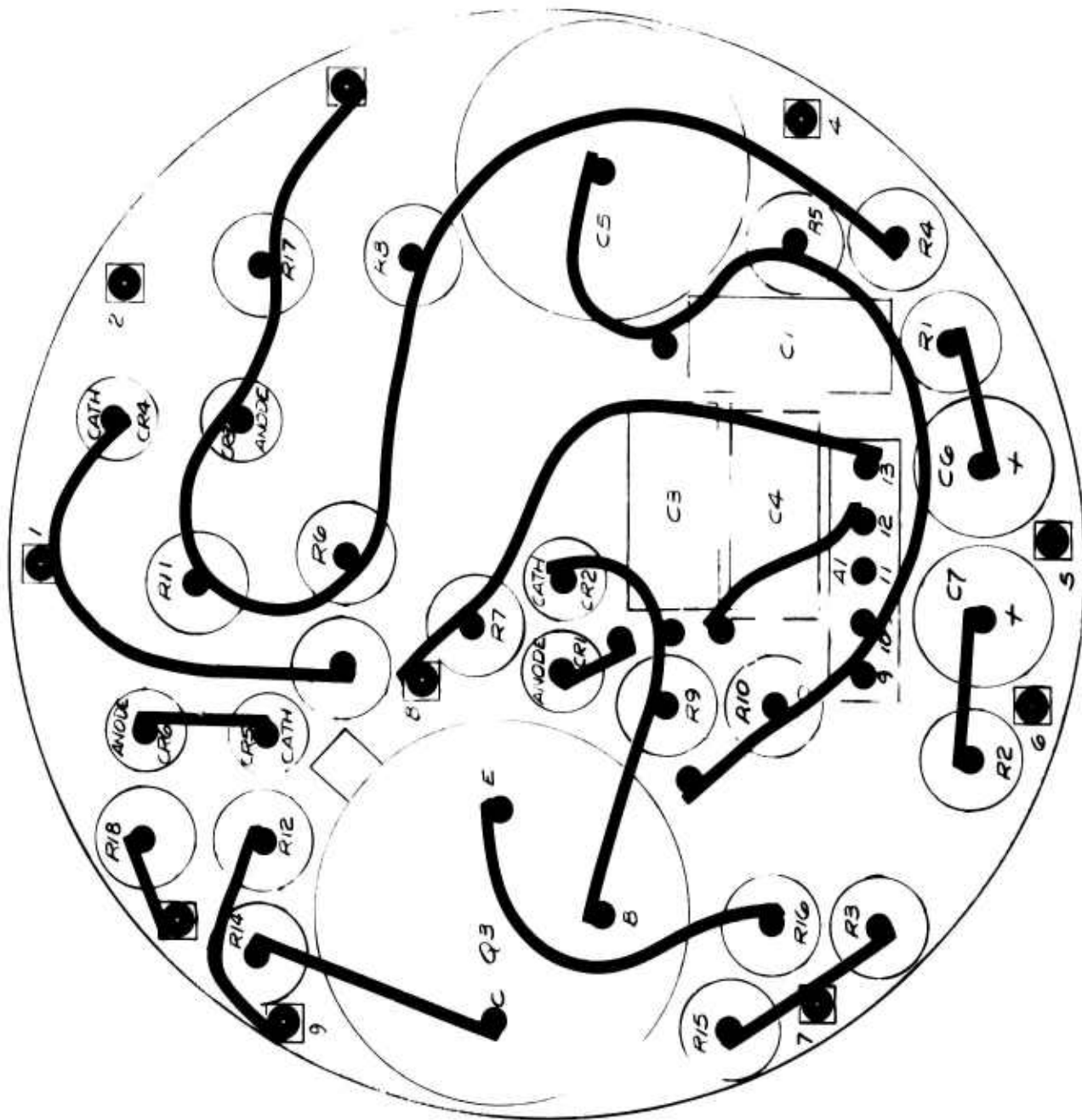
INPUT BUFFER



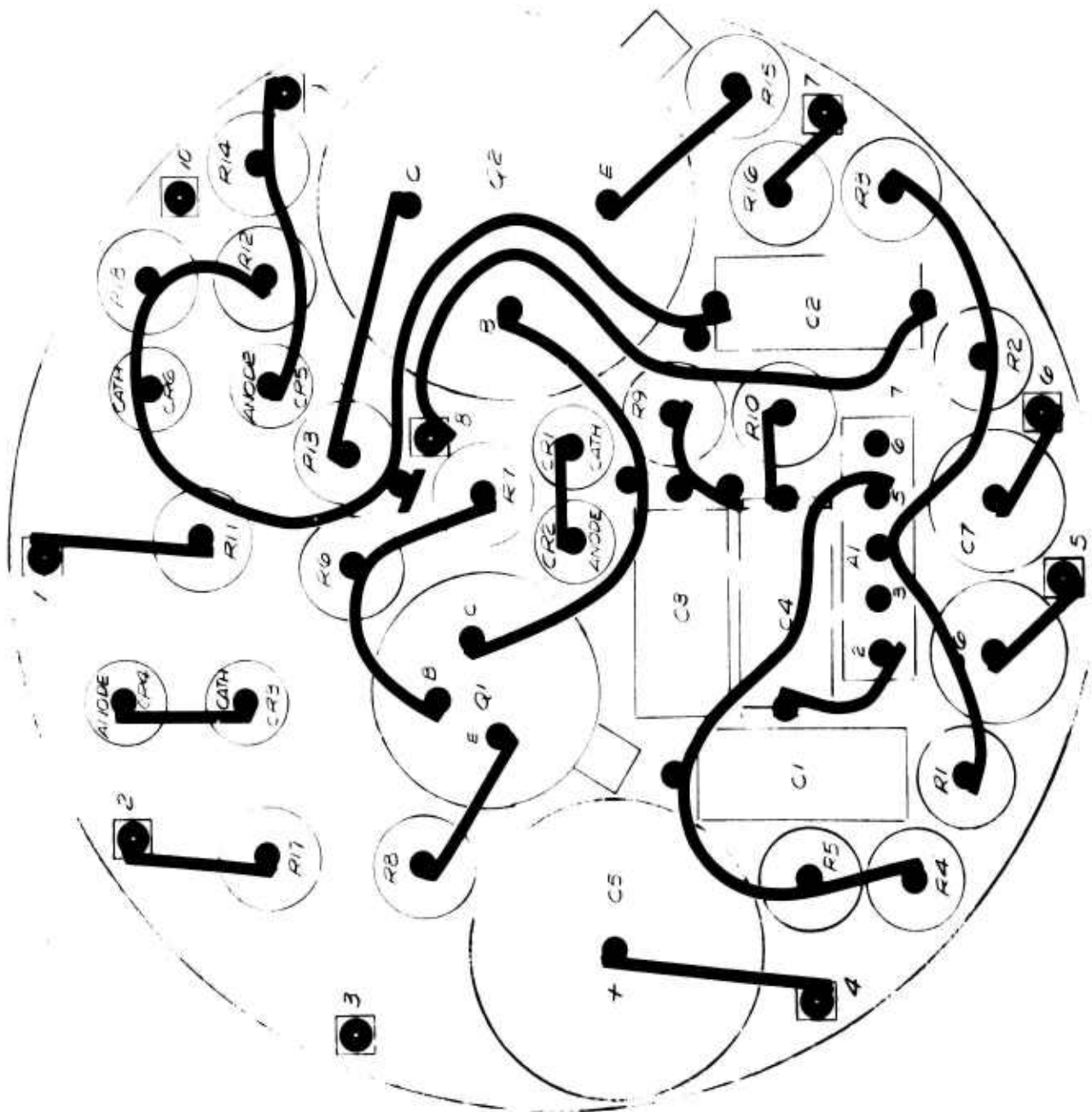
MODULE #2 -
POWER SUPPLY
71176



MODULE #2
POWER SUPPLY
SMB #216

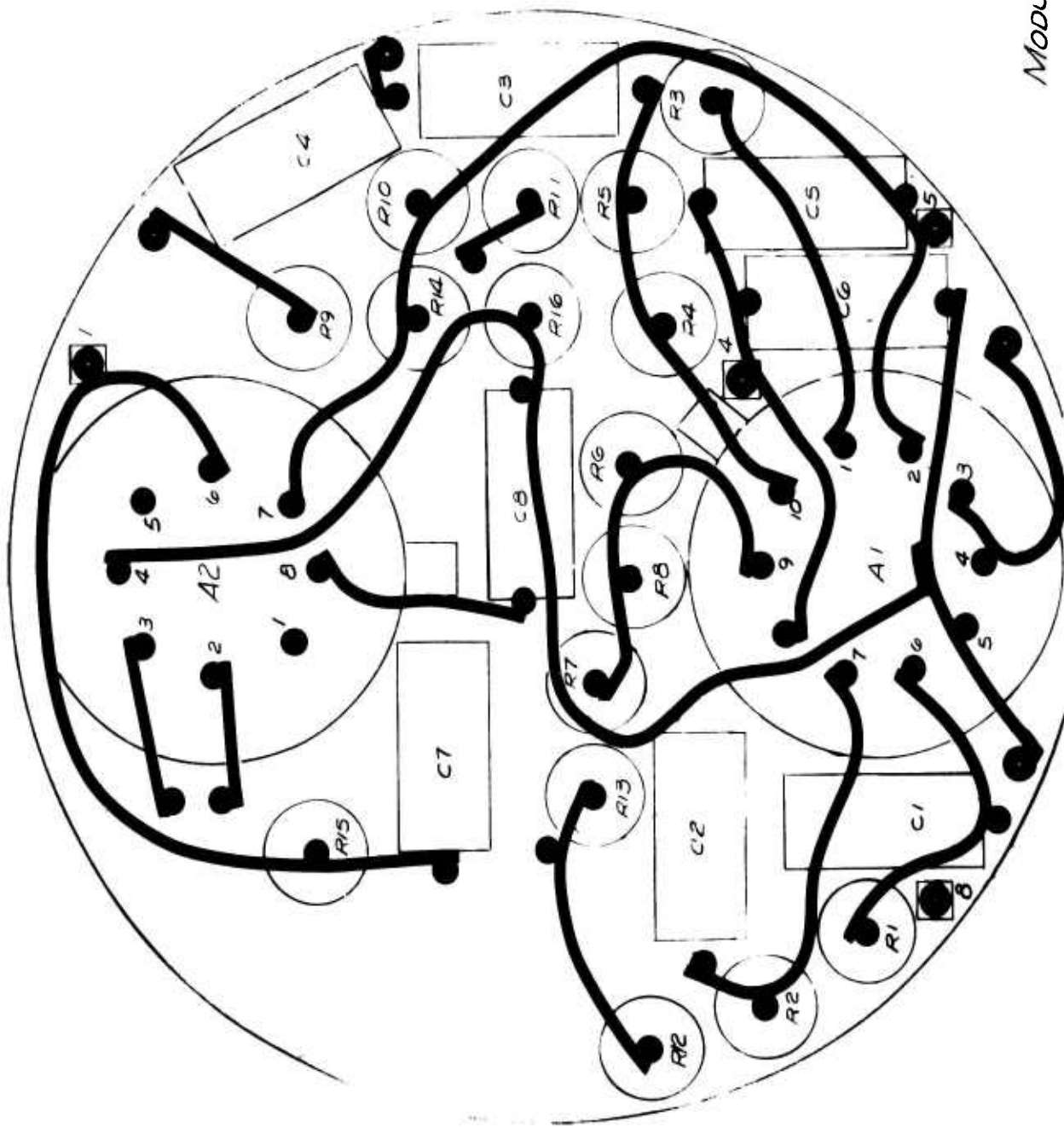


MODULE #3
POWER AMPLIFIER

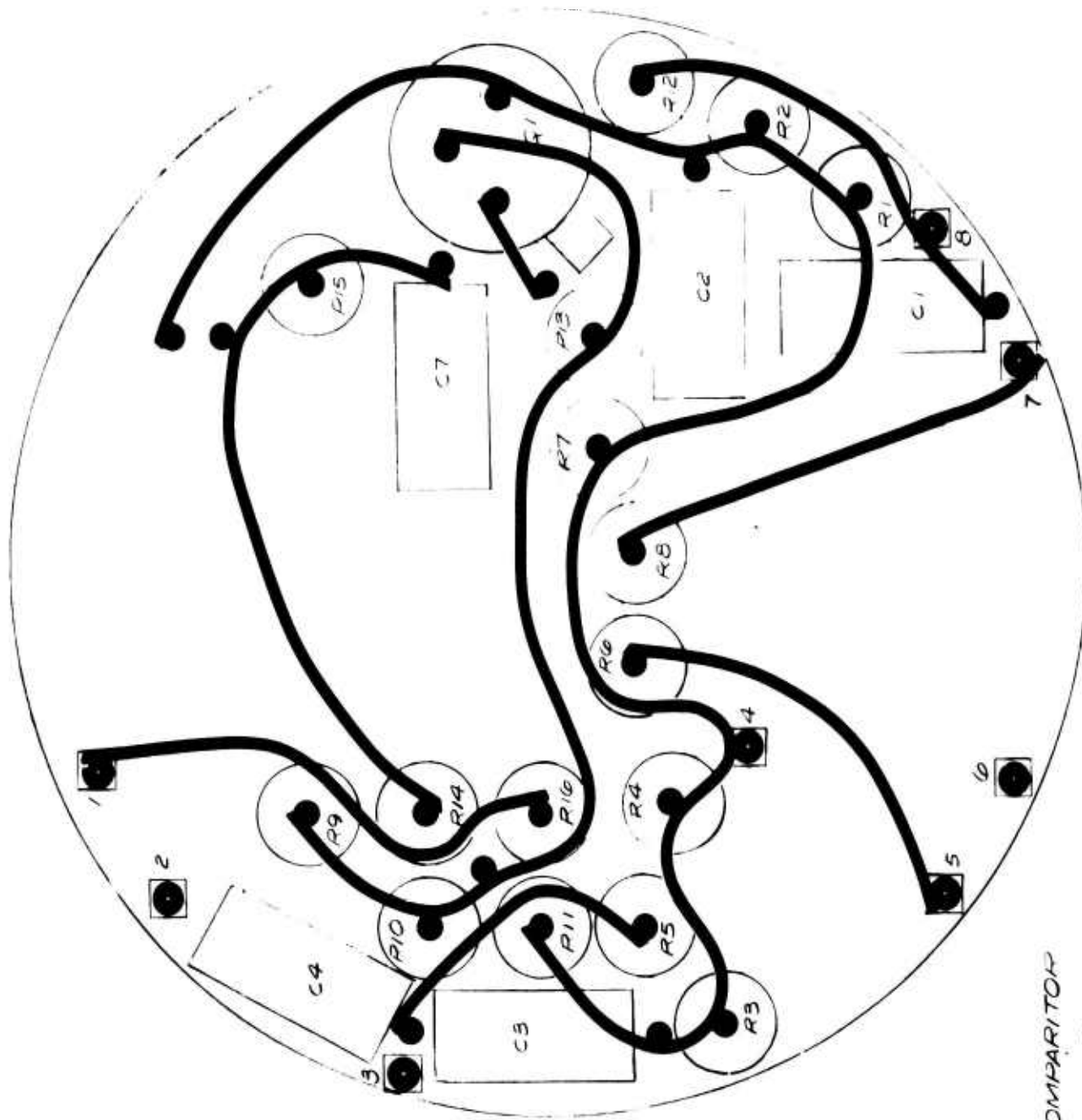


MODULE #3

POWER AMPLIFIER 6/2 6 2 7 2

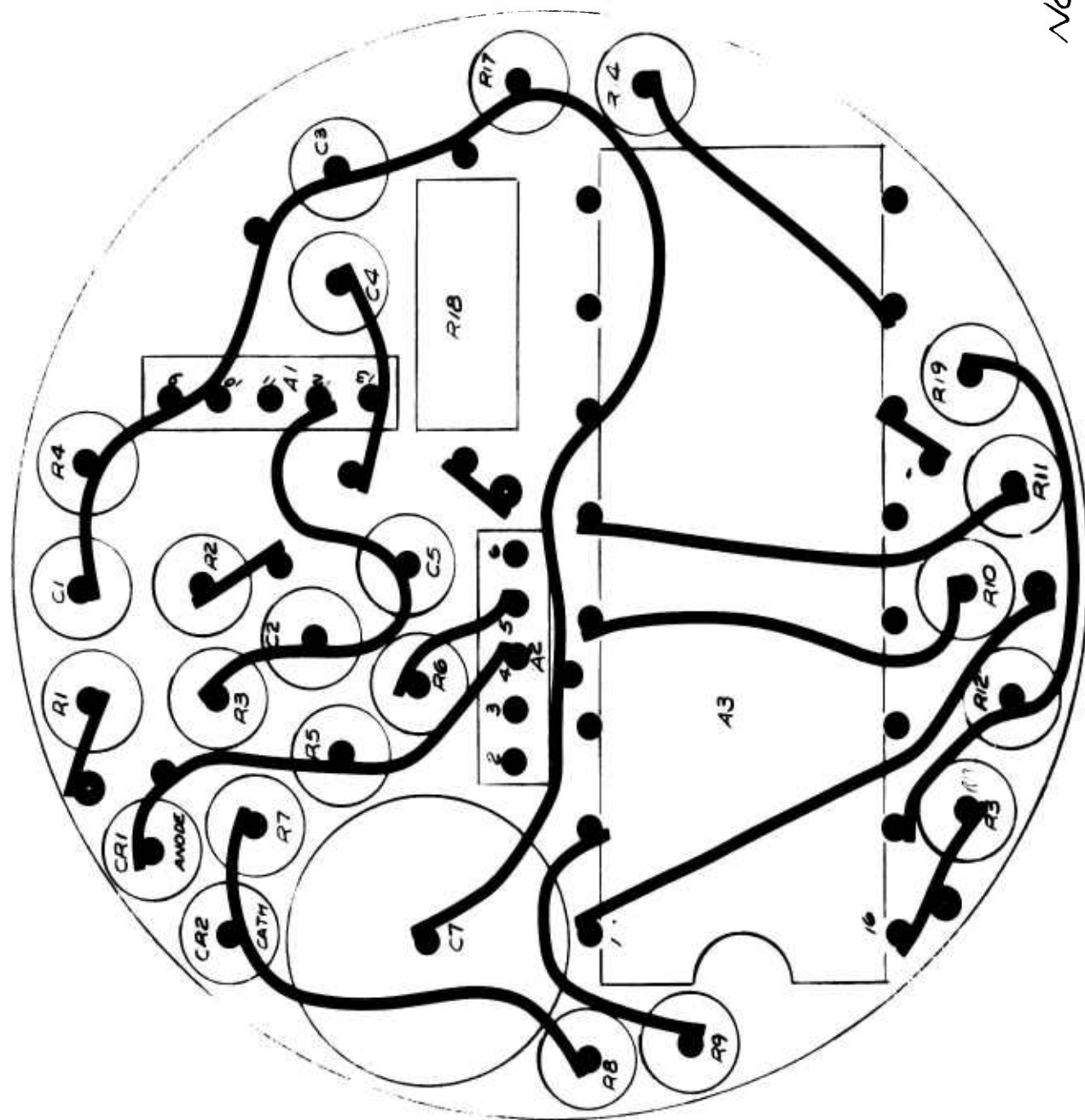


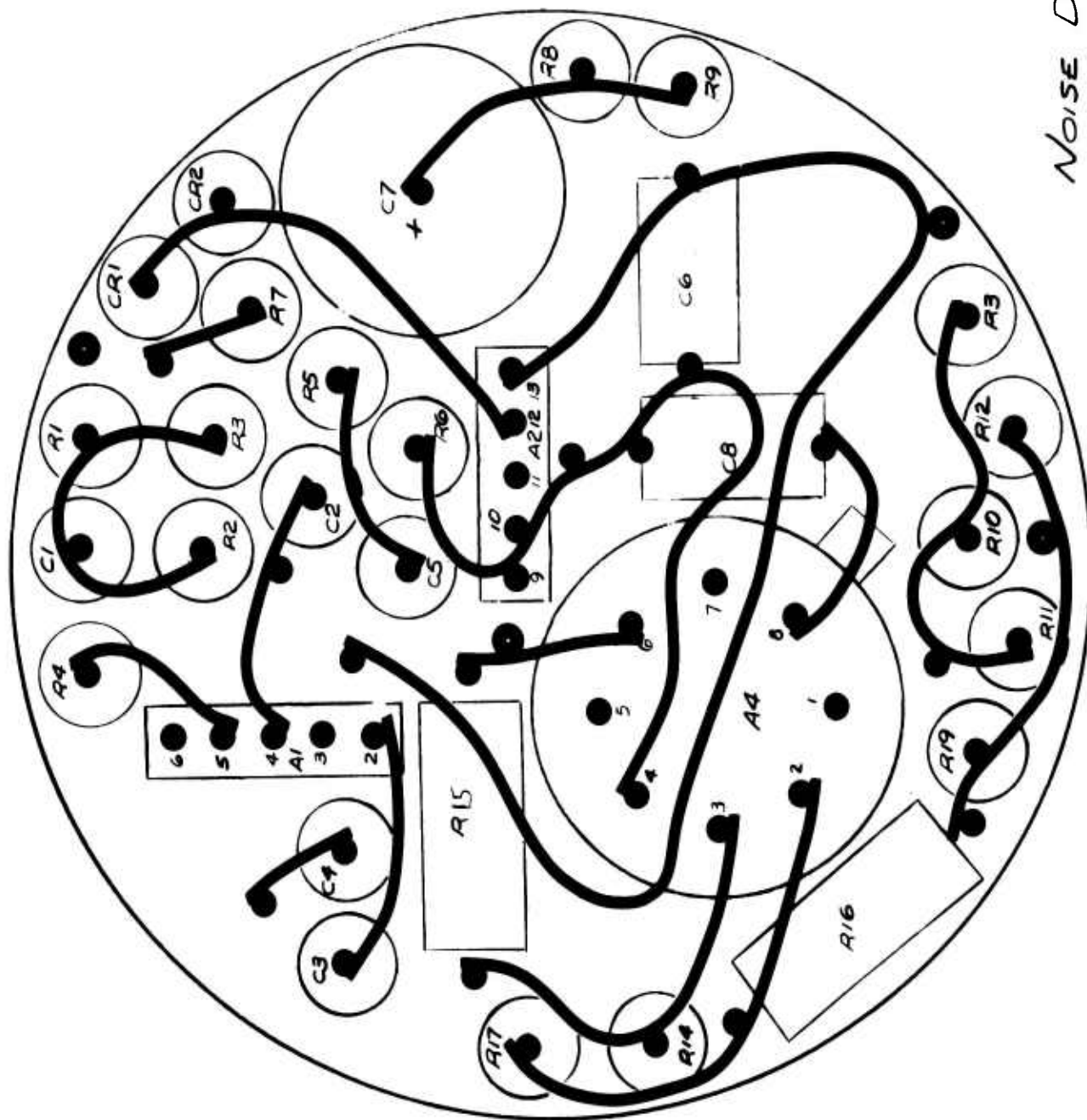
MODULE 4 PHASE COMPARATOR,
 & LOCK DETECTOR



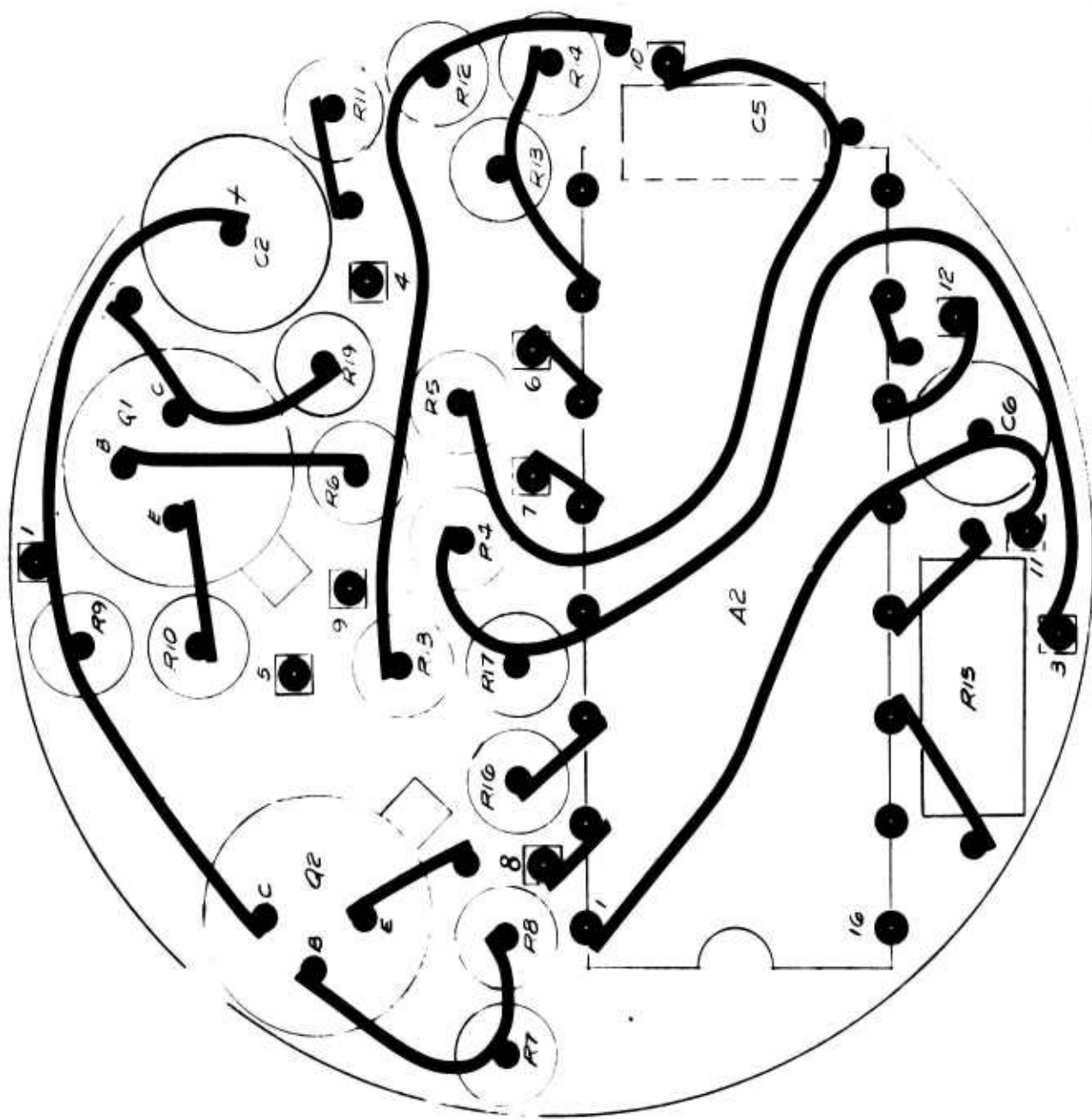
MODULE 4 - PHASE COMPARITOR
H86076 & LOCK DETECTOR

NOISE DETECTOR

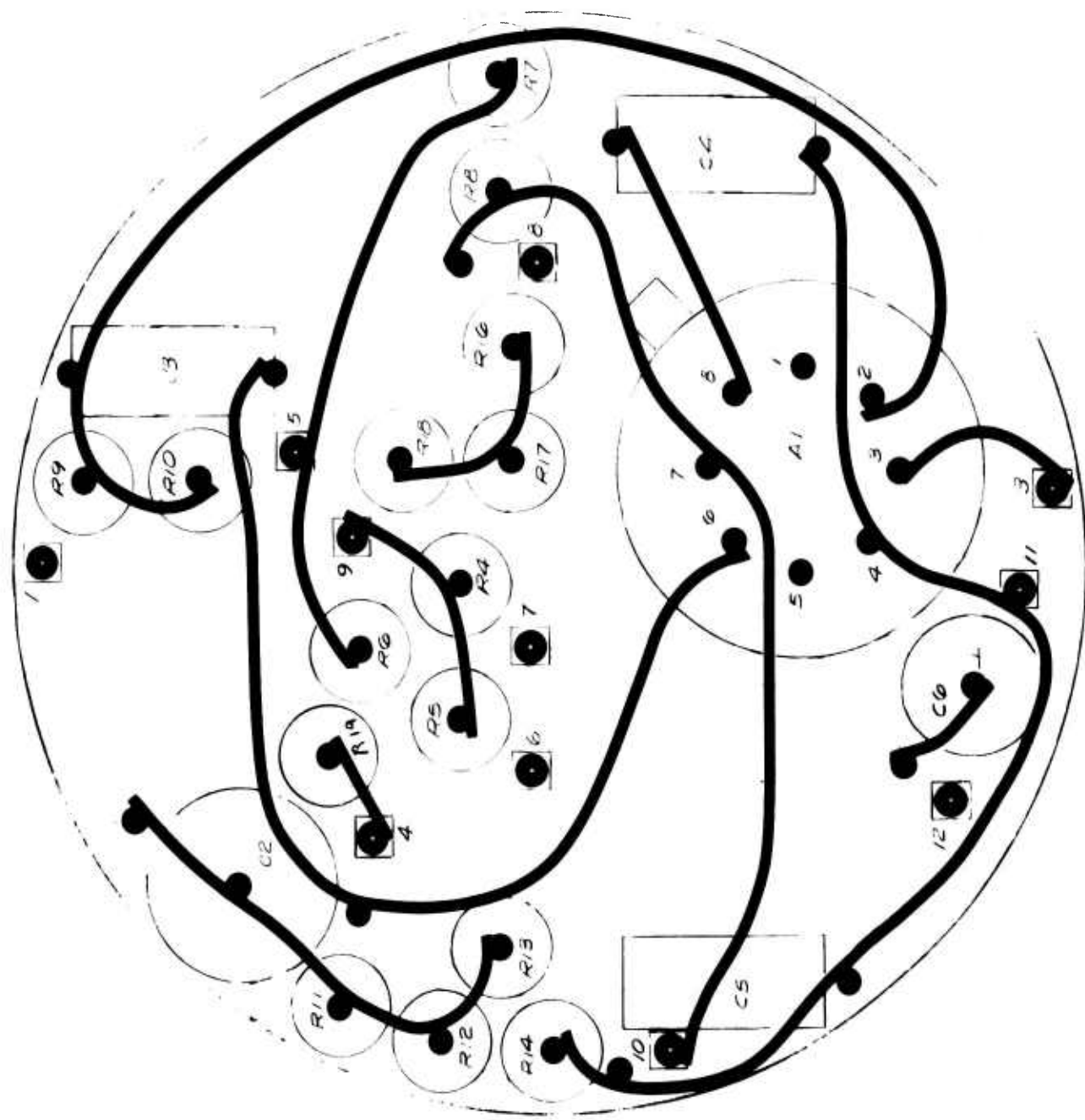




NOISE DETECTOR



MODULE #5 - INTEGRATOR & VCO
 4/2 6/22/70



MODULE #5 - INTEGRATOR & VCO
(REV 6-22-76)

APPENDIX C
ELECTRONIC COMPONENTS PARTS LIST

RESISTORS

PROGRAM RESONANT ACOUSTIC GAGE
 ASSEMBLY RAM
 SUB ASSEMBLY BUFFER

PART NO. _____
 PART NO. _____

PAGE 1 OF 2

PREPARED BY R. Eichhorn
 DATE 7-26-76
 SCHEMATIC _____

Circuit Number	Part Number and Construction	Status*	Military Specification	Manufacturer	Resistance (ohms)	Tolerance	Power Rating (watts)	Actual Power (watts)	Maximum Duty Cycle	Max. Bulk Air Temp (°C)	Screening Requirements
R1	RNR55K / HOLDER / METAL FILM		MIL-R-55102	DALE EMF 55-22	3.03K	2%	1/8 W				
R2	RCR07C / CARBON COMPOSITION		MIL-R-39003	ALLEN-BRADLEY 10F355	1M	5%	1/4 W				
R3	RNR55K		MIL-R-55102	DALE	19.6K	2%	1/8 W				
R4	RNR55K		"	"	2.15K	2%	1/8 W				
R5	RCR07C		MIL-R-39003	A.B.	1M	5%	1/4 W				
R6	RNR55K		MIL-R-55102	DALE	196K	2%	1/8 W				
R7	RNR55K		"	"	196K	2%	1/8 W				
R8	RNR55K		"	"	294K	2%	1/8 W				
R9	RCR07C		MIL-R-39003	A.B.	1M	5%	1/4 W				
R10	RNR55K		MIL-R-55102	DALE	100K	2%	1/8 W				
R11	RNR55K		"	"	19.6K	2%	1/8 W				
R12	RNR55K		"	"	19.6K	2%	1/8 W				
R13	RNR55K		"	"	10K	2%	1/8 W				
R14			"	"	3.32K	2%	1/8 W				
R15			"	"	14K	2%	1/8 W				
R16			"	"	19.6K	2%	1/8 W				
R17					19.6K						
R18			"	"		2%	1/8 W				

RESISTORS

PROGRAM

ASSEMBLY

SUB ASSY POWER SUPPLY

PART NO.

PART NO.

PREPARED BY

DATE _____

SCHEMATIC

R. Eichen

DATE 6-21-76

SCHEMATIC

Circuit Number	Part Number and Construction	Status*	Military Specification	Manufacturer	Resistance (ohms)	Tolerance	Power Rating (watts)	Actual Power (watts)	Maximum Duty Cycle	Max. Bulk Atr Temp (°C)	Screening Requirements
R1			MIL-R-55182	DALE EMF 55-22	1 Ω	20%		160 mW	100%		
R2	ANR 55K		MIL-R-55182		4 Ω		1/8 W	40	100		
R3	ANR 55K		MIL-R-55182		2.15K	2%	1/8 W	304	100		
R4			MIL-R-55182		2.15K	2%		0			
R5			MIL-R-55182		SELECO 29	2%		6.04			
R6	ANR 55K		MIL-R-55182		2.15K	2%	1/8 W		100		
R7					690			1.25	100		
R8					19.6K			5.36	100		
R9					19.6K			5.36	100		
R10					10K				100		
R11					3.03K			37.2	100		
R12					2.15K			21.2	100		

*See Figure 8 for code.

RESISTORS

PROGRAM _____
 ASSEMBLY RAN
 SUB ASSY Power Amplifier

PREPARED BY R. Eickhoff
 DATE 6-21-76
 SCHEMATIC _____

Circuit Number	Part Number and Construction	Status*	Military Specification	Manufacturer	Resistance (ohms)	Tolerance	Power Rating (watts)	Actual Power (watts)	Maximum Duty Cycle	Max. Bulk Air Temp (°C)	Screening Requirements
R1	ENR 55K/MOLDBO		MIL-R-55182		10K	20%	1/8 W		100%		
R2					10K				100		
R3					6.81K				100		
R4					19.6K				100		
R5					19.6K				100		
R6					10K				100		
R7					10K				100		
R8					3.32K				100		
R9					3.32K				100		
R10					14K				100		
R11					200				100		
R12					200				100		
R13					200				100		
R14					200				100		
R15					33.2				100		
R16					33.2				100		
R17	RWP-81 / POWSE		MIL-R-39007	DALG AGS-1	2.5	1%	1 W		100		
R18	RWE-81 / POWSE		MIL-R-29007	DALL AGS-1	2.5	1%	1 W		100		

*See Figure 8 for code.

RESISTORS

PROGRAM RESONANT ACOUSTIC GAGE PREPARED BY R. EICHMAN
 ASSEMBLY RAM PART NO. _____ DATE 6-21-76
 SUB ASSY OSCILLATOR PART NO. _____ SCHEMATIC _____

Circuit Symbol Number	Part Number and Construction	Status*	Military Specification	Manufacturer	Resistance (ohms)	Tolerance	Power Rating (watts)	Actual Power (watts)	Maximum Duty Cycle	Max. Bulk At Temp (°C)	Screening Requirements
R1	RNC55K				19.6K						
R2					10K						
R3					2.15K						
R4	RWR81W6810FP				680Ω						
R5					200Ω						
R6					10K						
R7					4.99K						
R8					3.83K						
R9	RNC55J				23.7K						
R10	RNC55J				16.2K						
R11					200Ω						
R12					56L						
R13					56L						
R14					100K						
					100K						

A-111101

RESISTORS

PREPARED BY R. F. C. 1000
DATE 6-21-76
SCHEMATIC _____

PROGRAM _____ PART NO. _____
ASSEMBLY RAM PART NO. _____
SUB ASSY PHASE COMPASS 1.6

Circuit Number	Part Number and Construction	Status*	Military Specification	Manufacturer	Resistance (ohms)	Tolerance	Power Rating (watts)	Actual Power (watts)	Maximum Duty Cycle	Max. Bulk Air Temp (°C)	Screening Requirements
R1	RNR55K / MOLOSO METAL FILM		MIL-R-55182		19.6K	2%	1/8 W	5.5 mW	100%		
R2									100		
R3									100		
R4								11.4	100		
R5					2.15K			1.14	100		
R6					SELECT				100		
R7									100		
R8									100		
R9					10K			2.2	100		
R10					19.6K			2.2	100		
R11									100		
R12					14.0K			20.4	100		
R13					14.0K			20.7	100		
R14					274K			1.32	100		
R15					140K			1.64	100		
R16					3.83K			5	100		

*See Figure 8 for code.

RESISTORS

PROGRAM RESONANT Acoustic GAGE
 ASSEMBLY RAM
 SUB ASSY NOISE DETECTOR

PART NO. _____
 PART NO. _____

PREPARED BY R EICHNER
 DATE 7-28-76
 SCHEMATIC _____

Circuit Number	Part Number and Construction	Status*	Military Specification	Manufacturer	Resistance (ohms)	Tolerance	Power Rating (watts)	Actual Power (watts)	Maximum Duty Cycle	Max. Bulk Temp (°C)	Screening Requirements
R1	RWR55K		MIL-R-55102	DALE EMF 55-20	6.81K		1/8W				
R2					6.81K						
R3					140K						
R4					140K						
R5					30.1K						
R6					140K						
R7					140K						
R8					200R						
R9					4.99K						
R10					SELECT						
R11					SELECT						
R12					680						
R13					100K						
R14					30.1K						
R15					30.1K						
R16					SELECT						
R17					30.1K						
R18					4.99K						

PREPARED BY F. VANU 3100101
DATE 7/28/76
SCHEMATIC

PROGRAM	REMARK	ACCOUNT	PAGE
ASSEMBLY	RAM		PART NO
SUB ASSY	MOUSE		PART NO
			PAGE 2 OF 2

[illegible]

*See Figure 8 for code.

PREPARED BY R. E. Cline
DATE 7-20-76
SCHEMATIC

PROGRAM	RESONANT ACOUSTIC	GATE
ASSEMBLY	RAM	PART NO.
SUB ASSY.	INPUT BUFFER	PART NO.

PREPARED BY R. E. C. 1122
DATE 7-20-76
SCHEMATIC

[illegible]

*See Figure 8 for code.

CATALYTORS

PREPARED BY R. C. ...
DATE 6-1-76
SCHEMATIC

PROGRAM	PART NO.
ASSEMBLY RA1	PART NO.
SUB ASSY. POWER SUPPLY	

[illegible]

*See Figure 8 for code.

PREPARED BY R. EICHMAN
DATE 6-21-76
SCHEMATIC

PROGRAM	PART NO.
ASSEMBLY	RAM
SUB ASSY.	POWER AMPLIFIER

[illegible]

****See Figure 8 for code.**

CAPACITORS

PREPARED BY R. E. ...
DATE 6-21-76
SCHEMATIC

PROGRAM	PART NO.
ASSEMBLY	RA-1
SUB ASSY.	PHASE COMPARATOR

[illegible]

*See Figure 8 for code.

PREPARED BY R. Eichen
DATE 6-21-76
SCHEMATIC _____

PROGRAM _____
ASSEMBLY RAM
SUB ASSY. OSCILLATOR

PART NO.

[illegible]

*See Figure 8 for code.

CAPACITORS

PREPARED BY R. E. C. (2000)
DATE 7-28-76
SCHEMATIC

PROGRAM	DESIGN	APP	PART NO.
ASSEMBLY	SINGLE	MODE	PART NO.
SUB ASSY	110	DESIGN	

[illegible]

***See Figure 8 for code.**

SEMICONDUCTORS

PREPARED BY F. VAN GILLEN III

DATE 4/30/76

SCHEMATIC

PROGRAM RESONANT ACOUSTIC GAGE

PART NO.

PART NO.

PROGRAM ALL
ASSEMBLY 0AM

ASSEMBLY

CLUB ASSEMBLY

15-2-11-12

[illegible]

*See Figure 8 for code.

RECORDED BY F. VAN GELDEREN

PREPARED BY F. VAN GILDERE

DATE 7/28/72

SCHEMATIC

PROGRAM

ASSEMBLY

SUB ASSY.

PART NO.

PART NO.

RAM

POWER SUPPLY

DX/PI-V

PREPARED BY R. EICHMAN
DATE 6-21-76
SCHEMATIC _____

PROGRAM _____ PART NO. _____
ASSEMBLY RAM PART NO. _____
SUB ASSY. Power Amplifier

Circuit Number	Part Number and Construction	Status*	Military Specification	Manufacturer	BV CEO			BV CBO			BV EBO			Rated PIV	Actual PIV	Rated Power (watts)	Actual Power (watts)	Max. Ambient Temp (°C)	Maximum Duty Cycle	Screening Requirements
					Rated	Actual		Rated	Actual		Rated	Actual								
Q1	JANTXV 2N2907A	S	19500/291		60		60		5				—	—	0.4					
Q2	JANTXV 2N3501	S	19500/366		150		150		6				—	—	1.0					
Q3	JANTXV 2N3637	S	19500/357		175		175		5				—	—	1.0					
Q4	JANTXV 2N3792	S	19500/379		60		60		7				—	—	150					
Q5	JANTX 2N5038	N	19500/439 (USAF)		90		150		7				—	—	140					
CR1	JANTXV 1N4148	S	19500/1116										75	75						
CR2	JANTXV 1N4148	S											75	75						
CR3	JANTXV 1N4148	S											75	75						
CR4	JANTXV 1N4148	S											75	75						
CR5	JANTXV 1N4148	S											75	75						
CR6	JANTXV 1N4148	S											75	75						

*See Figure 8 for code.

PROGRAM _____
ASSEMBLY RAM
SUB ASSY. PHILIPS COMPACT 1000

PART NO. _____
PART NO. _____

PROGRAM
ASSEMBLY
SUB ASSY

PREPARED BY R. E. GARDNER
DATE 6-21-76
SCHEMATIC _____

*See Figure 8 for code.

PROGRAM _____
ASSEMBLY RAM
SUB ASSY. OSCILLATOR

PART NO. _____
PART NO. _____

PREPARED BY R. EICHORN
DATE 6-21-76
SCHEMATIC

[illegible]

SEMICONDUCTORS

PREPARED BY 7-1-70
DATE 7-1-70
SCHEMATIC

PROGRAM	<u>RESIDENT ADOPT</u>	PART NO.
ASSEMBLY	<u>1014</u>	PART NO.
SUB ASSY.	<u>ADJ. MOUNTING</u>	

[illegible]

*See Figure 8 for code.

PROGRAM	REDAVANT ACCOUNT	G.A.E.
ASSEMBLY	RAM	PART NO.
SUB ASSY.	INPUT BUFFER	PART NO.

PREPARED BY R. E. Emerson
DATE 7-26-76
SCHEMATIC _____

[illegible]

*See Figure 8 for code.

MICROELECTRONICS

PREPARED BY R. E. Hoot
DATE 6-21-76
SCHEMATIC _____

PROGRAM _____
ASSEMBLY RAM
SUB ASSY. POWER SUPPLY

PART NO. _____

PART NO. _____

[illegible]

*See Figure 8 for code.

PROGRAM
ASSEMBLY RAM
SUB ASSY. POWER AMPL

PREPARED BY R. EICHSEN
DATE 6-21-76
SCHEMATIC _____

[illegible]

MICROELECTRONICS

PREPARED BY R EICHBERG
DATE 6-21-76
SCHEMATIC

PROGRAM	PART NO.
ASSEMBLY RAM	
SUB ASSY. P4A-2 COMPACT	

[illegible]

*See Figure 8 for code.

PROGRAM
ASSEMBLY RAM
SUB ASSY. OSCILLATOR

PREPARED BY R. BILCHEN
DATE 6-21-76
SCHEMATIC _____

[illegible]

PREPARED BY F VAN GILLIGNE
DATE 7/28/76
SCHEMATIC

PROGRAM	RESERVANT	ACQUISITIVE	GAGE
ASSEMBLY	RAM		PART NO.
SUB ASSY.	NOISE DETECTOR		PART NO.

[illegible]

*See Figure 8 for code.

APPENDIX D
NONSTANDARD PARTS APPROVAL REQUEST

NON STANDARD PARTS APPROVAL REQUEST

- (1) NSPAR No. ARG-002 (2) Date: 5/21/76
 (3) Prime Contractor: Acurex (4) Contract No. F047041-75-C-0164
 (5) Part Nomenclature: Multiplier (6) Part Used In: Acoustic Recession Gage
 (7) Circuit Symbol: N/A (8) Manufacturer: Analog Devices, Inc.
 (9) Mfgr. Part No. AD532SH (10) Specification: MIL-STD-883A Level B
 (11) Justification for Use:

See Page 2

(12) Application Data:

(13) Test Data/Remarks:

Prepared by Thomas E. Vyse
Signature

Requested by R. L. Eishon
Signature

Parts Control Board Action:

Step 1 - NSPAR

Approved _____
Interim ✓ (5/24/76)
Disapproved _____

[Signature]
Aerospace

SAMSO
[Signature]
Acurex

Step 2 - SCD

Approved _____
Interim _____
Disapproved _____

Aerospace

SAMSO

Acurex

Step I
See attached comments

ARG-002

- (11) There is no standard part available to perform this function. Approximately 14 transistors, 15 resistors, and one non-standard operational amplifier would be required to replace this device. (A schematic using mostly standard parts can be supplied upon request.) Engineering judgement indicates that reliability would be sacrificed by attempting to implement this function with standard parts.
- (12) This circuit will be used as a phase comparator, and one will be required per system.

In the circuit configuration which is planned, the device will be used under the following conditions:

<u>Condition</u>	<u>Rated Maximum</u>	<u>Max. Circ. Stress</u>	<u>% of Rating</u>
Supply Voltage	$\pm 22V.$	$\pm 11 V.$	50%
Power Consumption	500 MW.	66 MW.	13%

- (13) Acurex Products Division has used this device of this family type in standard products used in severe environments. Since they do not keep failure records, no specific data is available. However, the devices are not known to be a problem.

Devices of this same family have been used in the Acoustic Gage for the past year with no failures or performance degradation. (BREADBOARD & GROUND TEST ELECTRONICS)

Several other microcircuits (non-standard) are available to perform this function. This one has been chosen because it requires a minimum of external parts. Other devices also require variable resistors for trimming, which are definitely restricted on this program.

ARG-002

1. There was no indication that an alert search had been conducted. There is a recent alert (3/31/76) GD-A76-02 which specifies internal corrosion in AD532 device. Also there are several other alerts on ~~Ames~~ 500 series devices reporting bonding/open metallization problems and photolith deficiencies.
2. What is the qual status and environmental capability of the part? ✓
3. Has the supplier any records of other military program on which the part has been used and its track record? ✓
4. Is there just one part used per vehicle? *yes*
5. Any special handling plans required for this device?

NON STANDARD PARTS APPROVAL REQUEST

(1) NSPAR No. ARG-003 (2) Date: May 21, 1976
 (3) Prime Contractor: Acurex Corporation (4) Contract No. F047041-75-C-0164
 (5) Part Nomenclature: Operational Amplifier (6) Part Used In: Recession Gage
 (7) Circuit Symbol: N/A (8) Manufacturer: Harris Semiconductor
 (9) Mfgr. Part No. HA-2510-8 (10) Specification: MIL-STD-883 Level B
T0-86 Package

(11) Justification for Use:

None of the allowed group 1 operational amplifiers have the required power bandwidth for adequate circuit operation. A discrete substitute would require at least 10 transistors, 8 resistors, and would consequently be far less reliable.

(12) Application Data:

See Page 2

(13) Test Data/Remarks:

Acurex has been using the commercial grade of this amplifier for years, and they have proven themselves to be quite reliable.

Prepared by Thomas E. Vyk
 Signature

Requested by R L Eichen
 Signature

Parts Control Board Action:
Step 1 - NSPAR

Approved

Interim

Disapproved

✓ (3/25/76)

Aerospace

SAMSO

Acurex

Step 2 - SCD

Approved

Interim

Disapproved

Aerospace

SAMSO

Acurex

Step I
 see attached comments

(12) Application Data

The HA2510-8 will be used several places in the circuit.

1. As the input buffer amplifier.
2. In the 800 KHz noise detector as a 20 db amplifier.
3. As a basic amplifier in the transmitting crystal driving amplifier.

Worst case circuit usage will be:

<u>Condition</u>	<u>Rated Max</u>	<u>Max Circuit Use</u>	<u>% of Rating</u>
Absolute voltage V+ to V-	40.0V	32V (20.6)	80% 52.7.
Differential input voltage	+ 15V	< 1 Volt	< 10%
Peak Output Current	50 MA	10 MA	20%
Internal Power Dissipation	300 MW	102 MW 124	34% 41.7.

ARG-003

1. Justification for not maintaining at least a 50% derating on power dissipation required. *Derating required*
2. A thermal transfer analysis shall be provided showing maximum junction temperature.
3. There was no evidence that an alert search had been made. There have been several alerts written against the part. Basically it was for slow rate induced errors. GIDEP Report No. N7A73-01.
4. What is qual status and environmental capability?
5. How many parts per system are used? *3 prob 4*

NON STANDARD PARTS APPROVAL REQUEST

- (1) NSPAR No. ARG-004 (2) Date: May 21, 1976
 (3) Prime Contractor: Acurex (4) Contract No. F047041-75-C-0164
 (5) Part Nomenclature: Op Amp (6) Part Used In: RecessionGage
 (7) Circuit Symbol: N/A (8) Manufacturer: Fairchild Semi, Mt. View, Ca.
 (9) Mfgr. Part No. UA108AHMQB (10) Specification: Unique 38510 processed to Class B

(11) Justification for Use:

None of the group 1 operational amplifiers have low enough input bias currents to meet the required circuit performance.

(12) Application Data:

Will be used as an integrator to drive the voltage controlled oscillator at appropriate derating. In use the Op-Amp will be subjected to following stress:
 (Continued on page 2)

(13) Test Data/Remarks:

This operational amplifier has performed quite well in the breadboard tests. It is included in Part 2 of QPL38510 and has thus shown itself to be a highly reliable part.

Prepared by Thomas E. Nyse
 Signature

Requested by R. L. Eichen
 Signature

Parts Control Board Action:

Step 1 - NSPAR

Approved mtg/tes
 Interim (3/25/76)
 Disapproved _____

[Signature]
 Aerospace

[Signature]
 SAMS0
 Acurex

Step 2 - SCD

Approved _____
 Interim _____
 Disapproved _____

Aerospace

SAMS0

Acurex

step I
 see attached comments

<u>Condition</u>	<u>Maximum Rating</u>	<u>Maximum Voltage</u>	<u>% of Rating</u>
Supply Voltage	$\pm 20V$	$\pm 10V$	50%
Interval Power Dissipation	500 MW	12 MW	3%
Differential Input Current	$\pm 10MA$	$<\pm 1MA$	$<10\%$
Input Voltage	$\pm 10V$	$\pm 5V$	50%

ARG-004

1. What would the penalty be if standard parts were used? ✓
2. Was an alert search performed? ✓
3. Has the part been used on other military programs and was it satisfactory?
4. What is the environmental capability of part? 3F510
5. Any special attention plans for handling and assembly of this device into hardware?

1) Diff pair low current level, another transistor
1/2 Power Parts. L17108 low bias



NON STANDARD PARTS APPROVAL REQUEST

- 1141.221
- (1) NSPAR No. ARG-005 (2) Date: 6-21-76
(3) Prime Contractor: Acurex (4) Contract No. F04701-75-C-0164
(5) Part Nomenclature: Capacitor (6) Part Used In: Oscillator
(7) Circuit Symbol: _____ (8) Manufacturer: VITRAMON
(9) Mfr. Part No. CYR41E102G (10) Specification: _____

(11) Justification for Use:

The gage measurement accuracy is dependant upon a stable RC time constant for the voltage controlled oscillator. Thus a capacitor with a low temperature coefficient. No known standard part meets the requirement.

(12) Application Data:

Used as the timing capacitor for the voltage controlled oscillator.

Rated Voltage: 100 Vdc
Actual: 21 VMAX

(13) Test Data/Remarks:

Temperature coefficient ± 25 P.P.M., other capacitors available for this function are CCR05 ceramic (MIL-C-20)

Prepared by

Ronald L. Enslin
Signature

Requested by

Ronald L. Enslin
Signature

Parts Control Board Action:

Step 1 - NSPAR

Approved _____
Interim _____
Disapproved _____

Aerospace

SAMSO

Larry Combs
Acurex

Step 2 - SCD

Approved _____
Interim _____
Disapproved _____

Aerospace

SAMSO

Acurex



NON STANDARD PARTS APPROVAL REQUEST

- 7141 258
- (1) NSPAR No. ARG-006 (2) Date: 6-22-76
(3) Prime Contractor: Acurex (4) Contract No. F04701-75-C-0164
(5) Part Nomenclature: Transistor (6) Part Used In: Power Amplifier
(7) Circuit Symbol: _____ (8) Manufacturer: RCA
(9) Mfgr. Part No. JTX 2N5038 (10) Specification: MIL-S-19500E/439 (USAF)

(11) Justification for Use:

The power amplifier requires high current power transistors with fast switching times in order to avoid excessive currents at high frequencies. The available standard parts do not meet this requirement.

(12) Application Data:

Will be used in the power amplifier driving a reactive load at 10 KHz to 100 KHz (see page 2).

(13) Test Data/Remarks:

Part is available JTX and is thus a Group II part

Prepared by

Ronald L. Eichen
Signature

Requested by

Ronald L. Eichen
Signature

Parts Control Board Action:

Step 1 - NSPAR

Approved _____
Interim _____
Disapproved _____

Aerospace

SAMSO

[Signature]
Acurex

Step 2 - SCD

Approved _____
Interim _____
Disapproved _____

Aerospace

SAMSO

Acurex

ARG-000

(12) Application Data:

	<u>Rating</u>	<u>Actual</u>
Collector Base Voltage	150 V	32 V
Collector Emitter Voltage	90 V	32 V
Emitter Base Voltage	7 V	2 V
Continuous Collector Current	20 A	.5 A
Peak Collector Current	30 A	1 A
Continuous Base Current	5 A	.05 A
Power Dissipation	140 A	4 W



NON STANDARD PARTS APPROVAL REQUEST

- 7141 255
- (1) NSPAR No. ARG-007 (2) Date: 6-21-76
(3) Prime Contractor: Acurex (4) Contract No. F04701-75-C-0164
(5) Part Nomenclature: Function Generator (6) Part Used In: Acoustic Recession Gage
(7) Circuit Symbol: N/A (8) Manufacturer: Exar
(9) Mfgr. Part No. XR2206M (10) Specification: MIL-STD-883A Level B
(11) Justification for Use:

SEE PAGE 2

- (12) Application Data:

SEE PAGE 2

- (13) Test Data/Remarks:

SEE PAGE 2

Prepared by Ronald L. Eubank
Signature

Requested by Ronald L. Eubank
Signature

Parts Control Board Action:

Step 1 - NSPAR

Step 2 - SCD

Approved _____
Interim _____
Disapproved _____

Aerospace

Approved _____
Interim _____
Disapproved _____

Aerospace

SAMSO

SAMSO

Acurex

Acurex



NON STANDARD PARTS APPROVAL REQUEST

- 7/4/76
- (1) NSPAR No. ARG-008 (2) Date: 6-22-76
(3) Prime Contractor: Acurex (4) Contract No. F04701-75-C-0174
(5) Part Nomenclature: Transformer (6) Part Used In: Acoustic Recession Gage
(7) Circuit Symbol: T1 (8) Manufacturer: Quality Transformer
(9) Mfg. Part No. Not yet assigned (10) Specification: MIL-T-27D

(11) Justification for Use:

The Acoustic Recession Gage uses a piezoelectric ceramic crystal to induce an acoustic signal in the RV Nostetip. This crystal requires a high excitation voltage (about 100 volts RMS) to provide the required signal/noise rate. Since the maximum power supply available is only 28 volts D.C., a transformer is required to provide the high voltage.

(12) Application Data:

Transformer will drive a reactive load with a maximum of 8 VA RMS. Load will be tuned using the transformer primary inductance. Ratings will conform to MIL-T-27D. Frequency range will be 10 KHz - 100KHz.

(13) Test Data/Remarks:

Trnasformer design is not complete, pending final selection of piezoelectric crystal. Transformer will be wound on a torroid core, ferroxcube series 846T250, core material 3c8. Primary inductance approximately 1000 microhenries.

Prepared by Ronald L. Eichen
Signature

Requested by Ronald L. Eichen
Signature

Parts Control Board Action:

Step 1 - NSPAR

Step 2 - SCD

Approved _____
Interim _____
Disapproved _____

Aerospace

Approved _____
Interim _____
Disapproved _____

Aerospace

SAMSO

Acurex

SAMSO

Acurex

(11) Justification for Use:

There is no standard part which will perform this function. The requirement is for a precision voltage controlled oscillator with a sine-wave output, capable of operating from 10 KHz to 100 KHz with a linear, repeatable, and stable voltage to frequency relationship.

A circuit to perform this function using only standard parts would be quite complex. A preliminary investigation indicates that 39 transistors, 24 resistors, and one operational amplifier would be required to replace this one microcircuit. Although no reliability calculations have been made, engineering judgement is that the circuit made from standard parts would be far less reliable. (A sketch of the circuit using standard parts is available upon request.)

(12) Application Data:

This microcircuit is the key element which translates resonant frequency to voltage. It will be used once per system. The unit will be used in a circuit which will provide the following maximum stresses:

<u>Parameter</u>	<u>Rated Maximum</u>	<u>Max. Act. Voltage</u>	<u>Percent of Rating</u>
Power Supply Voltage	26 V	20.6 V 10.3	79% 40%
Power Dissipation	750 MW	350 MW 168 mw	47% 22%
Timing Current (Pin 7)	6 MA	0.2 MA	3%

(13) Test Data/Remarks:

16.3 mA max I

Exar Integrated Systems Inc is a well established semiconductor manufacturer in Sunnyvale, California. Acurex does not have a large amount of experience in using Exar parts, and no problems related to that manufacturer are presently known. Exar is set up for, and they actively screen parts to MIL-STD-883A. All classes.

There are several other microcircuits on the market which nearly meet the requirements but only one other circuit which could replace it (Intersil 8038-See ARG001). This particular microcircuit was chosen because of less power supply sensitivity and fewer external parts when used in the configuration necessary for performing the recession gage function.

The XR2206M does not use any processes listed as restricted in the parts control program plan, whereas the Intersil devices uses film resistors. This NSPAR supercedes and cancels ARG-001.